Isolation and Structure Elucidation of Bioactive Secondary Metabolites from Marine Sponges

(Isolierung und Struktur-Identifizierung von biologisch aktiven Naturstoffen aus marinen Schwämmen)

Inaugural - Dissertation
zur Erlangung des Doktorgrades
der Mathematisch – Naturwissenschaftlichen Fakultät
der Heinrich-Heine-Universität Düsseldorf

Vorgelegt von
Mostafa A. F. Abdelgawwad
aus Assiut, Ägypten

Düsseldorf, 2004

Gedruckt mit Genehmigung der Mathematisch-Naturwissenschaftlichen Fakultät
der Heinrich-Heine-Universität, Düsseldorf

Eingereicht am : 17.05.2004

Referent : Prof. Dr. Peter Proksch
Koreferent : Dr. Rainer Ebel, Juniorprofessor

Erklärung

Hiermit erkläre ich ehrenwörtlich, daß ich die vorliegende Dissertation „Isolierung und Struktur Identifizierung von biologisch aktiven Naturstoffen aus marinen Schwämme“ selbständig angefertigt und keine anderen als die angegebenen Quellen und Hilfsmittel benutzt habe. Ich habe diese Dissertation in gleicher oder ähnlicher Form in keinem anderen Prüfungsverfahren vorgelegt. Außerdem erkläre ich, daß ich bisher noch keine weiteren akademischen Grade erworben oder zu erwerben versucht habe.

Düsseldorf,

Mostafa A. F. Abdelgawwad

Acknowledgements

To the Almighty God “ALLAH” who has granted me all these graces to fulfil this work and who supported me and blessed me by His power and His mercy in all my life. To Him I extend my heartfelt thanks.

Many institutions and individuals were responsible for the crystallisation of this humble work, whose associations and encouragement have contributed to the accomplishment of the present thesis, and I would like to pay tribute to all of them.

I specially wish to express my sincere thanks and gratitude to Prof. Dr. **Peter Proksch**, chairman of the Department of Pharmaceutical Biology, Düsseldorf University, for his kindness, admirable supervision, direct guidance, generous considerations and valuable support during my stay in his department.

I would also wish to thank Dr. **Rainer Ebel**, of the same department for his direct guidance, valuable comments and suggestions and specially for sharing his expertise in both NMR spectroscopy and mass spectrometry.

I would also like to express my deep thanks to my sincere teacher Dr. **RuAngelie Edrada** for her guidance, fruitful discussions, constructive advises and particularly for sharing her expertise in isolation techniques, NMR data interpretation and revision of this thesis.

I am deeply indebted to Dr. **Victor Wray** (Gesellschaft für Biotechnologische Forschung, Braunschweig), for the measurement of the NMR spectra and his vital comments in the structure elucidation of the isolated compounds.

I am grateful to Dr**. R. van Soest** (Zoological Museum, University of Amsterdam) for the identification of the sponge materials.

I am thankful to both Dr. **Steube** of DSMZ (Deutsche Sammlung von Mikroorganismen und Zellkulturen) and Prof. Dr**. W.E.G. Müller** (Universität Mainz, Germany) for the cytotoxicity tests.

I am thankful to Dr. **Thomas Schmidt** (HHU Düsseldorf) for his kind help in the measurement of some compounds at the GC machine.

I would also like to express my gratefulness to Dr. **Peter Tommes**, Dr. **U. Matthiesen** (HHU Düsseldorf) and Dr. **Albrecht Berg** (HKI für Naturstofforschung, Jena) for the measurement of EIMS, FABMS and high resolution ms data.

I am thankful to the Egyptian Ministry of Higher Education, Missions Office for providing the financial support for my study in Germany.

My deep thanks are also to my friends, **Ziyad Baker** and **Wafaa Hassan** for their kind friendship, valuable help, encouragement and co-operation during my stay in Germany.

I would also like to extend my sincerest gratitude to my colleagues at the Department of Pharmaceutical Biology, Düsseldorf, **Franka, Carsten, Hefni, Sabrin, Gamal, Bärbel, Sofia, Tu, Yasman, Yosi, Ehab, Amal, Mohamed, Haofu, Nadine** and all the others for their help, friendship and for the good working atmosphere.

My special thanks to my colleague **Arnulf** for his help in the revision of the German summary in my thesis.

My deep thanks to **Maraika**, **Katja** and Mrs **Schlag** for their kindness and for always providing me with the materials and glassware which I needed in my work.

I would also like to express my gratefulness to the staff members of the Department of Pharmacognosy, Faculty of Pharmacy, Assiut University for providing me the basic science and for Prof. Dr. **Montaser Khalifah,** the Dean of Faculty of Pharmacy El-Minia University, Egypt for offering me such a kind of opportunity to study in Germany and their continuous encouragement and kind advises.

My deep thanks are also due to my supervisors for my Master thesis, Prof. Dr. **Ahmed Abdelrahman**, Prof. Dr. **Mohamed Salah** and Prof. Dr. **Mahmoud Hamed** for their motivations, recommendations and for teaching me very precious knowledge about Pharmacognosy and Phytochemistry.

I deeply appreciate my wife **Rasha,** for her vast understanding, everlasting moral support, continuous encouragement and for providing me an excellent environment and worthy atmosphere for doing my research work.

To my pretty kids, **Karim**, **Haisam** and **Hala** for their lovely smiles that can relive any kind of tiredness.

At this point, all my heartily thanks, my grand indebtedness and enthusiastic appreciation to my **mother**, my brother **Gawad** and my sister **Doaa** for their unfailing love, spiritual support and constant prayers.

At the end, my deeply thanks to my **Father**, who passed away, and I will never forget that he was the first person who instilled in me the love of science, May Almighty ALLAH bless him.

To All of you, **THANK YOU VERY MUCH**

Mostafa Abdelgawwad
Düsseldorf, Germany.

To my Family

Table of Contents

Zusammenfassung

Aus marinen Organismen wie Schwämmen, Pilzen und Bakterien isolierte Naturstoffe zeigen eine einzigartige strukturelle Vielfalt, die zu neuen Verbindungen mit medizinischem Nutzen führen könnte. Diese Arbeit behandelt Isolierung, Strukturaufklärung und Screening hinsichtlich biologischer Aktivität der Verbindungen einiger im Roten Meer und in Indonesien gesammelter mariner Schwämme unter Verwendung verschiedener chromatographischer und spektroskopischer Verfahren.

Die vier in dieser Arbeit verwendeten Schwämme und die daraus isolierten und in ihrer Struktur aufgeklärten Verbindungen sind in der folgenden Tabelle zusammengefaßt (Tabelle 5.1).

1. **Der Schwamm *Erylus lendenfeldi*, Rotes Meer**

Der Schwamm *Erylus lendenfeldi* wurde erschöpfend mit MeOH und Aceton extrahiert. Die vereinigten Extrakte wurden zur Trockne aufkonzentriert und mit Petrolether, EtOAc und *n*-BuOH gegen H_2O ausgeschüttelt. Da die EtOAc- und *n*-BuOH-Fraktionen große Ähnlichkeit aufwiesen, wurden sie vereinigt. Die vereinigte Fraktion (1.79 g) wurde mittels Mitteldruckflüssigkeitschromatographie (MPLC) unter Verwendung von Kieselgel als stationärer Phase und Elution mit CH_2Cl_2 / MeOH (70/30) getrennt. Die eluierten Fraktionen wurden einer semi-präparativen HPLC-Trennung an einer RP-18 Säule unterzogen, wobei drei Reinstoffe isoliert werden konnten: das bereits bekannte Saponin Erylosid A (**1**) und zwei neue Verbindungen, Erylosid K (**2**) und Erylosid L (**3**). Erylosid A zeigte moderate antibiotische und fungizide Aktivität gegenüber *B. subtilis*, *E. coli* und *C. albicans*.

2. **Der Schwamm *Negombata corticata*, Rotes Meer**

Wie zuvor beschrieben wurde auch dieser Schwamm erschöpfend mit MeOH und Aceton extrahiert. Die vereinigten Extrakte wurden zur Trockne aufkonzentriert und mit Petrolether, EtOAc, *n*-BuOH gegen H_2O ausgeschüttelt. Die Petrolether- und EtOAc-Fraktionen wurden vereinigt und einer konventionellen Säulenchromatographie, gefolgt von einer semipräparativen HPLC unterzogen.

Dabei wurden zwei bekannte Reinsubstanzen isoliert, nämlich das 14-gliedrige Lacton Latrunculin B sowie das ringoffene Derivat Latrunculin M (**4** und **5**). Latrunculin B besitzt

eine ausgeprägte antibiotische und antimykotische Aktivität und Zytotoxizität gegenüber verschiedenen Leukämiezelllinien.

3. **Der Schwamm *Pseudoceratina purpurea*, Indonesien**

Der Schwamm *Pseudoceratina purpurea* wurde ebenfalls erschöpfend mit MeOH und Aceton extrahiert. Die vereinigten Extrakte wurden zur Trockne aufkonzentriert und mit Petrolether, EtOAc und *n*-BuOH gegen H_2O ausgeschüttelt. Die EtOAc-Phase wurde unter Verwendung verschiedener Gradientensysteme einer MPLC unterzogen, gefolgt von konventioneller Säulenchromatographie und schließlich semipräparativer HPLC, wobei zehn bekannte Bromtyrosinalkoloide isoliert wurden (**6 - 15**). Einige dieser Verbindungen zeigten antibiotische, andere zytotoxische Aktivität.

4. **Der Schwamm *Rhabdastrella globostellata*, Indonesien**

Der Schwamm wurde mit MeOH und anschließend mit Aceton extrahiert, die Lösungsmittel unter vermindertem Druck entfernt. Der Rohextrakt wurde mit EtOAc gegen Wasser ausgeschüttelt. Die EtOAc-Phase wurde zur Gewinnung der verschiedenen Fraktionen einer VLC unter Verwendung eines Gradientensystems von 100% *n*-Hexan bis 100% EtOAc, dann 50% MeOH in EtOAc und schließlich 100% MeOH unterzogen. Jede Fraktion wurde durch konventionelle Flash-Chromatographie (CH_2Cl_2 – MeOH, 95:5 oder 9:1) gereinigt, gefolgt von semipräparativer Reversed-Phase-HPLC unter Verwendung verschiedener MeOH-Wasser-Gemische. Dabei wurden zwölf neue Isomalabarican-Triterpene (**17-19, 21-27, 29, 30**) und drei bekannte Verbindungen (**16, 20, 28**) isoliert. Einige dieser Verbindungen zeigten antibiotische Aktivität, wohingegen interessanterweise alle isolierten Verbindungen zytotoxische Aktivität gegenüber verschiedenen Krebszelllinien aufwiesen.

Zusammenfassend ist festzustellen, daß die vorliegende Arbeit Hinweise auf die Chemie der Schwämme gibt. Diese Hinweise bilden eine fundierte Grundlage für weitere Forschung und Nutzung dieser Schwämme.

1. Introduction

1.1. Significance of the study

The role of natural products from all sources in drug discovery has been reviewed recently [Gullo, *et al.,* 1994]. More comprehensive coverage has been given to plants over the past 10 years [Kinghorn, *et al.,* 1993; Chadwick, *et al.,* 1990]. Thus [Farnsworth, *et al.,* 1985] have reported that at least 119 compounds derived from 90 plant species can be considered as important drugs. Further evidence of the importance of the natural products is proved by the fact that close to half of the best selling pharmaceuticals were either natural products or their derivatives [O'Neill, *et al.,* 1993]. Over that past 10 years, there has been a resurgence of interest in the investigation of natural materials as a source of potential, new chemotherapeutic agents, but there are now signs that this interest is once more waning in favour of new approaches to drug discovery. Drugs of natural origin have been classified as original products, products derived semi synthetically from natural products, or synthetic products based on natural product models [Cragg, 1997].

It is well known that the oceans cover nearly three-fourth or over 70% of the world's surface. About 85% of all edible plant mass is produced by marine plants and about 80% of all known animal species live in or on water [Marderosian, 1969; Proksch, 1991]. Of these marine organisms, especially invertebrates are known to contain most of the novel secondary metabolites [Gribble, 1992]. Considering the great number of marine invertebrate species, only a small fraction of them has been examined from a chemical point of view [McCaffrey, *et al.,* 1985; Braekman, *et al.,* 1986]. Over the past 20 years marine secondary products have attracted growing interest due to their unique chemical features which, for example, frequently include halogen substituents [Scheuer, 1990]. Thousands of new marine natural products have been reported, proving marine natural organisms to be a rich and varied source of new structural classes of secondary metabolites [Faulkner, 1988, 1990]. By January of 1999, this figure had risen to approximately 10,000 [Jaspars, 1999]. A recent review provided an updated list of marine natural products which are currently under clinical trials (see Fig. 1.1 and Table 1.1) [Proksch, *et al.,* 2002].

Table 1.1: Selected marine natural products currently in clinical trials.

Source	Compounds	Disease area	Phase of clinical trials
Conus magnus (cone snail)	Ziconotide	pain	III
Ecteinascidia turbinata (tunicate)	Ecteinascidin 743	cancer	II/III
Dolabella auricularia (sea hare)	Dolastatin 10	cancer	II
Dolabella auricularia (sea hare)	LU103793[a]	cancer	II
Bugula neritina (bryozoan)	Bryostatin 1	cancer	II
Tridemnum solidum (tunicate)	Didemnin B	cancer	II
Squalus acanthias (shark)	Squalamine lactate	cancer	II
Aplidium albicans (tunicate)	Aplidine	cancer	I/II
Agelas mauritianus (sponge)	KRN7000[b]	cancer	I
Petrosia contignata (sponge)	IPL567,092[c]	inflammation/asthma	I
Pseudopterogorgia elisabethae (soft coral)	Methopterosin[d]	inflammation/wound	I
Luffariella variabilis (sponge)	Manoalide	inflammation/psoriasis	I
Amphiporus lactifloreus (marine worm)	GTS-21[e]	Alzheimer/schizophrenia	I

[a] Synthetic analogue of dolastatin 15

[b] Agelasphin analogue (α-galactosylceramide derivative)

[c] Synthetic analogue of contignasterol (IZP-94,005)

[d] Semisynthetic pseudopterosin derivative

[e] Also known as DMXBA

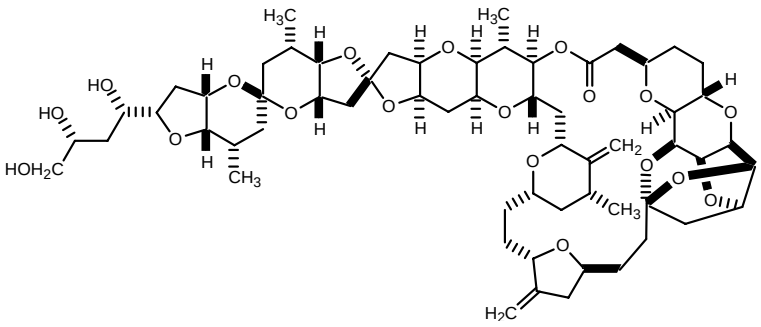

halichondrin B

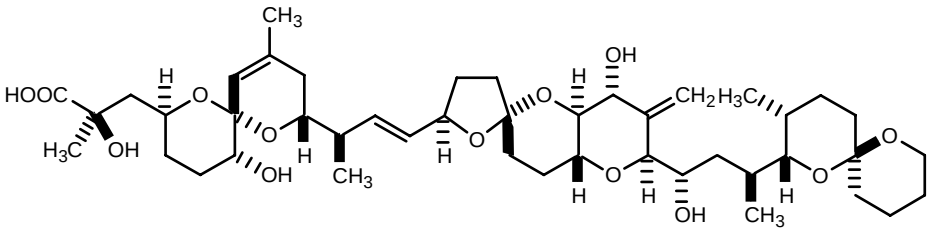

okadaic acid

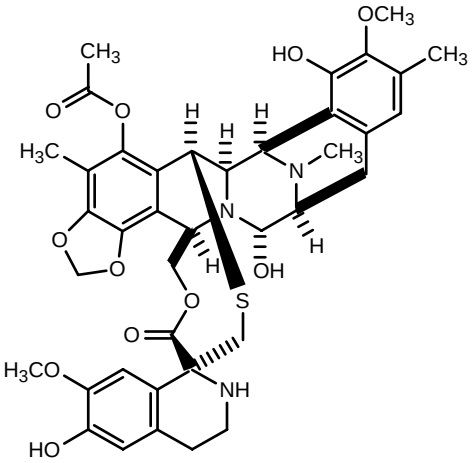

didemnin B

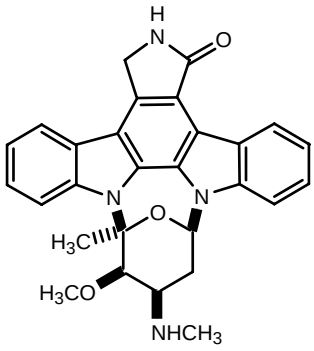

staurosporine

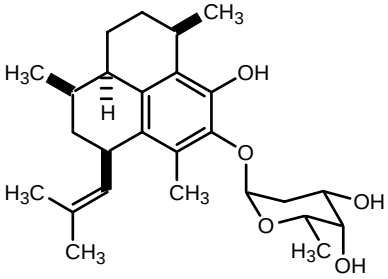

pseudopterosin E

Fig. 1.1: Promising candidates for new pharmaceuticals from marine origin

1.2. Antitumor pharmacology of marine natural products

[Luesch, *et al.,* 2000] reported on the isolation, structure determination and biological activity of a novel depsipeptide lyngbyabellin A from the marine cyanobacterium *Lyngbya majuscula.* Although lyngbyabellin A was observed to be cytotoxic to human nasopharyngeal and colon carcinoma cell lines and to disrupt specifically cellular microfilament networks in smooth muscle cells at concentrations of 0.01-5 μg/mL, it lacked *in vivo* activity when tested at sublethal doses against murine colon or mammary adenocarcinomas. On the other hand, two novel tetramic acids, melophlins A and B have been isolated from the sponge *Melophus sarassinorum* [Aoki, *et al.,* 2000]. These compounds reversed the ras-transformed phenotype of NIH3T3 fibroblasts at 5μg/mL. Cell cycle analysis by flow cytometry demonstrated that melophlins A and B arrested ras-transformed fibroblasts in the G_1 phase of the cell cycle, thus suggesting that melophlins reverse the transformed phenotype. These moderately cytotoxic marine agents may have potential as a new type of anticancer agent.

1.3. Marine natural products with immune-suppressive activity

Marine natural products have been investigated predominantly for their antimicrobial, cytotoxic, antitumor, antiviral and anti-inflammatory properties. Success in these areas is demonstrated by the agents now in pre-or clinical evaluation [König, *et al*., 1996]. Few marine natural products have been described as having immunosuppressive activity. The acridine alkaloid dercitin occurs in tunicates and has also been found in the deep water sponge *Dercitus sp*. Dercitin shows immunosuppressive activity in a murine derived, two-way mixed lymphocyte reaction (MLR) assay. This compound is however, highly cytotoxic with in *vivo* antitumor activity and thus more likely to be applied in cancer therapy [Gunawardana, *et al.,* 1988]. The most promising candidates for immunosuppressive therapy among marine natural products are discodermolide isolated from *Discodermia* species (see Fig. 1.2) and microcolin A (see Fig. 1.3). The isolated pure natural product discodermolide exhibited potent suppressive activity in the murine two-way MLR and concanavalin A stimulation of splenocyte cultures. It also suppressed the proliferation of human peripheral blood lymphocytes at relevant concentrations (<80.6 μM). Studies on its mechanism of action are not conclusive at this time, but most importantly, however, is the fact that it appears to differ from that of cyclosporine A. It does not inhibit interleukin-2 (IL-2) production but appears to modulate the expression of the IL-2 receptor [Longley, *et al.,* 1991].

1.4. Phospholipase A_2 (PLA_2) inhibitors from marine organisms

Few human ailments are as painful as those involving inflammation. Arthritis, gout, psoriasis, bee stings and many chemically induced oedemas are all examples of inflammatory conditions that result in considerable pain and swelling of the affected tissues. The inflammatory response is mediated by the biosynthesis of eicosanoids, such as, leukotrienes, prostaglandins and thromboxanes from arachidonic acid, as well as other autocoids released locally in response to an irritant. Phospholipase A_2 (PLA_2) is an enzyme that specifically catalyses the hydrolysis of the ester at the sn-2 position of a phospholipid to produce a lysophospholipid and a free fatty acid. The release of arachidonic acid from the sn-2 position of membrane phospholipids provides the substrate for the biosynthesis of eicosanoids**.** Thus, compounds that inhibit PLA_2 activity have been considered potential therapeutic agents in the treatment of inflammation [Potts, *et al.,* 1992]. Manoalide, a sesterterpenoid isolated from the Indo-pacific sponge *Luffariella variabilis* (see Fig. 1.4) [De Silva, *et al.,* 1980] is by far the most well characterised PLA_2 inhibitor from marine natural sources. Shortly after its discovery, a pharmacological evaluation revealed that manoalide is a potent analgesic and anti-inflammatory agent. Manoalide inhibited chemically induced oedemas in the mouse ear assay but did not inhibit arachidonic acid induced inflammation**,** indicating that inflammation is inhibited prior to the release of arachidonic acid [Jacobs, *et al.,* 1985]. The finding led to the discovery that manoalide directly and irreversibly inhibits PLA_2 enzymes from bee and cobra venoms [Glaser, *et al.,* 1986]. The significance of inhibition of extracellular PLA_2 enzymes by manoalide, in terms of its anti-inflammatory properties, has been addressed in studies aimed at determining the in *vivo* pathways that might be affected by manoalide. Manoalide was shown to inhibit the stimulated release of arachidonic acid from activated murine macrophages [Mayer, *et al.,* 1988]. The drug has also been demonstrated to inhibit phospholipase C (PLC) and to block calcium channels in a variety of cell models [Potts, *et al.,* 1992].

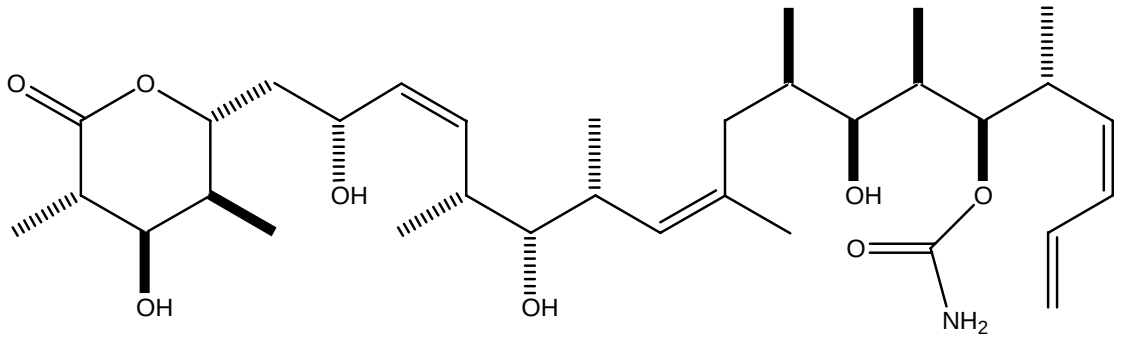

Fig. 1.2: Discodermolide

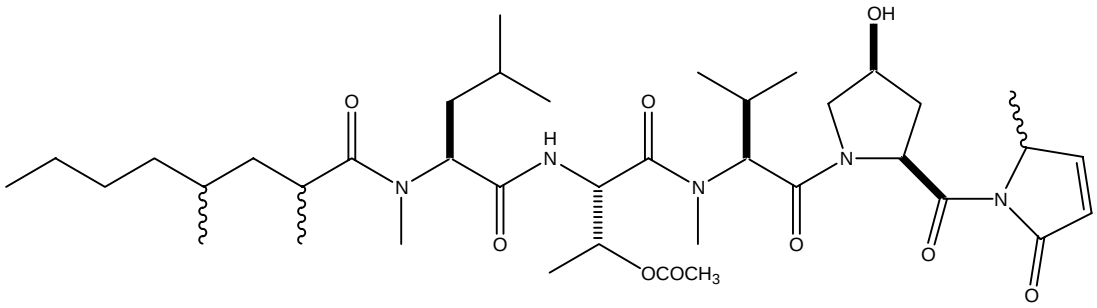

Fig. 1.3: Microcolin A

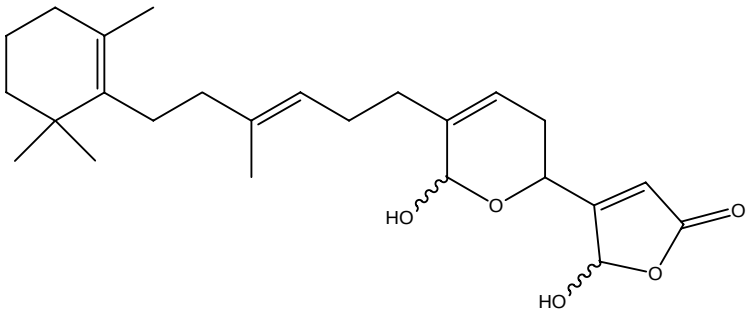

Fig. 1.4: Manoalide

1.5. Anatomy of Sponges

In the marine environment, sponges (phylum Porifera), are one of the most interesting groups of organisms regarding the accumulation of bioactive natural products [König, 1992; Sarma, *et al.,* 1993]. Sponges, or rather the skeletons of sponges, are mostly familiar from the few species in which the cleaned and dried meshwork of skeletal fibres is soft enough to be of use to humans. The rest of the more than 5,000 species of living sponges have skeletons that are too hard or scratchy, too filled with gritty particles, or too brittle and friable, to be commercially valuable. Sponges interest us for their many variations on a unique porous structure, from which the phylum "Porifera", the pore bearers takes its name [Pearse, *et al.,* 1987]. Unlike almost any other metazoans, sponges lack a nervous system and have no true musculature. Thus, locomotion is generally beyond them, and all species feed on food particles suspended in the water. No specialised reproductive, digestive, respiratory, sensory, or excretory organs are found in this group. Often, sponges are amorphous, asymmetrical creatures. In its simplest form, the typical sponge is a fairly rigid, perforated bag, whose inner surface is lined with flagellated cells. The empty space of this bag is called the spongocoel. The flagellated cells lining the spongocoel are called choanocytes (funnel cells), or collar cells in recognition of the cylindrical arrangement of the cytoplasmic extensions (collars) surrounding the proximal portion of each flagellum (Fig 1.5). The collars of sponge choanocytes are almost certainly homologous with those of protozoan choanoflagellates [Pechenik, 2000]. The porous nature of sponges makes them ideally suited for habitation by opportunistic crustaceans, various worms, etc. In addition to these macro-organisms, bacteria, blue-green algae and dinoflageliates are also observed in many species [Gerwick, *et al.,* 1992].

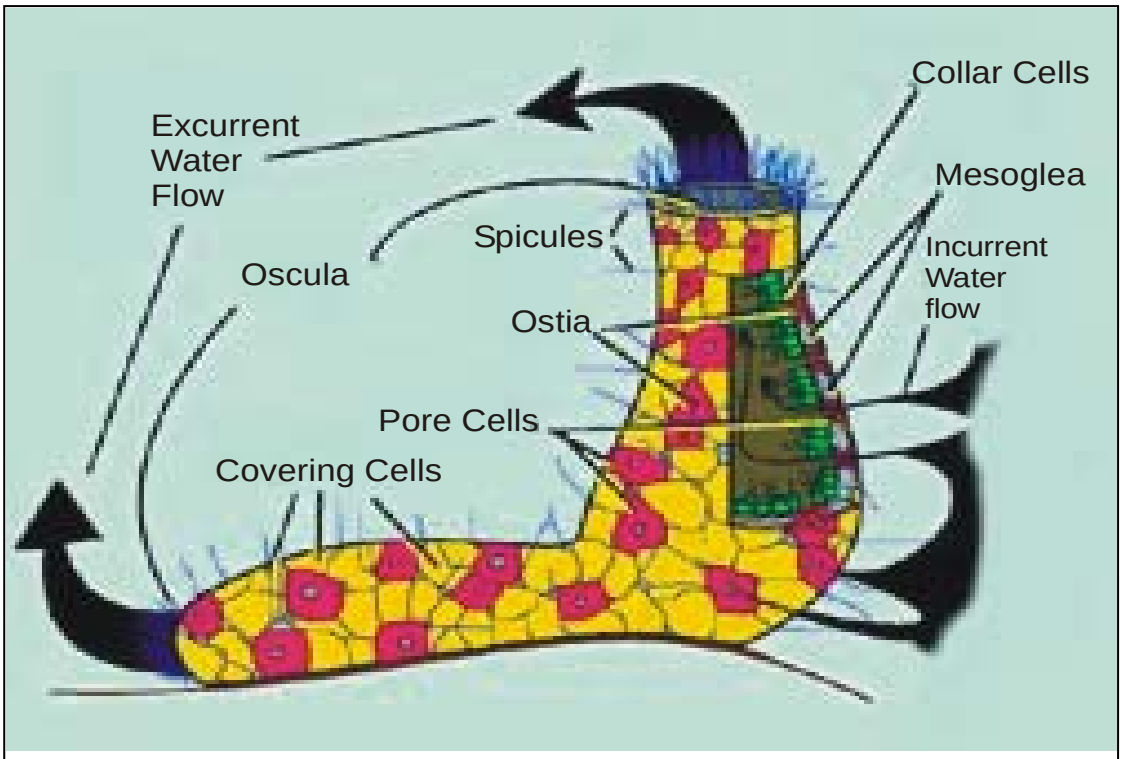

(a)

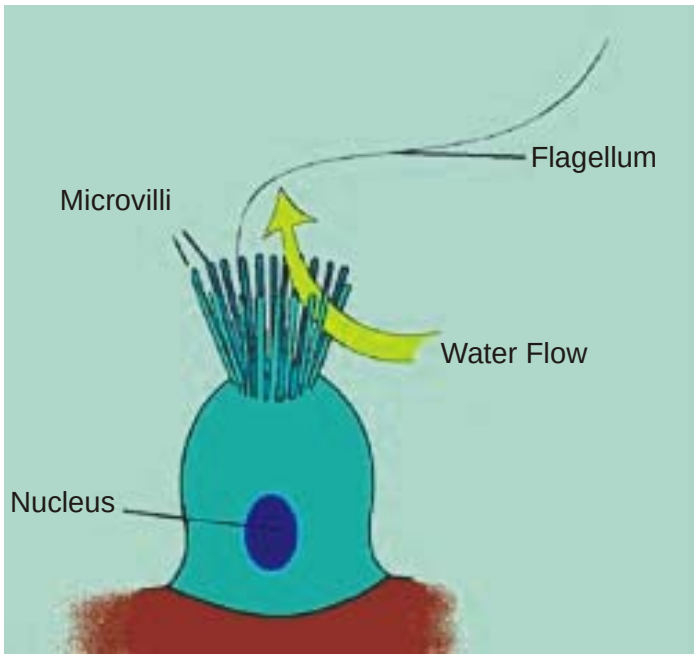

(b)

Fig. 1.5: a) Diagrammatic illustration of the body wall of a sponge

b) Detail of a choanocyte

It is generally assumed that the ecological success of sponges depends largely upon effective defence mechanisms that rely heavily on the accumulation of toxic or deterrent secondary compounds [Bakus, *et al.,* 1986; Sarma, *et al.,* 1993]. It is found that only a few fish species concentrate on sponges as their main diet [Randall, *et al.,* 1968]. This points out the ecological importance of these metabolites for the respective invertebrates and is corroborated by numerous studies which relate the accumulation of toxic natural products with their role as chemical defence to fight off potential predators (e.g. fishes) [Pawlik, *et al.,* 1995; Lindel, *et al.,* 2000] or to force back neighbours competing for space [Proksch, *et al.,* 1998; Proksch, 1999; McClintock, *et al.,* 2001]. The small number of fishes selecting sponges as their food source suggests that defensive properties of sponges, such as spicules (morphological defence) and noxious chemical substances (chemical defence), are highly effective in discouraging predation.

Most secondary products obtained from the sponges have been isolated from the whole body of the animals. It has been observed, however, that in some cases such as an unidentified maroon sponge, only the exterior tissues contained the deterrent substances [Burkholder, 1973].

1.6. Aim of the work

Sponges are among the well researched marine organisms primarily because of their size and abundance. 41% of discovered marine natural products have been isolated from sponges and hence they present an interesting source for the isolation of new compounds. This study is focused on the isolation of new or known metabolites from different sponge extracts which exhibit antibiotic or cytotoxic activities. These sponges were collected from either the Red Sea or Indonesia. Different chromatographic techniques were used to isolate the most biologically interesting compounds like TLC, CC, VLC, MPLC or semipreparative HPLC. Most of the isolated compounds were screened for antibiotic and cytotoxic activities. Antimicrobial activity was studied using the agar diffusion assay. Cytotoxicity was studied *in vitro* using different cell lines and with the brine shrimp (*Artemia salina*) lethality test.

2. Materials and Methods

2.1. Biological Materials

The sponges were collected off Aqaba, Red Sea (Jordan) or from the Baranglompo and Kapoposang islands in Indonesia. The sponges were collected by scuba or drop-off diving and voucher specimens were identified by Dr. Rob W.M. van Soest of the Zoological Museum, Amsterdam. The samples were frozen at -20 °C until workup. The freeze-dried samples were extracted with organic solvents and the resulting extracts were subjected to a series of biological assay for cytotoxicity, fungicidal and antibiotic activity.

2.1.1. *Erylus lendenfeldi*

The sponge *Erylus lendenfeldi* Thiele, 1903 (phylum Porifera, class Demospongiae, order Astrophorida, family Geodiidae), was collected in 2000 from the Gulf of Aqaba, Red Sea, Jordan at a depth of 32 ft. A voucher specimen has been deposited in the Zoological Museum, Amsterdam.

2.1.2. *Negombata corticata*

The sponge *Negombata corticata* Carter, 1879 (phylum Porifera, class Demospongiae, order Poecilosclerida, family Latrunculiidae), was collected in 2000 from the Gulf of Aqaba, Red Sea, Jordan at a depth of 32 ft. A voucher specimen has been deposited in the Zoological Museum, Amsterdam.

2.1.3. *Pseudoceratina purpurea*

The sponge *Pseudoceratina purpurea* (phylum Porifera, class Demospongiae, order Verongida, family Aplysinellidae) was collected in 1997 from Baranglompo island, Indonesia at a depth of 32 ft. A voucher specimen has been deposited in the Zoological Museum, Amsterdam under registration number ZMA POR. 17053, (see Fig. 2.1).

2.1.4. *Rhabdastrella globostellata*

The sponge *Rhabdastrella globostellata* Carter, (phylum Porifera, class Demospongiae, order Astrophorida, family Acorinidae) was collected in 1997 from Kapoposang island, Indonesia at a depth of 45 ft. It is shaped like a handball, hard and compressible, its external surface is red-brown with rounded protrusions. The internal is yellow in color. A voucher specimen has been deposited in the Zoological Museum, Amsterdam under registration number ZMA POR. 17166, (see Fig. 2.2).

Fig. 2.1: ***Pseudoceratina purpurea***

Fig. 2.2: ***Rhabdastrella globostellata***

2.2. Chemicals used

2.2.1. General laboratory chemicals

Agar-Agar	Merck
Anisaldehyde (4-methoxybenzaldehyde)	Merck
(-)-2- butanol	Merck
Chlorotrimethylsilane	Merck
Dimethylsulfoxide	Merck
Formaldehyde	Merck
L-(+) - Ascorbic acid	Merck
D- Glucose	Sigma
L- Glucose	Sigma
D- Galactose	Sigma
L- Galactose	Sigma
Nipagin A	Sigma
Hexamethyldisilazane	Merck
Hydrochloric acid	Merck
Potassium hydroxide	Merck
Pyridine	Merck
Concentrated sulfuric acid	Merck
Trifluroacetic acid (TFA)	Merck

2.2.2. Solvents

Acetone
Acetonitrile
Dichloromethane
Ethanol
Ethyl acetate
Hexane
Methanol
Petroleum ether

Solvents were purchased from the Institute of Chemistry, University of Düsseldorf. They were distilled prior to use and spectral grade solvents were used for spectroscopic measurements.

2.2.3. Chromatography

Pre-coated TLC plates (AluO, silica Gel 60 F254, layer thickness 0.2 mm	Merck
Pre-coated TLC plates (glass), RP-18, F254 S, layer thickness 0.25 mm	Merck
Silica Gel 60, 0.04-0.063 mm mesh size	Merck
Sephadex LH 20, 25-100 mm mesh size	Merck
HPLC Solvents:	
Methanol LiChrosolv HPLC	Merck
ortho-phosphoric acid 0.15%, pH 2.0 (prepared from ortho-phosphoric acid 85% p.a.)	Merck
Nanopure water	Barnstead

2.3. Equipment used

Balances	Mettler 200
	Mettler AT 250
	Mettler PE 1600
	Sartorius RC210P
Centrifuge	Kendro D-37520 osterde
Fraction collector	ISCO Cygnet
Freeze dryer	LYOVAC GT2, Pump TRIVAC D10E
Hot plates	Camag
Syringe	Hamilton 1701 RSN
Mill	Moulinex 354
Magnetic stirrer	Variomag Multipoint HP
Mixer	Braun
pH-Electrode	Inolab
	Behrotest PH 10-Set
Rotary Evaporator	Büchi Rotavap RE111
Drying ovens	Heraeus T 5050
Sonicator	Bandelin Sonorex RK 102
UV lamp	Camag (254 and 366 nm)

Vacuum desiccators	Savant Speed Vac SPD 111V Savant Refrigerator Vapour Trap RVT400, Pump Savant VLP80

HPLC equipment:

1. Gynkotek

Pump:	Gynkotek M40
HPLC Program:	Gynkosoft (v. 5.4)
Detector:	Gynkotek Photodiode Array Detector UVD 340
Autosampler:	Gynkotek Autosampler GINA 50
Printer:	NEC P60

II. Dionex

Pump:	Dionex P580A LPG
HPLC Program:	Chromeleon (V. 6.3)
Detector:	Dionex Photodiode Array Detector UVD 340S
Column thermostat:	STH 585
Autosampler:	ASI-100T

2.4. Chromatographic Methods

2.4.1. Thin layer chromatography (TLC)

TLC was performed on pre-coated TLC plates with Si gel 60 F_{254} (layer thickness 0.2 mm, E. Merck**,** Darmstadt, Germany**)** with either CH_2Cl_2:MeOH (95:5 and 9:1) for semi-polar compounds or Hexane:EtOAc (7:3) for non-polar compounds as mobile phases. TLC on reversed phase RP-18 F_{254} (layer thickness 0.25 mm, Merck, Darmstadt, Germany) was sometimes used for polar substances and using the different solvent systems of MeOH : water (9:1, 8:2, 7:3, 1:1). The compounds were detected from their UV absorbance at 254 and 366 nm or by spraying the TLC plates with anisaldehyde reagent followed by heating at 110 °C.

Anisaldehyde/H_2SO_4 Spray Reagent (DAB 10)

Anisaldehyde:	5 parts
Glacial Acetic Acid:	100 parts
Methanol:	85 parts
Conc. H_2SO_4	5 parts (added slowly)

The reagent was stored in an amber-coloured bottle and kept refrigerated until use. TLC was used to monitor the identity of each of the fractions and the qualitative purity of the isolated compounds. It was also utilised to optimise the solvent system that would be applied for column chromatography. TLC was also the suitable method to monitor the completion of a derivatization reaction.

2.4.2. Column chromatography

Crude extracts were subjected to repeated separation through column chromatography using appropriate stationary phases and solvent systems previously determined by TLC. The following separation systems were used:

a) stationary phase: Sephadex LH-20 (different sizes)
   solvent system: MeOH or MeOH: CH_2Cl_2 (1:1)

b) stationary phase: Silica gel (different sizes)
   solvent system: CH_2Cl_2: MeOH or Hexane:EtOAc.

c) stationary phase: RP-18 (different sizes)
   solvent system: MeOH: Nanopure water

2.4.3. Moderate pressure liquid chromatography (MPLC)

MPLC was used for the fast fractionation and even separation of crude extracts containing compounds with different polarity. The crude extract was dried and mixed with the silica gel (stationary phase) under pressure, while the silica gel was packed on special column under pressure also. The initial zone was then packed onto the tope of the column under pressure. The solvent system was then pumped under moderate pressure in a gradient manner starting from a non polar solvent such as n-Hexane until MeOH. The fractions were collected using a fraction collector.

2.4.4. Semi-preparative high pressure liquid chromatography (HPLC)

Semi-preparative HPLC was used for the isolation of pure compounds from fractions previously separated using column chromatography. Each injection consisted of 3 mg of the fraction dissolved in 1 mL of the solvent system. The solvent system was made of MeOH or acetonitrile and Nanopure water with or without 0.1% TFA, and pumped in gradient manner through the column at a rate of 5 mL/min. The eluted peaks were detected by the online UV detector were collected separately in Erlenmeyer flasks. The separation column (125 × 4 mm, i.d.) was pre-filled with Eurospher C-18 (Knauer, Berlin, Germany).

2.4.5. Analytical HPLC

Analytical HPLC was used to identify interesting peaks from extracts and fractions as well as to evaluate the purity of isolated compounds. The gradient used started with 10:90 [MeOH : nanopure H_2O (0.1% o-phosphoric acid) to 100% MeOH in 35 minutes. In some cases, special programs were used. Peaks were detected by UV-VIS diode array detector.

2.4.6. Vacuum liquid chromatography

Vacuum liquid chromatography (VLC) is a useful method for initial isolation procedure for large amounts of sample. The apparatus consists of a 500 mL sintered glass Büchner filter funnel with an inner diameter of 12 cm. Fractions were collected in Erlenmeyer flasks. Silica gel 60 was packed to a hard cake at a height of 5 cm under applied vacuum. The sample used was covered onto a small amount of silica gel using volatile solvents. The resulting sample mixture was then packed onto the top of the column. Step gradient elution with a non-polar solvent (Hexane) and increasing the amounts of a polar solvents (EtOAc, MeOH) gave successive fractions. The flow was produced by vacuum and the column was allowed to run dry after each fraction collected.

2.4.7. Gas chromatography

Gas chromatography was used to determine the nature and the absolute stereochemistry of sugar units (D or L forms). The sugar fraction of each compound was injected in the GC after hydrolysis and butanolysis using a special program. The samples were analyzed by comparison of the retention times with those observed for the authentic, commercially standards available.

2.4.8. Flash chromatography

Flash chromatography was used for rapid isolation of certain types of compounds which may be affected by light such as isomalabaricane tritepenoids. A silica gel GF_{254} pre-packed column was used and the sample was dissolved in a small volume of the solvent used. The resulting mixture was then packed onto the top of the column using special syringe. The flow rate was maintained by an air pump. The eluent was collected by a fraction collector and the separation was followed up by TLC.

2.5. Procedure for the isolation of secondary metabolites

2.5.1. Isolation of secondary metabolites from the sponge *Erylus lendenfeldi*

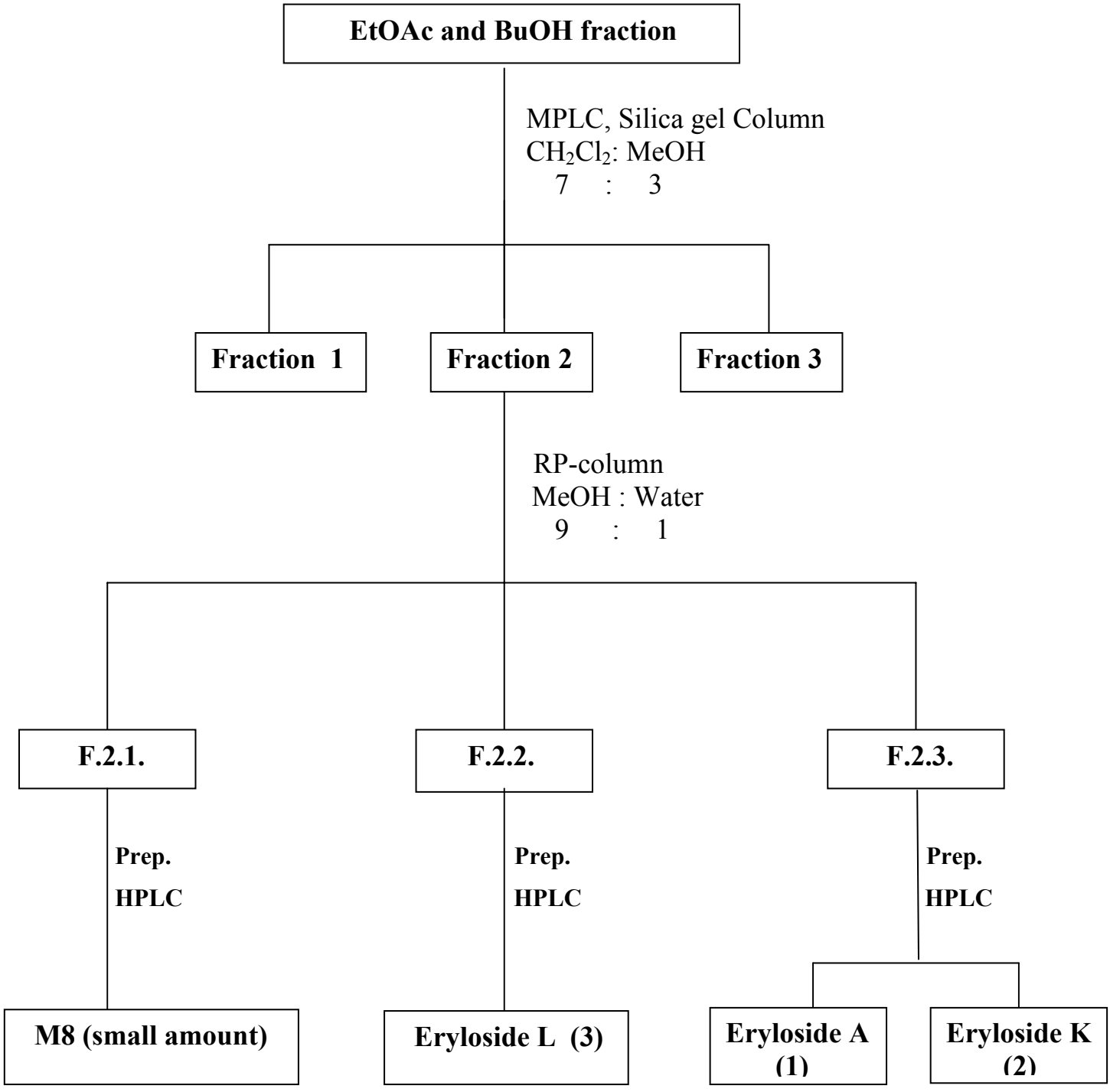

2.5.2. Isolation of secondary metabolites from the sponge *Negombata corticata*

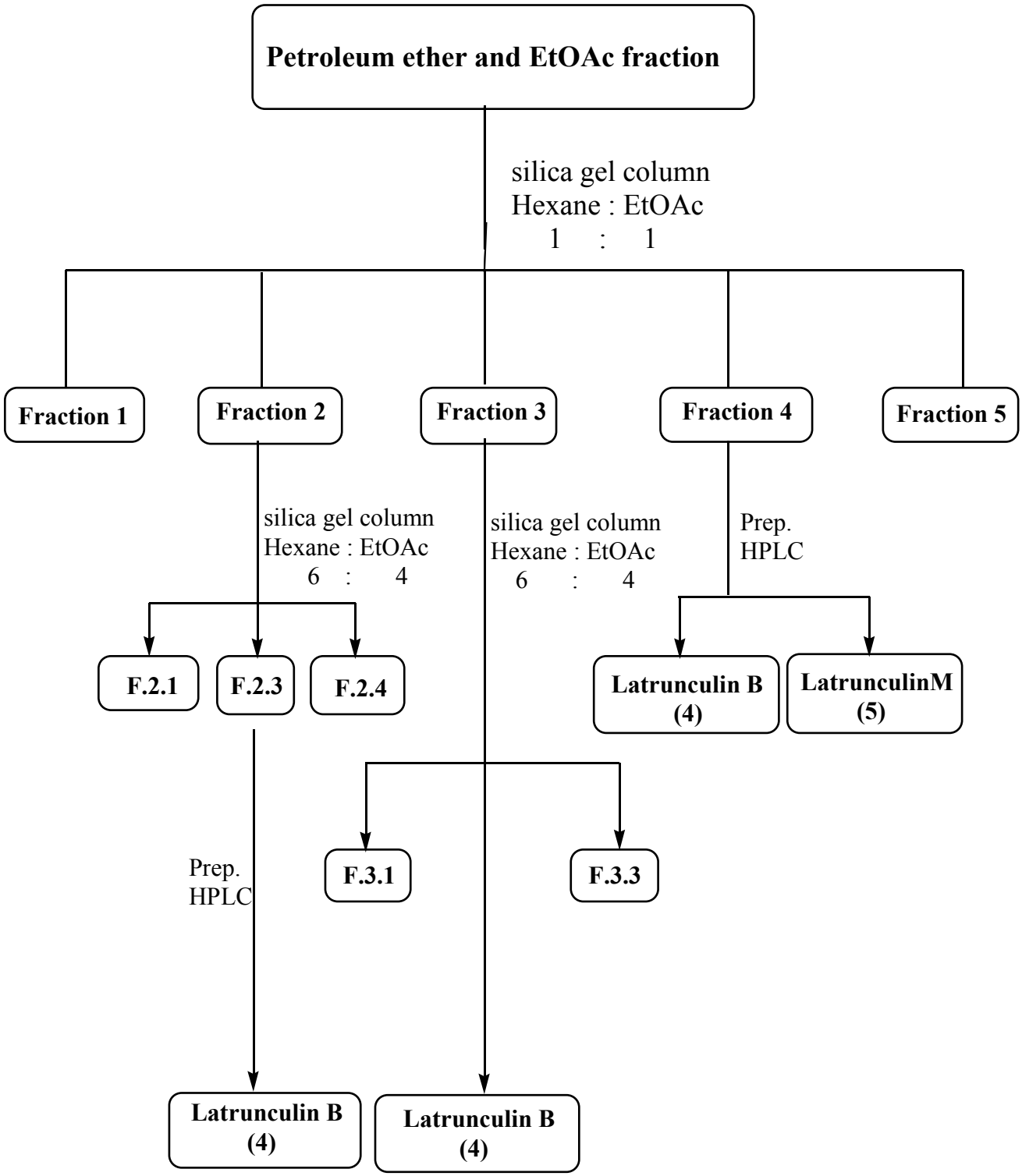

2.5.3. Isolation of secondary metabolites from the sponge *Pseudoceratina purpurea*

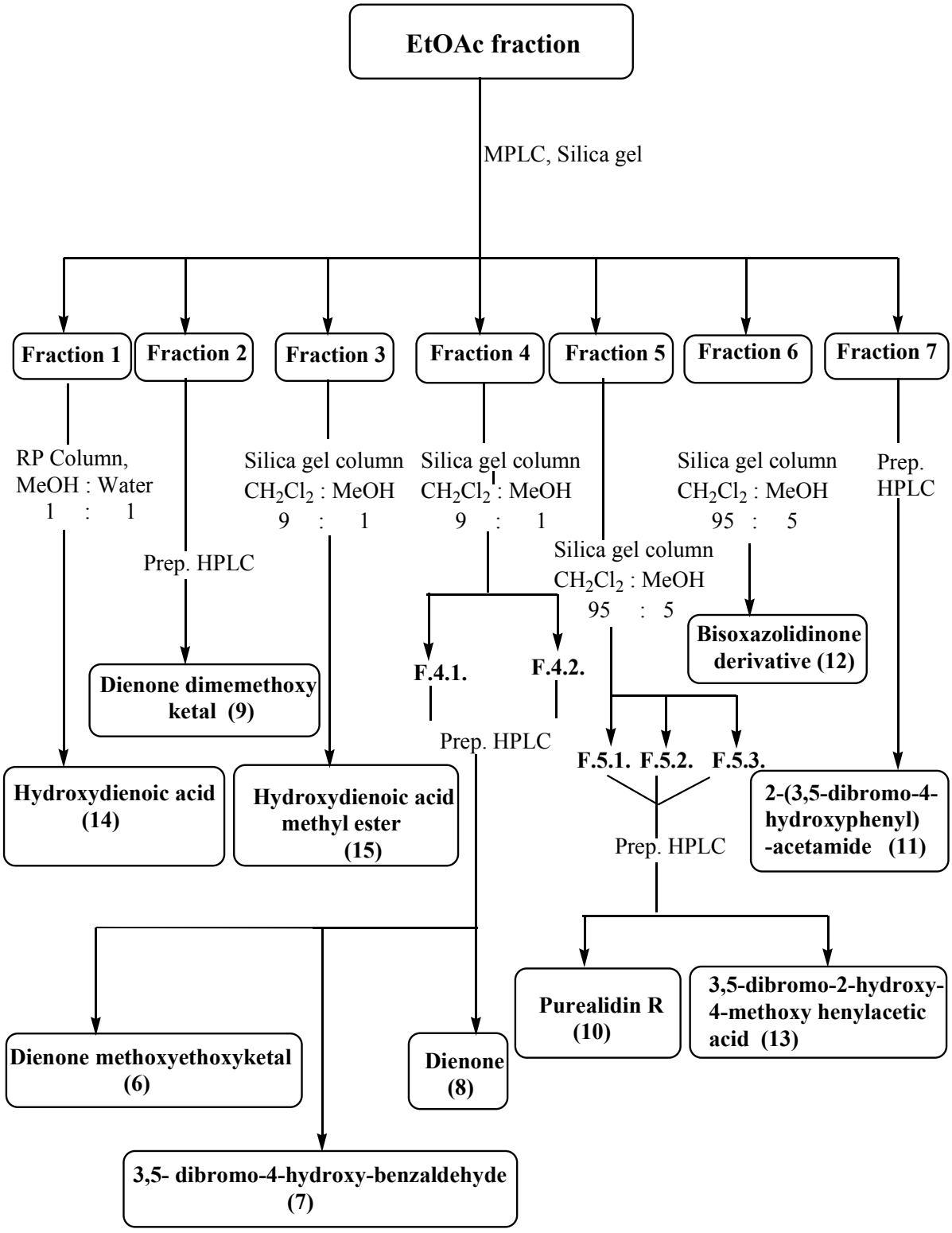

2.5.4 Isolation of secondary metabolites from the sponge *Rhabdastrella globostellata*

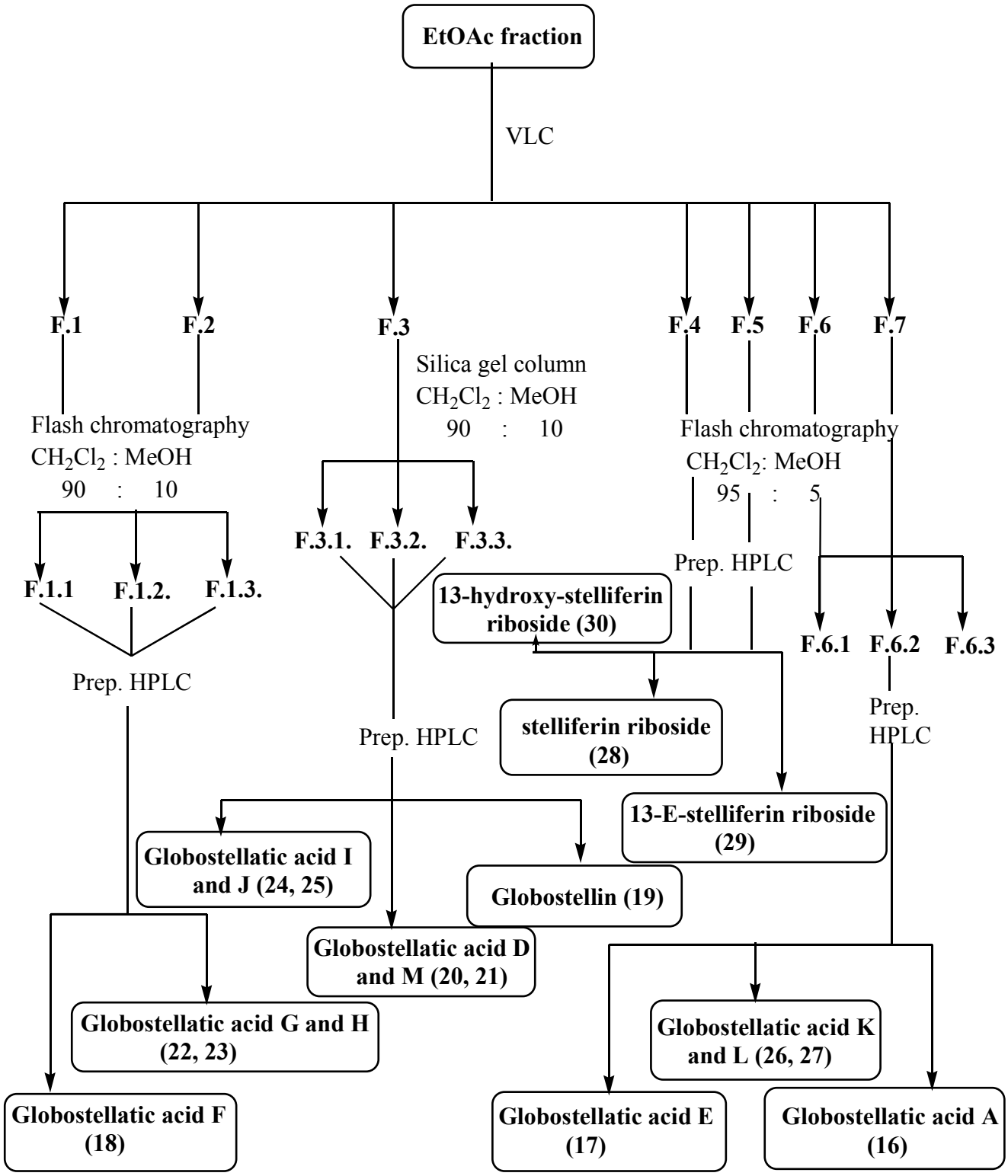

2.6. Structure elucidation of the isolated secondary metabolites

2.6.1. Mass spectrometry (MS)

Low resolution MS. Low resolution mass spectra were measured by EI and FAB-MS on a Finnigan MAT 8430 mass spectrometer. Measurements were done by Dr. Peter Tommes, Institute of Anorganische and Struktur Chemie, HHU Düsseldorf.

EIMS (electron impact mass spectroscopy) analysis involves vaporizing a compound in an evacuated chamber and then bombarding it with electrons having 25.80 eV (2.4-7.6 MJ/mol) of energy. The high energy electron stream not only ionises an organic molecule (requiring about 7-10 eV) but also causes extensive fragmentation (the strongest single bonds in organic molecules have strengths of about 4 eV). The advantage is that fragmentation is extensive, giving rise to a pattern of fragment ions which can help to characterise the compound. The disadvantage is the frequent absence of a molecular ion.

FABMS (fast atom bombardment) was the first widely accepted method that employs energy sudden ionization. FAB is useful for compounds, especially polar molecules, unresponsive to either EI or CI mass spectrometry. It enables both non-volatile and high molecular weight compounds to be analyzed. In this technique, a sample is dissolved or dispersed in a polar and relatively non-volatile liquid matrix, introduced into the source on a copper probe tip. Next, this matrix is bombarded with beam of atoms of about 8 Kev. It uses a beam of neutral gas (Ar or Xe atoms) and both positive and negative ion FAb spectra can be obtained.

High resolution MS. High resolution is achieved by passing the ion beam through an electrostatic analyser before it enters the magnetic sector. In such a double focusing mass spectrometer, ion masses can be measured with an accuracy of about 1 ppm. With measurement of this accuracy, the atomic composition of the molecular ions can be determined. HREIMS was measured at the national research of natural and biomimetic drugs, Beijing Medical University, China and HKI für Naturstofforschung, Jena.

ESIMS (electron spray ionization) is a method for ejecting ionized molecules from a solution by creating a fine spray of highly charged droplets in the presence of a strong electric field. This type of ionization is highly conductive to the formation of multiply charged molecules.

LC/MS. High pressure liquid chromatography (HPLC) is a powerful method for the separation of complex mixtures, especially when many of the components may have similar polarities. If a mass spectrum of each component can be recorded as it elutes from the LC column, quick characterisation of the components is greatly facilitated. Usually, ESIMS (electron spray ionisation mass spectrometry) is interfaced with LC to make an effective on-line LC/MS. HPLC/ESI-MS was carried out using a Finnigan LC QDECA mass spectrometer connected to a UV detector. The samples were dissolved in water/MeOH mixtures and injected to HPLC/ESI-MS set-up. HPLC was run on a Nucleosil C-18 reversed-phase column. Measurements were done at Institute of Pharmaceutical Biology, HHU Düsseldorf. For standard MS/MS measurements, a gradient of 10:90 (acetonitrile: nanopure H_2O (0.1% HCOOH) to 100 % acetonitrile in 35 minute was used.

2.6.2. Nuclear magnetic resonance spectroscopy (NMR)

NMR measurements were done at the Institut für Anorganische Chemie und Makromolekulare Chemie of HHU Düsseldorf. ^{1}H and ^{13}C spectra were recorded at 300º K on Bruker DPX 300, ARX 400, 500 or AVANCE DMX 600 NMR spectrometers. All 1D and 2D spectra were obtained using the standard Bruker software. The samples were dissolved in different solvents (i.e. DMSO-d_6, $CDCl_3$, and CD_3OD), the choice of which was dependent on the solubility of the samples. Residual solvent signals were used as internal standards (reference signal). The observed chemical shift (δ) values were given in ppm and the coupling constants (*J*) in Hz.

2.6.3. Optical activity

Optical rotation was determined on a Perkin-Elmer-241 MC polarimeter by measuring the angle of rotation at the wavelength of 546 and 579 nm of a mercury vapour lamp at room temperature (25 ºC) in a 0.5 mL cuvette with 0.1 dm path length. The specific optical rotation was calculated using the expression:

$$[\alpha]_D^{20} = \frac{[\alpha]_{579} \times 3.199}{4.199 - \frac{[\alpha]_{579}}{[\alpha]_{546}}}$$

With $[\alpha]^{20}_{D}$ = the specific rotation at the wavelength of the sodium D-line, 589 nm, at a temperature of 20 ºC.

$[\alpha]_{579}$ and $[\alpha]_{546}$ = the optical rotation at wavelengths 579 and 546 nm, respectively, calculated using the formula:

$$[\alpha]_{\lambda} = \frac{100 \times \alpha}{I \times c}$$

Where α = the measured angle of rotation in degrees,

I = the length in dm of the polarimeter tube,

c = the concentration of the substance expressed in g/100 mL.

2.7. Acid Hydrolysis and GC Analysis

A solution of eryloside A (1.5 mg) was hydrolysed by treatment with 3 N HCl and stirred at 80 °C for about 5 h. The solution was concentrated using N_2. The residue was re-dissolved in (-)-2- butanol (0.5 mL) and one drop of trifluoroacetic acid. The solution was transferred to an ampoule while was sealed and heated at 130 °C in an oven overnight until complete butanolysis. The solution was concentrated to dryness in a vacuum evaporator and then connected to the freeze dryer overnight until complete dryness. The residue was then treated with hexamethyldisilazane-chlorotrimethylsilane-pyridine (0.1 mL, 1 : 1 : 5) for 30 min at room temperature. The solution was then centrifuged and the supernatant (1 μL) was analysed by GC on HP-5 column. The injectionport and detector temperatures were 200 °C and 220 °C, respectively. The temperature gradient was programmed as linear increase from 135 °C to 200 °C at 1 °C/min. Four Peaks of the hydrolysate were detected at 37.49, 40.11, 42.43, 43.49 minutes, which was in agreement with the four peaks obtained for authentic D-galactose at 37.50, 40.15, 42.44, 43.45 minutes treated simultaneously in the same manner, [Leontein, *et al.;* Gerrit, *et al.,* 1977].

2.8. Biological Test Methods

2.8.1. Brine-shrimp assay

This technique is an *in vivo* lethality test with a tiny crustacean, the brine shrimp (*Artemia salina* Leach). It has been previously utilised in various bioassay systems including the analysis of pesticide residues, mycotoxins, stream pollutants, anaesthetics, dinoflagellate toxins, morphine-like compounds, toxicity of oil dispersants, cocarcinogenicity of phorbol esters and toxicants in marine environments [Meyer, *et al.,* 1982]. This test takes into account the basic premise that pharmacology is simply toxicology at a lower dose, and that toxic

substances might indeed elicit, at a lower non-toxic dose, interesting pharmacological effects. The procedure determines LC_{50} values in μg/mL of active compounds and extracts in the brine medium.

Sample preparation. The test samples were dissolved in a suitable organic solvent and the appropriate amount was transferred to a 10 mL sample vial. For crude extracts, 0.5 μg of the compounds were used and various concentrations of the pure compound. The samples were then dried under nitrogen and reconstituted with 20 μL DMSO. Control vials containing the same amount of DMSO were also prepared.

Hatching of the eggs. Brine shrimp eggs (Dohse, Aquaristik GmbH, Bonn, Germany) were hatched in a small tank filled with artificial sea water which was prepared with a commercial salt mixture (Sera Sea-Salt, Aquaristik GmbH, Bonn, Germany) and distilled water. After 48 h, 20 nauplii were collected by pipette (counted macroscopically in the stem of the pipette against a lighted background) and transferred into each test sample vial. Artificial sea water was then added to make 5 mL. The vials were maintained under illumination. Survivors were counted, with the aid of a magnifying glass after 24 hours and the percent deaths at each dose and control were determined. The LC_{50} values were determined using the probit analysis method. The LD_{50} was derived from the best fit line obtained by linear regression analysis.

2.8.2. Fish-feeding assay

In the experiment with *Blennius sphinx* fishes, food pieces treated with sponge extracts were given to the fishes at the same time as untreated food pieces. If the fishes showed a preference to the untreated food pieces, this meant the extract had fish feeding deterrent activity.

In the natural habitat some sponges show self defence against predators with the aid of their secondary metabolites, due to this the extracts have been tested in their natural concentration as present in the sponge. The amount of extract in 10 mL sponge was determined, by the following equation:

$$\text{Density} = \frac{\text{Wet weight}}{\text{Volume}}$$

The preparation of food pieces

The total extract was dissolved in a certain volume of suitable solvent and a volume equal to 10 mL sponge was calculated. 1.053 g food granules were grinned to a fine powder in a mortar and put in round bottom flask, and then the volume of the extract solution (10 mL sponge) was added, mixed well and evaporated to dryness. At the end the food/ extract mixture was detached from the wall of the flask by spatula (Flask A).

0.189 g agar was weighed into an Erlenmeyer flask, then 9.5 mL distilled water was added. The flask was closed with aluminium foil, boiled on a water bath for four minutes and then cooled to 55 ºC (Flask B).

The content of the flask B was added to the sponge extract and mixed well to give the treated food (Experiment).

The untreated food was prepared analogous to the previous steps, but instead of the extract, the respective amount of pure solvent was used (blank).

Both types of food (experiment and blank) were poured into a frame, this frame containing two openings 2.5 x 25 cm. Under the frame there was a network and plastic foil. One of the openings was filled with experiment and the other was filled with blank, both were distributed to yield 2 mm thickness. After cooling of the agar the frame was removed and the food remained on the network. Six pieces were cut from blank and experiment, each 10 squares wide. Each of the blank and the experiment diet was attached to metallic body to sink in the aquarium.

Fish feeding experiment

Six food bands were put in the aquarium at the same time. The food pieces were observed until one third of the food in each band had been consumed. The food free squares were counted and the percentage of eaten food from both experiment and blank were calculated.

$$\text{Percentage of eaten food from experiment} = \frac{e \times 100}{t}$$

$$\text{Percentage of eaten food from blank} = \frac{b \times 100}{t}$$

e = number of food free squares from experiment

b = number of food free squares from blank

t = total number of food free squares (for experiment and blank).

The fishes used in this experiment were collected from the Mediterranean Sea near Elba Island, Italy.

2.8.3. Antibacterial activity

Microorganisms. Crude extracts and the isolated pure compounds were tested for activity against the following standard strains: gram-positive bacteria *Bacillus subtilis* **168** and *Staphylococcus aureus* **ATCC 25923**, gram-negative bacteria *Escherichia coli* **ATCC 25922** and *Escherichia coli* **HB 101**.

Culture preparation. The agar diffusion assay was performed according to the Bauer-Kirby-Test (DIN 58940). Prior to testing, a few colonies (3 to10) of the organism to be tested were subcultured in 4 ml of tryptosesoy broth (Sigma, Germany) and incubated for 2 to 5 h to produce a bacterial suspension of moderate cloudiness. The suspension was diluted with sterile saline solution to a density visually equivalent to that of a $BaSO_4$ standards, prepared by adding 0.5 ml of 1% $BaCl_2$ to 99.5 ml of 1% H_2SO_4 (0.36 N). The prepared bacterial broth was inoculated onto Müller-Hinton-Agar plates (Difco, USA) and dispersed by means of sterile beads.

Agar diffusion assay. For screening, aliquots of the test solution were applied to sterile filter-paper discs (5 mm diameter, Oxoid Ltd.) to give a final disc loading concentration of 500 μg for crude extracts and various concentrations (50, 25, 10, 5 and 1μg/disk) for pure compounds. The impregnated discs were placed on agar plates previously seeded with the selected test organisms, along with discs containing solvent blanks. The plates were incubated at 37 ˚C for 24 h. Antimicrobial activity was recorded as the clear zone of inhibition surrounding the disc (diameter measured in mm).

2.8.4. Cytotoxicity test

Cytotoxicity tests were carried out by both Dr. Klaus Steube of DSMZ (Deutsche Sammlung von Mikroorganismem und Zellkulturen GmBH, Braunschweig, Germany) and Prof. Dr. W.E.G. Müller (Mainz University, Germany).

Human leukemia cell lines used by Dr. Steube were U-937 [Sundstrom, *et al.,* 1976], JURKAT [Schneider, *et al.,* 1977] and THP-1 [Tsuchiya, *et al.,* 1980]. On the other hand, cancer cells used by Dr. Müller were L5178Y, HELA, and PC12.

Leukemia cell lines as U-937, JURKAT and THP-1 were grown in plastic flasks (Nunc, Wiesbaden, Germany). All cultures were propagated using standardized media supplemented with 10-20% heat-inactivated fatal bovine serum and were cultivated at 37 °C in a humidified atmosphere containing 5% CO_2.

The freeze-dried compounds were dissolved in EGMME (ethylene glycol monomethyl ether) or DMSO, diluted in RPM1-1640 culture medium and stored frozen at -20 °C. At the final dilution used in the experiments, the EGMME/DMSO concentration was 0.1%.

For the experiments, exponentially growing cells (viability of >90% as measured by trypan blue exclusion) were harvested, washed and re-suspended in fresh medium at a final concentration ranging between 2 and 4 x 10^5 cells/mL (depending on the cell line). Total cell number and viability were determined in a cell counting chamber after staining the cells with trypan blue. Aliquots of 90 µL were seeded out into 96-well flat-bottom culture plates (Nunc, Wiesbaden, Germany). Ten mL of medium with the solvent EGMME/DMSO or the different concentrations of the test compound were added. After 48 h incubation period, the extent of cytotoxicity was evaluated by the MTT assay or by the Thy assay. In the latter, cytotoxicity was determined by incorporation of [^{3}H] thymidine. Radioactive incorporation was carried out for the last 3 h of the 48 h incubation period. One µCi of [methyl-^{3}H] thymidine (Amersham-Buchler, Braunschweig, Germany; specific activity 0.25 mCi/µmol) was added in a 20µL volume to each well. Cells were harvested on glass fibre filters with a multiple automatic sample harvester, and radioactivity was determined in a liquid scintillation count (1209 Rackbeta, LKB, Freiburg, Germany).

The cytotoxicity against L5178Y mouse lymphoma cells, Hela cervix carcinoma cells, and PC12 brain tumour cells of the rats was determined using the microculture tetrazolium (MTT) assay, and compared to that of untreated controls [Carmichael, *et al.,* 1987]. Of the test samples, stock solutions in ethanol 96% (v/v) were prepared. Exponentially growing cells were harvested, counted and diluted appropriately. Of the cell suspension, 50 µL containing 3750 cells were pipetted into 96-well microtiter plates. Subsequently, 50 µL of a solution of

the test samples containing the appropriate concentration was added to each well. The concentration range was 3 and 10 µg/mL. The small amount of ethanol present in the wells did not affect the experiments. The test plates were incubated at 37 °C with 5% CO_2 for 72 h. A solution of 3-(4,5-dimethylthiazol-2-yl)-2,5-diphenyltetrazolium bromide (MTT) was prepared at 5 mg/mL in phosphate buffered saline (PBS; 1.5 mM KH_2PO_4, 6.5 mM Na_2HPO_4, 137 mM NaCl, 2.7 mM KCl; pH 7.4) and from this solution, 20 µL was pipetted into each well. The yellow MTT penetrates the healthy living cells and in the presence of mitochondrial dehydrogenases, MTT is transformed to its blue formazan complex. After an incubation period of 3 h 45 min at 37 °C in a humidified incubator with 5% CO_2, the medium was centrifuged (15 min, 20 °C, 210 x g) with 200 µL DMSO, the cells were lysed to liberate the formed formazan product. After thorough mixing, the absorbance was measured at 520 nm using a scanning microtiter-well spectrophotometer. The colour intensity is correlated with the number of healthy living cells.

Cell survival was calculated using the formula:

$$\text{Survival (\%)} = 100 \times \frac{\text{(absorbance of treated cells - absorbance of culture medium)}}{\text{(absorbance of untreated cells - absorbance of culture medium)}}$$

All experiments were carried out in triplicates and repeated three times. As controls, media with 0.1% EGMME/DMSO were included in the experiments.

3. Results

3.1. Isolated compounds from the sponge *Erylus lendenfeldi*

Erylosides are terpene glycosides possessing either steroidal or pentasterol aglycones with two or more sugar moieties which have been isolated from several species of the genus *Erylus*. These include erylosides A and B, C and D which were isolated from different species of the genus *Erylus* [Carmely, *et al.,* 1989; Valeria, *et al*., 1992], eryloside E from *Erylus goffrilleri* [Gulavita, *et al*., 1994], eryloside F from *Erylus formosus* [Stead, *et al*., 2000] and erylosides G-J from *Erylus nobilis* [Jongheon, *et al*., 2001], (see Fig 3.1). A new neuraminidase inhibitory triterpenoidal saponin, nobiloside was also isolated from the marine sponge *Erylus nobilis* [Takada, *et al.,* 2002]. From the Caribbean sponge *Erylus formosus* a triterpene tetrasaccharide, formoside has been isolated [Jaspars, *et al*., 1994]. In addition to the previous, three cytotoxic glycolipids have been isolated from another species of the genus *Erylus* [Goobes, *et al*., 1996] and a new IL-6 receptor antagonist, erylusamine B has been isolated from *Erylus placenta* [Sata, *et al*., 1994].

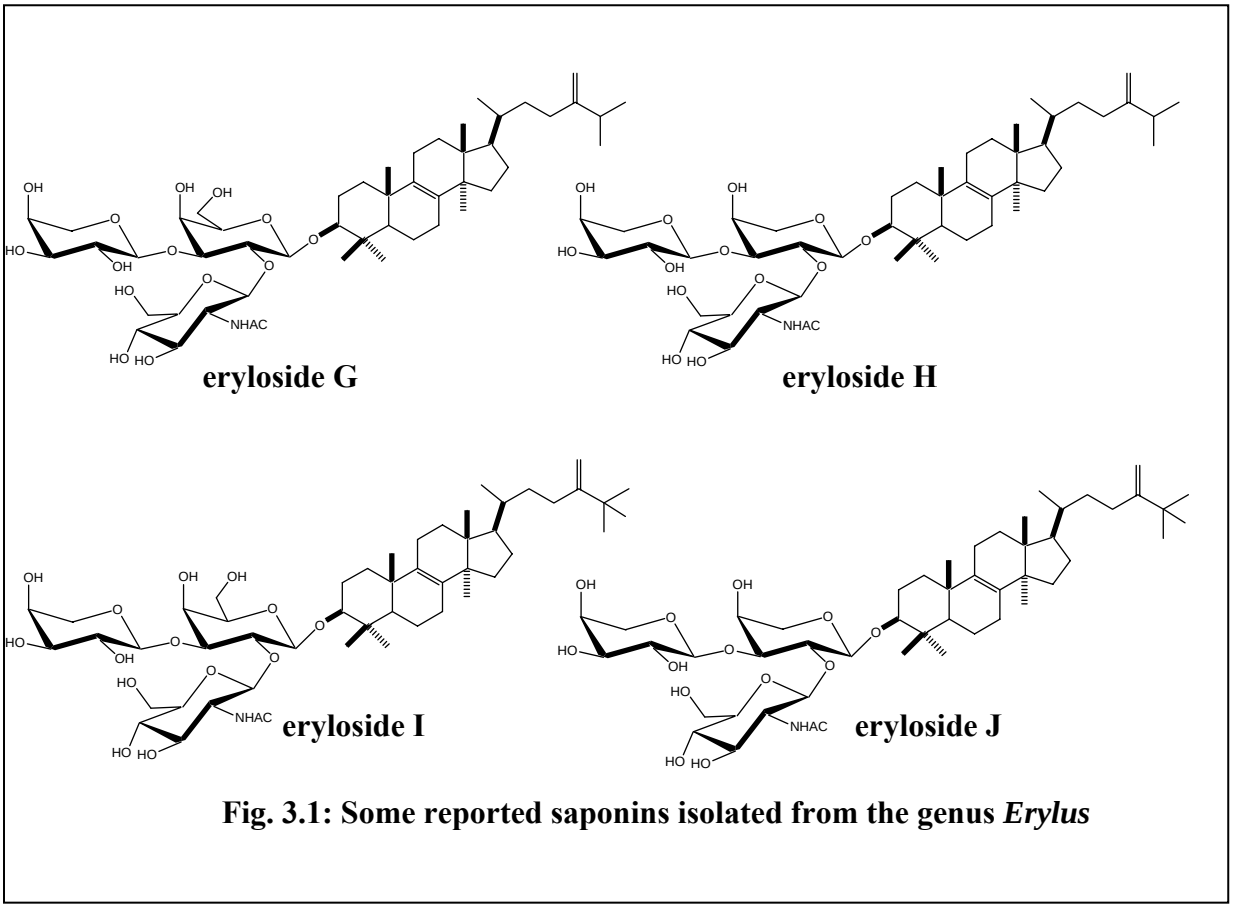

Fig. 3.1: Some reported saponins isolated from the genus *Erylus*

Screening of the extracts of collected sponges from the Red Sea in the fish feeding bioassay revealed that both *Erylus lendenfeldi* and *Negombata corticata* had a strong deterrent activity (see Fig 3.2). Chemical investigation of the ethyl acetate and butanol fractions of *Erylus lendenfeldi* yielded the known steroidal saponin eryloside A in addition to two new steroidal saponins, eryloside K and L.

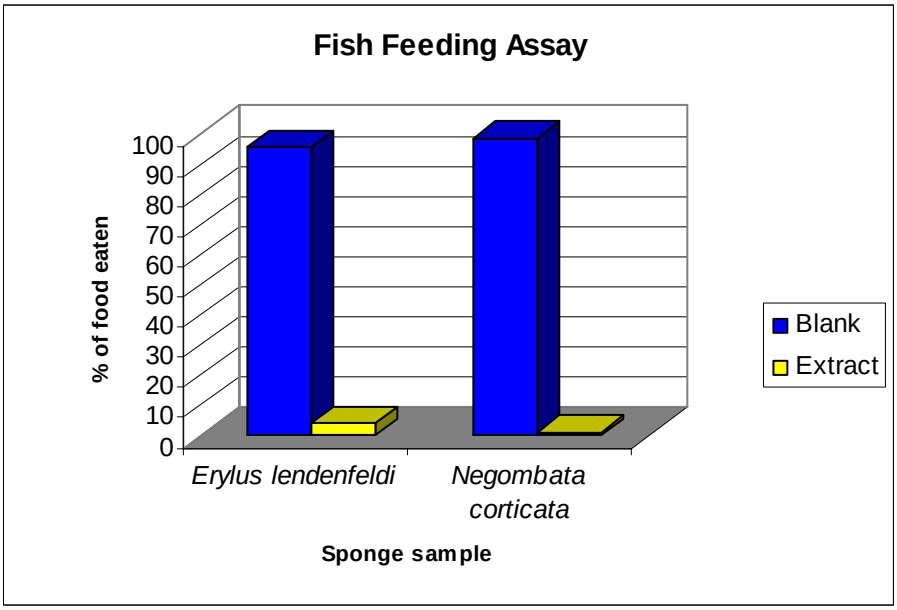

Fig. 3.2: Fish feeding assay of some Red Sea sponges

3.1.1. Eryloside A (1, known compound)

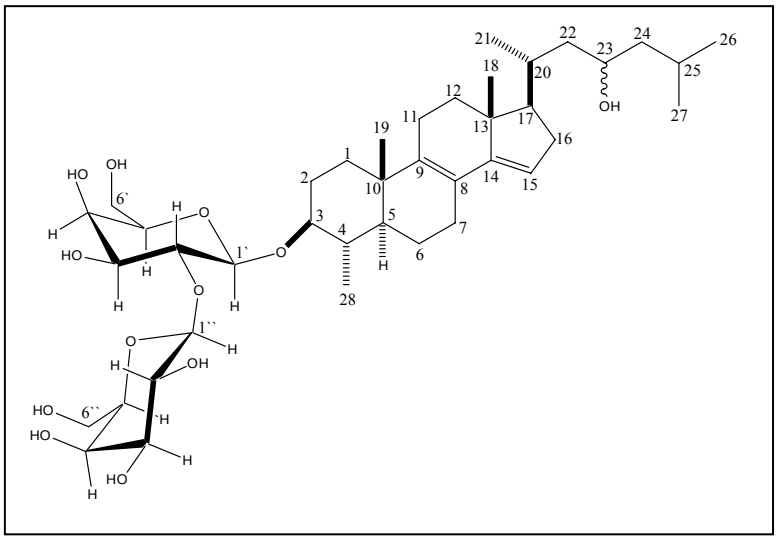

Eryloside A (**1**) was obtained as white amorphous powder, $[\alpha]_D^{20}$ +11 (*c* = 0.3, MeOH); UV (MeOH) λ_{max} 249 nm. The negative HRESIMS showed a pseudomolecular ion peak at m/z 737.4867 $[M - H]^-$ (100); (see Fig 3.3). This molecular weight in conjunction with the 1D and 2D NMR data is compatible with the molecular formula $C_{40}H_{66}O_{12}$. In the ^1H NMR and COSY spectra of compound **1** (see Table 3.1 and Fig 3.4) the presence of a number of resonances between 3.00 and 5.50 ppm, two anomeric protons (4.48 ppm, d, *J* = 7.7 Hz and 4.60 ppm, d, *J* = 7.8 Hz) and six methyl groups at the range from 0.90 to 1.31 ppm suggested that compound **1** is a steroidal glycoside with two sugar moieties. This was also confirmed from the ^{13}C NMR and DEPT experiment (see Fig. 3.5) which revealed the presence of 40 carbons, 28 of which belong to the aglycone and 12 carbons for the two sugar moieties. The aglycone carbons include six methyls, 9 methylenes, 8 methines and 5 quaternary carbons (see Table 3.1). Comparison of the NMR data and the molecular weight of compound **1** with those of the previously reported steroidal saponins isolated from the genus *Erylus* in combination with a careful inspection of the COSY and HMBC spectra allowed for a complete assignment of all signals. Compound **1** is identical with the known compound eryloside A [Carmely, *et al*., 1989].

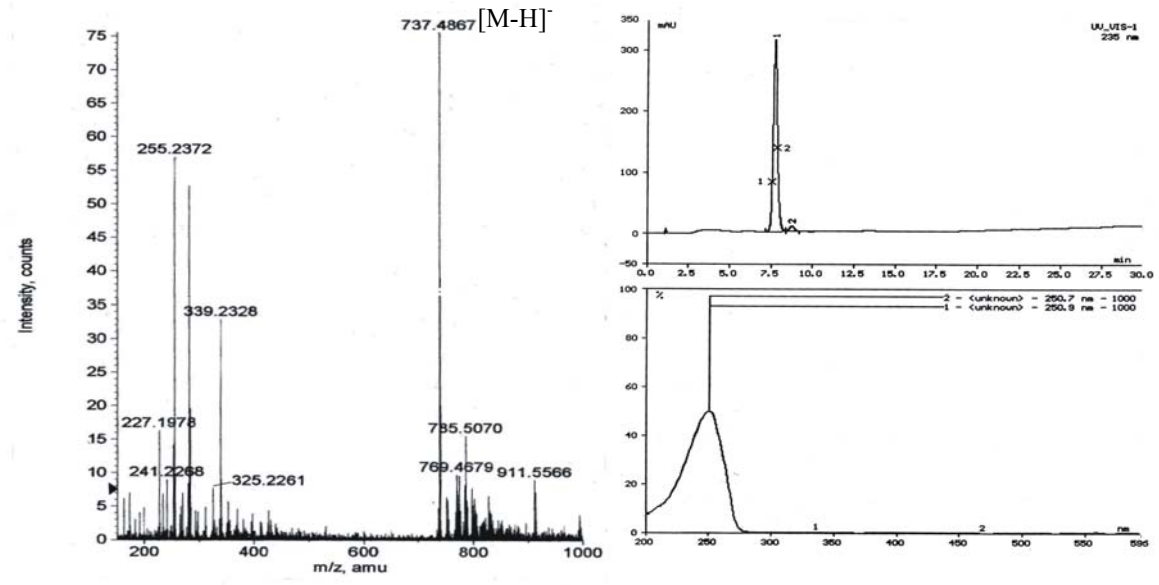

HREIMS **UV**

Fig. 3.3: UV and HREIMS spectra of compound 1

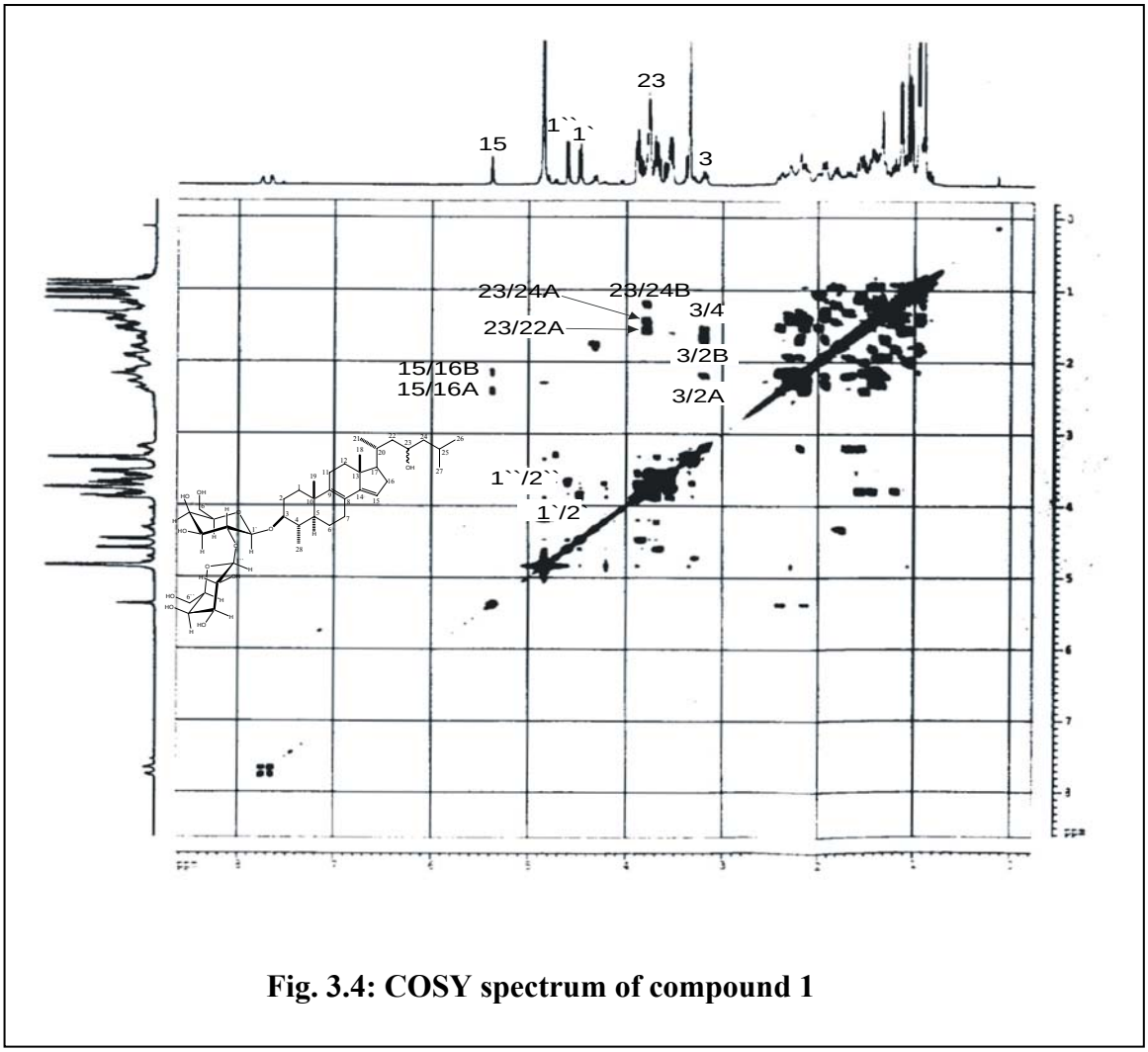

Fig. 3.4: COSY spectrum of compound 1

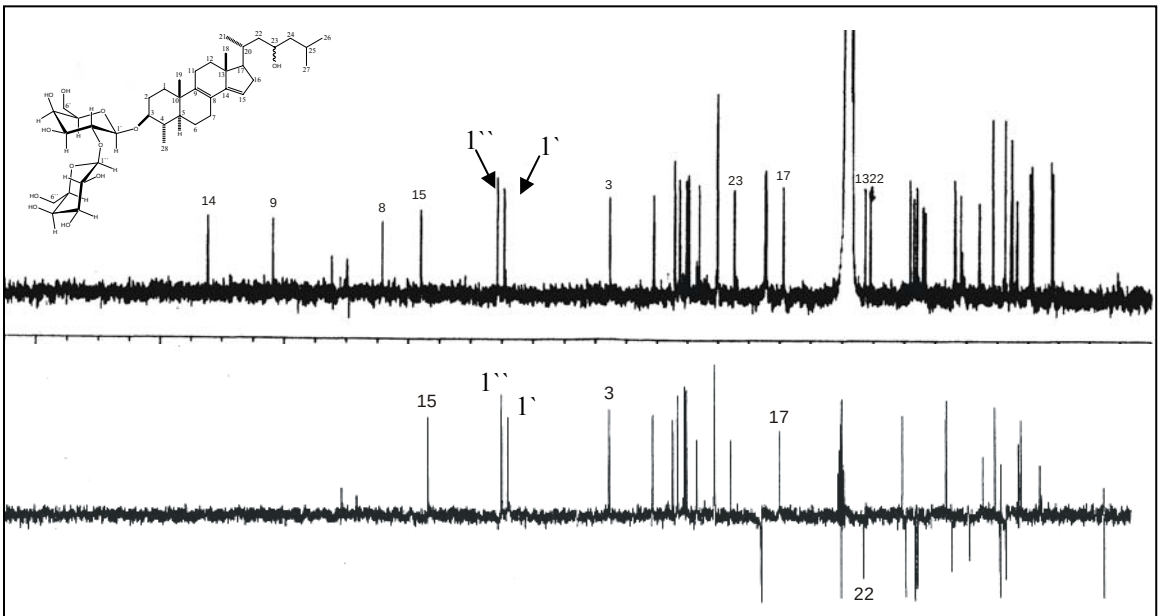

F ig. 3.5: ^{13}C NMR (top) and DEPT spectra (bottom) of compound 1

3.1.2. Eryloside K (2, new compound)

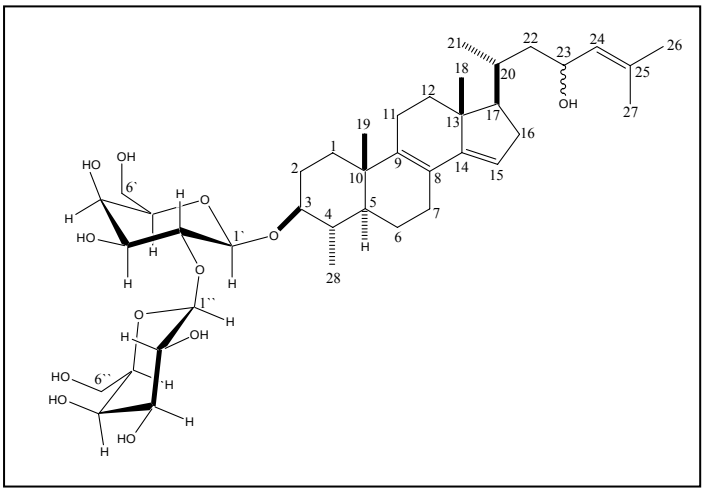

Eryloside K (**2)** was obtained as white amorphous powder (1.8 mg); $[\alpha]_D^{20}$ +6 (*c* = 0.2, MeOH), UV (MeOH) λ_{max} 249 nm (see Fig. 3.6). The negative HRESIMS showed a pseudomolecular ion peak at *m/z* 735.5121 $[M - H]^-$. This molecular weight in conjunction with the 1D and 2D NMR data is compatible with the molecular formula $C_{40}H_{64}O_{12}$. ^{1}H NMR and COSY experiment of **2** (see Fig. 3.7) revealed that it is closely related to eryloside A. Detailed comparison of ^{1}H NMR and COSY spectra of compound **2** with that for **1** (see Table 3.1) revealed an additional olefinic proton at 5.22 ppm suggesting the presence of an additional double bond which is in compatible with its molecular weight. The peak at 1.81 ppm for H-25 found in compound **2** was absent in **1**. In addition, the downfield shift for H-23 (4.46 ppm) was not observed in comparison to **1**. The presence of a strong correlation in the COSY spectra of compound **2** between H-23 and the additional olefinic proton suggested that the position of the double bond is between C-24 and C-25 in the side chain. Furthermore, the presence of a long range homoallylic coupling between this additional olefinic proton and the two methyl groups (26 and 27) in the COSY spectrum confirmed the position of the extra double bond at C-24 and C-25. This is in agreement with the downfield shift of the two methyl groups (26 and 27) at 1.72 and 1.75 ppm, respectively in compound **2**. The chemical shift and coupling pattern of the conspicuous H-3 at 3.20 ppm (dt, *J* = 10.2, 4.5 Hz) were consistent with those reported for 3β-hydroxyl, 4β-H, 5α-H steroids [Carmely, *et al*., 1989]. The ^{1}H NMR of the sugar part of **2** has no difference in comparison with that of compound **1**. On the basis of the coupling constants between H-3` and H-4` (axial-equatorial, 3.5 Hz) and also H-3`` and H-4`` (axial-equatorial, 3.4 Hz) it was evident that the two sugar moieties should be β-D-galactopyranosyl units. The linkage between the two ß-D-galactopyranosyl units was established to be at C-2` (1``,2`-β-D- galactose) as observed from the downfield

shifts of H-2` and H-2`` in $^{1}$H NMR and the upfield shifts of H-3` and H-3``. The identity of the sugar moieties was confirmed by an acidic hydrolysis and GC analysis in which the D-configuration for both galactose units was also confirmed.

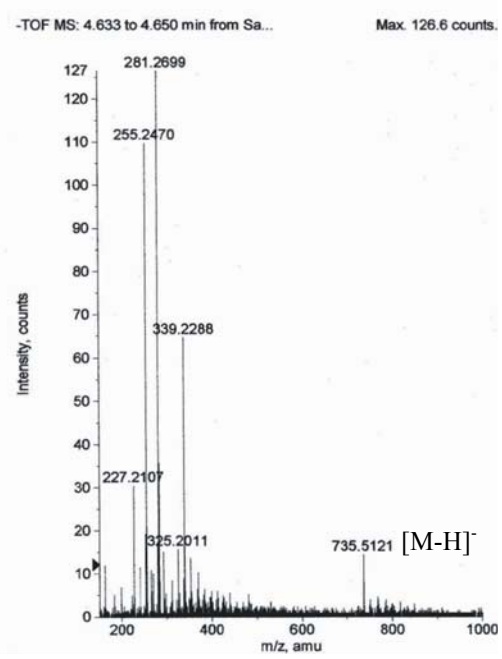

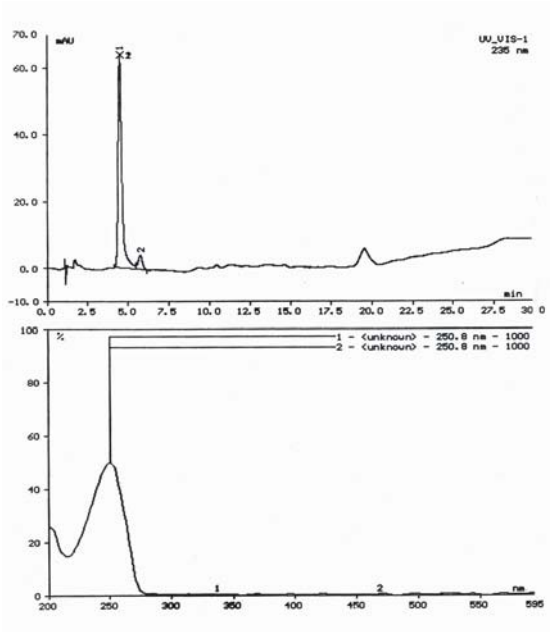

HREIMS **UV**

Fig. 3.6: UV and HREIMS spectra of compound 2

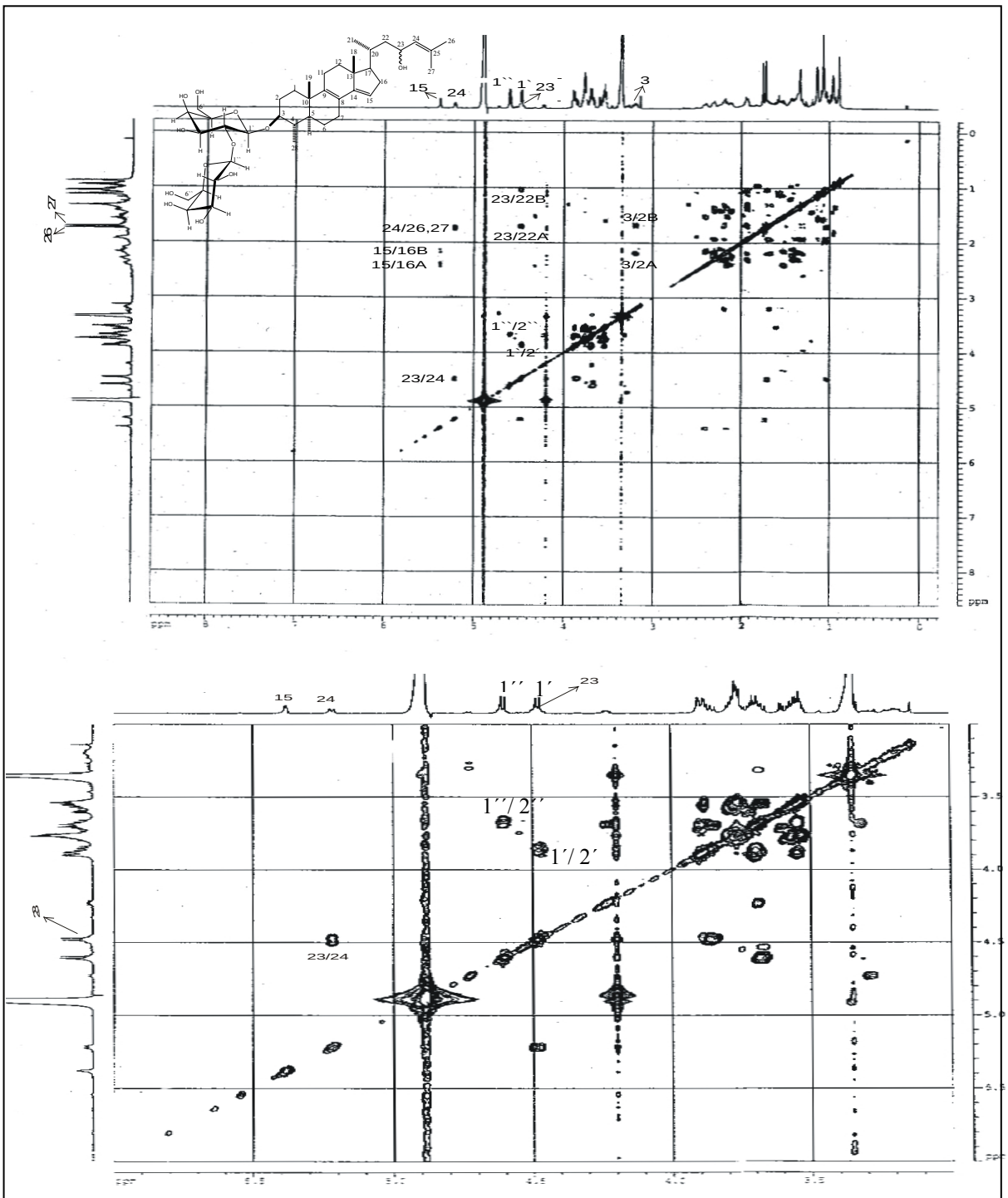

Fig. 3.7: Total COSY spectrum (top) and enlargement (bottom) of compound 2

3.1.3. Eryloside L (3, new compound)

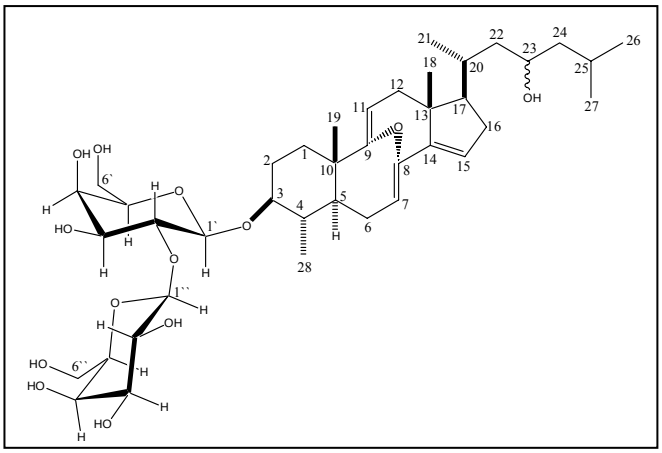

Eryloside L (**3**) was obtained as a white amorphous powder (5.2 mg); $[\alpha]_D^{20}$ +23 (*c* = 0.2, MeOH); UV (MeOH) λ_{max} 202 nm. The negative HRESIMS showed a pseudomolecular ion peak at *m/z* 751.4704 $[M - H]^-$ (see Fig 3.8). This molecular weight is in accordance with the molecular formula $C_{40}H_{64}O_{13}$. Comparison between the NMR data of compound **3** and those of **1** revealed that this compound is also closely related to eryloside A. The full inspection of the ^{1}H NMR and COSY spectra of **3** (see Fig. 3.9 and Table 3.2) revealed the presence of three olefinic protons at 4.85, 5.05, 5.43 ppm, six methyls at the range from 0.90 to 1.25 ppm, and two very clear anomeric protons at 4.48 ppm (d, J = 7.7 Hz) and 4.60 ppm (d, J = 7.8 Hz), the latter indicating the presence of two sugar moieties. These findings were corroborated by its ^{13}C NMR and DEPT data (see Fig 3.10 and Table 3.2) which revealed the presence of 40 carbons. Careful inspection of the ^{13}C and DEPT NMR showed that this compound consists of two parts; one contains 28 carbons which is the aglycone part and the two sugar moieties which contain 12 carbons. The aglycone part consists of six methyls, 7 methylenes, 10 methines, and 5 quaternary carbons. The presence of three methines at 107.4, 113.9 and 122.9 ppm suggested the presence of three double bonds which is in agreement with its ^{1}H NMR data. On the other hand the presence of three quaternary carbons at 151.5, 153.0, 169.8 ppm suggested the occurrence of an oxygen bearing-olefinic carbon. Detailed interpretation of COSY and TOCSY (see Fig. 3.11) spectral data resulted in the elucidation of the presence of three spin systems (A, B and C). A strong correlation in the TOCSY experiment between the two protons in position 1 and the protons on positions 2, 3, 4, 5, 6, and 7 revealed the first spin system (A). A correlation between H-11 and the two protons on position 12 clarified the second spin system (B) and agreed with the cross peak between H-11

and the methine protons on position 12 in the COSY spectrum. The first and second spin systems determined the position of the oxygen bridge between C-8 and C-9 which was also confirmed by the downfield shifts of C-8 at 153.0 ppm and C-9 at 169.8 ppm in the ^{13}C NMR spectrum in comparison to compound **1**. Furthermore, strong correlation in the TOCSY spectrum between H-15 and the protons in positions 16, 17, 20, 21, 22, 23, 24, 25, 26, and 27 revealed the third and last spin system (C). The downfield shifts of H-17, H-5, H_2-6, H-11, H_2-12 in the ^{1}H NMR of **3** in comparison to that of **1** which is in agreement with ^{13}C NMR of **3** suggested that the positions of the three double bonds are between C-7, 8; C-9,11 and C-14,15. This is confirmed by the chemical shift of H-15 and C-14. The positions of the double bonds were also corroborated by a full inspection of the HMBC spectrum of **3** (see Fig 3.12 and Table 3.2). The strong correlation between H-12 and C-9; CH_3-18 and C-14; CH_3-19 and C-9, C-1 and finally H-12 and C-17; CH_3-18 and C-13 confirmed the connection between the three spin systems (see Fig 3.12). The attachment of the sugar moiety to the aglycone in compound **3** was established to be at position 3 through the strong cross peak between H-3 and the anomeric carbon C-1` in HMBC spectrum. The relative stereochemistry of the hydroxyl group at C-3 as equatorial was determined by the mutual correlations observed between H-3 /CH_3-28 and H-5, and H-5 /CH_3-28 in the ROESY spectrum. The nature of the sugar unit was confirmed by an acidic hydrolysis and GC analysis in which the D-configuration of the two galactose units was also assigned. The 8α, 9α-oxido stereochemistry is suggested by the downfield chemical shift of H-5 to 2.46 ppm implying the oxygen function and H-5 to be located on the same face of the molecule [D´Auria, *et al.*, 1991].

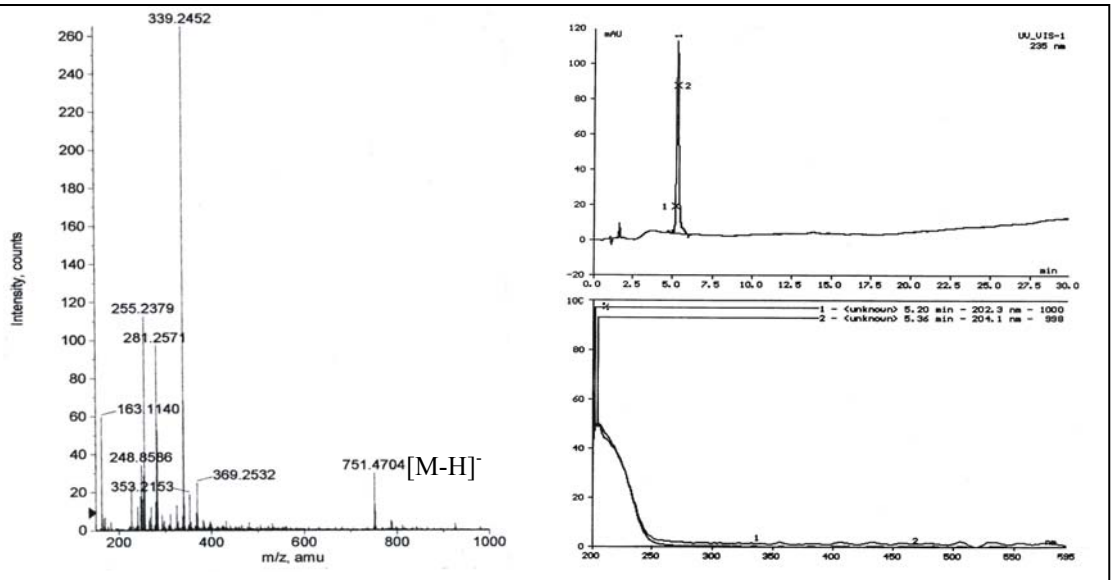

HREIMS **UV**

Fig. 3.8: HREIMS and UV spectra of compound 3

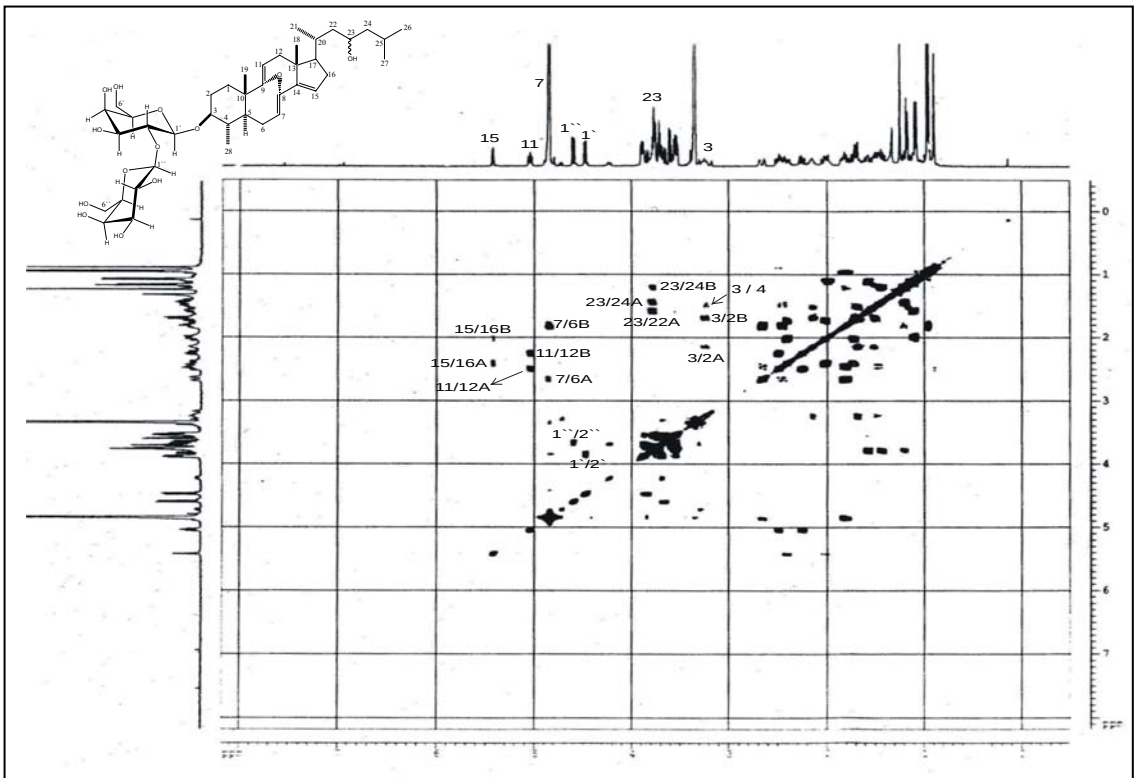

Fig. 3.9: COSY spectrum of compound 3

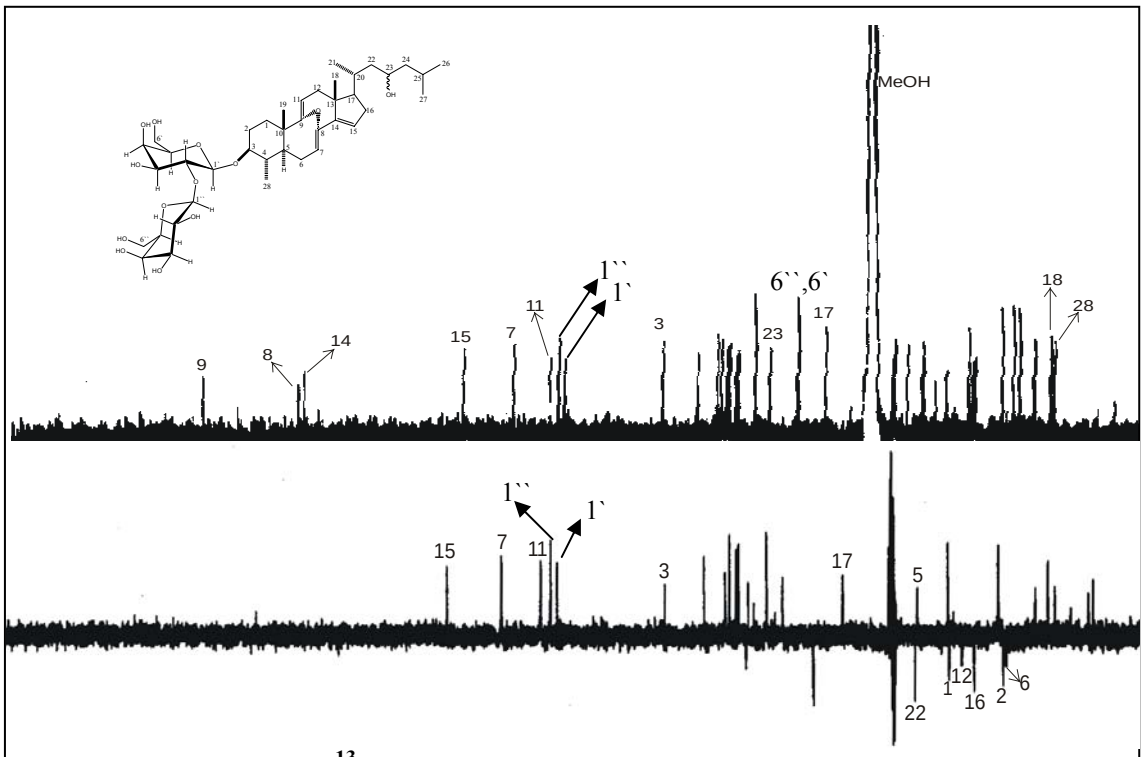

Fig. 3.10: ^{13}C NMR (top) and DEPT spectra (bottom) of 3

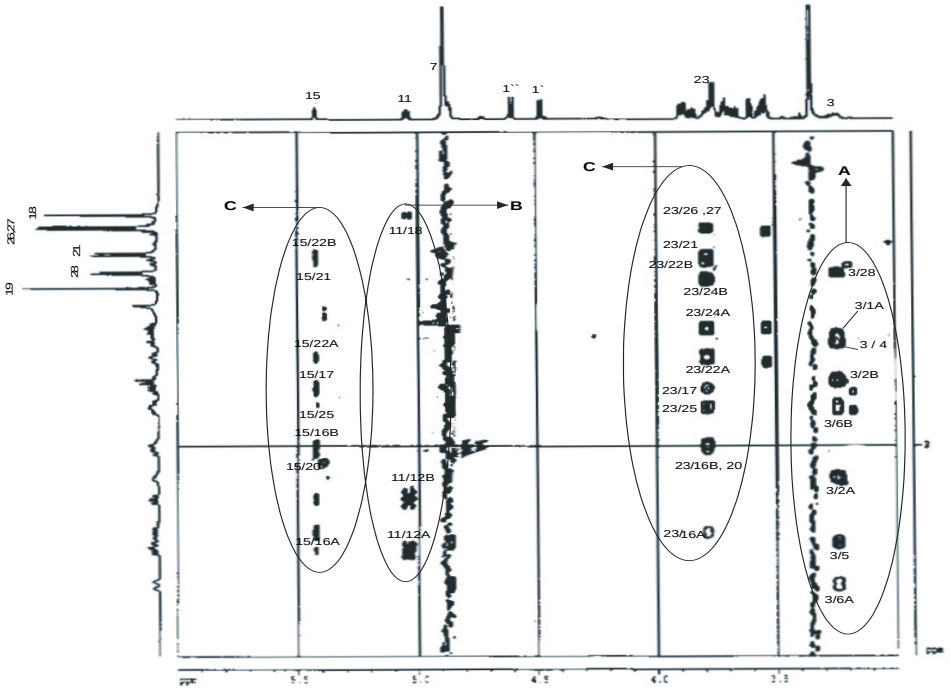

Fig. 3.11: Part of the TOCSY experiment of compound 3 showing three different spin systems (A, B and C)

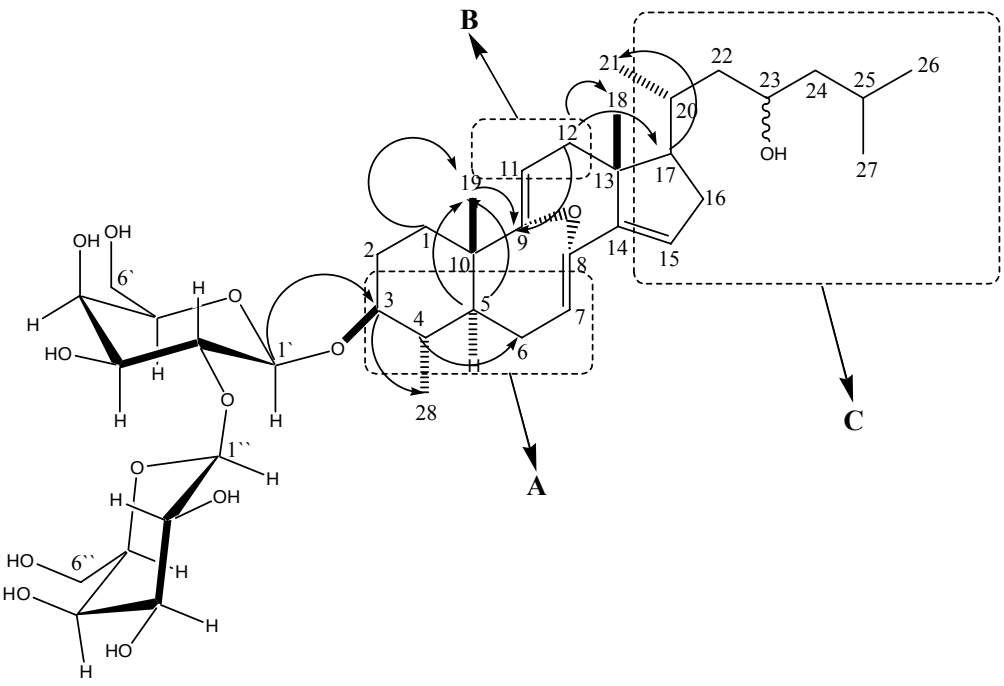

Fig. 3.12: Some HMBC correlations of compound 3 connecting the three spin systems A, B and C

Table 3.1: NMR data of compounds 1, 2

Position	^{1}H NMR, (ppm), multiplicity (Hz) of 1	^{1}H NMR, (ppm), multiplicity (Hz) of 2	^{13}C NMR (ppm) of 1
1A	1.93 m	1.94 m	36.6 t
1B	1.34 m	1.31 m	-
2A	2.22 m	2.19 m	30.9 t
2B	1.69 m	1.69 m	-
3	3.35 (1H, dt, 4.6, 10.4 Hz)	3.21 (1H, dd, 10.2, 4.5 Hz)	87.7 d
4	1.53, m	1.57, m	39.1 d
5	1.01, m	0.98, m	under solvent
6A	1.93 m	1.43 m	21.9 t
6B	1.29 m	1.19 m	-
7A	2.29 m	2.24 m	22.8 t
7B	2.14 m	2.11 m	-
8	-	-	124.3 s
9	-	-	141.9 s
10	-	-	38.0 s
11A	2.35 m	2.33 m	28.0 t
11B	1.99 m	2.19 m	-
12A	2.11 m	1.93 m	38.5 t
12B	1.40 m	1.39 m	-
13	-	-	46.3 s
14	-	-	152.4 s
15	5.38 br s	5.37 br s	118.0 d
16A	2.40 m	2.40 m	37.0 t
16B	2.20 m	2.14 m	-
17	1.47, m	1.52, m	59.4 d
18	0.90 (3H, s)	0.89 (3H, s)	16.2 q
19	1.07 (3H, s)	1.07 (3H, s)	19.8 q
20	2.01, m	1.82, m	31.8 d
21	1.03 (3H, d, 6.4 Hz)	0.96 (3H, d, 6.6 Hz)	19.4 q
22A	1.56 m	1.70 m	45.5 t
22B	1.22 m	1.03 m	-
23	3.63, m	4.47, m	67.4 d
24A	1.43 m	5.22 dt (1H, 8.4, 1.2 Hz)	under solvent
24B	1.18 m	-	-
25	1.81, m	-	25.8 d
26	0.96 (3H, d, 6.5 Hz)	1.72 (3H, d, 1.1 Hz)*	22.7 q
27	0.96 (3H, d, 6.5 Hz)	1.75 (3H, d, 1.02 Hz)*	23.7 q
28	1.13 (3H, d, 6.3 Hz)	1.14 (3H, d, 6.3 Hz)	15.9 q
1′	4.48 (1H, d, 7.7 Hz)	4.48 (1H, d, 7.8 Hz)	104.7 d
2′	3.86 (1H, dd, 9.2, 7.6 Hz)	3.85 (1H, dd, 9.4, 7.8 Hz)	80.5 d
3′	3.69, m	3.70, m	75.2 d
4′	3.88 (1H, br d, 3.6 Hz)	3.88 (1H, dd, 3.5, 0.8 Hz)	70.1 d
5′	3.56, m	3.55, m	76.3 d
6′A	3.77 m	3.80 m	62.2 t
6′B	3.77 m	3.79 m	-
1′′	4.60 (1H, d, 7.8 Hz)	4.61 (1H, d, 7.8 Hz)	105.7 d
2′′	3.67 (1H, dd, 9.7, 7.6 Hz)	3.68 (1H, dd, 9.8, 7.8 Hz)	73.1 d
3′′	3.55, m	3.53 , m	74.8 d
4′′	3.74, m	3.76, m	70.1 d
5′′	3.55, m	3.58, m	77.1 d
6′′A	3.67 m	3.74 m	62.3 t
6′′B	3.67 m	3.72 m	-

These compounds were measured in CD_3OD at 500 MHz.

***** These values may be interchanged.

Table 3.2: NMR data of compound 3

Position	^{1}H NMR (ppm), multiplicity (Hz) of 3	^{13}C NMR (ppm) of 3	HMBC correlations of (3) H ⟶ C
1A	1.70 m	39.8 t	19
1B	1.51 m	-	
2A	2.16 m	31.0 t	
2B	1.65 m	-	
3	3.35, m	87.0 d	5, 28, 1´
4	1.47, m	40.1 d	6, 28
5	2.46, m	45.1 d	19
6A	2.66 m	30.5 t	4
6B	1.88 m	-	
7	4.85, br s	113.9 d	
8	-	153.0 s	-
9	-	169.8 s	-
10	-	42.8 s	-
11	5.05 (1H, dd, 7.9, 5.8 Hz)	107.4 d	
12A	2.75 (1H, d, 8.1 Hz)	37.7 t	9, 13, 14, 17, 18
12B	2.25 (1H, dd, 13.3, 8.1 Hz)	-	
13	-	under solvent	-
14	-	151.5 s	-
15	5.43 br s	122.9 d	
16A	2.39 m	35.8 t	20
16B	2.07 m	-	
17	1.76, m	57.4 d	18, 21
18	0.90 (3H, s)	17.1 q	12, 13, 14, 17
19	1.25 (3H, s)	20.1 q	1, 5, 9, 10
20	2.00, m	31.8 d	16, 21
21	1.08 (3H, d, 6.4 Hz)	19.9 q	17, 20, 22
22A	1.58 m	45.4 t	21
22B	1.13 m	-	
23	3.76, m	67.5 d	
24A	1.43 m	49.1 t	25, 26, 27
24B	1.22 m	-	
25	1.81, m	25.8 d	24, 26, 27
26	0.99 (3H, d, 6.6 Hz)	22.6 q	24, 25, 27
27	0.99 (3H, d, 6.6 Hz)	23.7 q	24, 25, 26
28	1.17 (3H, d, 6.3 Hz)	16.4 q	3, 4, 5
1´	4.48 (1H, d, 7.7 Hz)	104.7 d	3, 3`
2´	3.84 (1H, dd, 9.6, 7.7 Hz)	80.6 d	
3´	3.60, m	75.5 d	
4´	3.88 (1H, br d, 3.3 Hz)	70.1 d	
5´	3.53, m	76.3 d	
6´A	3.69 m	62.2 t	
6´B	3.72 m	-	
1´´	4.60 (1H, d, 7.8 Hz)	105.8 d	
2´´	3.67 (1H, dd, 9.7, 7.8 Hz)	73.2 d	
3´´	3.54, m	74.9 d	
4´´	3.71, m	70.1 d	
5´´	3.59, m	77.1 d	
6´´A	3.72 m	62.3 t	
6´´B	3.69 m	-	

The compound was measured in CD_3OD at 500 MHz.

Bioactivity

Eryloside A (**1**) was the first saponin isolated from the genus *Erylus* by [Carmely, *et al*., 1989]. It was reported that this compound has antitumor activity against P388 cells with an lC_{50}= 4.2 μg/mL. However this compound proved inactive when tested against JURKAT, THP-1 and MM-1 cell lines. On the other hand, **1** showed antifungal activity against *Candida albicans* but was inactive against *S. aureus*. Furthermore, eryloside F has been reported to have a potent and relatively selective thrombin receptor antagonist activity [Stead, *et al*., 2000]. It is reported also that nobiloside which is a tritepenoidal saponin isolated from the sponge *Erylus nobilis* inhibited the enzyme neuraminidase from the bacterium *Clostridium perfringens* with an IC_{50} value of 0.46 μg/mL [Takada, *et al.,* 2002].

In the present study, compound **1** showed a moderate activity against *B. subtilis*, *E. coli*, and *C. albicans* at a concentration 10 μg per disc, while it was inactive against *S. aureus* (see Table 3.3). On the other hand, the isolated pure compounds from *Erylus lendenfeldi* **1** and **2** showed a moderate activity in the brine shrimp bioassay while compound **3** was inactive (see Table 3.4).

Table 3.3: Zones of inhibition in agar – plate diffusion assay.

Compound*	**Zone of inhibition (mm)**			
	S. aureus	***E. coli***	***B. subtilis***	***C. albicans***
1				
(5 μg)	-	-	-	-
(10 μg)	-	6 mm	7 mm	7 mm

(-): negative
* amount tested at μg per disc

Table 3.4: Brine-shrimp lethality test for compounds 1, 2 and 3

Compound	**Brine-shrimp mortality rate at a concentration of**	
	0.5 mg	**0.25 mg**
1	50%	0%
2	50%	0%
3	0%	0%

3.2. Isolated compounds from the marine sponge *Negombata corticata*

The family Latrunculiidae is characterised by the presence of marine toxins like latrunculin A, B, C, D, and M (see Fig 3.13). Colonies of *Latrunculia magnifica* have never been observed to be damaged or eaten by fish [Neeman, *et al.,* 1975]. When squeezed manually, these sponges exude a reddish fluid accompanied by a strong odour. This exudate causes fish to immediately flee, leading to death within minutes [Groweiss, *et al*., 1983]. The latrunculins are the first known 2-thiazolidinone-bearing marine macrolides. They were found to cause major alteration in specific cytoskeletal proteins [Groweiss, *et al*., 1983; Kashman, *et al*., 1985; Blasberger, *et al*., 1989]. Recentely, latrunculin S was isolated from the sponge *Fasciospongia rimosa* [Tanaka, *et al.,* 1996]. As mentioned before (see page 31), the total extract of the sponge *Negombata corticata* collected from the Red Sea showed a strong deterrent activity in the fish feeding assay, so it was decided to investigate this sponge.

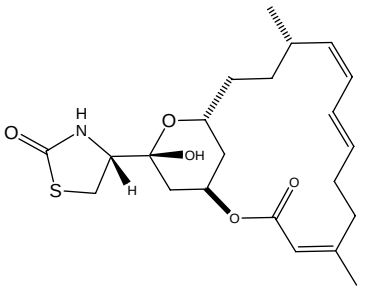

Latrunculin A

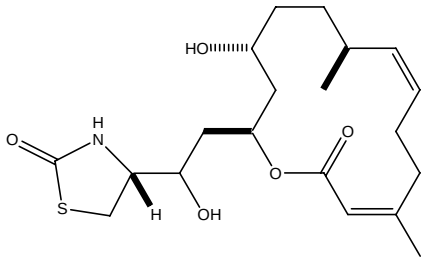

Latrunculin C

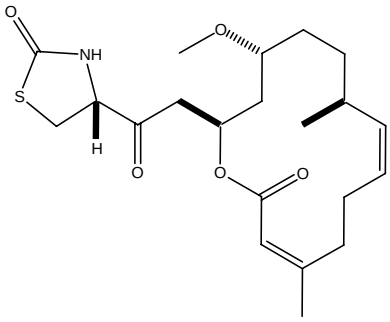

Latrunculin D

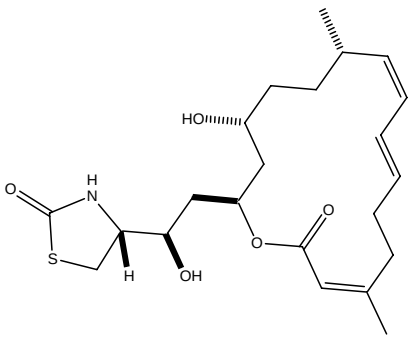

Latrunculin S

Fig. 3.13: Some latrunculins isolated from family Latrunculiidae

3.2.1. Latrunculin B (4, known compound)

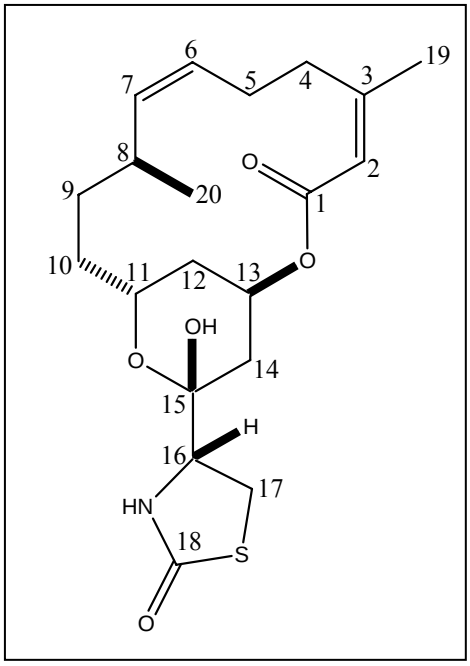

Latrunculin B (**4**) was obtained as yellow oily substance ($[\alpha]_D$ +98 (*c* = 0.5, $CHCl_3$; UV (MeOH) λ_{max} 216 nm). The negative HREIMS showed a pseudomolecular ion peak at *m/z* 394.1920 $[M - H]^-$ (100), while the positive ESIMS gave a peak at *m/z* 378 which was revealed as $[M+H-(H_20)]^+$ (see Fig. 3.14). The ^1H NMR spectrum of compound **4** (see Fig. 3.15 and Table 3.5) showed the presence of one methyl doublet at 0.94 ppm with a coupling constant of 6.6 Hz, one olefinic methyl doublet at 1.91 ppm with a coupling constant of 1.1 Hz due to a homoallylic coupling, a triplet at 4.24 ppm with a coupling constant of 11 Hz, three doublets of doublets at 4.26, 3.47 and 3.39 ppm and finally, four signals in the region between 5.00 and 6.00 ppm. A full inspection of the ^{13}C NMR (see Fig. 3.16 and Table 3.5) and the DEPT spectra revealed the presence of 20 carbons consisting of two methyls, seven methylenes, seven methines and four quaternary carbons. Comparison between the NMR spectra of compound **4** and those reported for latrunculin B [Groweiss, *et al.,* 1983] showed that compound **4** is identical to latrunculin B. The complete assignment of NMR signals of compound **4** was done through analysis of its 2D NMR spectra which includes COSY (see Fig. 3.17), HMQC and HMBC. From the COSY spectrum the position of the N*H* can be determined through the cross peak between N*H* and H-16 while the presence of a cross peak from H-2 to CH_3-19, and H-7 to CH_3-20 through homoallylic coupling indicated the positions of the two methyls. On the other hand, from the HMBC spectrum, the strong correlation

between H-16 and C-14, C-15, C-17, C-18 confirmed the connection between the thiazolidinone and the tetrahydropyran rings. The cross peak between H-13 and both C-1 and C-15 as well as H-2 with C-1, C-2, C-4, C-19 confirmed the position of the carbonyl group at C-1 and revealed to presence of a macrolide system (see Fig. 3.18 and Table 3.5). Two further olefinic protons (H-6 and H-7) were found to resonate at 5.25 and 5.04 ppm, respectively with a coupling constant of 11.2 Hz proving the *Z* (*cis*)-configuration of the double bond. The relative stereochemistry of compound **4** was determined through comparison of the coupling constant values of **4** with those reported for latrunculin B.

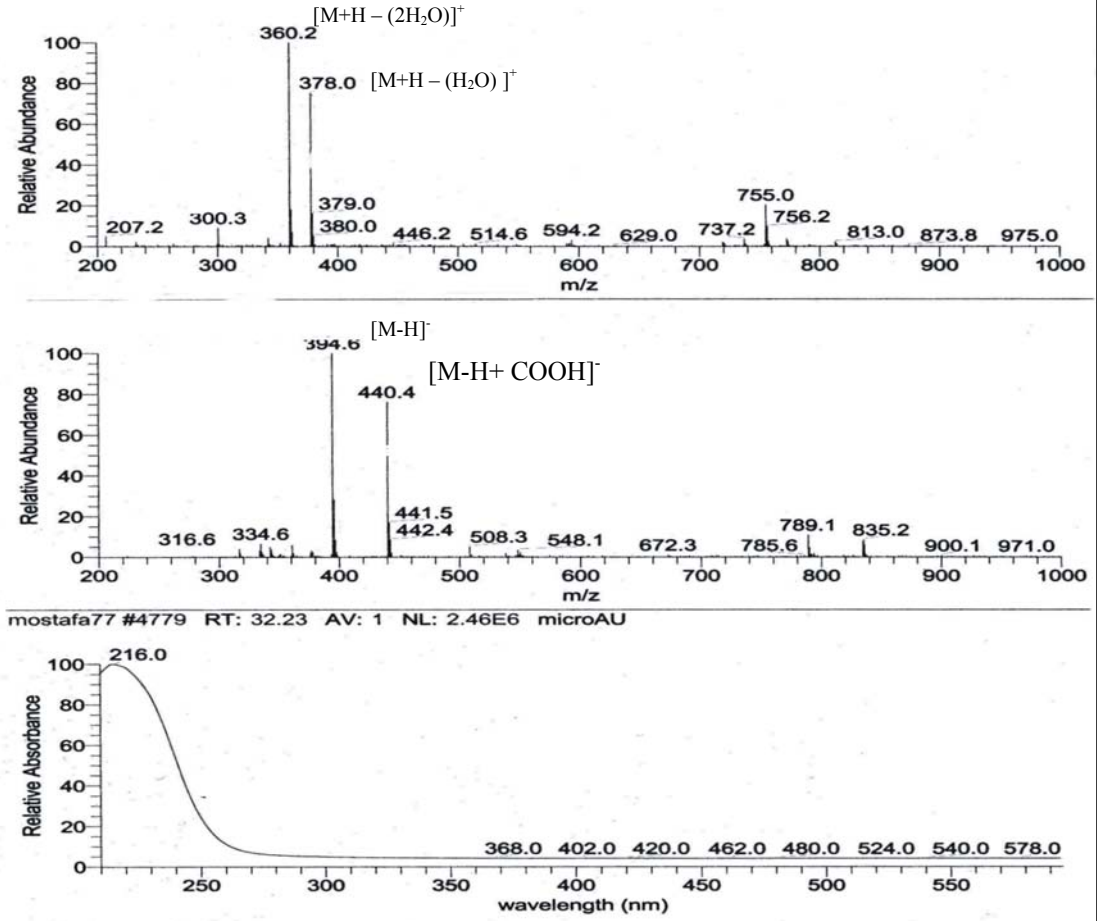

Fig. 3.14: (+) ESI mass (top),(-) ESI mass (middle) and UV spectra (bottom) of compound 4

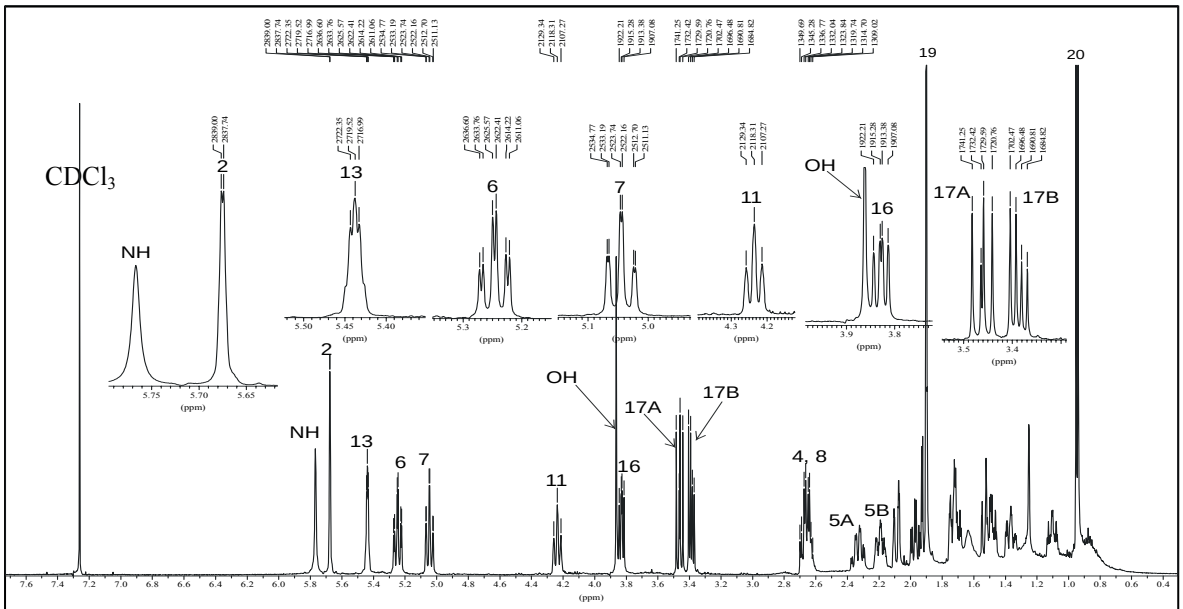

Fig. 3.15: ^{1}H NMR spectrum of latrunculin B (compound 4)

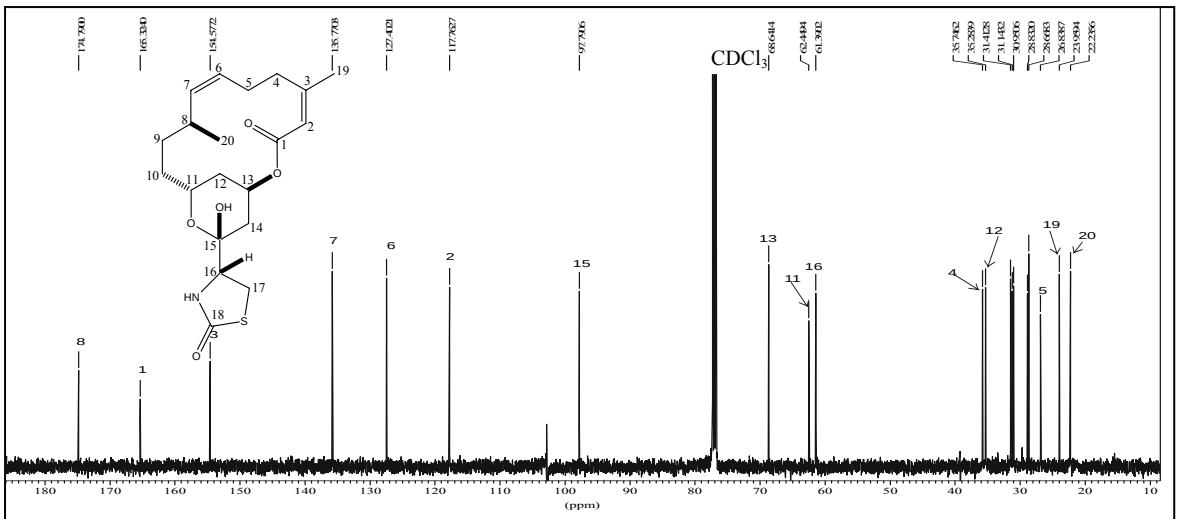

Fig. 3.16: ^{13}C NMR spectrum of latrunculin B (compound 4)

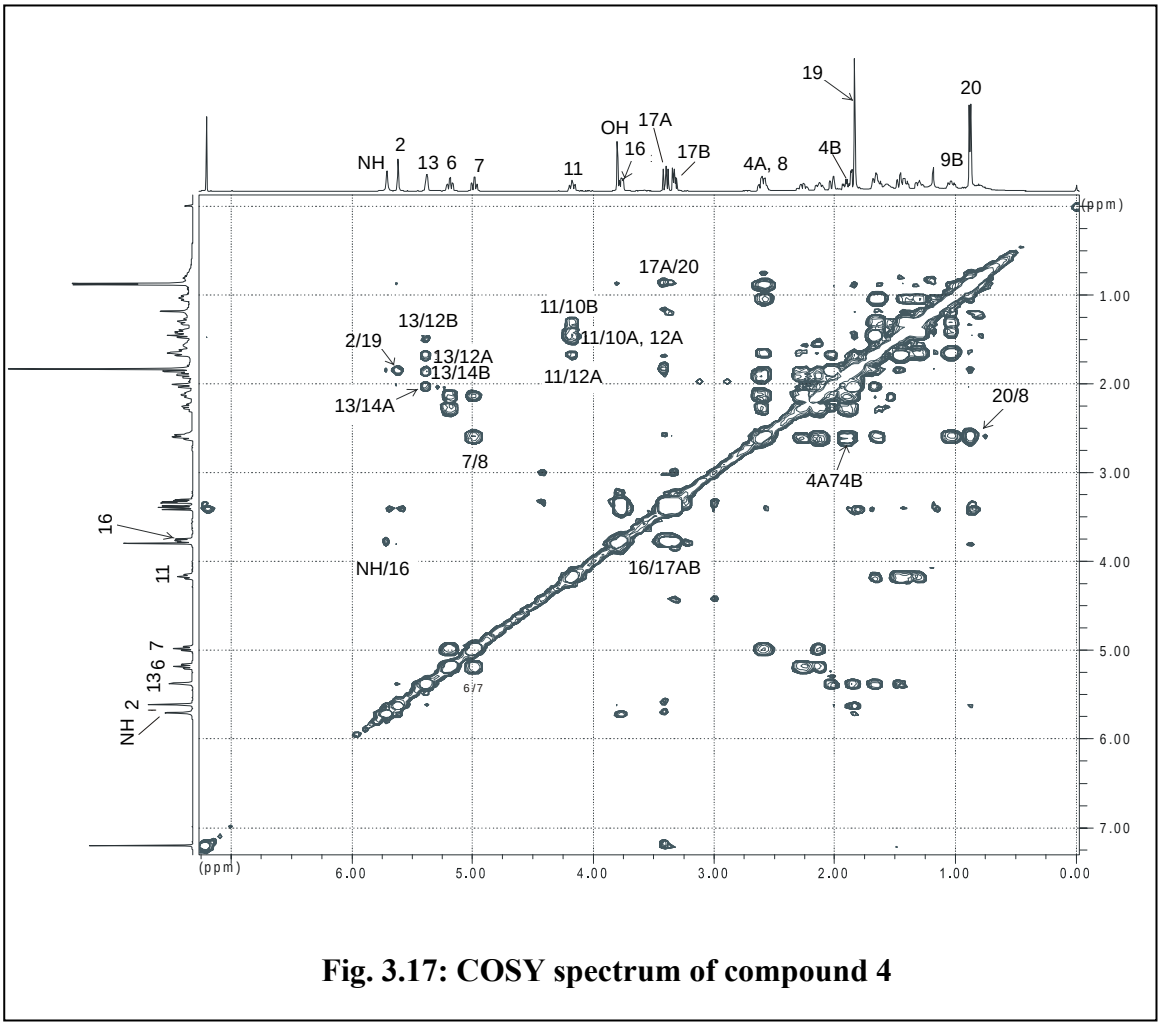

Fig. 3.17: COSY spectrum of compound 4

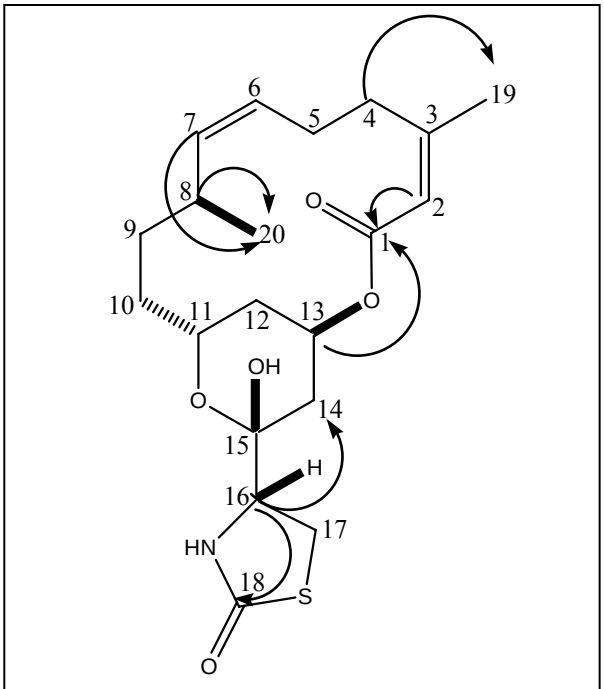

Fig. 3.18: Some HMBC correlations of 4

Table 3.5: NMR data of compound 4

Position	^{1}H NMR (ppm), multiplicity (Hz)	^{13}C NMR (ppm)	HMBC correlations H ⟶ C
1	-	165.3 s	-
2	5.68 (d, 1.5 Hz)	117.8 d	1, 3, 4, 19
3	-	154.6 s	-
4A	2.66, m	35.8 t*	3, 6, 19
4B	1.93 m	-	3, 6, 19
5A	2.34, m	26.8 t	3, 4, 6, 7
5B	2.18 m	-	3, 4, 6, 7
6	5.25 (ddd, 11.3, 11.3, 3.2 Hz)	127.4 d	4, 5, 8
7	5.04 (ddd, 11.1, 11.1, 1.9 Hz)	135.8 d	5, 8, 20
8	2.66, m	28.8 d	6, 7, 8, 9, 10, 20
9A	1.77, m	31.2 t **	7, 10, 20
9B	1.09 m	-	7, 10, 20
10A	1.40, m	31.4 t **	9, 11
10B	1.36 m	-	9, 11
11	4.24 (br t, 11 Hz)	62.5 d	9, 10, 13
12A	1.78, m	35.3 t *	14
12B	1.52 m	-	14
13	5.42 (br t, 2.5 Hz)	68.7 d	1, 11, 15
14A	2.14, m	31.0 t	12, 13, 15
14B	1.92 m	-	12, 13, 15
15	-	97.8 s	-
16	3.83 (dd, 8.5, 6.2 Hz)	61.4 d	14, 15, 17, 18
17A	3.46 dd (11.9, 9.1 Hz)	28.7 t	15, 16, 18
17B	3.39 (dd, 11.7, 6.0 Hz)	-	15, 16, 18
18	-	174.8 s	-
19	1.91 (d, 1.2 Hz)	24.0 q	2, 3, 4
20	0.94 (d, 6.6 Hz)	22.2 q	7, 8
O*H*	3.87, br s	-	-
N*H*	5.81, br s	-	-

*, ** These values may be interchanged

The compound was measured in $CDCl_3$ at 500 MHz.

3.2.2. Latrunculin M (5, known compound)

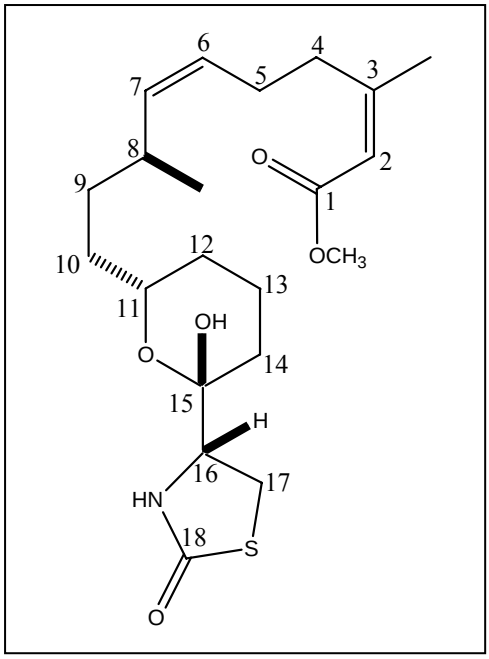

Latrunculin M (**5**) was obtained as yellow oily substance ($[\alpha]_D^{20}$ +35 (*c* = 0.143, MeOH; UV (MeOH) λ_{max} 216 nm). The negative ESIMS gave a peak at *m/z* 411 $[M-H]^-$ with the molecular formula $C_{21}H_{33}NO_5S$, which is compatible with peaks at *m/z* 394.3 $[M+H-(H_2O)]^+$ and at *m/z* 362.4 $[M+H-(H_2O+CH_3OH]^+$ in the positive ESIMS (see Fig. 3.19). The ^{1}H NMR spectrum of compound **5** (see Fig. 3.20 and Table 3.6) revealed that it is closely related but not identical to **4**. It is evident that compound **5** has the same set of olefinic protons as compound **4**, i.e. it has a broad singlet at 5.68 ppm for H-2 and signals at 5.34 ppm (dt) for H-6, and 5.11 ppm (br t) for H-7. The absence of a signal at 5.44 ppm for H-13 in compound **5** in comparison to that in **4** suggested that the macrolide ring had been opened in **5**. The presence of an additional methoxy group in compound **5** as well as the observed mass difference of 16 mass units indicated **5** to be methyl-13-deoxy latrunculin B carboxylate. Comparison between the ^{1}H NMR data of compound **5** and that reported for latrunculin M [Blasberger, *et al*., 1989] confirmed that the structure of compound **5** is identical to the latter.

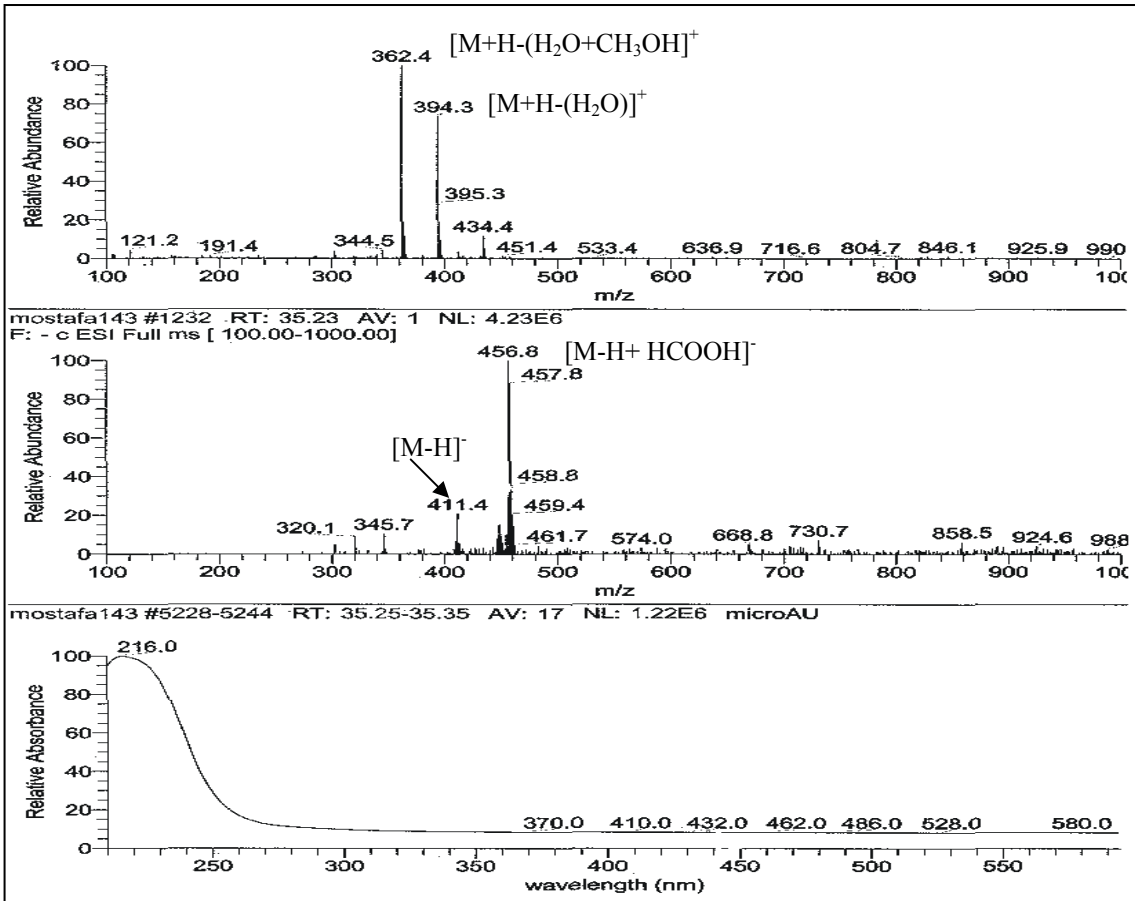

Fig. 3.19: (+) ESI mass (top), (-) ESI mass (middle) and UV spectra (bottom) of compound 5

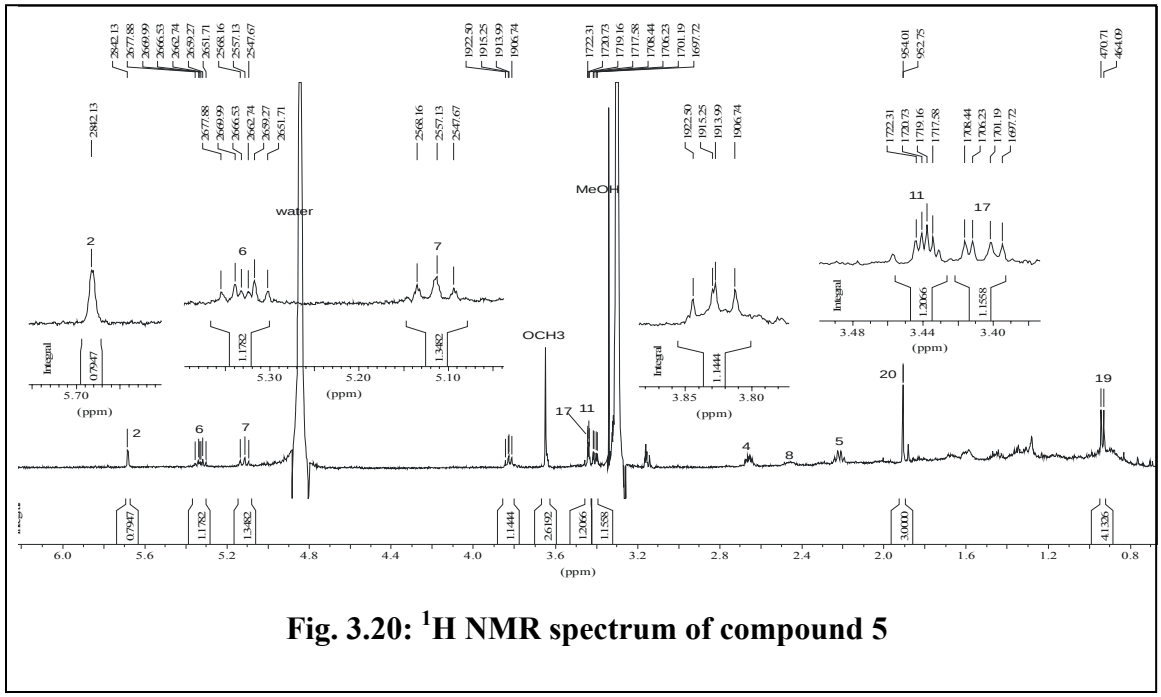

Fig. 3.20: ^{1}H NMR spectrum of compound 5

Table 3.6: NMR data of compound 5

Protons	^{1}H NMR (ppm), multiplicity (Hz)
1	-
2	5.68, br s
3	-
4A,B	2.66, (2H, m)
5A,B	2.2 (2H, m)
6	5.33 (dt, 11.0, 7.6 Hz)
7	5.11 (br t, 9.5 Hz)
8	2.45, m
9A	1.28, m
9B	1.15, m
10A	1.32, m
10B	1.28, m
11	3.44, m
12A	1.52, m
12B	1.08, m
13A	1.76, m
13B	1.69, m
14A	1.61, m
14B	1.50, m
15	-
16	3.83 (dd, 8.5, 7.3 Hz)
17A,B	3.41 (2H, dd, 8.5, 3.5 Hz)
18	-
19	1.92 (d, 1.26 Hz)
20	0.94 (d, 6.6 Hz)
OCH_3	3.65, s

The compound was measured in CD_3OD at 500 MHz.

Bioactivity

Different fractions of the sponge *Negombata corticata* showed a strong activity in the brine shrimp bioassay (see Table 3.7). They also showed a strong activity against different gram positive and gram negative bacteria and also exhibited antifungal activity. The isolated pure compounds from *Negombata corticata* also displayed strong activity against both gram positive and gram negative bacteria (see Table 3.8). As previously mentioned, the latrunculins disrupt microfilament organisation and exert profound effects on the morphology of non-muscular cells without affecting the organisation of the microtubular system [Spector, *et al*., 1983 and 1989]. Biological activity screening of latrunculin B showed a strong activity as antitumor agent against different leukemia cells (See Table 3.9).

Table 3.7: Brine-shrimp lethality test for different fractions of the marine sponge *Negombata corticata*

Fraction	Brine-shrimp mortality rate at a concentration of	
	0.5 mg/mL	**1 mg/mL**
Hexane	100 %	100 %
Ethyl acetate	100 %	100 %
Aqueous	60 %	50 %

Table 3.8: Agar plate diffusion assay of fractions and pure compounds from *Negombata corticata*.

Fraction* /Compound	Zone of inhibition (mm)			
	S. aureus	***E. coli***	***B. subtilis***	***C. albicans***
Hexane fraction				
(5 µg)	12	10	-	7
(10 µg)	12	10	-	7
EtOAc fraction				
(5 µg)	6	11	7	18
(10 µg)	6	11	7	18
Butanol fraction				
(5 µg)	7	12	7	15
(10 µg)	7	12	7	15
Latrunculin B (4)				
(5 µg)	7	10	14	7
(10 µg)	14	15	14	15

* amount tested at µg per disc.

(-): negative

Table 3.9: Cytotoxicity test for compound 4 (latrunculin B)

Concentration (μg/mL)	% of Growth rate in different cell lines		
	JURKAT	**THP-1**	**U-937**
1	93	100	97
5	82	48	53
10	80	42	41
25	60	26	22
50	38	4	10
100	7	0	12

3.3. Isolated compounds from the marine sponge *Pseudoceratina purpurea*

Sponges belonging to the order Verongidae have yielded a wide variety of tyrosine metabolites [Ambrosio, *et al.*, 1982], usually based on 3,5-dibromo-tyrosine or less frequently 3-bromo, 3-chloro-, 3,5-dichloro-, or 3-bromo-5-chloro-tyrosine [Kazlauskas, *et al.*, 1981; Ambrosio, *et al.*, 1984]. In many cases, a single tyrosine unit is involved, as with dienone (dibromoverongiaquinol) [Ambrosio, *et al.*, 1982 and 1984] and aeroplysinin-1 [Fattorusso, *et al.*, 1972]. Other metabolites entail two or more tyrosine units through either amide bonding, as in aerothionin and homoaerothionin which also incorporate biogenic amines [Moody, *et al.*, 1972] or ether bonds as in bastadins [Kazlauskas, *et al.*, 1981] or both bond types exemplified by fistularin-3 [Gopichand, *et al.*, 1979] (see Fig. 3.21). The different fractions of the marine sponge *Pseudoceratina purpurea* collected from Baranglompo Island, Indonesia in 1997 showed a moderate activity in the brine shrimp bioassay (see Table 3.10). Search for bioactive substances from marine organisms lead to the isolation of ten bromotyrosine alkaloids (**6-15**) from the ethyl acetate fraction. The structures were elucidated on the basis of spectroscopic data (^{1}H-NMR, ^{13}C NMR, COSY, HMQC, and HMBC) in combination with mass spectrometry.

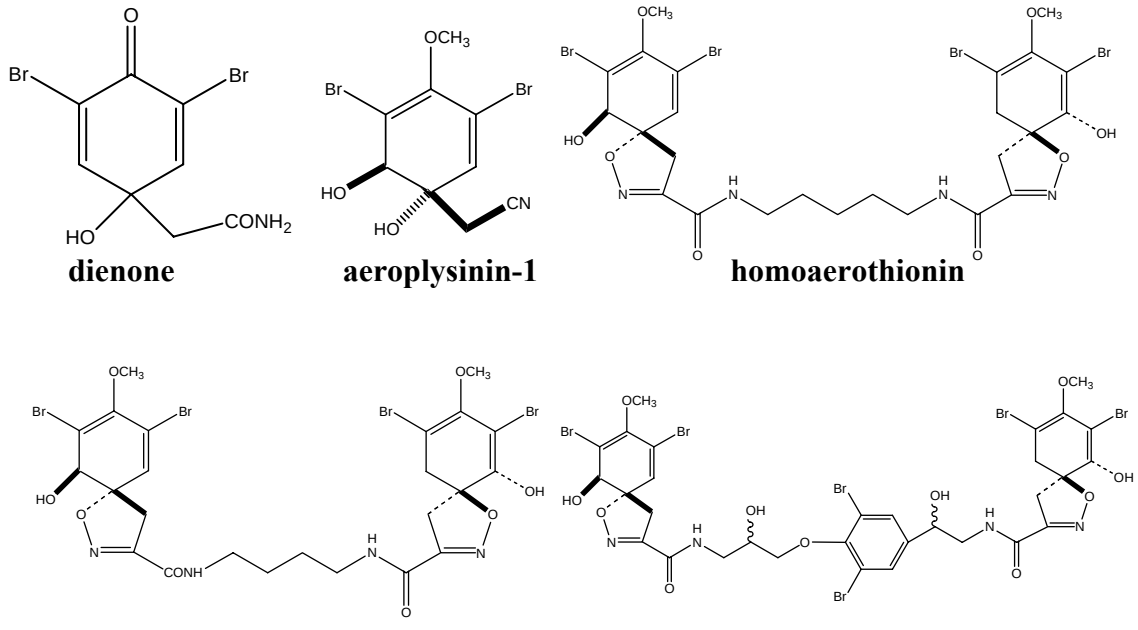

Fig. 3.21: Some bromotyrosine alkaloids isolated from sponges of the order Verongidae

Table 3.10: Brine-shrimp lethality test for different fractions of the marine sponge *Pseudoceratina purpurea*

Fraction	Brine-shrimp mortality rate (%) at a concentration of	
	0.5 mg/mL	**1 mg/mL**
Hexane	100 %	100 %
Ethyl acetate	55 %	55 %
Aqueous	0 %	0 %

3.3.1. Dienone methoxyethoxyketal (6, known compound)

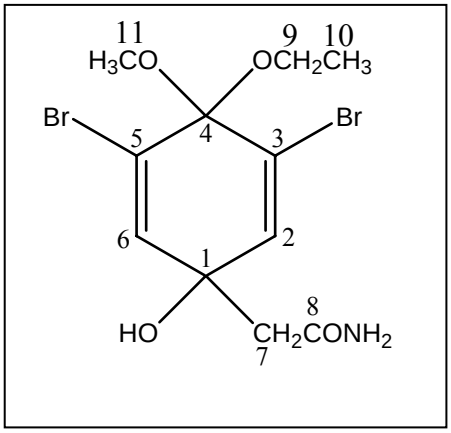

Compound **6** was isolated as pure white amorphous powder. FABMS gave a cluster with the ratio 1:2:1 at *m/z* 406:408:410 (8%) for $[M+Na]^+$ which indicated the presence of two bromine atoms. Two important fragmentation peaks appeared at *m/z* 352:354:356 (18%) for $[M+H-(MeOH)]^+$ and at *m/z* 338:340:342 (12%) for $[M+H-(EtOH)]^+$ (see Fig. 3.22). This molecular weight is compatible with the molecular formula $C_{11}H_{15}Br_2NO_4$. In the ^{1}H-NMR spectrum of compound **6** (see Fig. 3.23, Table 3.11), the presence of two meta-coupled doublet aromatic protons at 6.69 ppm, in addition to the presence of another characteristic singlet at 2.52 ppm (2H) suggested that this compound may be a bromotyrosine alkaloid. This was confirmed from the full inspection of the ^{13}C NMR spectrum (see Fig. 3.24, Table 3.11) of **6** which revealed the presence of 10 carbons consisting of one methyl, one methoxy, two methylenes, two methines and five quaternary carbons. The signal at 173.8 ppm was

indicative of a carbonyl group. The comparison of the NMR data of compound **6** with those reported for the known compound dienone-methoxyethoxyketal [Andersen, *et al*., 1973] confirmed the structure of **6** to be identical to the latter compound. As already reported [Andersen, *et al*., 1973], no optical rotation could be measured, suggesting that **6** was isolated as a 1:1 mixture of both possible stereoisomers.

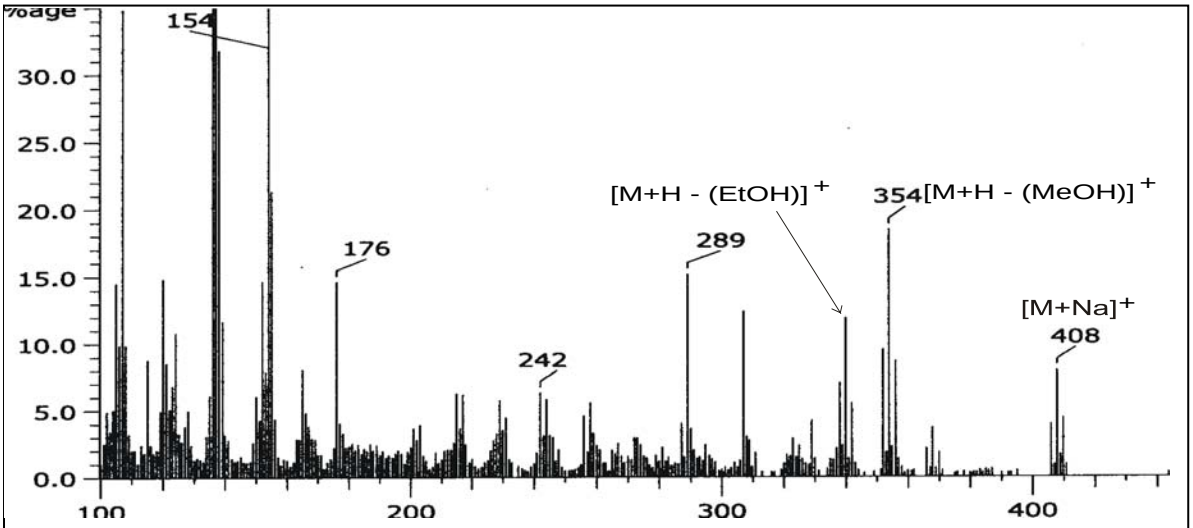

Fig. 3.22: FABMS spectrum of compound 6

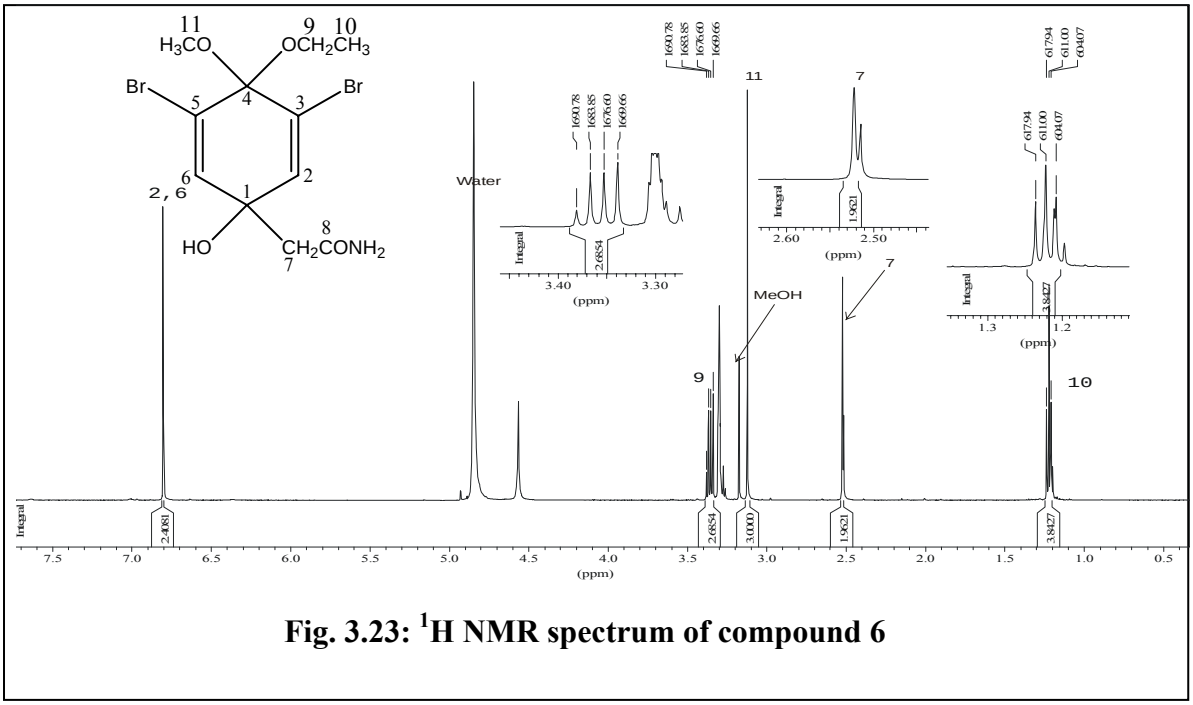

Fig. 3.23: ^{1}H NMR spectrum of compound 6

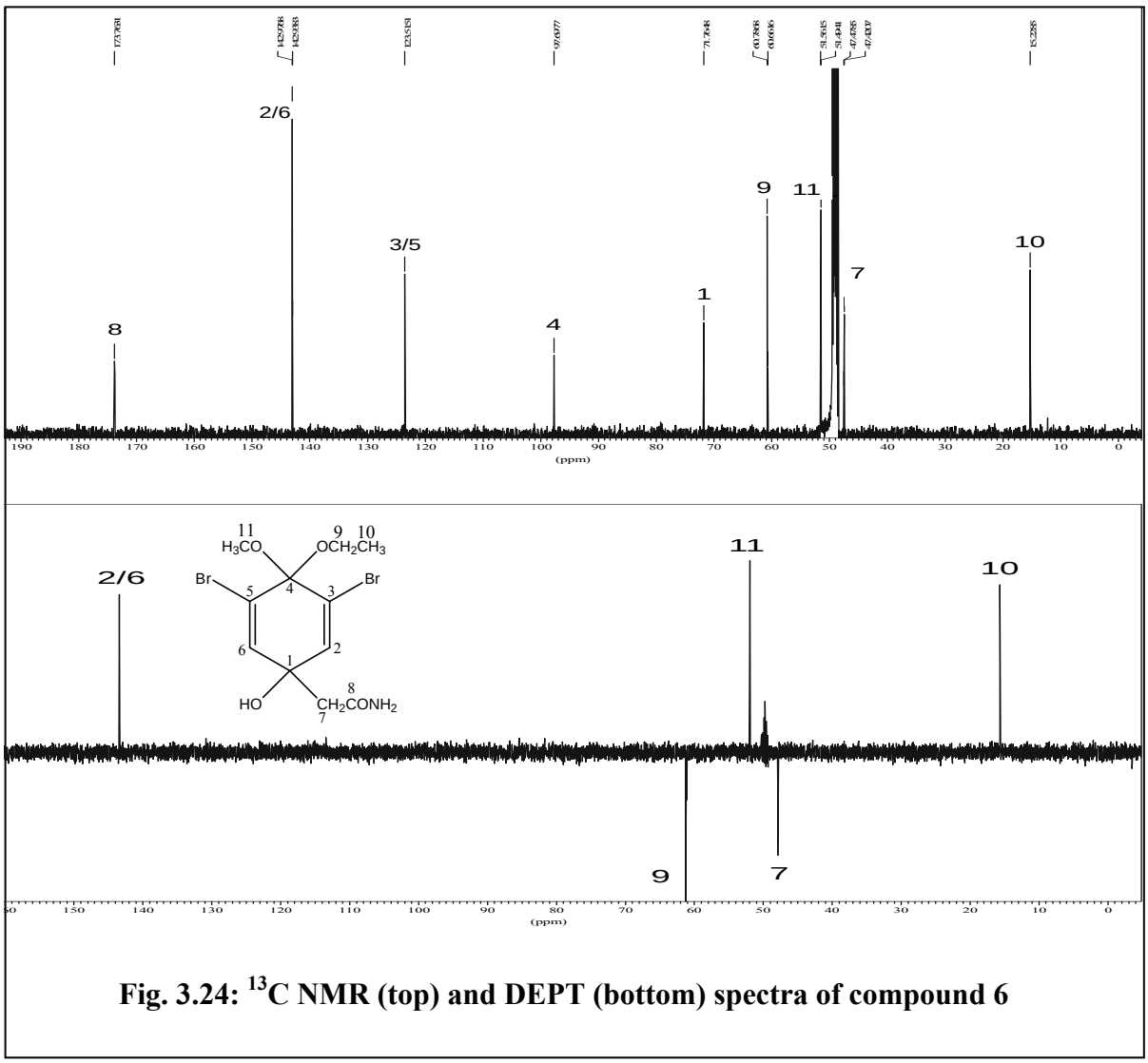

Fig. 3.24: ^{13}C NMR (top) and DEPT (bottom) spectra of compound 6

Table 3.11: NMR data of compound 6

Position	^{1}H NMR (ppm), multiplicity (Hz)	^{13}C NMR (ppm)
1	-	71.8 s
2/6	6.69 (2H, d, 1.5 Hz)	143.0 d
3/5	-	123.5 s
4	-	97.7 s
7A,B	2.52 (2H, s)	47.4 t
8	-	173.8 s
9A,B	3.36 (2H, q, 6.9 Hz)	60.7 t
10	1.22 (3H,t, 6.9 Hz)	15.2 q
11	3.13 (3H, s)	51.5 q

The compound was measured in CD_3OD at 500 MHz.

3.3.2. 3, 5- Dibromo-4-hydroxy-benzaldehyde (7, known compound)

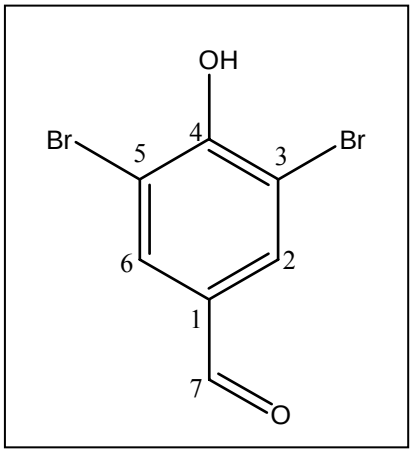

Compound **7** was isolated as yellow oil. It has $UV_{(MeOH)}$ absorbance at λ_{max} 228 and 278 nm. The negative ESIMS gave a cluster with the ratio 1:2:1 at *m/z* 277:279:281 $[M-H]^-$ indicating the presence of two bromine atoms (see Fig. 3.25). This molecular weight is compatible with the molecular formula $C_7H_4Br_2O_2$. With only three signals, the ^1H NMR spectrum of compound **7** was very simple (see Fig. 3.26, Table 3.12). A singlet at 9.22 ppm was characteristic for the presence of an aldehydic proton (H-7) while a singlet for two protons at the aromatic region suggested the presence of a symmetrical tetra-substituted benzene ring. Finally, the presence of the singlet at 8.35 ppm was assigned to a phenolic hydroxyl group. Using the mass and ^1H NMR data, the structure of **7** was confirmed.

Table 3.12: NMR data of compound 7

Position	**^1H NMR (ppm), multiplicity (Hz)**
2/6	7.70 (2H, s)
7A,B	9.22(1H, s)
O*H* at C-1	8.35 (1H, s)

The compound was measured in DMSO-d_6 at 500 MHz.

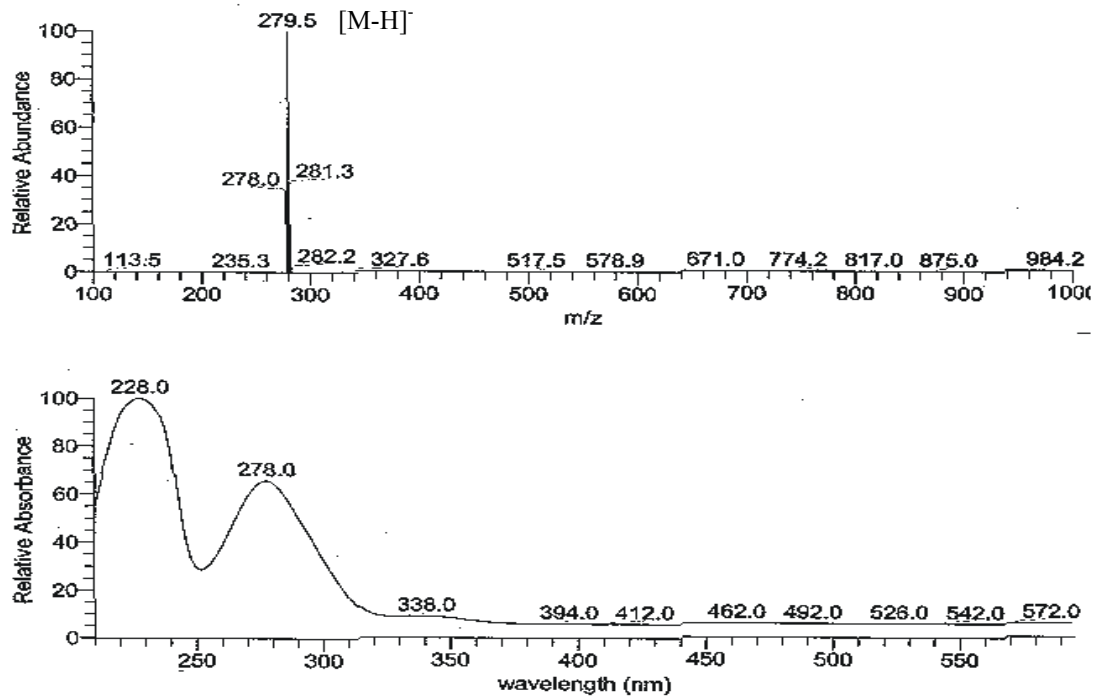

Fig. 3.25: (–) ESI spectrum (top) and UV spectrum (bottom) of compound 7

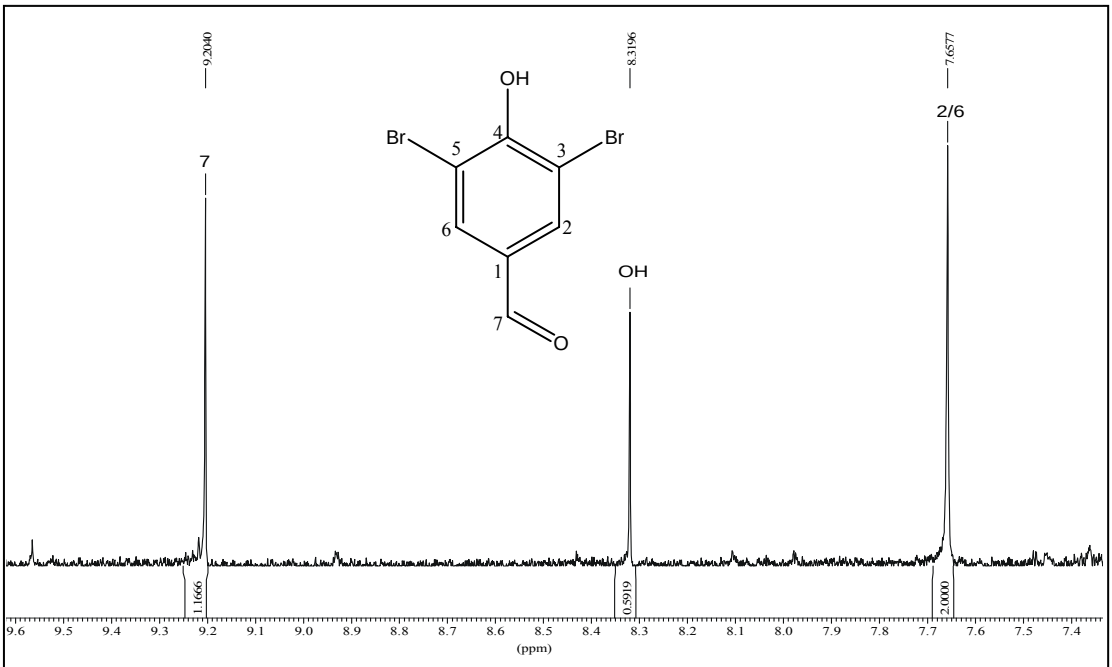

Fig. 3.26: ^{1}H NMR spectrum of compound 7

3.3.3. Dienone (8, known compound)

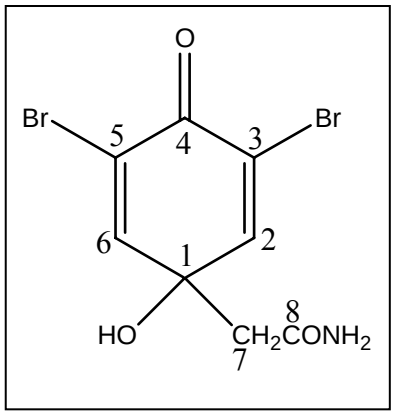

Compound **8** was isolated as a yellow oily substance with UV absorbance at λ_{max} 260 nm (MeOH). The positive ESIMS gave a cluster at *m/z* 324:326:328 as 1:2:1 $[M+H]^+$ indicating the presence of two bromine atoms (see Fig. 3.27). This was compatible with the molecular formula $C_8H_7Br_2NO_3$. The structure of **8** was confirmed using ^{1}H-NMR (see Fig. 3.28 and Table 3.13) and by comparison with data reported for the previously known dienone [Sharma, *et al*., 1967a, and b]. This compound is optically inactive because of its symmetry.

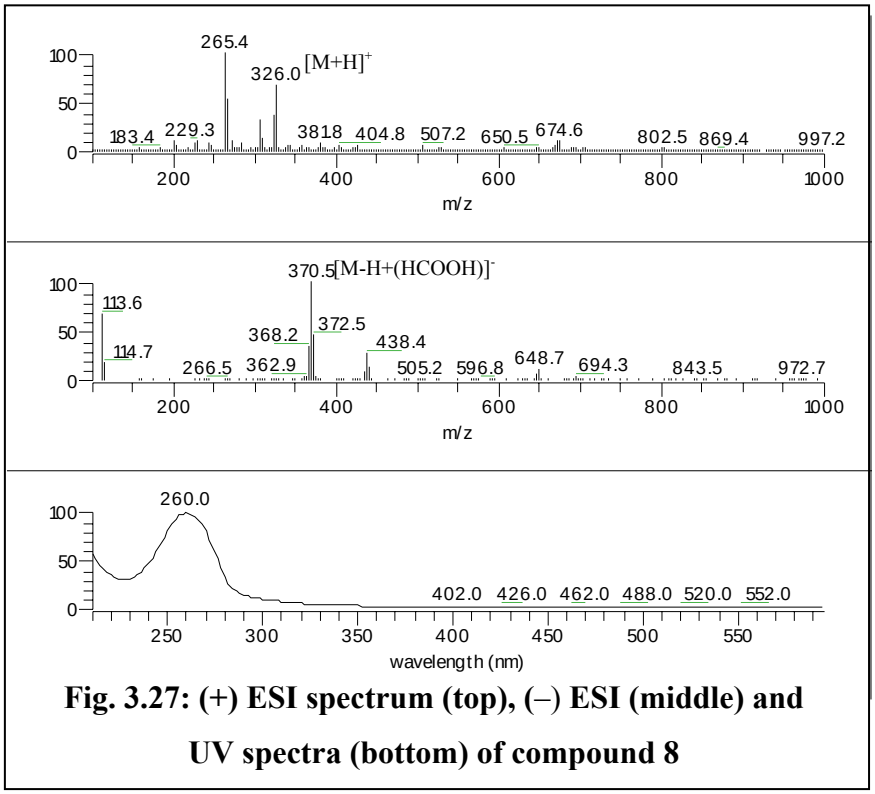

Fig. 3.27: (+) ESI spectrum (top), (–) ESI (middle) and UV spectra (bottom) of compound 8

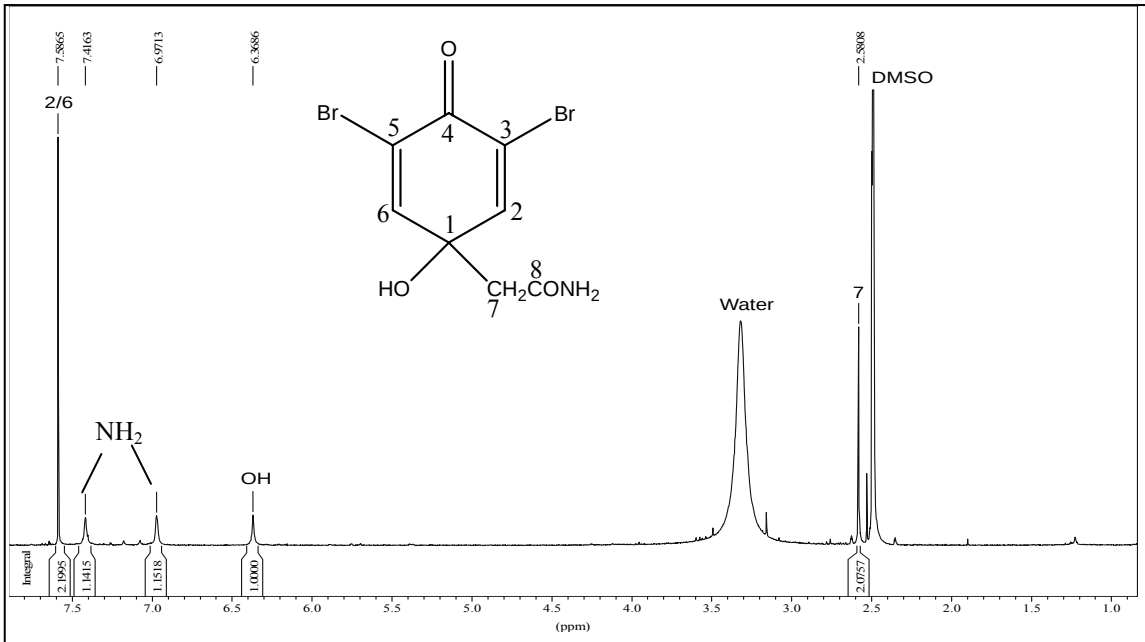

Fig. 3.28: ^{1}H NMR spectrum of compound 8

Table 3.13: NMR data of compound 8

Position	^{1}H NMR (ppm), multiplicity (Hz)
2/6	7.59 (2H, s)
7A,B	2.62 (2H, s)
O*H*	6.38 (1H, br s)
NH_2	6.98 (1H, br s), 7.43 (1H, br s)

The compound was measured in DMSO-d_6 at 500 MHz.

3.3.4. Dienone dimethoxyketal (9, known compound)

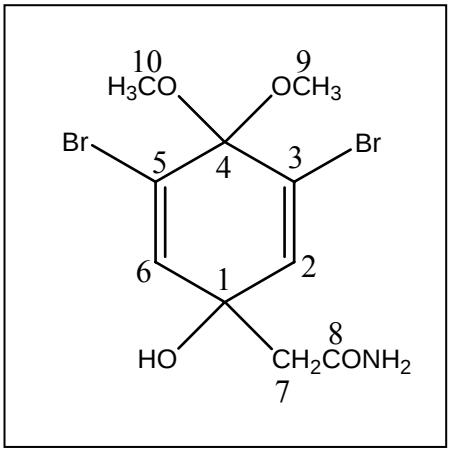

Compound **9** was isolated as yellow oil with the UV maximum absorbance at λ_{max} 218 (MeOH). The positive ESIMS gave a cluster at 338: 340: 342 for $[M+H-(MeOH)]^+$ with the ratio 1:2:1 indicating the presence of two bromine atoms. On the other hand, the negative ESIMS gave a cluster at *m/z* 414:416:418 for $[M-H + (HCOOH)]^-$ (see Fig. 3.29). This molecular weight is compatible with the molecular formula $C_{10}H_{13}Br_2NO_4$. Comparison between the ^1H NMR spectra of compound **9** (see Fig. 3.30 and Table 3.14) to that of dienone (see Fig. 3.28) revealed that the two compounds are closely related. The most important difference was the presence of two additional singlets at 2.98 and 3.04 ppm for two methoxy groups. The two methoxy groups appeared at two different chemical shifts because they are chemically but not magnetically equivalent. On the other hand, the upfield chemical shift of H-2/6 at 6.79 ppm in comparison to that in dienone suggested that compound **9** is a dimethoxyketal of dienone where the carbonyl group is substituted with two methoxy groups [Andersen, *et al*., 1973]. The structure of **9** was confirmed by comparison of the mass and ^1H NMR data with those reported for the known compound dienone-dimemethoxyketal [Sharma, *et al*., 1970]. This compound is optically inactive like dienone because of its symmetry.

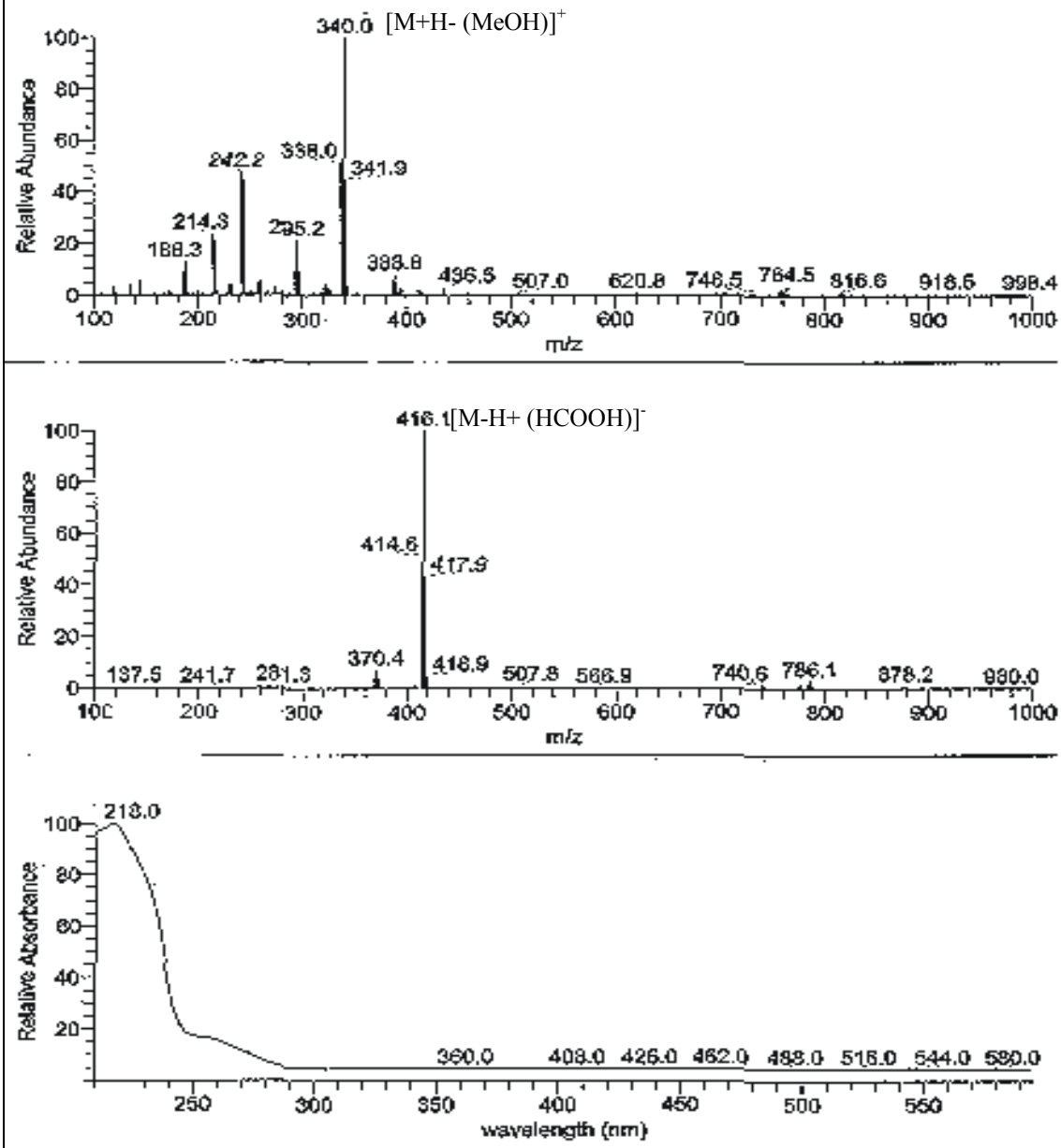

Fig. 3.29: (+) ESI spectrum (top), (–) ESI (middle) and UV spectra (bottom) of compound 9

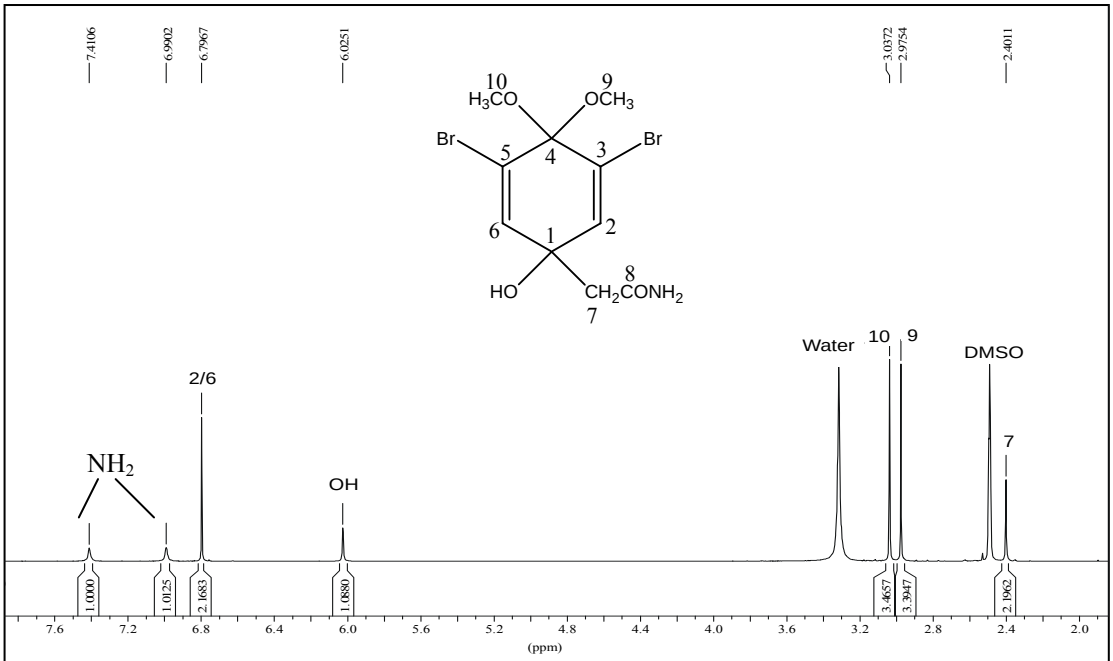

Fig. 3.30: ^{1}H NMR spectrum of compound 9

Table 3.14: NMR data of compound 9

Position	^{1}H NMR (ppm), multiplicity (Hz)
2/6	6.79 (2H, s)
7A,B	2.40 (2H, s)
9*	2.98 (3H, s)
10*	3.04 (3H, s)
O*H*	6.03 (1H, s)
NH_2	7.00 (1H, br s), 7.42 (1H, br s)

The compound was measured in DMSO-d_6 at 500 MHz.
* These values may be interchanged.

3.3.5. Purealidin R (10, known compound)

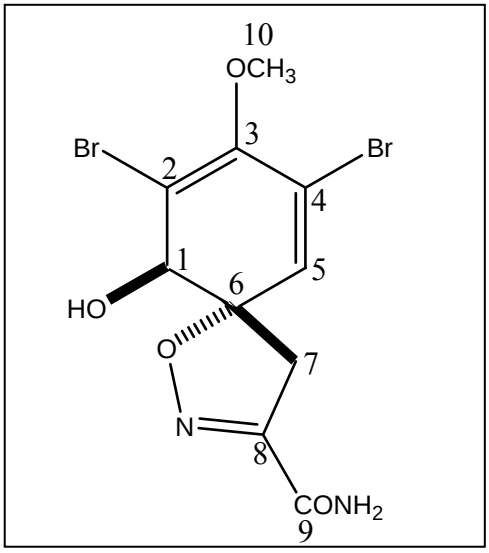

Compound **10** was isolated as a yellow oil with UV absorbance at λ_{max} 228 and 288 nm and $[\alpha]_D^{20}$ = +21.5, (c = 0.041, MeOH). The EIMS of compound 10 showed an isotope pattern of 1:2:1 for the $[M]^+$ 380:382:384 (3%) and two other fragments at 336:338:340 (5%), 304:306:308 (15%), indicative of the presence of two bromine atoms (see Fig. 3.31). This molecular weight is compatible with the molecular formula $C_{10}H_{10}Br_2N_2O_2$. The ^{1}H NMR spectrum (see Fig. 3.32 and Table 3.15) exhibited signals typical for a spirocyclohexadienylisoxazoline ring at 3.91 ppm (s, H-1), 6.58 ppm (s, H-5) and 3.18, 3.58 ppm (two doublets, 1 H each, *J* = 18.3 Hz, C*H*$_2$-7) [Gao, *et al*., 1999]. Furthermore, the spectrum contained a signal at 3.64 ppm which indicated the presence of a methoxy group. Comparison of the UV, mass spectrum, optical rotation and ^{1}H NMR data of compound **10** with those reported for the known compound purealidin R confirmed the structure [Kobayashi, *et al*., 1995]. The relative stereochemistry at C-1 and C-6 of the spiroisoxazole ring was deduced to be *trans* between the hydroxyl group at C-1 and the oxygen atom in the isoxazoline ring from the proton chemical shift of 3.91 ppm for H-1 [Nishiyama, *et al.,* 1985). It was confirmed that compound **10** was dextrorotatory from the comparison of the sign of the optical rotation with that reported for purealidin R indicating that the configurations at C-1 and C-6 are 1*R* and 6*S* [McMillan, *et al*., 1981].

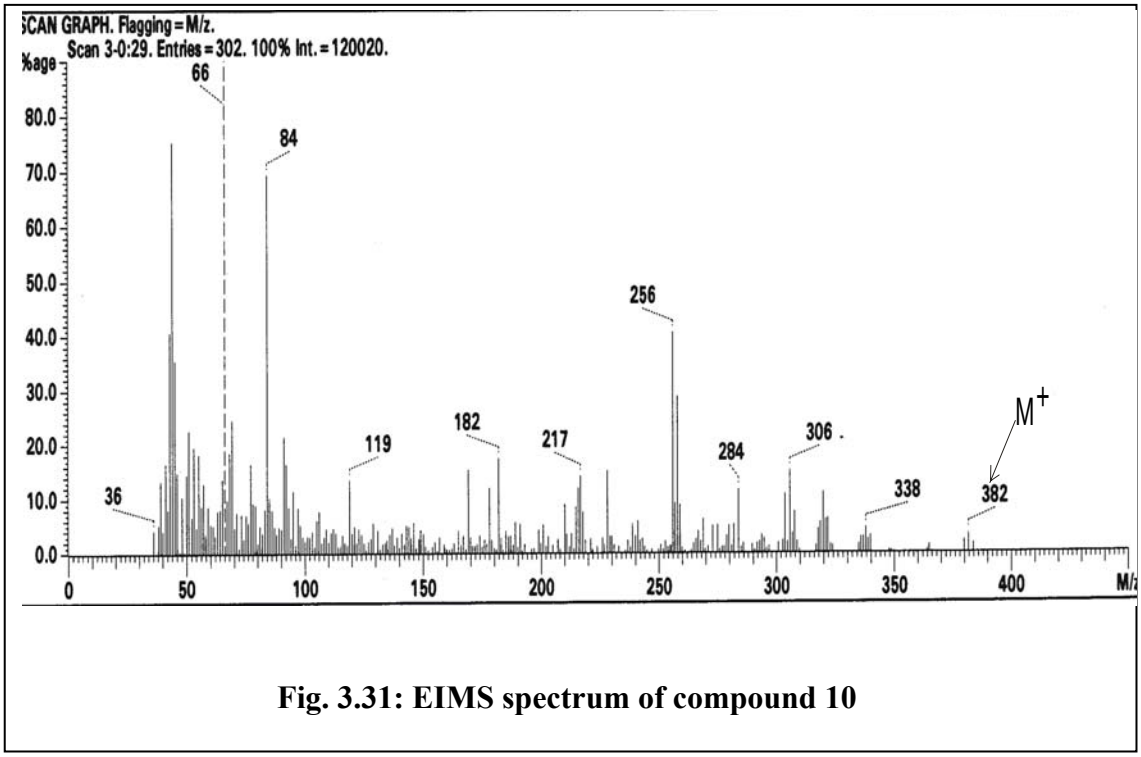

Fig. 3.31: EIMS spectrum of compound 10

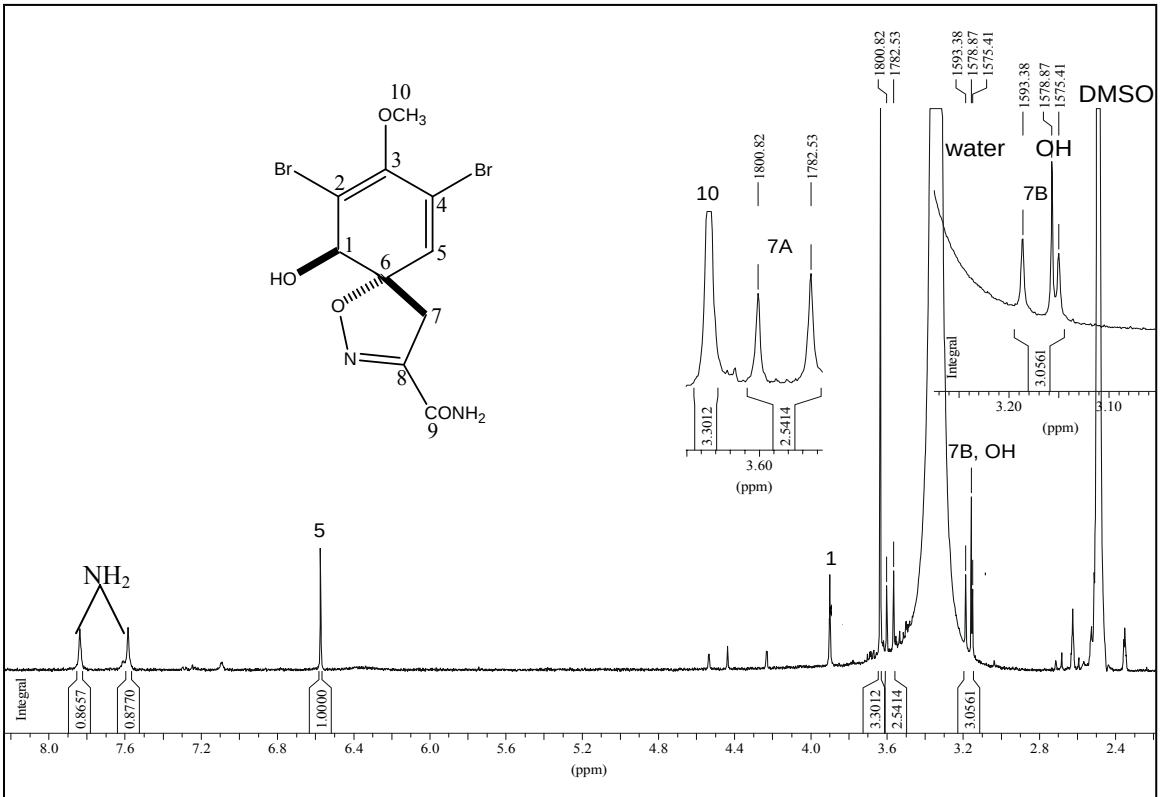

Fig. 3.32: ^{1}H NMR spectrum of compound 10

Table 3.15: NMR of compound 10

Position	^{1}H NMR (ppm), multiplicity (Hz)
1	3.91 (1H, s)
5	6.58 (1H, s)
7A	3.58 (1H, d, 18.3 Hz)
7B	3.18 (1H, d, 18.3 Hz)
O*C*H_3	3.64 (3H, s)
O*H*	3.17 (1H,s)
NH_2	7.59 (1H, br s), 7.84 (1H,br s)

The compound was measured in DMSO-d_6 at 500 MHz.

3.3.6. 2-(3, 5-Dibromo-4-hydroxyphenyl)-acetamide (11, known compound)

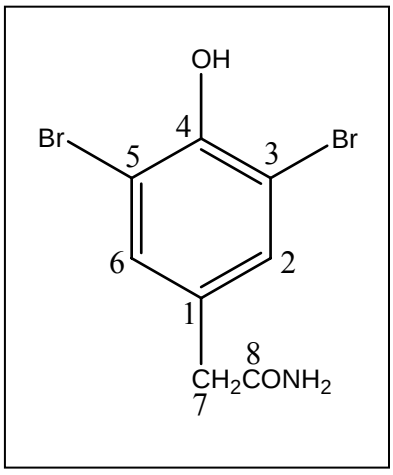

Compound **11** was isolated as yellow oil with UV absorbance at λ_{max} 212 and 290 nm (MeOH). The positive ESIMS of compound **11** showed a cluster at *m/z* 308:310:312 $[M+H]^+$ with the ratio 1:2:1 indicating the presence of two bromine atoms (see Fig. 3.33). This molecular weight is compatible with the molecular formula $C_8H_7Br_2NO_2$. The ^{1}H NMR of compound **11** (see Fig. 3.34 and Table 3.16) was very simple. It only showed a signal at 7.32 ppm (2H, s, H-2 and H-6), 3.21 ppm (2H, s, H-7A and H-7B) and two signals at 6.88 and 7.40 ppm (br s) for NH_2. According to the ^{1}H NMR data of compound **11** and also the mass

spectra, it was clear that **11** is a bromotyrosine alkaloid derivative. The HMBC spectral analysis of **11** (see Fig. 3.35) showed a strong cross peak between H-7 and C-2/6 and C-8 which confirmed the position of the carbonyl group. On the other hand, the cross peak between H-2/6 and C-3/5 confirmed the position of the two bromine atoms. Comparison of the ^{1}H NMR and HMBC data of compound **11** with those reported for the known bromotyrosine alkaloid 2-(3,5-dibromo-4-hydroxyphenyl)-acetamide [Chib, *et al.*, 1978] confirmed the structure of **11** to be identical to the other.

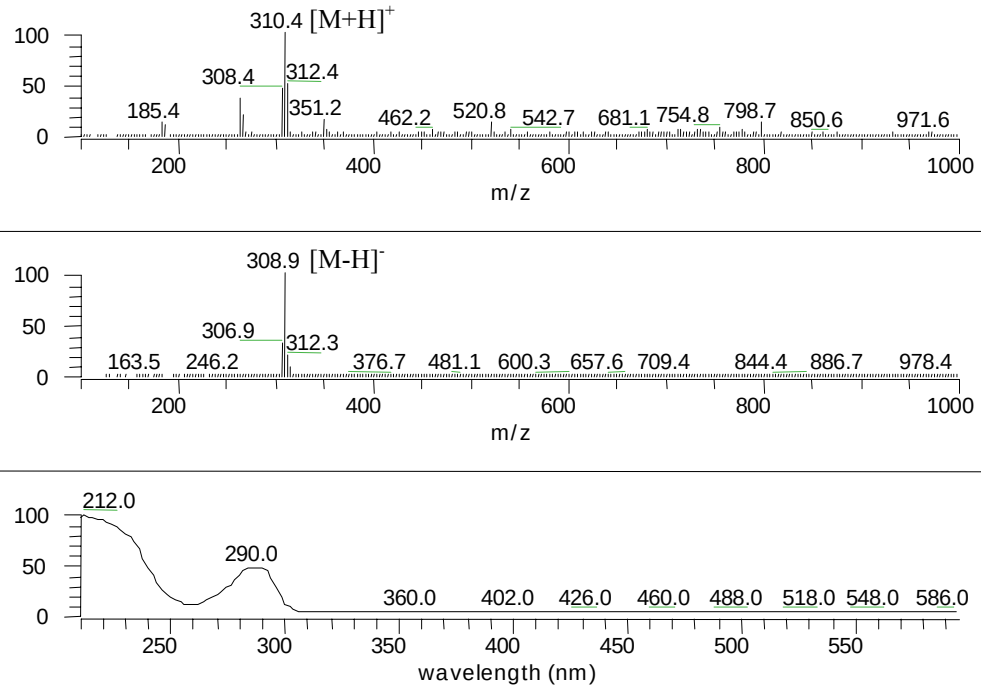

Fig. 3.33: (+) **ESI (top), (-) ESI (middle) and UV spectra (bottom) of compound 11**

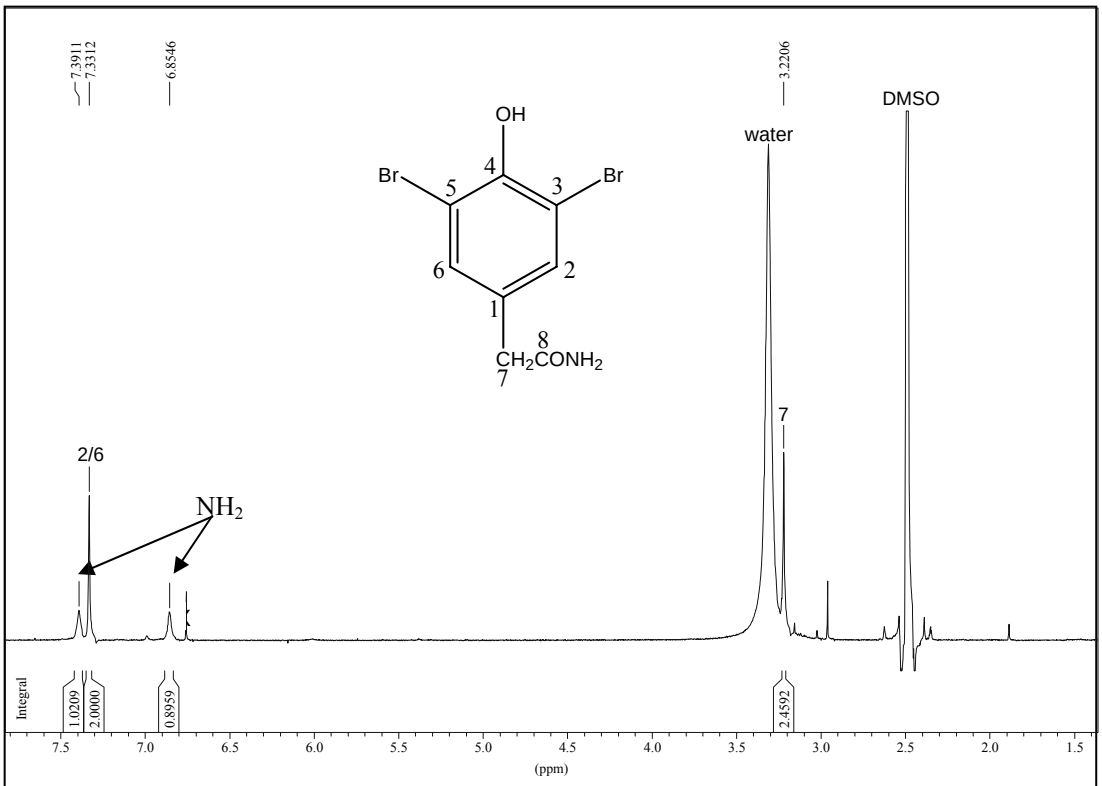

Fig. 3.34: ^{1}H NMR spectrum of compound 11

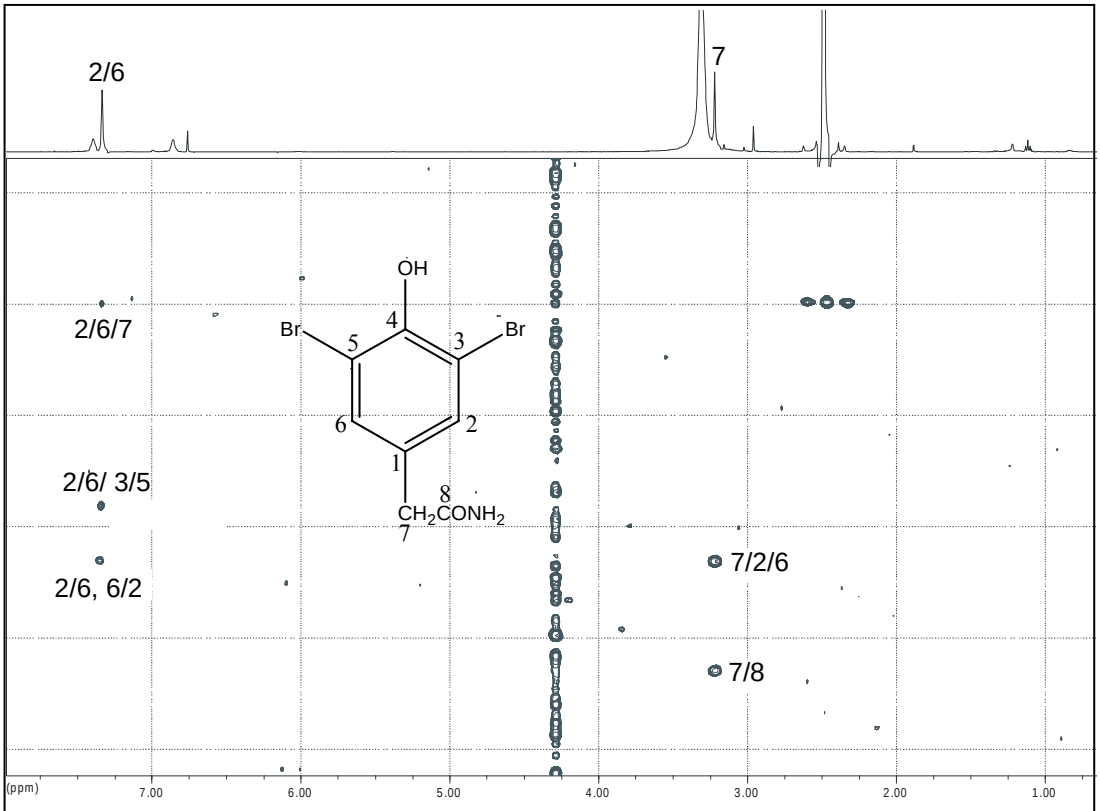

Fig. 3.35: HMBC spectrum of compound 11

Table 3.16: NMR data of compound 11

Position	^{1}H NMR (ppm), multiplicity (Hz)	^{13}C NMR (ppm)*	HMBC correlations H ⟶ C
2/6	7.32 (2H, s)	132.7 d	7, 3, 5
3/5	-	112.6 s	2/6
7A,B	3.21 (2H, s)	40.2 t	2/6, 8
8	-	171.6 s	-
NH_2	6.88 (1H,br s), 7.40 (1H, br s)	-	-

The compound was measured in DMSO-d_6 at 500 MHz.
* Obtained from the HMBC spectrum.

3.3.7. Bisoxazolidinone derivative (12, known compound)

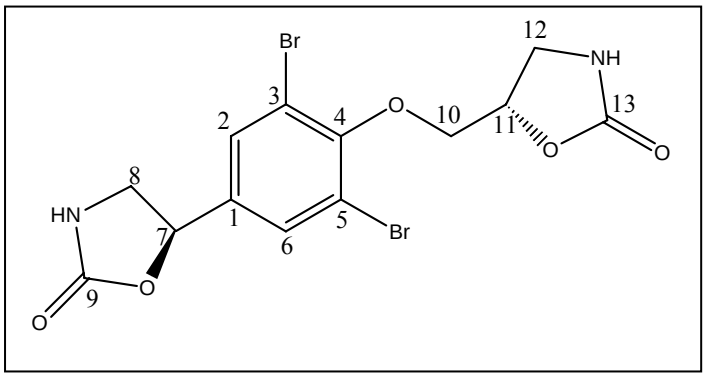

Compound **12** was isolated as a yellow oil with the UV absorbance at λ_{max} 218 and 275 nm (MeOH) and $[\alpha]_D^{20}$ = +20.2 (*C* = 0.064, MeOH). The negative ESIMS of compound **12** showed a cluster at *m/z* 433:435:437 $[M-H]^-$ with the ratio 1:2:1 indicating the presence of two bromine atoms (see Fig. 3.36). This molecular weight is compatible with the molecular formula $C_{13}H_{12}Br_2N_2O_5$. The ^{1}H NMR spectrum of **12** (see Fig. 3.37 and Table 3.17) revealed the presence of a singlet at 7.73 ppm for two protons (H-2 and H-6) which suggested the presence of a symmetric aromatic ring. This is compatible with the presence of a peak at 130.5 ppm for two carbons in the ^{13}C NMR spectrum (see Fig. 3.38 and Table 3.17). Furthermore, the ^{13}C NMR spectrum displayed a peak at 117.7 ppm which was attributed to a symmetrical aromatic carbon bearing bromine. Full inspection of the ^{1}H, ^{13}C and DEPT NMR

spectra of **12** revealed three methylene carbons, four methine carbons, two carbamide groups at 158.2, 158.5 ppm and four quaternary carbons of the tetra-substituted benzene ring. On the other hand, the COSY spectrum (see Fig. 3.39) indicated two spin systems in addition to the singlet for two aromatic protons at 7.73 ppm. This confirmed the presence of two oxazolidinone rings in addition to the aromatic ring. The connection of the three rings was determined through a strong correlation in the HMBC spectrum (see Fig. 3.40) between H-7 and C-2, C-6; H-12 and C-10 and C-13. Furthermore, the strong correlation between H-2/H-6 with C-4 (^3J) and H-8A and H-8B with C-1 (^3J) confirmed the position of the two bromine atoms at C-3/C-5. This is compatible with the upfield shift of C-3/C-5 at 117.7 ppm in comparison to that of C-2/C-6 at 130.5 ppm. The chemical shifts of the two carbamide groups were indirectly determined through their correlations in the HMBC spectrum. The structure of **12** was confirmed by comparison of the NMR data of **12** with those reported for the known bisoxazolidinone derivative [Borders, *et al*., 1974]. Concerning the absolute streochemistry of **12**, it is clear that, four stereoisomers (R, R), (R, S), (S, R) and (S, S) at the two chiral carbon atoms C-7 and C-11 respectively are possible. Three of them (R,S), (S,R) and (R,R) were isolated from nature, while the last form (S,S) has not yet been encountered uptill now [Norte, *et al.,* 1988, Makarieva *et al.,* 1981 and Borders, *et al*., 1974]. Comparison of the optical rotation, the ^{1}H NMR chemical shifts and coupling constants of the oxazolidinone moiety of compound **12** and those reported for the different stereoisomers confirmed that compound **12** is the (R, S) form as previously isolated from Borders' group.

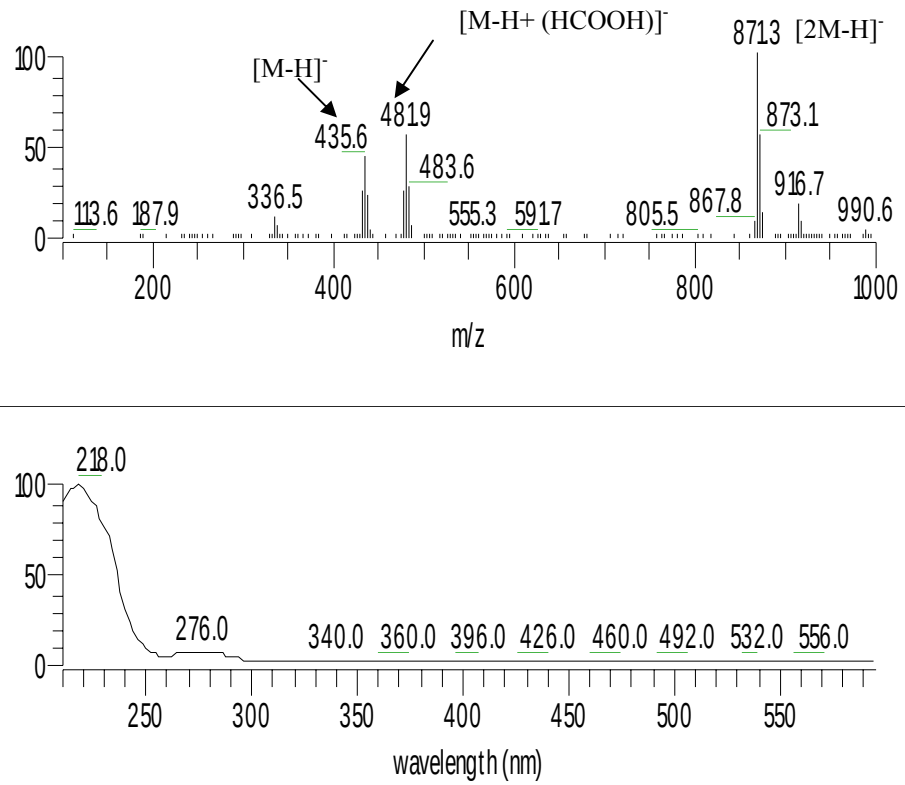

Fig. 3.36: (–) ESI (top) and UV spectra (bottom) of compound 12

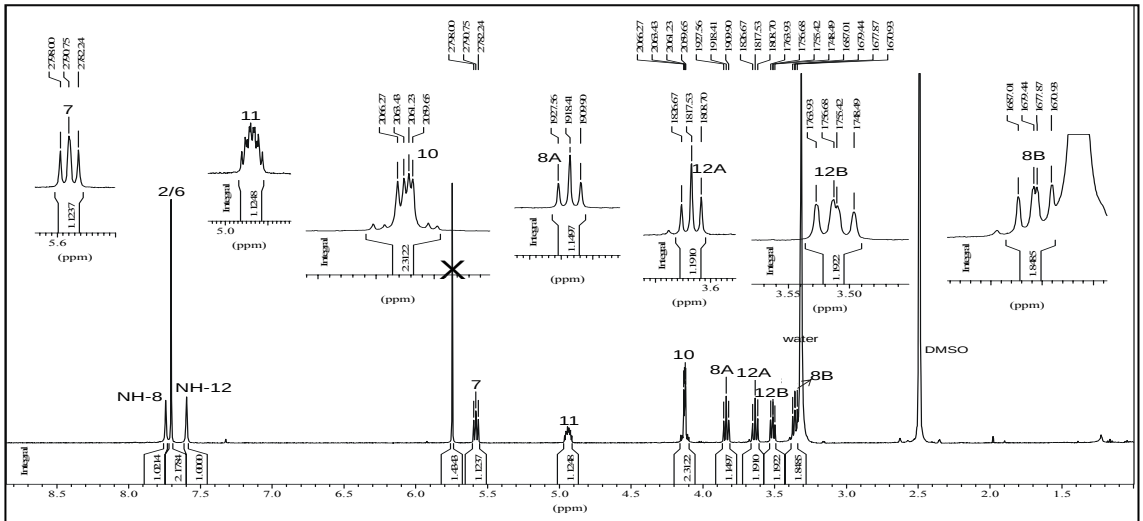

Fig. 3.37: ^{1}H NMR spectrum of compound 12

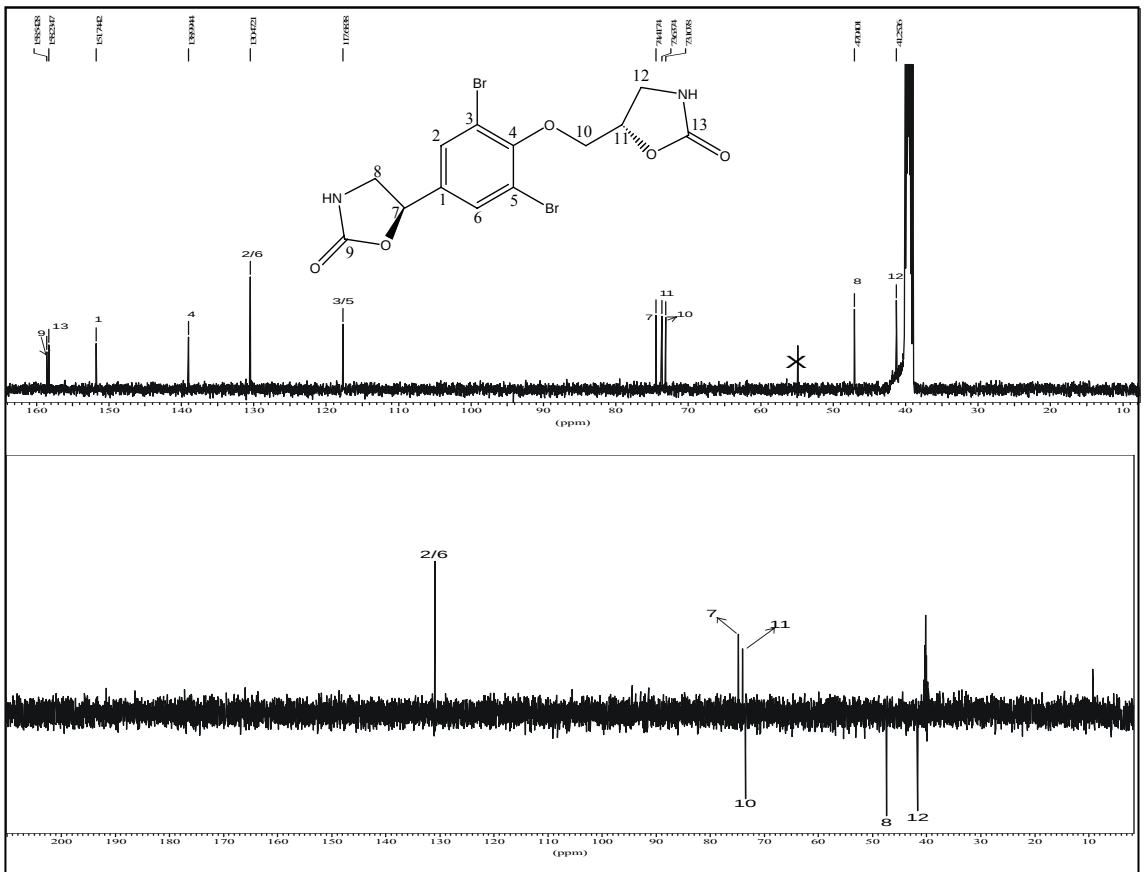

Fig. 3.38: ^{13}C NMR (top) and DEPT (bottom) spectra of 12

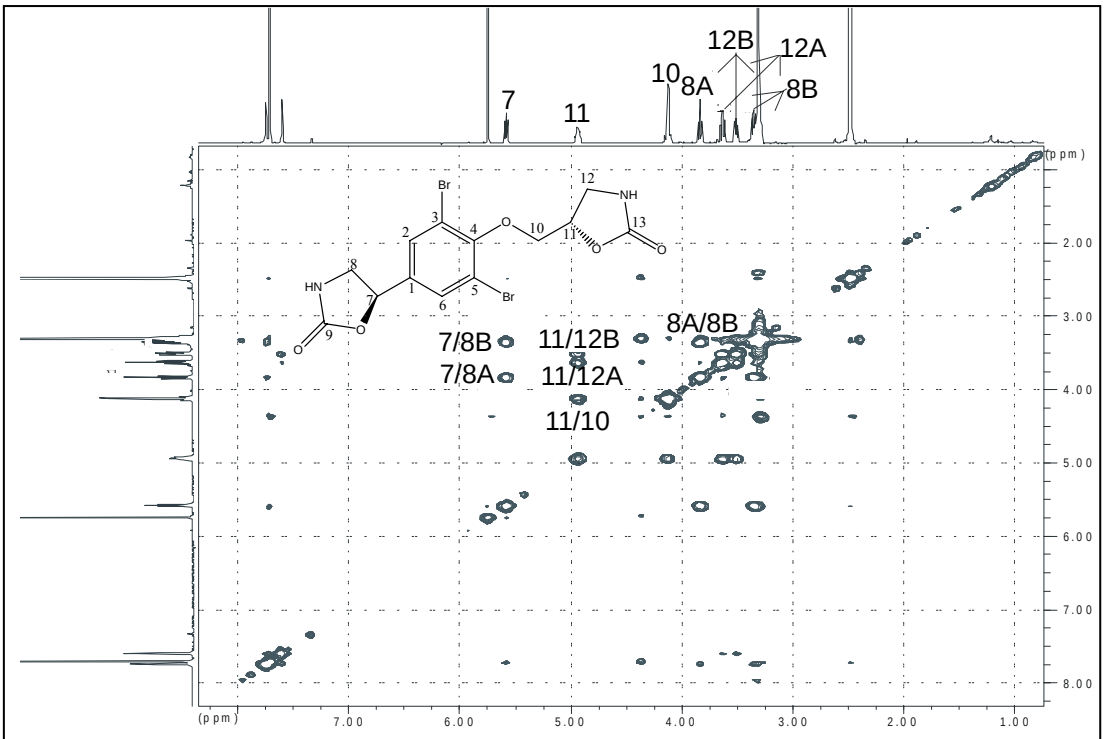

Fig. 3.39: COSY spectrum of compound 12

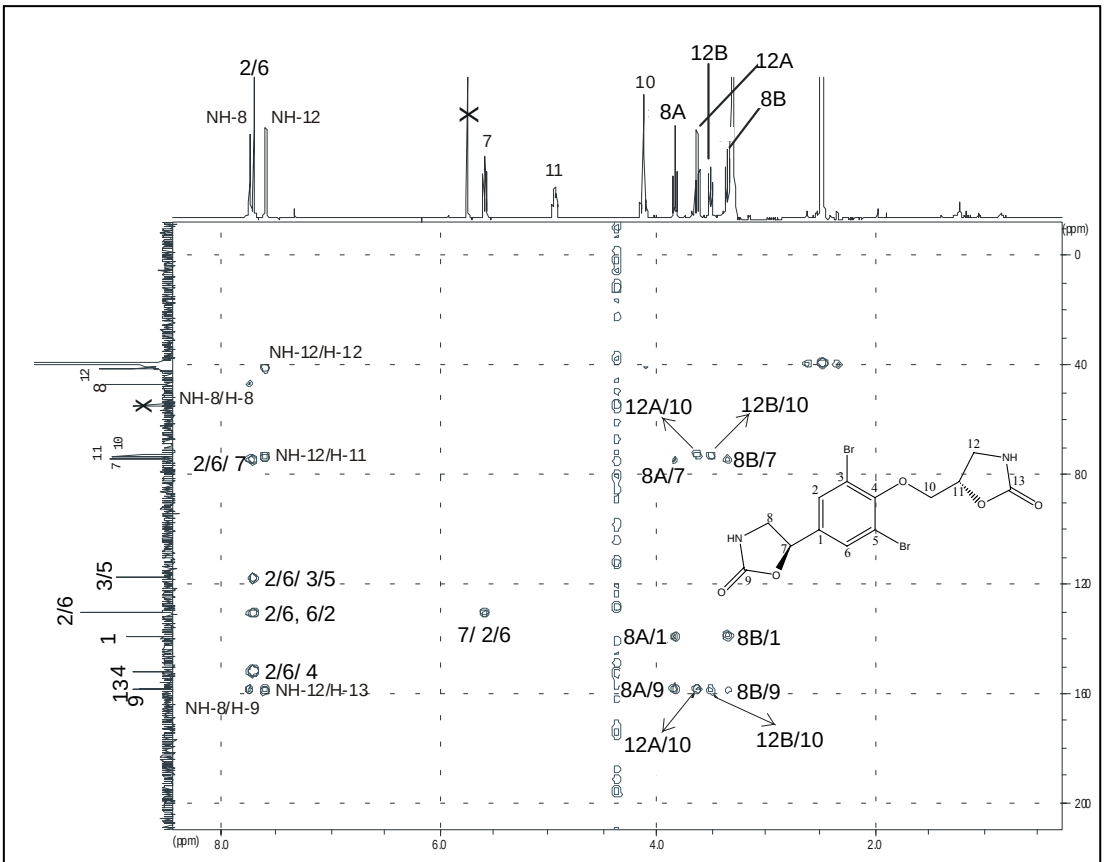

Fig. 3.40: HMBC spectrum of compound 12

Table 3.17: NMR data of compound 12

Position	^{1}H NMR (ppm), multiplicity (Hz)	^{13}C NMR (ppm)	HMBC correlations H → C
1	-	139.0 s	
3/5	-	117.7 s	
2/6	7.73 (2H, s)	130.5 d	7, 3/5, 4
4	-	151.7 s	
7	5.58 (1H, t, 8.5 Hz)	74.4 d	2/6
8A	3.84 (t, 8,5 Hz)	47.0 t	1, 7 , 9
8B	3.41 (dd, 8.5, 6.9 Hz)	-	1, 7 , 9
9	-	158.5 s	
10A,B	4.14 (2H, m)	73.1 t	
11	4.95, m	73.6 d	
12A	3.65 (t, 8.8 Hz)	41.3 t	10, 13
12B	3.53 (t, 8.2 Hz)	-	10, 13
13	-	158.2 s	
N*H*-8	7.78 (1H, s)	-	7, 8 , 9
N*H*-12	7.60 (1H, s)	-	11, 12 , 13

The compound was measured in DMSO-d_6 at 500 MHz.

3.3.8. 3, 5-Dibromo-2-hydroxy-4-methoxyphenylacetic acid (13, new natural product)

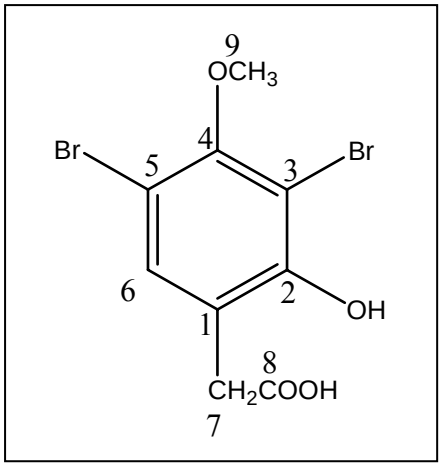

Compound **13** was isolated as yellow oil with UV absorbance at λ_{max} 218 and 290 nm. The HREIMS showed a cluster at *m/z* 338:340:342 $[M]^+$ with a ratio 1:2:1 indicating the presence of two bromine atoms (see Fig. 3.41). This molecular weight is compatible with the molecular formula $C_9H_8Br_2O_4$. The ^1H NMR of compound **13** (see Fig. 3.42 and Table 3.18) showed the presence of a methoxy group at 3.76 ppm (3H, s), a methylene at 3.57 ppm (2H, s), an aromatic proton at 7.42 ppm and two broad singlets at 12.41 and 6.55 ppm for an acidic hydroxyl group and phenolic OH group, respectively. On the other hand, the ^{13}C and DEPT spectra (see Fig. 3.43 and Table 3.18) also revealed one methoxy, one methylene, one methine, five quaternary carbons and one carbonyl group. The downfield chemical shift of the methylene group at 3.57 ppm suggested that this methylene is attached to the carbonyl group which is confirmed by the presence of a cross peak between H-7 and C-8 in the HMBC spectrum (see Fig. 3.44). The attachment of this methylene group with the benzene ring was confirmed by a strong ^3J correlation with C-2/6 and ^2J correlation with C-1 in the HMBC spectrum. Furthermore, the position of the methoxy group was confirmed through the strong correlation between the methoxy protons and C-4 in the HMBC spectrum. Thus, compound **13** was identified as 3, 5-dibromo-2-hydroxy-4-methoxyphenylacetic acid. This compound was so far only reported as a degradation product of the known compound homoaerothionin [Moody, *et al*., 1972], but has never been isolated as a true natural product until now.

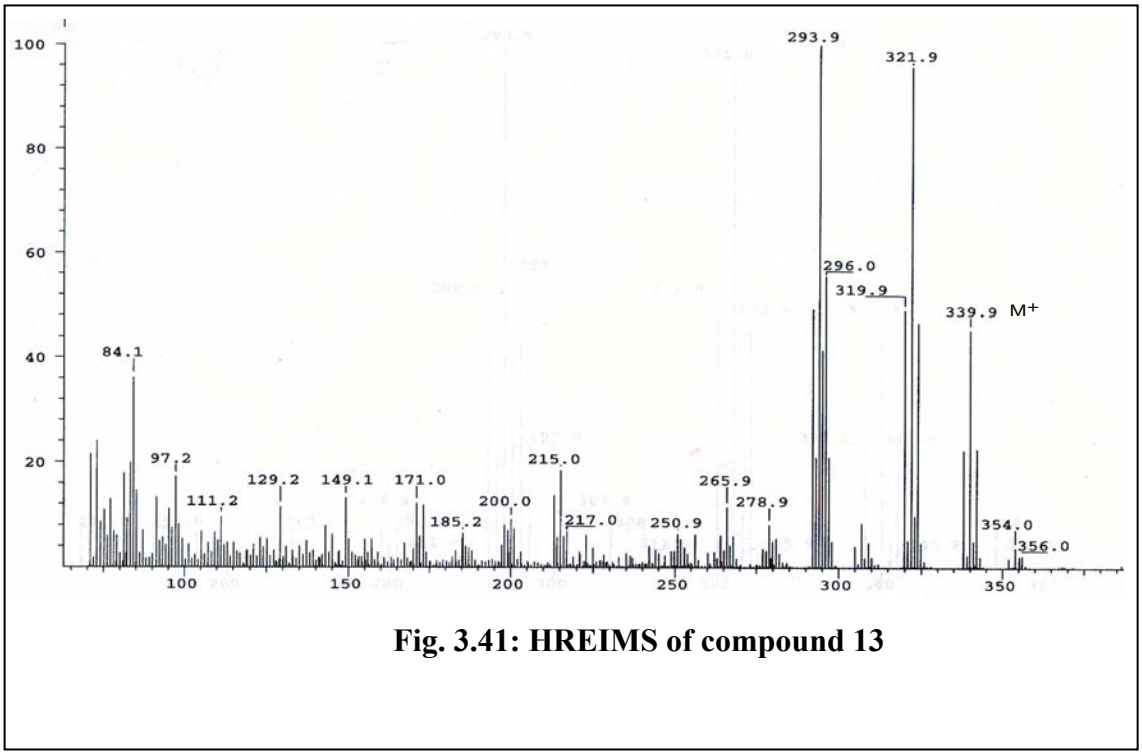

Fig. 3.41: HREIMS of compound 13

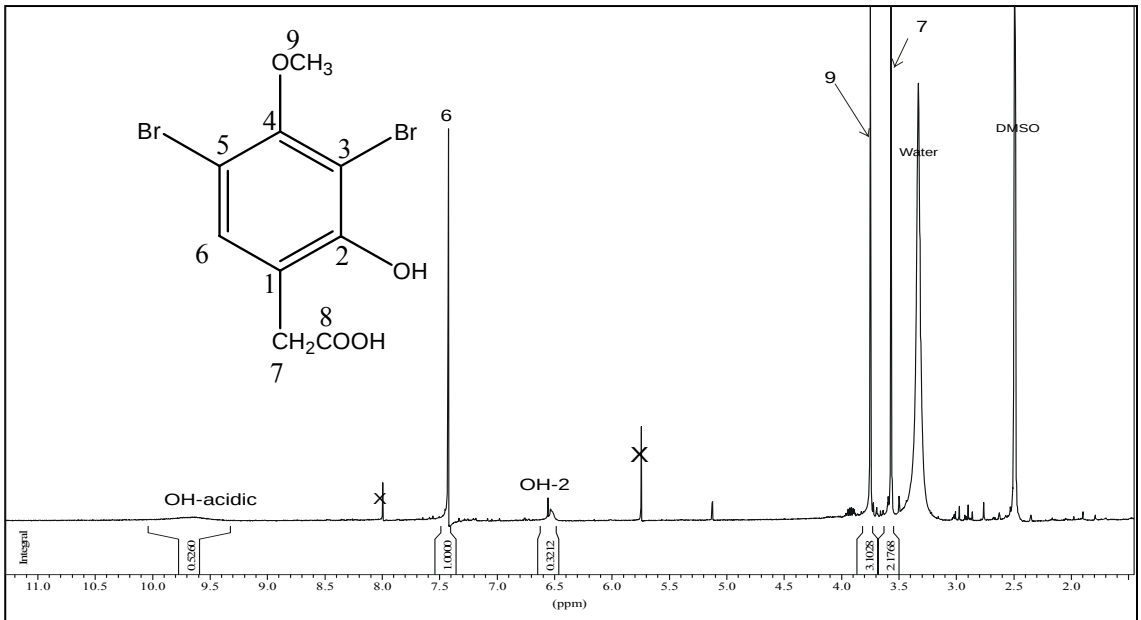

Fig. 3.42: ^{1}HNMR spectrum of 13

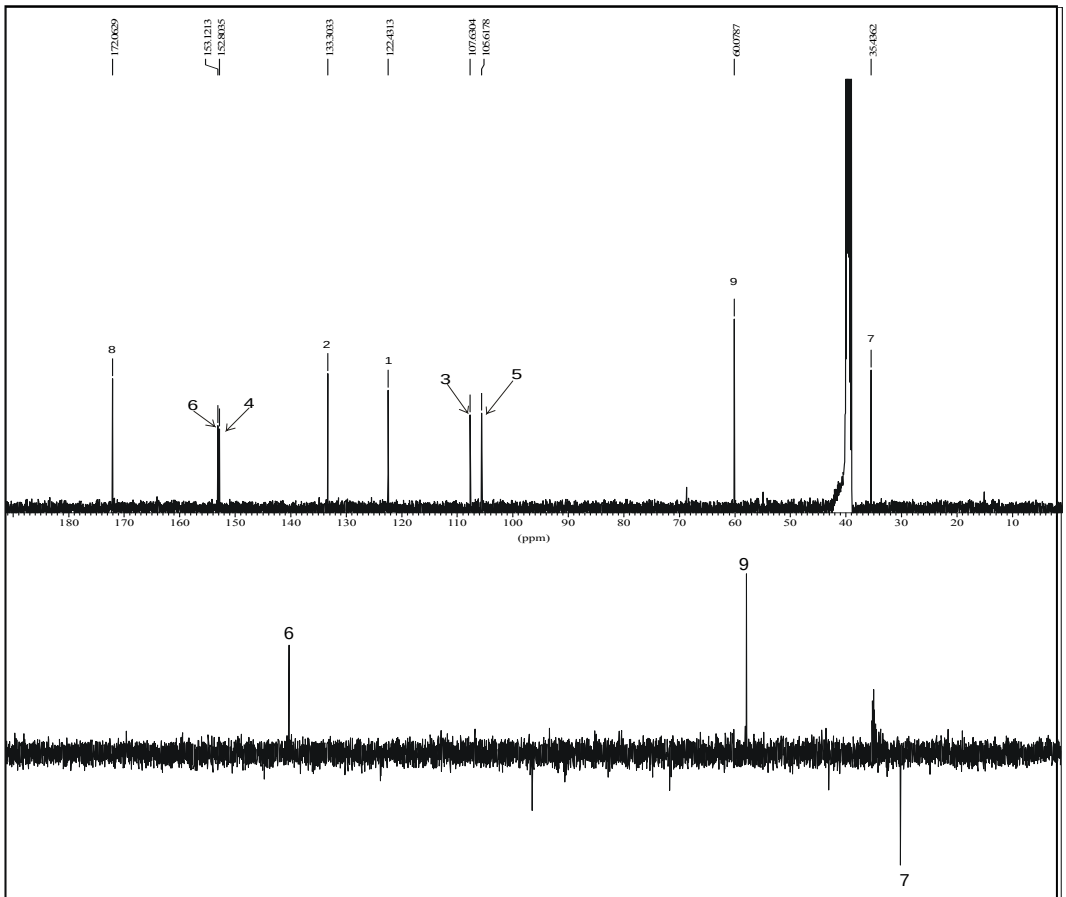

Fig. 3.43: ^{13}C NMR (top) and DEPT (bottom) spectra of compound 13

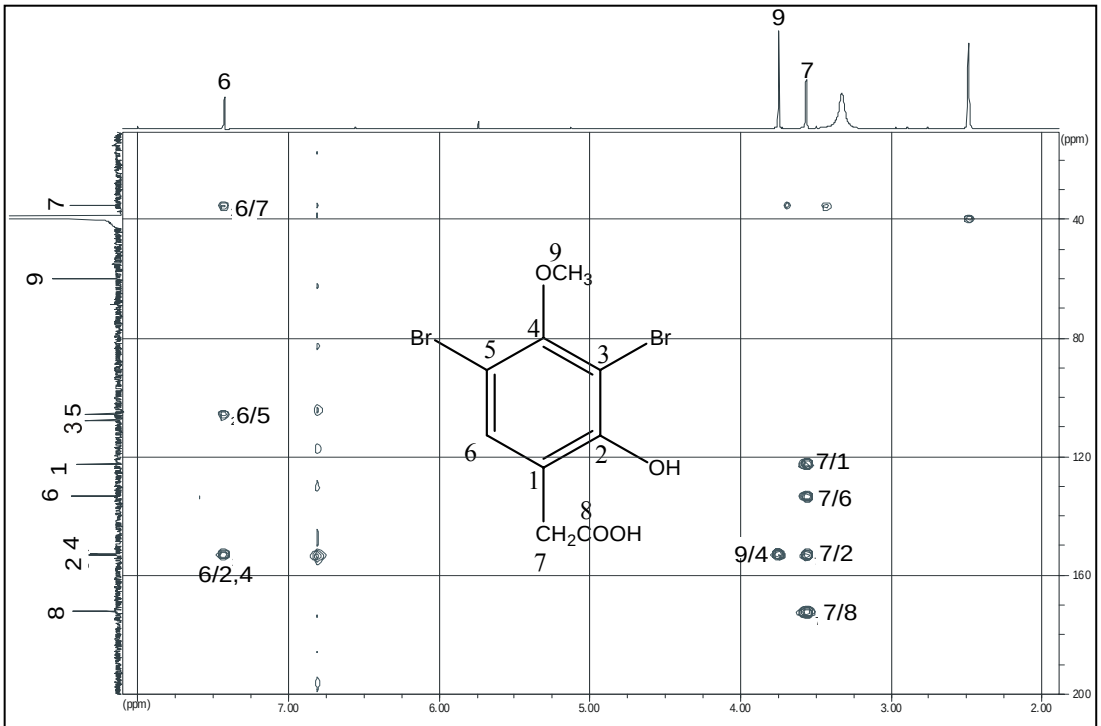

Fig. 3.44: HMBC spectrum of compound 13

Table 3.18: NMR data of compound 13

Position	^{1}H NMR (ppm), multiplicity (Hz)	^{13}C NMR (ppm)	HMBC correlations H → C
1	-	122.4 s	
6	7.42 (1H, s)	133.3 d	2, 4, 5, 7
3	-	107.6 s	
4	-	152.8 s	
5	-	105.6 s	
2	-	153.1 s	
7A,B	3.57 (2H, s)	35.4 t	1, 2, 6, 8
8	-	172.0 s	
9	3.76 (3H, s)	60.1 q	
O*H*-2	6.55 (1H, s)	-	2
O*H*-acidic	12.41 (1H, s)	-	4

The compound was measured in DMSO-d_6 at 500 MHz.

3.3.9. Hydroxydienoic acid (14, known compound)

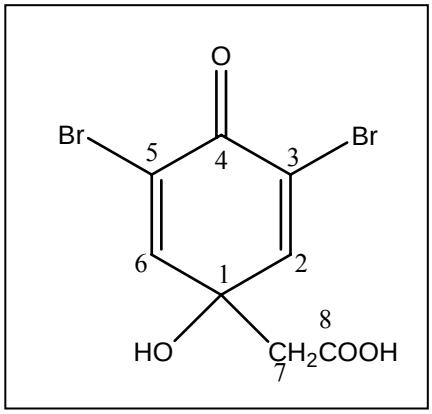

Compound **14** was isolated as yellow oil with UV absorbance at λ_{max} 258 nm. The negative ESIMS of compound **14** showed a cluster at *m/z* 323:325:327 $[M-H]^-$ with the ratio 1:2:1 indicating the presence of two bromine atoms (see Fig. 3.45). This molecular weight is compatible with the molecular formula $C_8H_6Br_2O_4$ which was also confirmed from the HREIMS. The ^{1}H NMR spectrum of compound **14** (see Fig. 3.46 and Table 3.19) revealed the

presence of a singlet at 7.69 ppm for two protons (H-2/6), a singlet at 2.78 ppm for two protons indicating the presence of a methylene group (H-7) attached to a carbonyl function (C-8). This was confirmed by the presence of a cross peak between H-7 and C-8 in the HMBC spectrum (see Fig. 3.46). Furthermore, the ^{1}H NMR spectrum showed also two broad singlets at 12.45, 6.40 ppm indicating the presence of an acidic OH group and another normal OH group, respectively. The comparison between the ^{1}H NMR data of compound **14** and that reported for the known compound dienone (**8**) (see page 61) suggested that compound **14** is closely related to **8** with the exception that it contained a carboxylic acid function instead of an amide group as in dienone. This was confirmed by the difference of one mass unit in the molecular weight between compound **14** and dienone. The full ^{13}C NMR data of **14** (see Table 3.19) was assigned through the HMBC spectrum. It was reported that hydroxydienoic acid (**14**) was first synthesized from the known compound dienone dimethoxyketal (**9**) [Sharma, *et al*., 1970], but was later obtained as a natural product from the sponge *Aplysina thiona* [Cruz, *et al*., 1990].

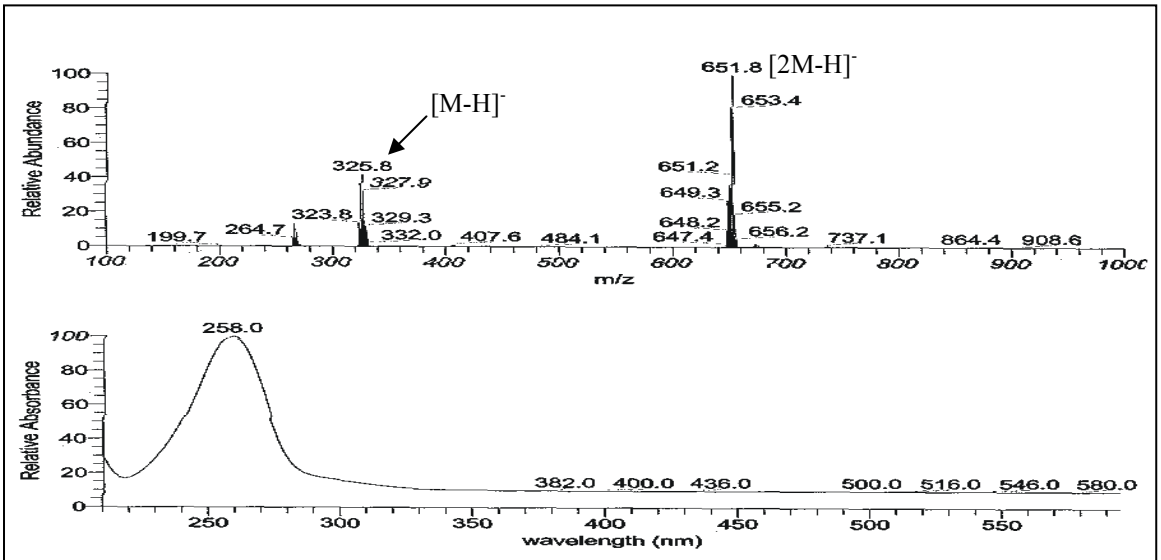

Fig. 3.45: (–) **ESI (top) and UV spectra (bottom) of compound 14**

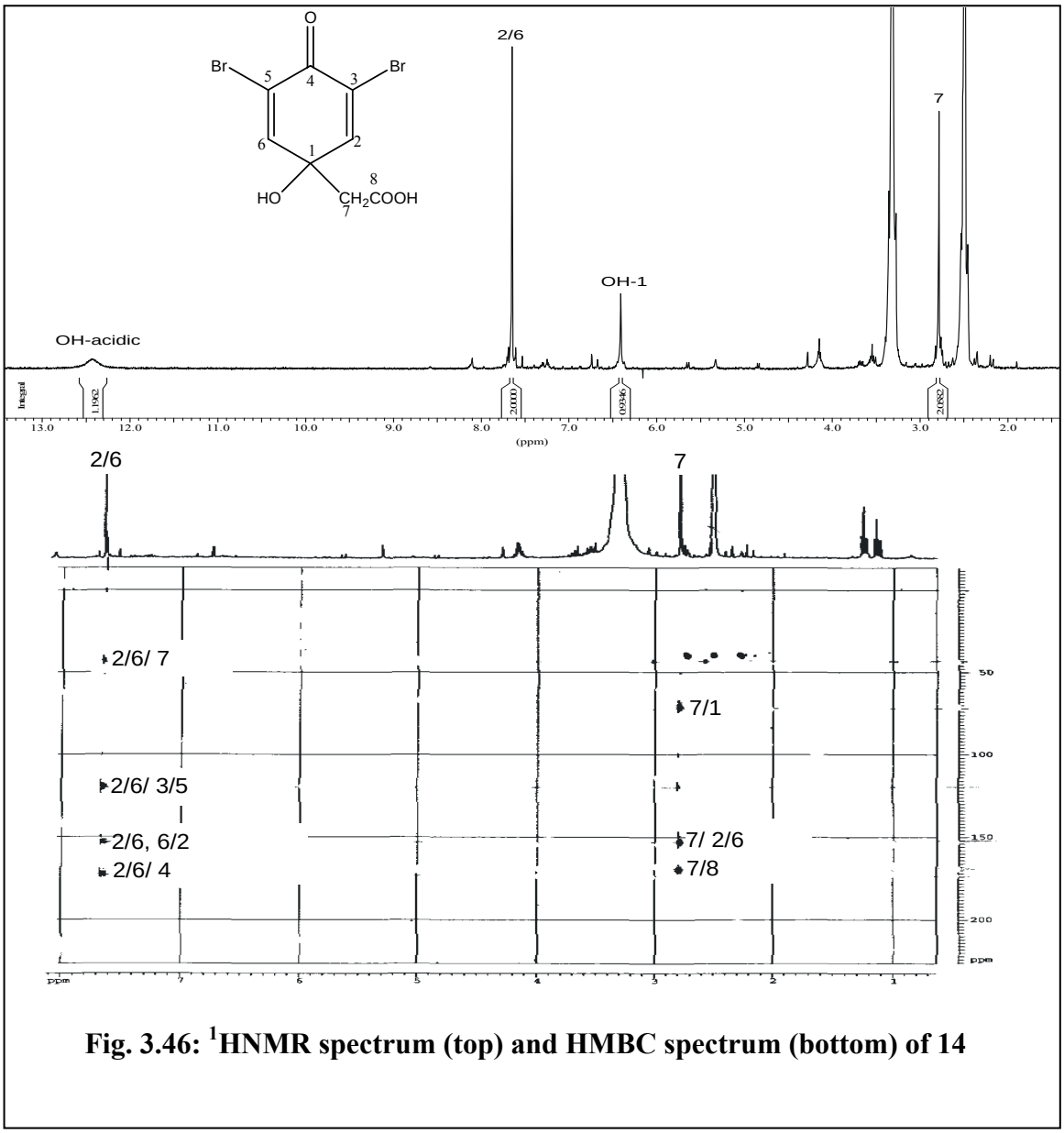

Fig. 3.46: ^{1}HNMR spectrum (top) and HMBC spectrum (bottom) of 14

Table 3.19: NMR data of compound 14

Position	^{1}H NMR (ppm), multiplicity (Hz)	^{13}C NMR (ppm)*	HMBC correlations H ⟶ C
1	-	71.1 s	
3/5	-	119.2 s	
2/6	7.69 (2H, s)	152.8 d	3, 4,5, 7
4	-	172.1 s	
7A,B	2.78 (2H, S)	43.1 t	1, 2/6, 8
8	-	169.6 s	
O*H* at C-1	6.40 (1H, br s)	-	
O*H* acidic	12.45 (1H, br s)	-	

The compound was measured in DMSO-d_6 at 500 MHz.
* Obtained from the HMBC spectrum.

3.3.10. Hydroxydienoic acid methyl ester (15, new natural product)

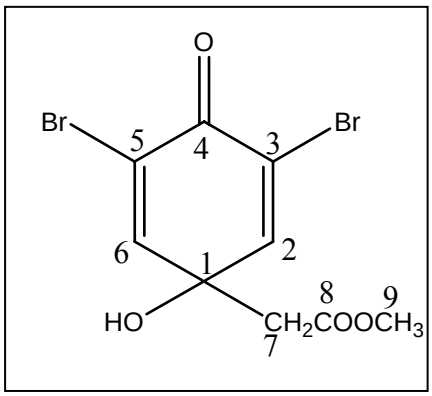

Compound **15** was isolated as yellow oil with the UV absorbance at λ_{max} 258 nm. The negative ESIMS of compound **15** showed a cluster at *m/z* 337:339:341 with the ratio 1:2:1 $[M-H]^-$ indicating the presence of two bromine atoms (see Fig. 3.47). This molecular weight is compatible with the molecular formula $C_9H_8Br_2O_4$ which was also confirmed from the HREIMS. The ^{1}HNMR spectrum of **15** (see Fig. 3.48 and Table 3.20) is closely related to that of compound **14**. Both differ by the presence of an additional methoxy group at 3.68 ppm (3H, s) for compound **15** and the absence of the broad singlet at 12.45 ppm for the acidic OH.

This suggested that compound **15** is the methyl ester congener of compound **14.** The position of the methoxy group was confirmed through a strong cross peak in the HMBC spectrum (see Fig. 3.49) between the methoxy group and C-8. The downfield shift of the methylene group, H_2-7 at 2.85 ppm (2H, s) in the ^{1}HNMR spectrum suggested that this methylene is attached to a carbonyl group. This was further confirmed by cross peaks between H_2-7 and C-8, C-1, C-2/6 in the HMBC spectrum. Some ^{13}C assignments of compound **15** (see Table 3.20) were obtained indirectly through the HMBC spectrum.

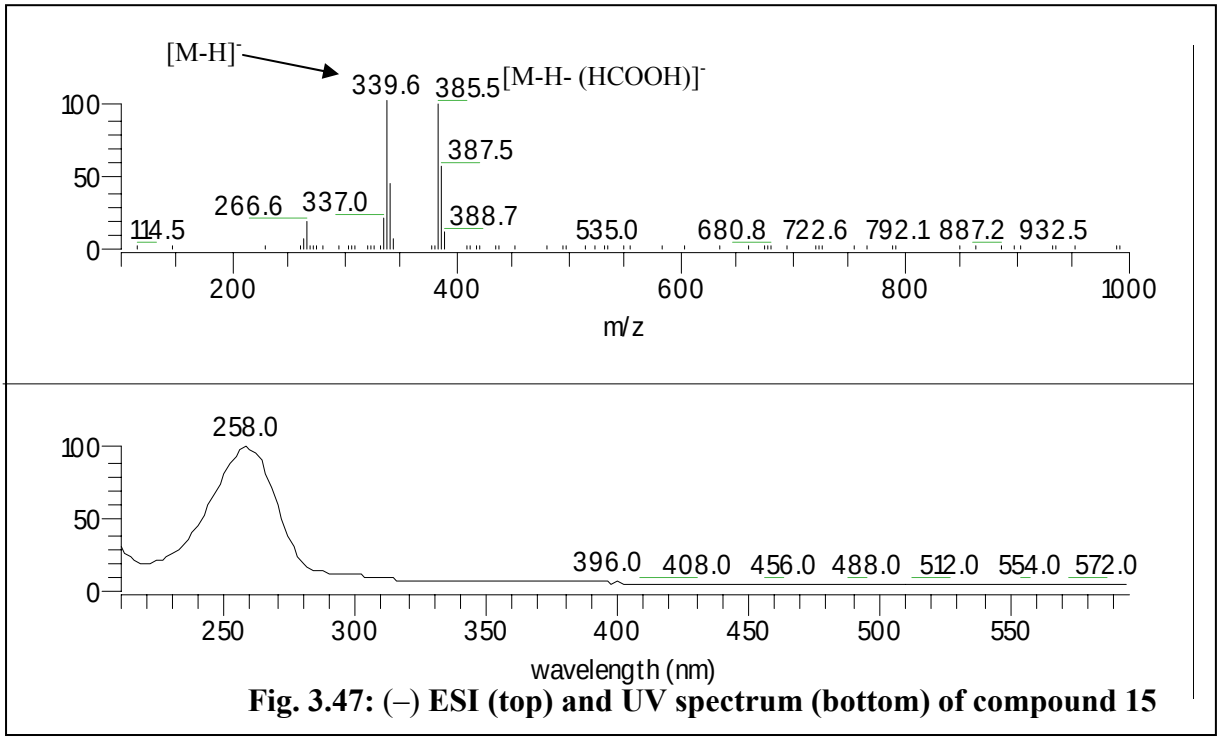

Fig. 3.47: (–) ESI (top) and UV spectrum (bottom) of compound 15

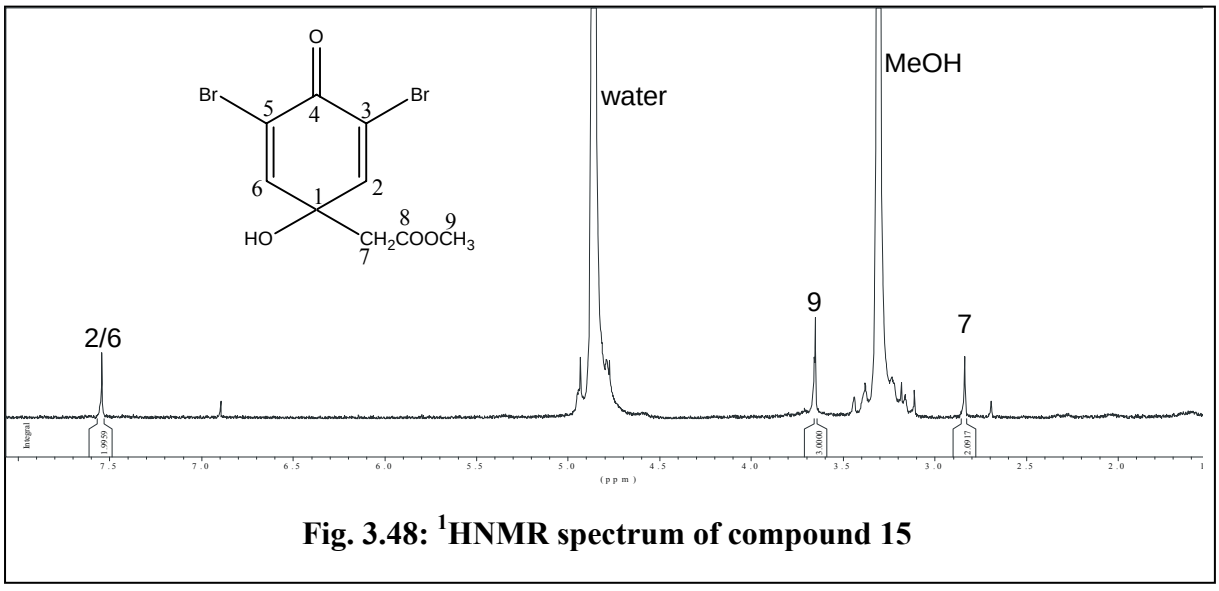

Fig. 3.48: ^{1}HNMR spectrum of compound 15

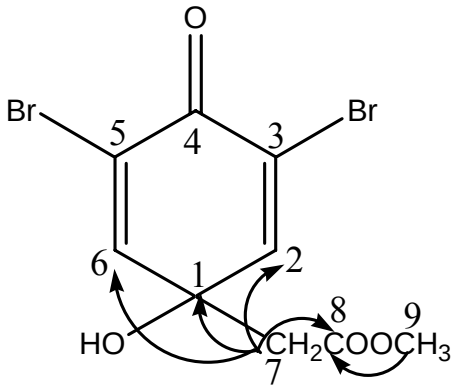

Fig. 3.49: Some HMBC correlations of 15

Table 3.20: NMR data of compound 15

Position	^{1}H NMR (ppm), multiplicity (Hz)	^{13}C NMR (ppm)*	HMBC correlations H ⟶ C
1	-	72.0 s	
3/5	-		
2/6	7.95 (2H, S)	152.3 d	
4	-		
7A,B	2.85 (2H, S)	44.1 t	1, 2/6, 8
8	-	170.2 s	
9	3.68 (3H, S)		8

The compound was measured in MeOD at 500 MHz.

* Obtained from the HMBC analysis.

Bioactivity

Different fractions of sponge *Pseudoceratina purpurea* showed a strong activity against different gram positive and gram negative bacteria and displayed also antifungal properties. On the other hand, some of the isolated pure compounds from *Pseudoceratina purpurea* only showed a moderate activity against some types of bacteria (see Table 3.21) while the other compounds were inactive. In our search for new cytotoxic drugs all the isolated compounds from *Pseudoceratina purpurea* were tested against different cancer cell lines. Four compounds showed activity with different percentages while the other compounds were inactive. The results are summarised in (Table 3.22).

Table 3.21: Agar plate diffusion assay of fractions and pure compounds from *Pseudoceratina purpurea*.

Fraction / Compound *	Zone of inhibition (mm)				
	S. aureus	***E. coli***	***B. subtilis***	***C. albicans***	***S. cerevisia***
Hexane fraction					
(5 µg)	7	-	10	-	n.t.
(10 µg)	7	-	10	-	n.t.
EtOAc fraction					
(5 µg)	15	9	12	-	n.t.
(10 µg)	15	9	12	-	n.t.
Butanol fraction					
(5 µg)	20	10	15	15	n.t.
(10 µg)	20	10	15	15	n.t.
Aqueous fraction					
(5 µg)	10	9	12	10	n.t.
(10 µg)	10	9	12	10	n.t.
Dienone (8)					
(50 µg)	n.t.	11	9	n.t.	-
(100 µg)	n.t.	7	11	n.t.	-
Hydroxydienoic acid (14)					
(50 µg)	n.t.	-	-	n.t.	-
(100 µg)	n.t.	8	-	n.t.	-
Hydroxydienoic acid methyl ester (15)					
(50 µg)	n.t.	-	8	n.t.	-
(100 µg)	n.t.	-	12	n.t.	-

n.t. = not tested. * amount tested at µg per disk
(-): negative

Table 3.22: Cytotoxicity test for the isolated compounds from *Pseudoceratina purpurea*

Compounds (10 μg/mL)	**% of Growth rate in different cell lines**		
	JURKAT	**THP-1**	**U-937**
3,5- dibromo-4-hydroxy-benzaldehyde (7)	12	0	0
Dienone (8)	100	46	30
Dienone dimethoxyketal (9)	0	15	20
Hydroxydienoic acid (14)	100	60	63

3.4. Isolated compounds from the marine sponge *Rhabdastrella globostellata*

The malabaricanes first known as malabaricol were isolated from the wood of the *Alianthus malabarica* tree. The malabaricanes are yellow pigments characterised by a tricyclic terpenoid core and a conjugated, polyene side chain [Chawla, *et al*., 1967; Sobti, *et al*., 1968; Patou, *et al*., 1989]. Isomalabaricane triterpenes have been isolated from several genera of marine sponges [Tasdemir, *et al*., 2002; Meragelman, *et al*., 2001; Zampella, *et al.*, 2000]. They differ from the malabaricanes by having a *trans-syn-trans* ring junction about the tricyclic moiety instead of *trans-anti-trans* (see Fig. 3.50). In the search for biologically active metabolites from marine invertebrates, twelve new cytotoxic triterpenes (**17 - 19, 21 - 27** and **29 - 30**) were isolated from the Indonesian sponge *Rhabdastrella globostellata* in addition to the known compounds globostellatic acids A (**16**) and D (**20**) [Ryu, *et al*., 1996] and the glycoside congener, stelliferin riboside (**28**) [Tabudravu, *et al.,* 2001].

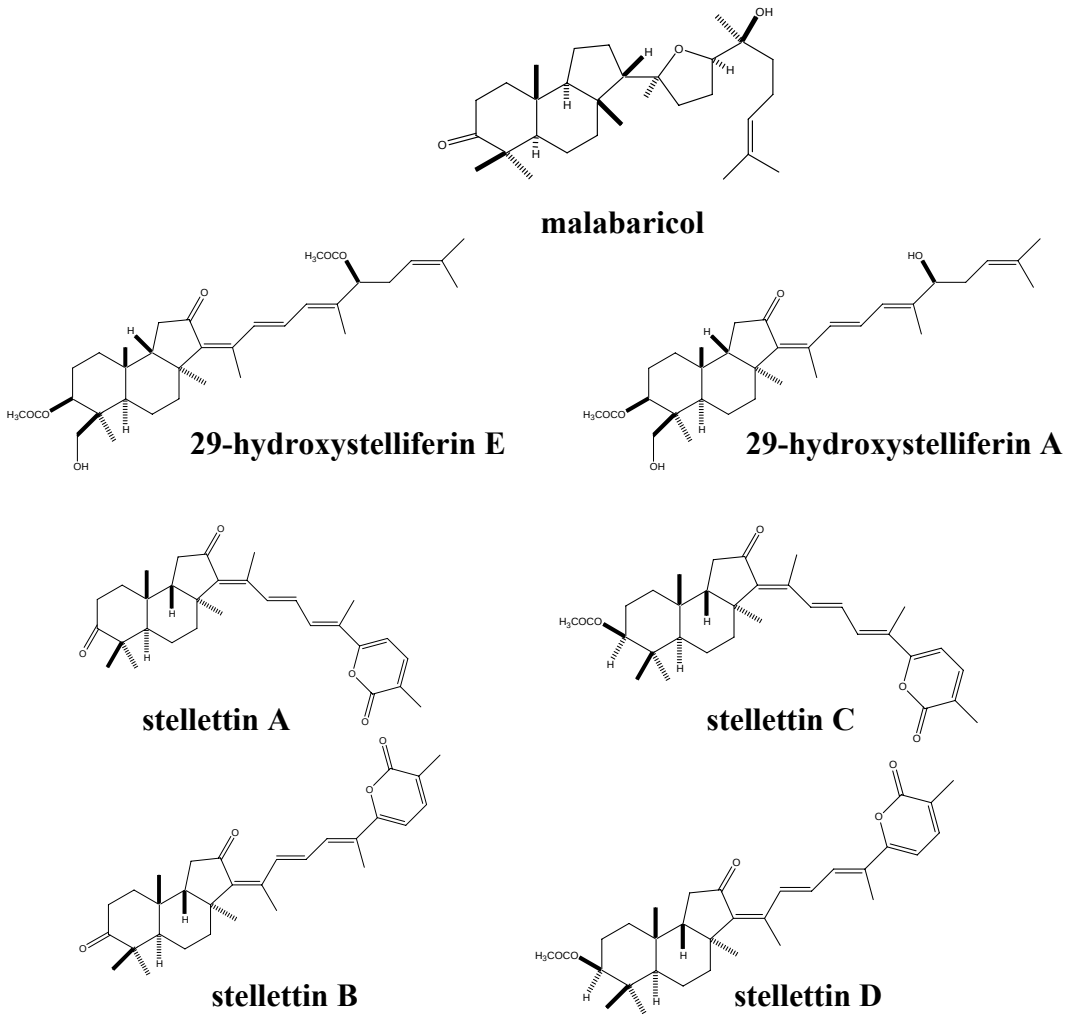

Fig. 3.50: Some malabaricanes and isomalabaricanes previously isolated from plants and marine sponges

3.4.1. Globostellatic acid A (16, known compound)

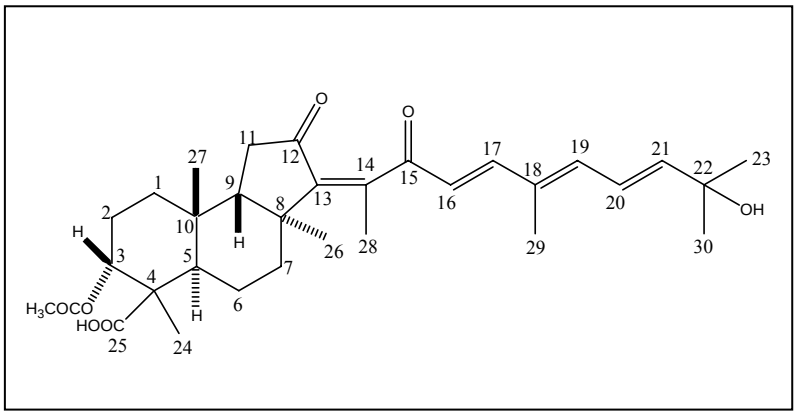

Compound **16** was obtained as yellow oily substance, $[\alpha]_D^{20}$ – 35 (*c* = 0.174, MeOH). It showed UV absorption at λ_{max} 234 and 329 nm (MeOH). The positive ESIMS showed a pseudomolecular ion peak at *m/z* 541 $[M+H]^+$. This molecular weight is compatible with the molecular formula $C_{32}H_{44}O_7$. The ^1H NMR spectrum of **16** (see Fig. 3.51 and Table 3.23) showed the presence of five methyls on sp3 quaternary carbons, two olefinic methyls at 1.91 and 1.98 ppm, an acetyl at 2.06 ppm, an oxygenated methine at 5.42 ppm and five olefinic protons. These data suggested that compound **16** is either a malabaricane or an isomalabaricane triterpene. The COSY spectrum of **16** (see Fig. 3.52) provided the assignment of the side chain and the tricyclic portion of the molecule. The COSY spectrum showed a cross peaks between H-16 and H-17 then H-19 to H-20 and further to H-21. A homoallylic coupling between C*H*$_3$-29 and H-19 was also observed. On the other hand, the position of the isopropyl group was confirmed by the cross peak between C*H*$_3$-23 and C*H*$_3$-30 with C-22 (^2J) and C-21 (^3J) in the HMBC spectrum. Furthermore, C*H*$_3$-28 showed strong correlations with C-15 and C-13 which confirmed the position of the carbonyl group at C-15 and the connection of the side chain to the tricyclic moiety. The structure of **16** was confirmed by comparison of its NMR data with those reported for the known compound globostellatic acid A [Ryu, *et al*., 1996]. The relative stereo-structure of **16** was also identical to the known compound as determined by their comparable coupling constant data.

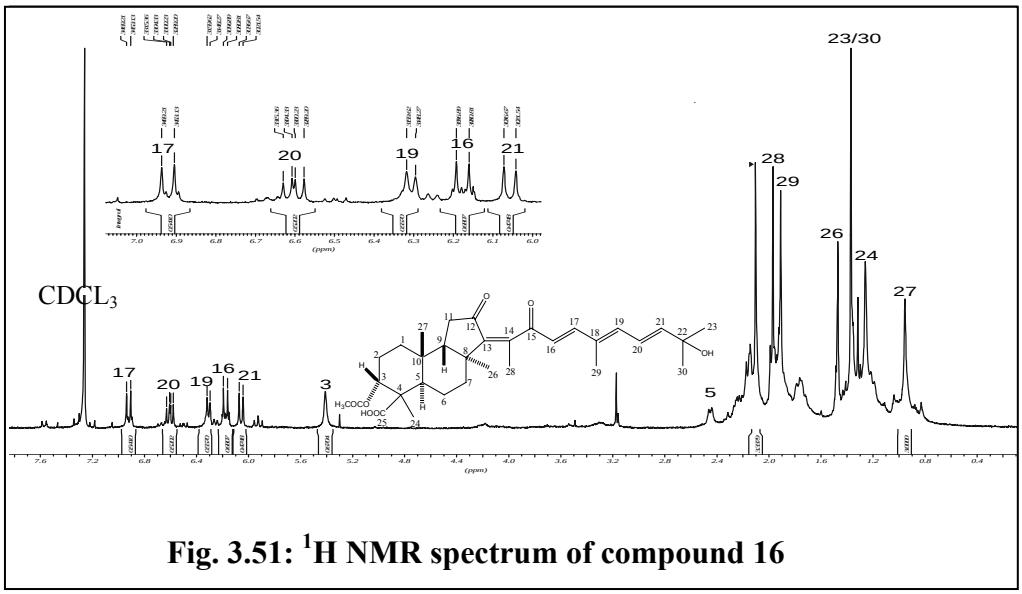

Fig. 3.51: ^{1}H NMR spectrum of compound 16

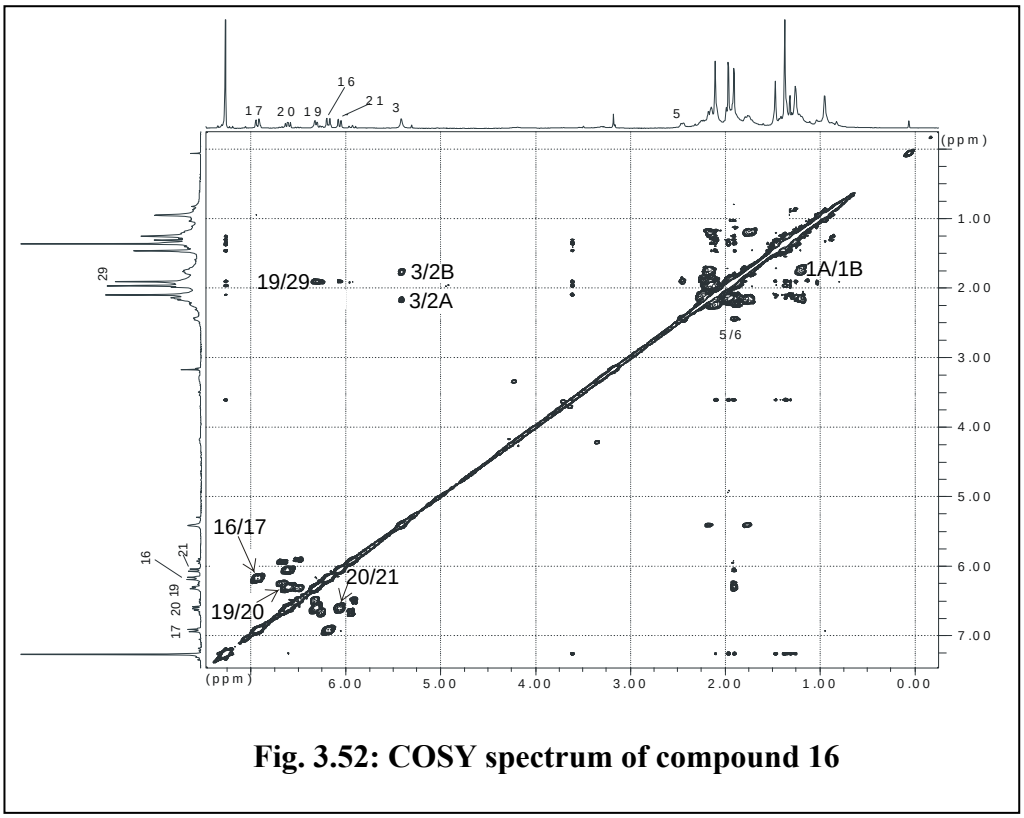

Fig. 3.52: COSY spectrum of compound 16

3.4.2. Globostellatic acid E (17, new compound)

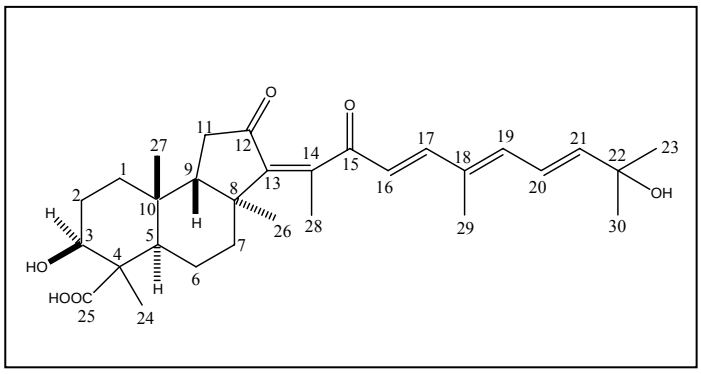

Globostellatic acid E (**17**) was obtained as yellow oily substance, $[\alpha]_D^{20}$ – 19 (*c* = 0.182, MeOH). It showed a pseudomolecular ion peak in the negative ESIMS at *m/z* 497 $[M-H]^-$. The molecular formula $C_{30}H_{43}O_6$ $[M+H]^+$ was established by HRESIMS ($C_{30}H_{43}O_6$, *m/z* 499.3069, calcd. 499.3061). It has UV absorptions at λ_{max} 234 and 329 nm (MeOH). The UV absorption at λ_{max} 329 nm was indicative of the presence of a highly conjugated polyene chromophore. The ^{1}H NMR spectrum of **17** (see Fig. 3.53 and Table 3.23) indicated that this compound shared the same isomalabaricane triterpenoid structure as globostellatic acids [Ryu, *et al*., 1996]. The conjugated polyene system in **17** was shorter than that in globostellatic acids B and C but identical to the one in globostellatic A (**16**) [Ryu, *et al*., 1996] as revealed by UV data (λ_{max} 329 nm). This is compatible with the fact that, the higher the conjugated system, the greater is the bathochromic shift of the UV absorbance of the compound. Analysis of the ^{1}H NMR and ^{1}H-^{1}H COSY spectra of compound **17** (see Fig 3.53) revealed the presence of five methyls at 0.95, 1.25, 1.36 (6H) and 1.47 ppm, two olefinic methyls at 1.91 and 1.96 ppm, an oxygenated methine at 4.18 ppm and five olefinic protons which are characteristic signals for the malabaricane or isomalabaricane triterpenes. Comparison between ^{1}H NMR data of compound **17** and the reported data of globostellatic acid A (**16**) [Ryu, *et al*., 1996] showed the absence of the acetyl group at 2.06 ppm in compound **17** in addition to the upfield shift of the oxygenated methine at 4.18 ppm instead of 5.41 ppm in **16**. Thus, it was found to contain a hydroxyl group in position 3 instead of an acetoxy group. This is compatible with the difference of 42 mass unit in the molecular weight between compound **17** and globostellatic acid A (**16**). Complete assignment of protons and carbons data of compound **17** has been elucidated using ^{1}H NMR, COSY, ^{13}C NMR, HMQC (see Fig. 3.54) and HMBC (see Table 3.23) spectral analysis. ^{13}C NMR data (see Table 3.23) for the tricyclic moiety indicated that **17** had an isomalabaricane skeleton comparable with the published data [Zhang,

et al., 2001]. The relative stereostructure of **17** was elucidated through a ROESY experiment. The presence of a cross peak between H-5 and CH_3-26 as well as H-9 and CH_3-27 confirmed the isomalabaricane nucleus of compound **17**. The correlation between H-3 and /H-5 revealed the relative stereochemistry of H-3 as being α and the hydroxyl group as being β. Furthermore, the cross peaks between H-16/CH_3-29 and H-20/CH_3-29 indicated the 16(*E*), 18(*E*), 20 (*E*) form of the side chain. This is confirmed also, through the coupling constant values $J_{16,17}$ = 16.1 Hz, $J_{20,21}$ = 15.0 Hz. Comparison between the ^{13}C values of CH_3-26,28 in compound **17** with those reported in compound **16** confirmed the 13 (*Z*) form of compound **17**.

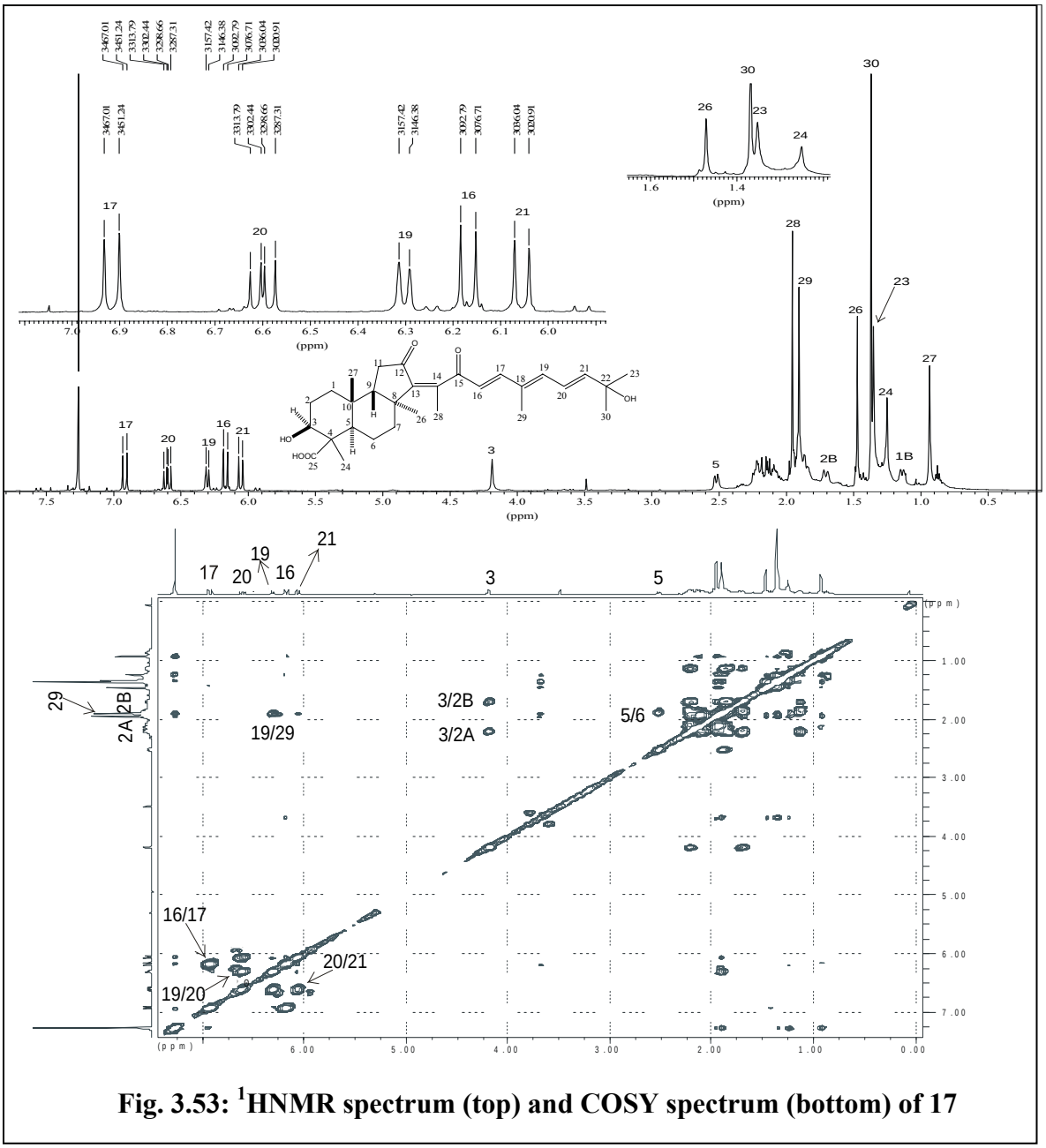

Fig. 3.53: ^{1}HNMR spectrum (top) and COSY spectrum (bottom) of 17

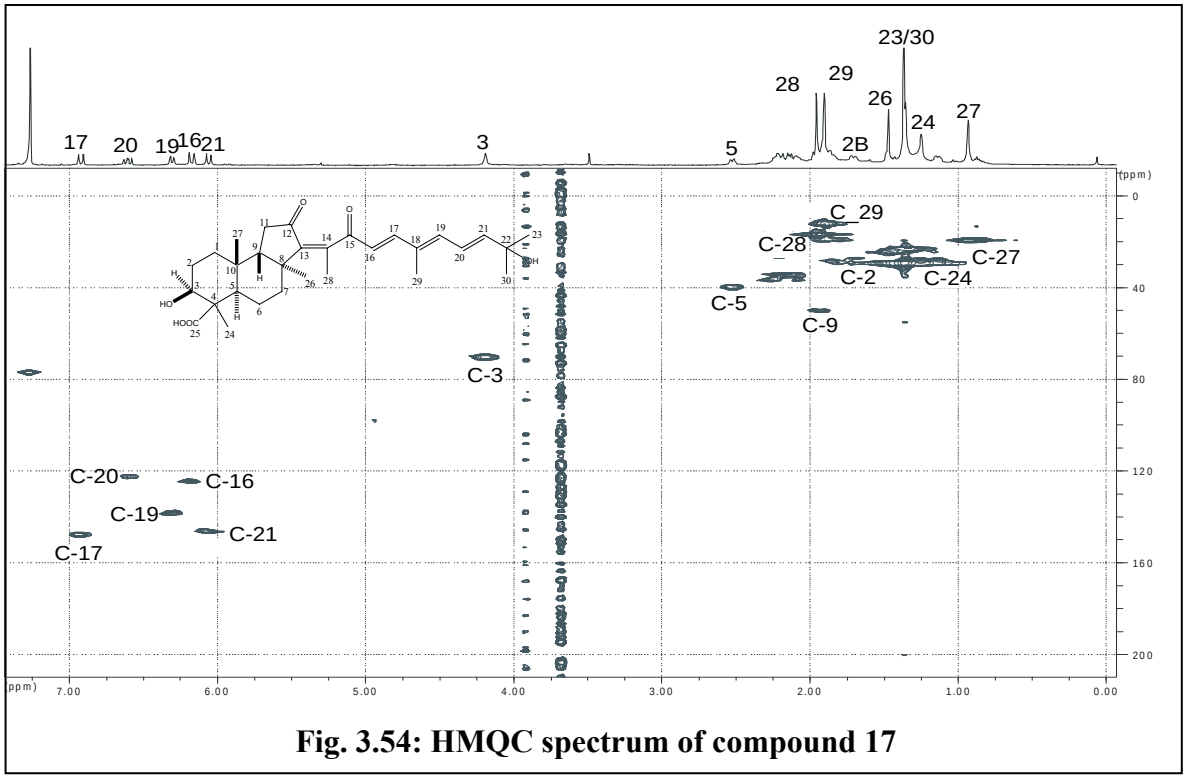

Fig. 3.54: HMQC spectrum of compound 17

3.4.3. Globostellatic acid F (18, new compound)

Globostellatic acid F (**18**) was obtained as yellow oily substance, $[\alpha]_D^{20}$ – 32.5 (*c* = 0.025, MeOH). It showed a pseudomolecular ion peak in the negative ESIMS at *m/z* 497 $[M-H]^-$. This molecular weight is compatible with the molecular formula $C_{30}H_{42}O_6$. The conjugated polyene system in **18** was the same as in compound **17**. This is confirmed from the UV absorption at λ_{max} 225 and 331 nm (MeOH). The molecular weight, ^{1}H NMR (see Fig. 3.55 and Table 3.24) and COSY spectral data of compound **18** revealed that it is a stereo-isomer of compound **17**. The ^{1}H NMR spectrum of **18** was similar to that of **17** except for the signal for H-17 which appeared more downfield (7.61 ppm) with slight downfield shifts for H-16, 19, 20 and 21 indicating that compound **18** is a steroisomer of globostellatic acid E (**17**). The coupling constant values of the olefinic protons in **18**, $J_{16,17}$ = 16.0 Hz and $J_{20,21}$ = 15.0 Hz confirmed the 16(*E*), 20(*E*) form as compound **17**. Unfortunately, the isolated amount of compound **18** was very small (0.8 mg). This compound needs further spectral analysis to confirm its structural form.

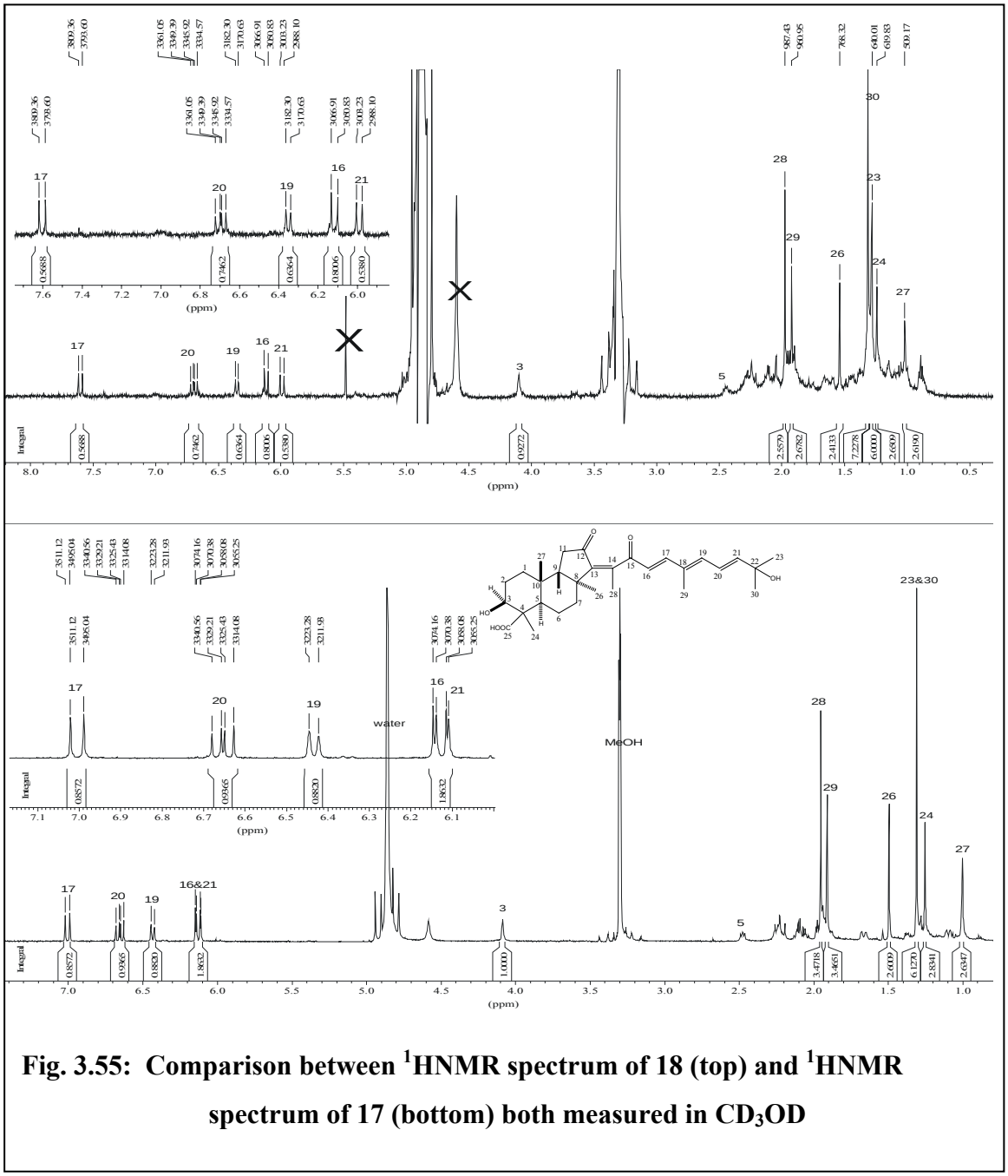

Fig. 3.55: Comparison between ^{1}HNMR spectrum of 18 (top) and ^{1}HNMR spectrum of 17 (bottom) both measured in CD_3OD

3.4.4. Globostellin (19, new compound)

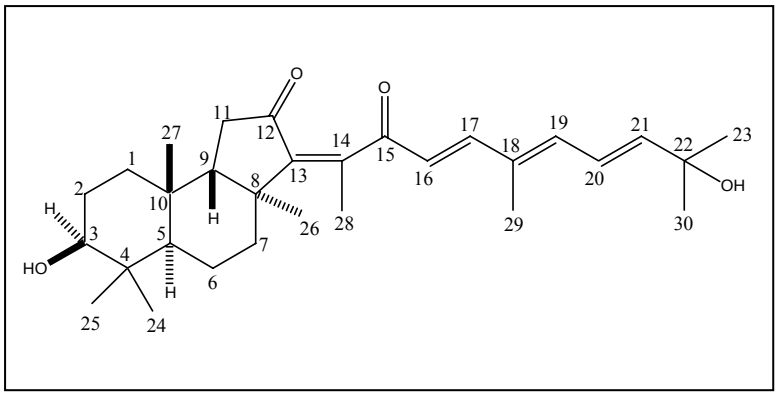

Globostellin (**19**) was obtained as yellow oily substance, $[\alpha]_D^{20}$ + 65 (*c* = 0.052, MeOH). It showed a pseudomolecular ion peak in the positive ESIMS at *m/z* 469 $[M+H]^+$. The molecular formula $C_{30}H_{45}O_4$ $[M+H]^+$ was established by HRESIMS ($C_{30}H_{45}O_4$ *m/z* 469.3290, calcd 469.3320). The UV absorption of compound **19** at λ_{max} 231 and 329 nm indicated that this compound is related to the other isomalabaricane triterpenoid compounds. The ^{1}H NMR spectral data of compound **19** (see Fig. 3.56 and Table 3.24) are closely related to those of compound **17** with the exception of the presence of an additional methyl singlet at 1.01 ppm, and the upfield shifts of H-3 at 3.52 ppm (dd, 4.7, 11.4 Hz) and H-5 at 1.73 ppm. The upfield shift of H-3 in compound **19** suggested that the additional methyl is attached to C-4, replacing the carboxyl group found in **17**. This is compatible with the difference of 30 mass units in the molecular weight between **17** and **19** and by a ^3J coupling between CH_3-24 and C-5 and ^2J coupling between CH_3-25 and C-4 in addition to the coupling between the two geminal methyls in the HMBC spectrum (see Fig. 3.57 and Table 3.24). The coupling constant of 11.7 Hz between H-3 and H-2β indicated axial orientation of H-3 and consequently, the hydroxyl group at C-3 followed the β- configuration [Oku, *et al.*, 2000]. All protons were assigned using ^{1}H NMR and COSY (see Fig. 3.58) spectra. The structure of compound **19** was confirmed by comparison of the protons of the tricylic moiety with those reported for stelliferin D [Tsuda, *et al.*, 1991].

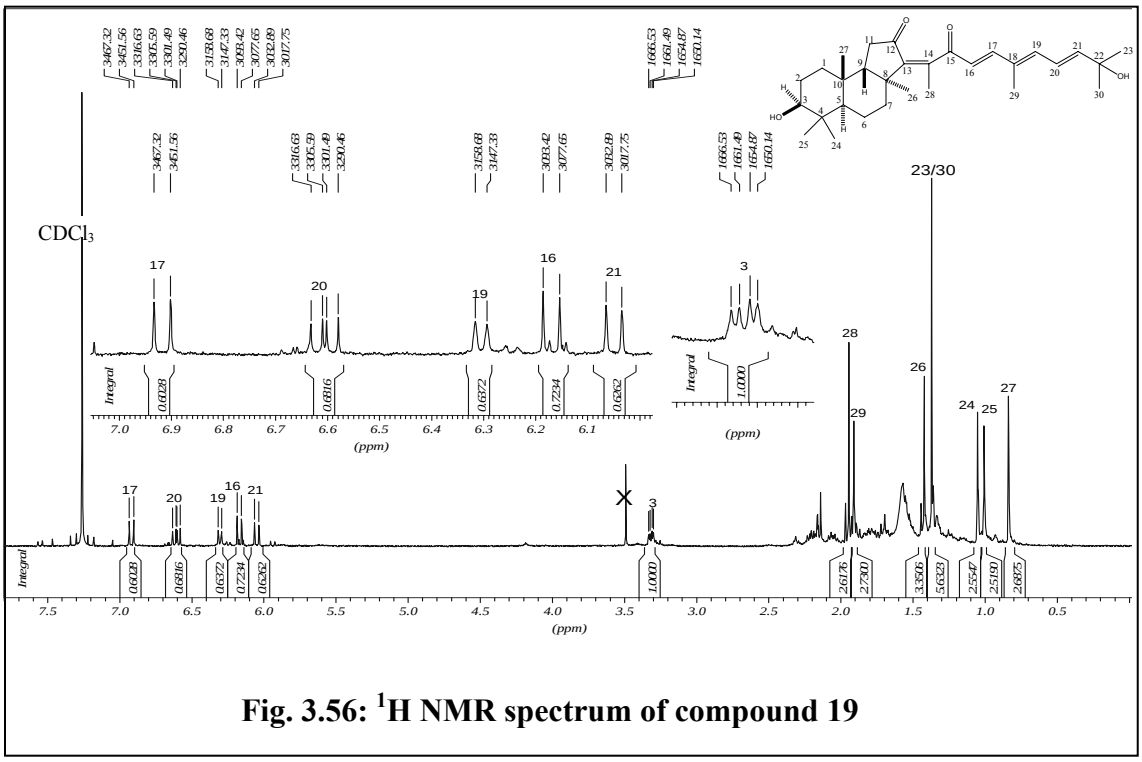

Fig. 3.56: ^{1}H NMR spectrum of compound 19

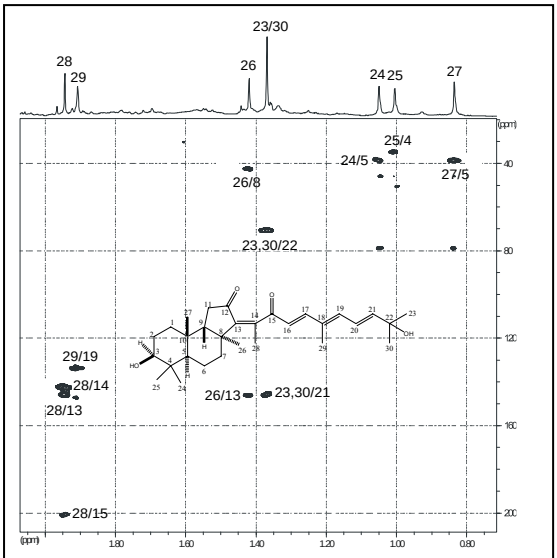

Fig. 3.57: Part of the HMBC spectrum of compound 19

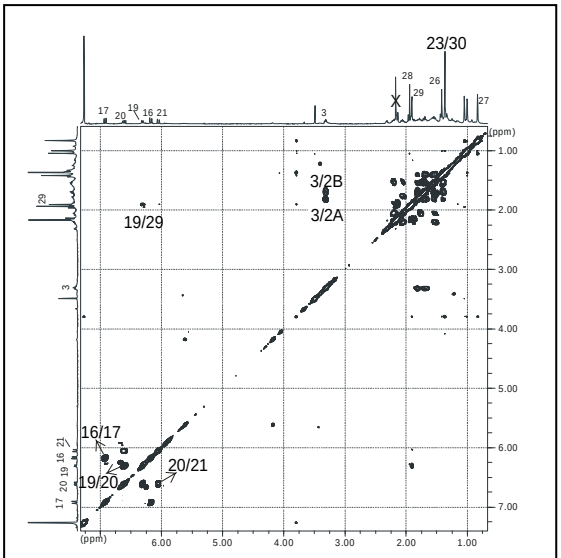

3.58: COSY spectrum of compound 19

Table 3.23: NMR data of compounds 16-17

position	^{1}H NMR (ppm), multiplicity (Hz) of 16	^{1}H NMR (ppm), multiplicity (Hz) of 17	^{13}C NMR (ppm) of 17	HMBC correlations of 17 H ⟶ C
1A	2.18 m	1.89 m	30.1 t	
1B	1.19 m	1.18 m	-	
2A	2.16 m	2.21 m	27.5 t	
2B	1.77 m	1.73 m	-	
3	5.42 br s	4.18 br s	70.4 d	24
4	-	-	47.6 s	-
5	2.44 m	2.33 m	39.9 d	24, 27
6A,B	1.92 (2H, m)	1.88 (2H, m)	19.5 t	
7A	2.13 m	2.23 m	36.7 t	26
7B	2.05 m	2.09 m	-	
8	-	-	42.9 s	-
9	1.90 m	1.94 m	50.1 d	27
10	-	-	36.9 s	-
11A	2.23 m	2.20 m	34.7 t	
11B	2.12 m	2.13 m	-	
12	-	-	*	-
13	-	-	146.3 s	-
14	-	-	142.9 s	-
15	-	-	204.0 s	-
16	6.19 (1H, d, 16.1 Hz)	6.18 (1H, d, 16.1 Hz)	124.5 d	
17	6.92 (1H, d, 16. 1 Hz)	6.93 (1H, d, 16.1 Hz)	147.7 d	
18	-	-	133.9 s	-
19	6.32 (1H, d, 11.4 Hz)	6.3 (1H, d, 11.0 Hz)	138.4 d	29
20	6.61 (1H, dd, 15.1, 11.4 Hz)	6.6 (1H, dd, 15.0, 11.0 Hz)	122.4 d	
21	6.07 (1H, d, 15.1 Hz)	6.06 (1H, d, 15.0 Hz)	146.2 d	
22	-	-	71.1 s	-
23	1.38 (3H, s)	1.36 (3 H, s)	29.8 q	21, 22, 30
24	1.26 (3H, s)	1.25 (3H, s)	23.5 q	3, 4. 5, 25
25	-	-	181.6 s	-
26	1.47 (3H, s)	1.47 (3H, s)	24.8 q	7, 6, 13
27	0.96 (3H, s)	0.95 (3H, s)	19.6 q	5, 9, 10
28	1.98 (3H, s)	1.96 (3H, s)	17.1 q	13, 14, 15
29	1.91 (3H, s)	1.91 (3H, s)	12.4 q	17, 18, 19
30	1.38 (3H, s)	1.36 (3H, s)	29.8 q	21, 22, 23
31	-	-	-	-
COC*H*$_3$	2.06 (3H, s)	-	-	-

* Not observed.

Spectra were measured in $CDCl_3$ at 500 MHz.

Table 3.24: NMR data of compounds 18-19

Position	^{1}H NMR (ppm), multiplicity (Hz) of 18	^{1}H NMR (ppm), multiplicity (Hz) of 19	HMBC correlations of 19 H → C
1A	1.89 m	1.56 m	
1B	1.18 m	1.43 m	
2A	2.21 m	1.84 m	
2B	1.73 m	1.70 m	
3	4.12 br s	3.52 (1H,dd, 11.4, 4.7 Hz)	
4	-	-	-
5	2.33 m	1.73 m	
6A	1.88 (2H, m)	1.78 m	
6B	-	1.53 m	
7A	2.23 m	2.22 m	
7B	2.09 m	2.07 m	
8	-	-	-
9	1.94 m	1.90 m	
10	-	-	-
11A	2.20 m	2.15 (2H, m)	
11B	2.13 m	-	
12	-	-	-
13	-	-	-
14	-	-	-
15	-	-	-
16	6.12 (1H, d, 16.0 Hz)	6.17 (1H, d, 15.8 Hz)	
17	7.61 (1H, d, 16.0Hz)	6.92 (1H, d, 15. 8 Hz)	
18	-	-	-
19	6.35 (1H, d, 11.5Hz)	6.31 (1H, d, 11.1 Hz)	
20	6.69 (1H, dd, 15.0, 11.5 Hz)	6.67 (1H, dd, 15.1, 11.1 Hz)	
21	6.00 (1H,d, 15.0 Hz)	6.05 (1H, d, 15.1 Hz)	
22	-	-	-
23	1.32 (3H, s)	1.37 (3H, s)	21, 22, 30
24	1.24 (3H, s)	1.05 (3H, s)*	5
25	-	1.01 (3H, s)*	4
26	1.53 (3H, s)	1.42 (3H, s)	8, 13
27	1.08 (3H, s)	0.84 (3H, s)	5
28	1.98 (3H, s)	1.94 (3H, s)	13, 14, 15
29	1.93 (3H, s)	1.91 (3H, s)	19
30	1.32 (3H, s)	1.37 (3H, s)	21, 22, 23
	-	-	-
	-	-	-

Spectra were measured in $CDCl_3$ for **19** and in MeOD for **18** at 500 MHz.

* These values may be interchanged.

3.4.5. Globostellatic acid D and M (20, 21, known and new compound respectively)

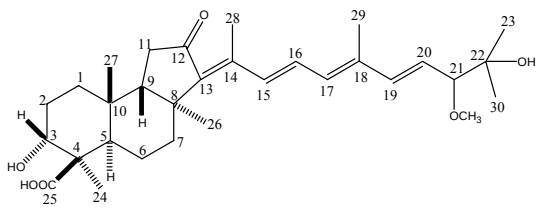

Globostellatic acid D (Δ^{13} = *E*)

known

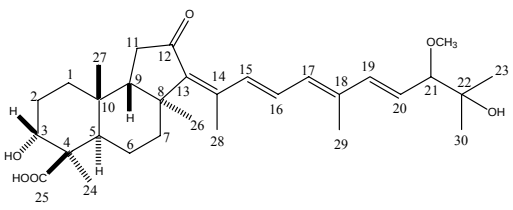

Globostellatic acid M (Δ^{13} = *Z*)

new

Globostellatic acid M (**21**) was obtained as a 2:1 isomeric mixture with the known compound globostellatic acid D (**20**). The positive ESIMS of this mixture showed a pseudomolecular ion peak at *m/z* 515 $[M+H]^+$. The molecular formula $C_{31}H_{47}O_6$ $[M+H]^+$ was established by HRESIMS ($C_{31}H_{47}O_6$ *m/z* 515.3351, calcd 515.3374). Comparison between the ^{1}H NMR spectrum of this mixture (see Fig. 3.59 and Table 3.25) and that reported for the known compound globostellatic acid D (**20**) [Ryu, *et al.*, 1996] revealed the presence of a second isomer, i.e. globostellatic acid M. In the ^{1}H NMR spectrum of this isomeric mixture, most of the signals of the two compounds were either overlapped or with small but distinguishable chemical shift differences. The most characteristic difference between the two compounds was the downfield shift of resonance for the olefinic signal H-15 at 8.05 ppm in compound **21** which indicated that it was located in the deshielding region of the carbonyl group, thus assigned to H-15 of the 13-*Z*-isomer, in comparison to that for the known 13-*E*-form (**20)** at 6.67 ppm which indicated that it was located in the shielding region of the carbonyl group [Rao, *et al.*, 1997; McCabe, *et al.*, 1982]. This is compatible with the upfield shift of C*H*$_3$-28 at 2.08 ppm in compound **21** instead of 2.32 ppm in compound **20**. The full assignment of the ^{1}H NMR data of the two substances was done through the differentiation of the spine systems of each in the COSY spectrum. It was not possible to differentiate the ^{13}C NMR chemical shifts of both compounds by the HMQC and HMBC spectra (see Fig. 3.60 and Table 3.25). The relative stereochemistry of the tricyclic moiety was determined through ROESY correlations between the pairs H-9/C*H*$_3$-27, as well as H-5/C*H*$_3$-26, clearly establishing a *trans-syn-trans* stereochemistry corresponding to an isomalabaricane skeleton, whereas a strong cross peak between H-5 and C*H*$_3$-24 revealed α-configuration of the methyl group at C-4. On the other hand, the presence of a strong correlation in the ROESY spectrum

between H-3 and CH_3-27 confirmed the relative stereochemistry of the hydroxyl group to follow the α-configuration.

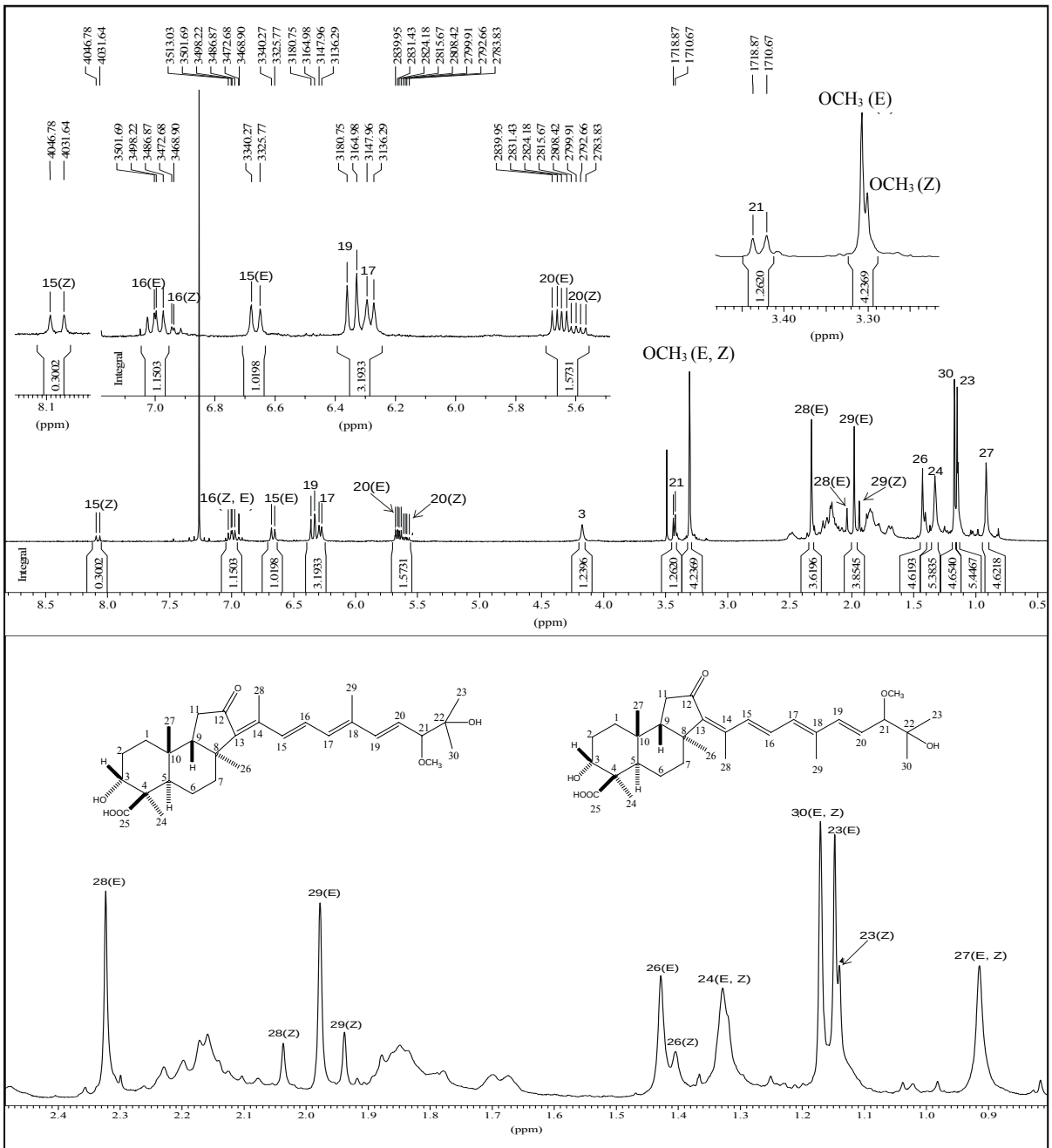

Fig. 3.59: ^{1}H NMR of compounds 20 and 21 (top) with enlargement of the methyl region (bottom)

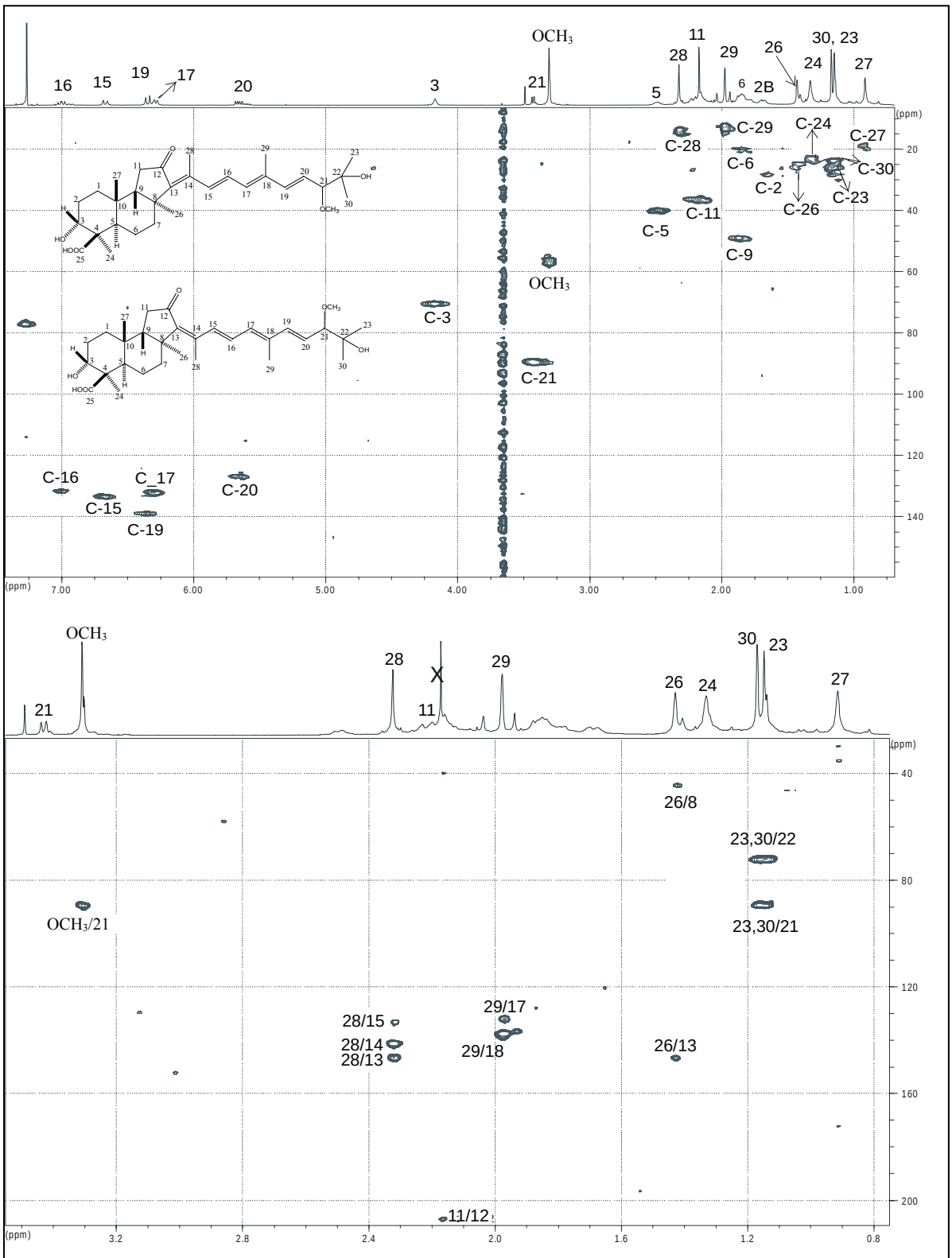

Fig. 3.60: HMQC spectrum (top) and part of HMBC spectrum (bottom) of compounds 20 and 21

Table 3.25: NMR data of compounds 20 and 21

position	^{1}H NMR (ppm), multiplicity (Hz) of 20	^{1}H NMR (ppm), multiplicity (Hz) of 21	^{13}C NMR (ppm) of 20, 21*	HMBC correlations of 20, 21 H ⟶ C
1A	1.95 m	1.95 m	30.3 t	
1B	1.17 m	1.17 m	-	
2A	2.21 m	2.21 m	28.7 t	
2B	1.69 m	1.69 m	-	
3	4.08 br s	4.08 br s	70.7 d	
4	-	-	***	-
5	2.51, (1H, br d, 11.8 Hz)	2.51 (1H, br d, 11.8 Hz)	40.2 d	
6A,B	1.89 (2H, m)	1.89 (2H, m)	20.4 t	
7A	2.23 m	2.23 m	***	
7B	2.09 m	2.09 m	-	
8	-	-	45.0 s	-
9	1.87 m	1.87 m	49.4 d	
10	-	-	35.9 s	-
11A	2.23 m	2.23 m	36.8 t	12
11B	2.19 m	2.19 m	-	
12	-	-	207.7 s	-
13	-	-	146.8 s	-
14	-	-	141.5 s	-
15	6.67 (1H, d, 14.8 Hz)	8.05 (1H, d, 15.0 Hz)	133.3 d	
16	7.00 (1H,dd, 14.8, 11.4 Hz)	7.05 (1H, dd, 15.0, 11.0 Hz)	131.8 d	
17	6.28 (1H, d, 11.4 Hz)	6.25 (1H, d, 11.0 Hz)	132.1 d	
18	-	-	137.7 s	
19	6.34 (1H, d, 15.7 Hz)	6.39 (1H, d, 15.8 Hz)	138.8 d	
20	5.65 (1H, dd, 15.7, 8.8 Hz)	5.70 (1H, dd, 15.8, 8.0 Hz)	126.8 d	
21	3.43 (1H, d, 8.8 Hz)	3.45 (1H, d, 8.0 Hz)	89.8 d	O*CH*$_3$
22	-	-	72.5 s	
23	1.17 (3H, s)	1.16 (3H, s)	24.1 q **	21, 22, 30
24	1.33 (3H, s)	1.25 (3H, s)	23.5 q	
25	-	-	***	-
26	1.43 (3H, s)	1.43 (3H, s)	24.9 q	8, 13
27	0.91 (3H, s)	0.98 (3H, s)	18.8 q	5, 10
28	2.32 (3H, s)	2.08 (3H, s)	15.1 q	13, 14, 15
29	1.98 (3H, s)	1.97 (3H, s)	13.5 q	18, 17
30	1.15 (3H, s)	1.14 (3H, s)	26.2 q**	21, 22, 23
OC*H*$_3$	3.30 (3H, s)	3.30 (3H, s)	57.0 q	

These compounds were measured in $CDCl_3$ at 500 MHz.

* Obtained from the HMQC and HMBC spectra.

** These values may be interchanged.

*** Not observed.

3.4.6. Globostellatic acid G and H (22, 23, new compounds)

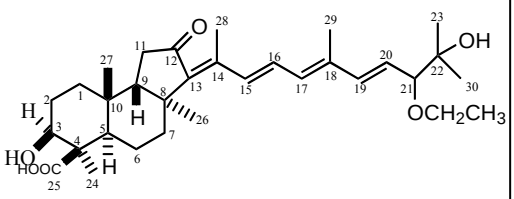

Globostellatic acid G

$\Delta^{13} = E$

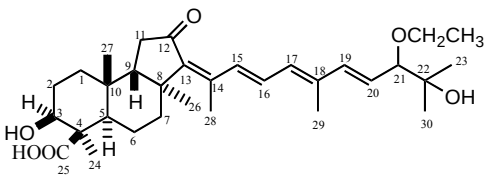

Globostellatic acid H

$\Delta^{13} = Z$

Globostellatic acid G (**22**) and Globostellatic acid H (**23**) were obtained as a 2:1 isomeric mixture. Attempts to separate this mixture were unsuccessful. The positive ESIMS of this mixture showed a pseudomolecular ion peak at *m/z* 529 $[M+H]^+$. This molecular weight is compatible with the molecular formula $C_{32}H_{48}O_6$. The ^{1}H NMR spectra of **22** and **23** (see Fig. 3.61 and Table 3.26) showed the presence of five methyl singlets, one methyl triplet, two olefinic methyls, five olefinic protons, two oxygenated methines and one oxygenated methylene. Comparison between the ^{1}H NMR spectra of compounds **22** and **23** with that reported for globostellatic acid D (**20**) [Ryu, *et al.,* 1996] revealed that compounds **22** and **23** are closely related to the latter except for the presence of two additional peaks at 3.33 and 3.59 ppm (2H, m), indicating the presence of an additional oxymethylene group. This is compatible with the absence of the methoxy group in compounds **22** and **23**, and the presence of an additional methyl triplet in the upfield region (1.19 ppm) with a coupling constant 7.2 Hz, suggesting the presence of an ethoxy group in compounds **22** and **23** instead of a methoxy as in **20**. A strong cross peak between the two protons of the oxymethylene group (CH_2-31) and CH_3-32 in COSY experiment (see Fig. 3.62) suggested that compounds **22** and **23** are the ethoxy derivatives of globostellatic acid D (**20**). The position of the ethoxy group was confirmed by the downfield shift of H-21 (3.55, d, 8.2 Hz) indicating that it is an oxygenated methane, in addition to a strong homoallylic cross peak between H-21 and H-19 as observed from the COSY spectrum. Full ^{1}H NMR data assignments for compounds **22** and **23** were obtained by careful analysis of ^{1}H NMR and COSY spectra. The chemical shifts of the carbons were all assigned by full inspection of HMQC and HMBC spectra (see Fig. 3.63 and Table 3.26). The coupling constants $J_{15,16}$ = 14.5 Hz, $J_{19,20}$ = 15.4 Hz suggested 15*E*, 17*E*, 19*E* geometries in both compounds. The upfield shift for the olefinic signal at 6.66 ppm in compound **22** indicated that it was located in the shielding region of the carbonyl group and should be assigned to H-15 of the 13-*E*-isomer [Rao, *et al.*, 1997; Ravi, *et al.,* 1981]. This is

compatible with the downfield shift of the C*H*$_3$-28 singlet at 2.33 ppm. On the other hand, the downfield shift for H-15 at 8.08 ppm in compound **23** indicated that it was located in the deshielding region of the carbonyl group and should be assigned to H-15 of the 13-*Z*-isomer [McCormick, *et al.*, 1996; McCabe, *et al.,* 1982]. This is also compatible with the upfield shift of C*H*$_3$-28 at 2.04 ppm. The relative stereochemistry of the tricyclic moiety was determined through ROESY correlations between the pairs H-9/C*H*$_3$-27, as well as H-5/C*H*$_3$-26, which clearly established a *trans-syn-trans* stereochemistry corresponding to an isomalabaricane skeleton, whereas a strong cross peak between H-5 and C*H*$_3$-24 revealed α-configuration of the methyl group at C-4. Furthermore, the presence of a strong correlation between H-3 and C*H*$_3$-24 and a weak but distinct correlation between H-3 and H-5 revealed α-configuration of H-3 and a 3β-hydroxyl function.

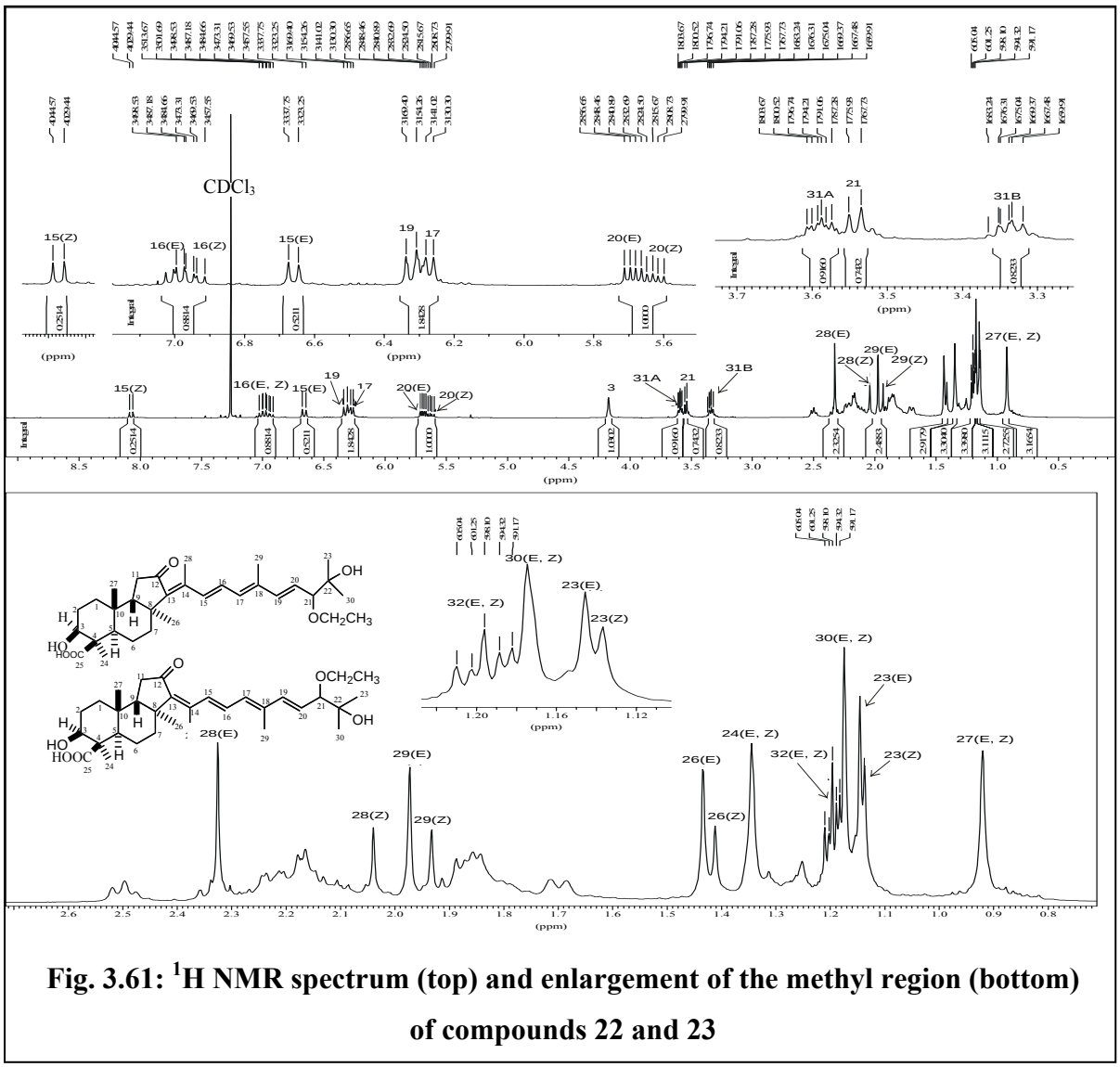

Fig. 3.61: ^{1}H NMR spectrum (top) and enlargement of the methyl region (bottom) of compounds 22 and 23

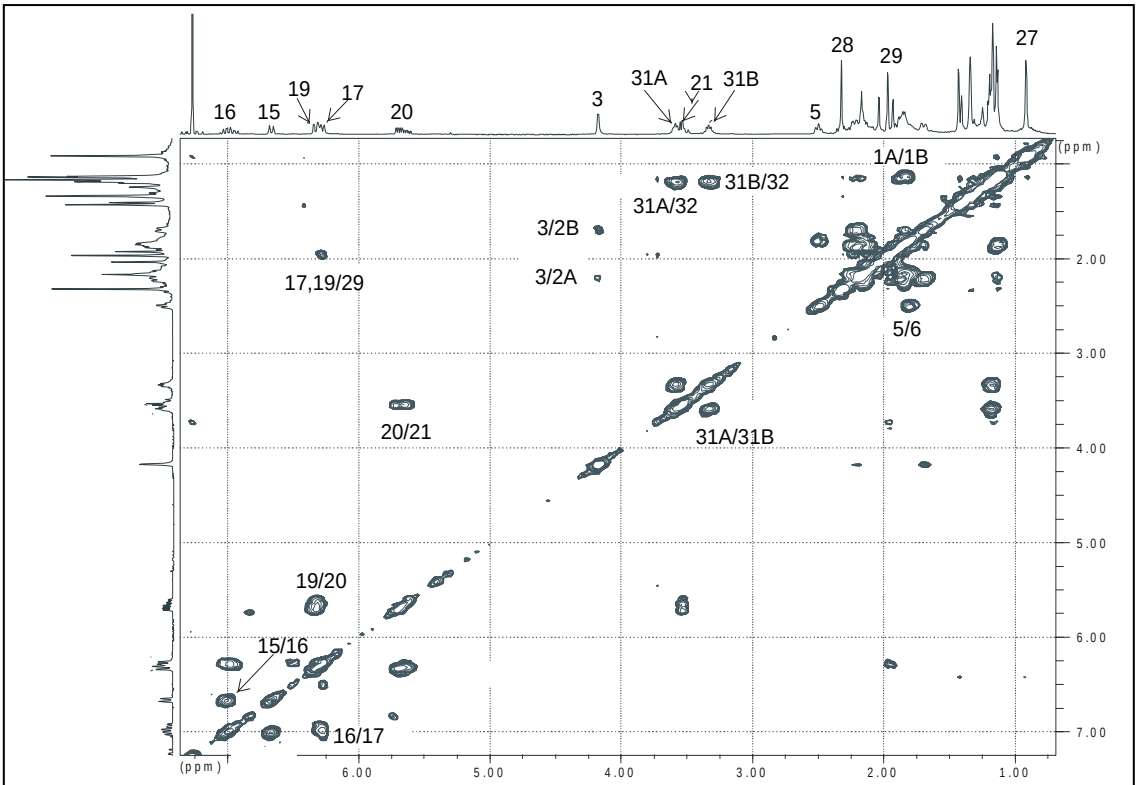

Fig. 3.62: COSY spectrum of compounds 22 and 23

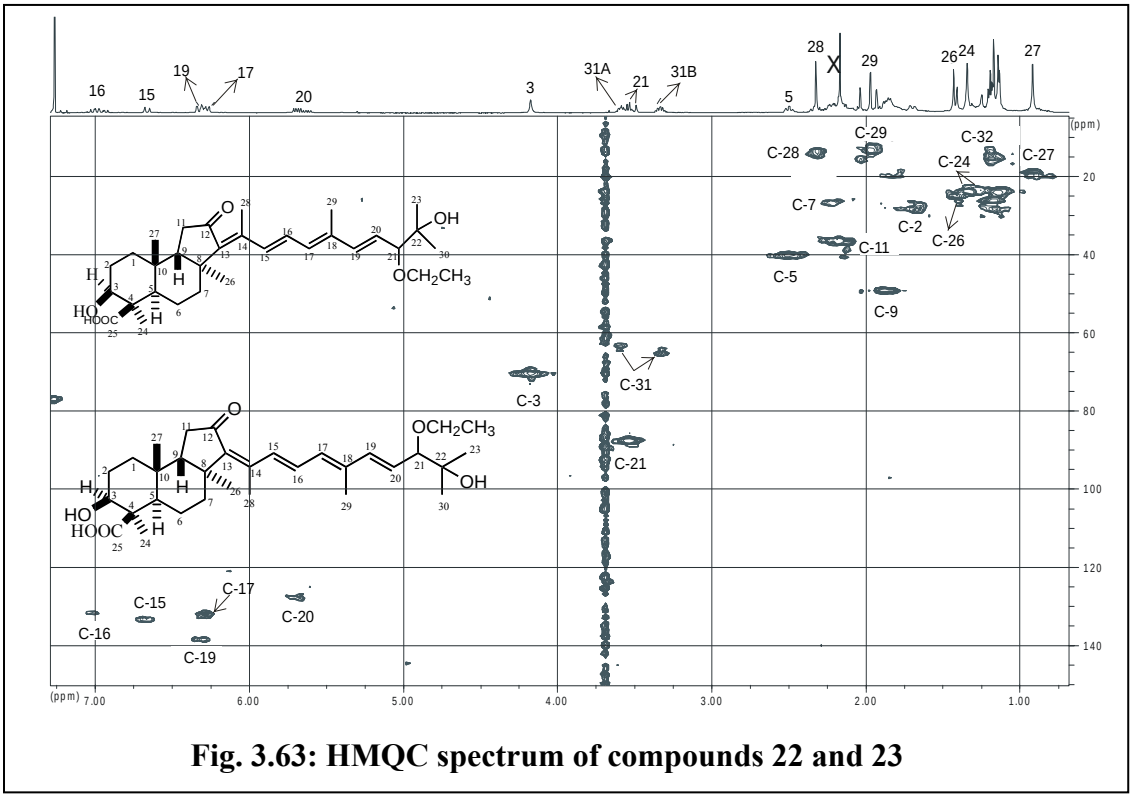

Fig. 3.63: HMQC spectrum of compounds 22 and 23

Table 3.26: NMR data of compounds 22 and 23

Position	^{1}H NMR (ppm), multiplicity (Hz) of 22	^{1}H NMR (ppm), multiplicity (Hz) of 23	^{13}C NMR (ppm) of 22, 23*	HMBC correlations of 22, 23 H → C
1A	1.87 m	1.87 m	28.5 t	
1B	1.19 m	1.19 m	-	
2A	2.22 m	2.22 m	26.9 t	
2B	1.70 m	1.70 m	-	
3	4.19 br s	4.19 br s	70.7 d	
4	-	-	48.0 s	-
5	2.49 m	2.49 m	40.2 d	
6A,B	1.82 (2H, m)	1.82 (2H, m)	20.0 t	
7A	2.19 m	2.19 m	40.2 t	
7B	2.11 m	2.11 m	-	
8	-	-	45.4 s	-
9	1.88 m	1.88 m	49.1 d	
10	-	-	37.0 s	-
11A	2.28 m	2.28 m	36.5 t	12
11B	2.21 m	2.21 m	-	
12	-	-	207.7 s	-
13	-	-	147.2 s	-
14	-	-	142.0 s	-
15	6.66 (1H, d,14.5 Hz)	8.08 (1H, d, 14.5 Hz)	133.3 d	
16	6.99 (1H,dd, 14.5, 11.5 Hz)	6.94 (1H,dd, 14.5, 11.5 Hz)	131.6 d	
17	6.27 (1H,d, 11.5 Hz)	6.27 (1H,d, 11.5 Hz)	132.0 d	
18	-	-	138.1 s	
19	6.33 (1H, d, 15.4 Hz)	6.33 (1H, d, 15.4 Hz)	138.2 d	
20	5.69 (1H,dd, 15.4, 8.2 Hz)	5.62 (1H,dd, 15.4, 8.2 Hz)	127.8 d	
21	3.55 (1H, d, 8.2 Hz)	3.55 (1H, d, 8.2 Hz)	88.3 d	
22	-	-	73.2 s	-
23	1.17 (3H, s)	1.17 (3H, s)	26.1 q	21, 22, 30
24	1.35 (3H, s)	1.35 (3H, s)	23.7 q	4, 5, 25
25	-	-	182.7 s	-
26	1.43 (3H, s)	1.41 (3H, s)	25.1 q	8, 13
27	0.92 (3H, s)	0.92 (3H, s)	19.3 q	9, 10
28	2.33 (3H, s)	2.04 (3H, s)	14.2 q	13, 14, 15
29	1.97 (3H, s)	1.93 (3H, s)	13.3 q	17, 18, 19
30	1.15 (3H, s)	1.14 (3H, s)	24.1 q	21, 22, 30
31A	3.59 m	3.59 m	64.6 t	32
31B	3.33 m	3.33 m	-	
32	1.19 (3H, t, 7.2 Hz)	1.19 (3H, t, 7.2 Hz)	15.2 q	31

These compounds were measured in $CDCl_3$ at 500 MHz.

* Obtained from the HMQC and HMBC spectra.

3.4.7. Globostellatic acid I and J (24, 25, new compounds)

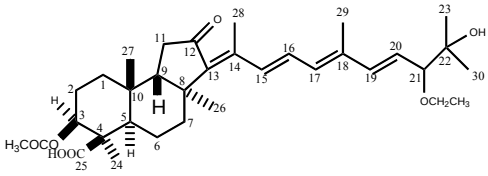

Globostellatic acid I
$\Delta^{13} = E$

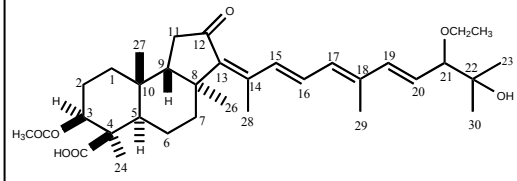

Globostellatic acid J
$\Delta^{13} = Z$

Globostellatic acid I (**24**) and globostellatic acid J (**25**) were also obtained also as a 2:1 isomeric mixture. Attempts to separate this mixture by using different chromatographic techniques were unsuccessful. The positive ESIMS of this isomeric mixture showed a pseudomolecular ion peak at *m/z* 593 $[M+Na]^+$. This molecular weight is compatible with the molecular formula $C_{34}H_{50}O_7$. The ^1H NMR spectrum of compounds **24** and **25** (see Fig. 3.64 and Table 3.27) revealed that this isomeric mixture is closely related to the previous compounds mixture **22** and **23**. Comparison between the molecular weight of the isomeric mixture **22, 23** and that for isomeric mixture **24, 25** indicated that the difference was 42 mass units. This indicated that compounds **24** and **25** may have an additional acetoxy group possibly at C-3 instead of a hydroxyl group as in compounds **22** and **23**, which is characteristic for many isomalabaricane triterpenoids. This proposal was confirmed by the presence of an additional acetyl group signal at 2.09 ppm (3H, s) in compounds **24** and **25** in comparison to compounds **22** and **23**. This is compatible with the downfield shift of H-3 in compounds **24** and **25** which appeared at 5.43 ppm (1H, br s) in comparison to that in compounds **22** and **23** which appeared at 4.19 ppm. Careful analysis of ^1H NMR and COSY spectra of compounds **24** and **25** showed that the rest of the proton signals of this isomeric mixture was identical with those shown for compounds **22** and **23**. The coupling constant values $J_{15,16}$ = 15.1 Hz, $J_{19,20}$ = 15.8 Hz suggested the 15*E*, 17*E*, 19*E* geometries in both compounds **24** and **25** which is also characteristic for isomalabaricane triterpenoids. Like in compound **22**, the upfield shift of the resonance for the olefinic H-15 signal at 6.67 ppm in compound **24** showed that it is a 13-*E*-isomer. This is compatible with the downfield shift of the CH_3-28 singlet at 2.34 ppm. On the other hand, the downfield shift of the olefinic H-15 signal at 8.08 ppm in compound **25** exhibited the 13-*Z*-isomer. This is also compatible with the upfield shift of the CH_3-28 singlet at 2.05 ppm. ROESY spectral data indicated that compounds **24** and **25** have the same relative stereochemistry as shownn for **22** and **23**.

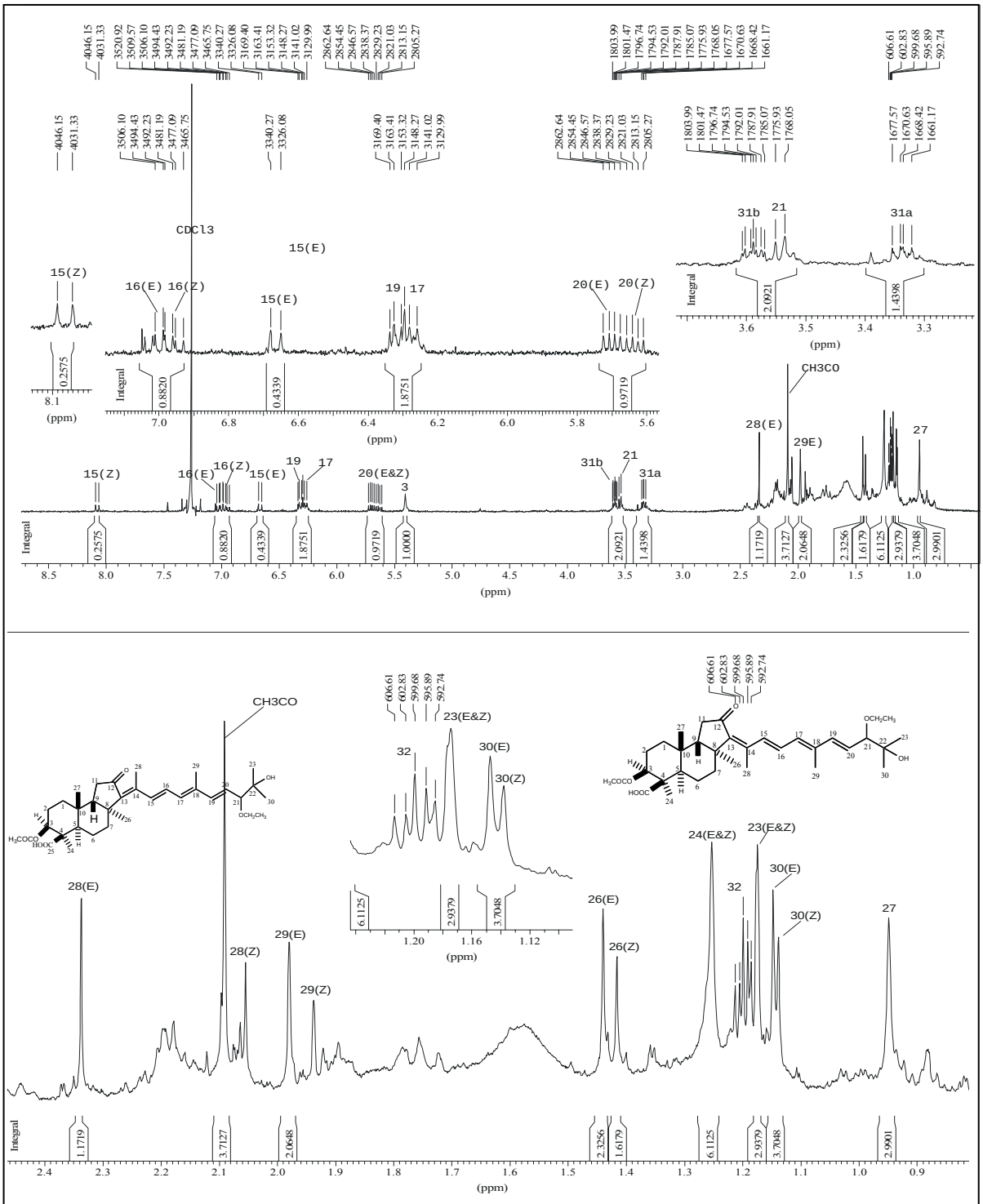

Fig. 3.64: ^{1}H NMR spectrum (top) and enlargement of the methyl region (bottom) of compounds 24 and 25

Table 3.27: NMR data of compounds 24 and 25

Position	^{1}H NMR (ppm), multiplicity (Hz) of 24	^{1}H NMR (ppm), multiplicity (Hz) of 25
1A	1.79 m	1.79 m
1B	1.20 m	1.20 m
2A	2.18 m	2.18 m
2B	1.78 m	1.78 m
3	5.43 br s	5.43 br s
4	-	-
5	2.46 m	2.46 m
6A,B	1.84 (2H, m)	1.84 (2H, m)
7A	2.19 m	2.19 m
7B	2.11 m	2.11 m
8	-	-
9	1.90 m	1.90 m
10	-	-
11A	2.28 m	2.28 m
11B	2.21 m	2.21 m
12	-	-
13	-	-
14	-	-
15	6.67 (1H, d, 15.1 Hz)	8.00 (1H, d, 15.1 Hz)
16	7.01 (1H, dd, 15.1, 11.3 Hz)	6.96 (1H, dd, 15.1, 11.3 Hz)
17	6.28 (1H, d, 11.3 Hz)	6.28 (1H, d, 11.3 Hz)
18	-	-
19	6.32 (1H, d, 15.3 Hz)	6.32 (1H, d, 15.3 Hz)
20	5.70 (1H, dd, 15.8, 8.0 Hz)	5.63 (1H, dd, 15.8, 8.0 Hz)
21	3.54 (1H, d, 8.0 Hz)	3.54 (1H, d, 8.0 Hz)
22	-	-
23	1.18 (3H, s)	1.18 (3H, s)*
24	1.26 (3H, s)	1.26 (3H, s)
25	-	-
26	1.44 (3H, s)	1.42 (3H, s)
27	0.95 (3H, s)	0.95 (3H, s)
28	2.34 (3H, s)	2.05 (3H, s)
29	1.98 (3H, s)	1.94 (3H, s)
30	1.15 (3H, s)	1.14 (3H, s) *
31A	3.59 m	3.59 m
31B	3.34 m	3.34 m
32	1.19 (3H, t, 7.2 Hz)	1.19 (3H, t, 7.2 Hz)
$COCH_3$	2.09 (3H, s)	2.09 (3H, s)

These compounds were measured in $CDCl_3$ at 500 MHz.
* These values may be interchangeable.

3.4.8. Globostellatic acid K and L (26, 27, respectively, new compounds)

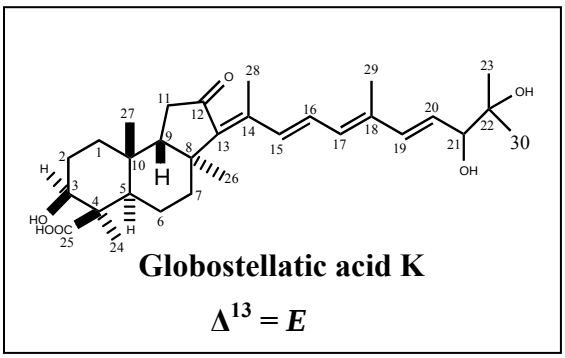

Globostellatic acid K

$\Delta^{13} = E$

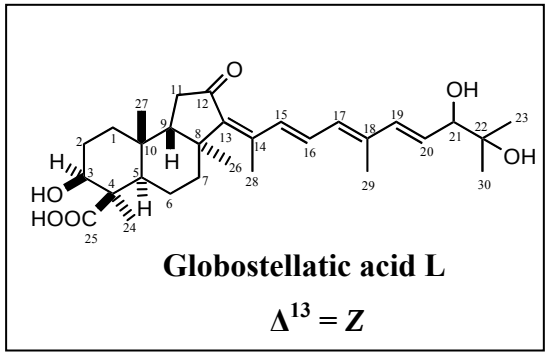

Globostellatic acid L

$\Delta^{13} = Z$

Globostellatic acid K (**26**) and globostellatic acid L (**27**) were also obtained as a 2:1 isomeric mixture. As the previous compounds, attempts to separate this mixture by using different chromatographic technique were unsuccessful. The positive ESIMS of this isomeric mixture showed a pseudomolecular ion peak at *m/z* 501 $[M+H]^+$. This molecular weight is compatible with the molecular formula $C_{30}H_{44}O_6$. The ^1H NMR spectrum of compounds **26** and **27** was closely related to that of compounds **22** and **23** (see page 103) which indicated that this mixture is also related to the isomalabaricane triterpenoids. Full inspection of the ^1H NMR data of compounds **26** and **27** (see Fig. 3.65 and Table 3.28) revealed the presence of five methyl singlets, two olefinic methyls, five olefinic protons and two oxygenated methines. Comparison between the ^1H NMR data of compounds **26** and **27** and those of compounds **22** and **23** showed the absence of the methyl triplet at 1.19 ppm and also the absence of two protons at 3.33 and 3.59 ppm for an oxygenated methylene. Furthermore, H-21 appeared as a triplet at 3.92 ppm in compounds **26** and **27** instead of a doublet at 3.55 ppm as in compounds **22** and **23**. The presence of a strong correlation between H-21 and H-22 in the COSY spectra of compounds **26** and **27** suggested that C-21 in these compounds carried a hydroxyl group instead of an ethoxy group as in compounds **22** and **23.** This proposal was confirmed by 28 mass unit differences in the molecular weight between the isomeric mixture **26** and **27** and the isomeric mixture **22** and **23.** This indicated the loss of C_2H_4 group (see page 103). The complete carbon assignment in compounds **26** and **27** was done indirectly from their HMQC and HMBC spectra (see Fig. 3.66 and Table 3.28). The 15*E*, 17*E*, 19*E* geometries in both compounds **26** and **27** are also typical for all the isomalabaricane triterpenoids as determined through their coupling constants. The 13-*E*-isomer of compound **26** was determined by the upfield shift of the resonance for the olefinic H-15 signal at 6.72 ppm which is compatible with the downfield shift of C*H*$_3$-28 at 2.30 ppm. The downfield shift of the resonance for the olefinic H-15 signal at 8.05 ppm in compound **27** suggested a 13-*Z*-isomer. This was

compatible with the upfield shift of CH_3-28 at 2.07 ppm. The relative stereochemistry of the tricyclic moiety of compounds **26** and **27** was also determined through the ROESY correlation between the pairs H-5/CH_3-26 as well as H-9/CH_3-27, which clearly established a *trans-syn-trans* stereochemistry corresponding to the isomalabaricane skeleton.

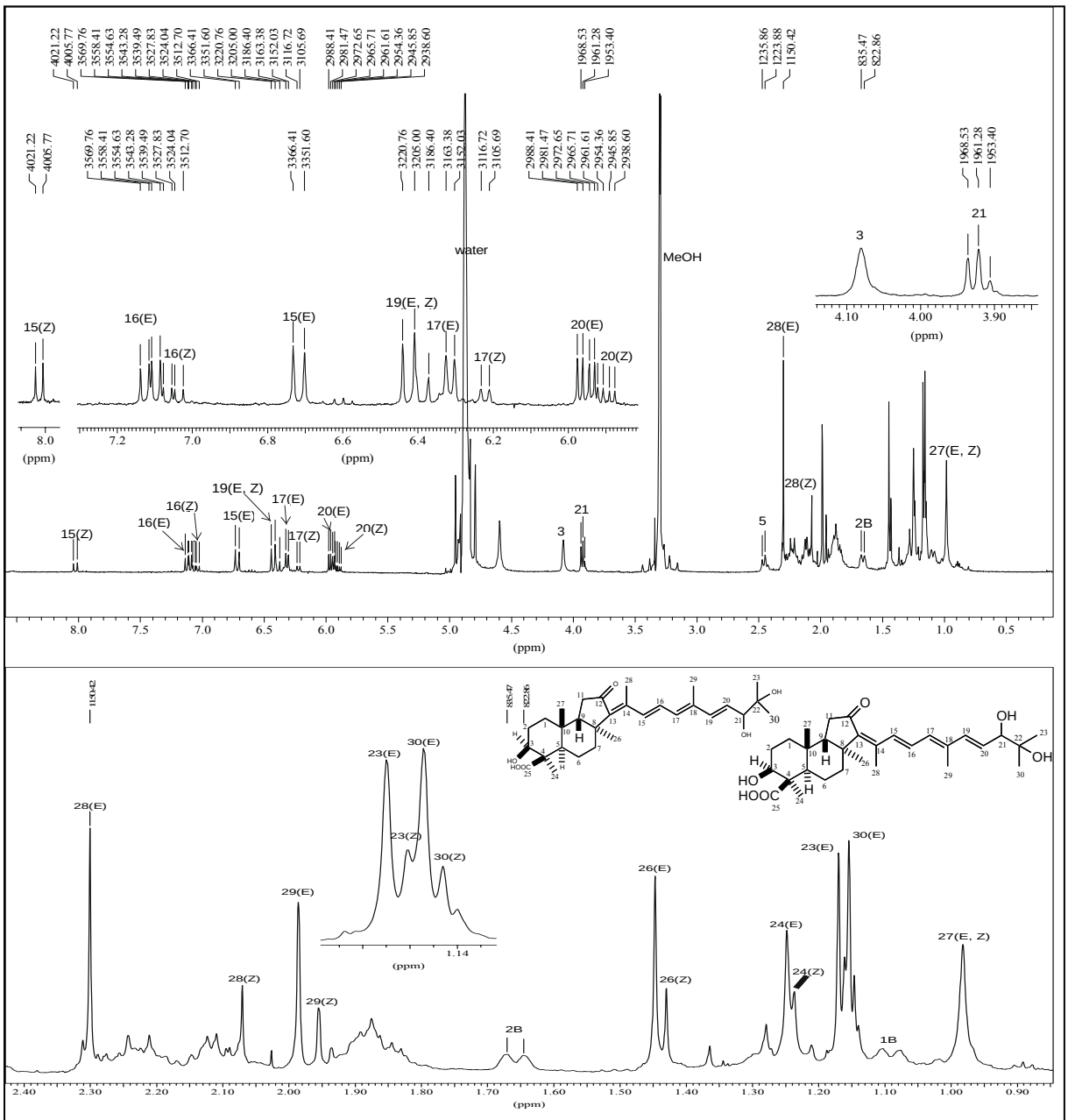

Fig. 3.65: ^{1}H NMR spectrum (top) and enlargement of the methyl region (bottom) of compounds 26 and 27

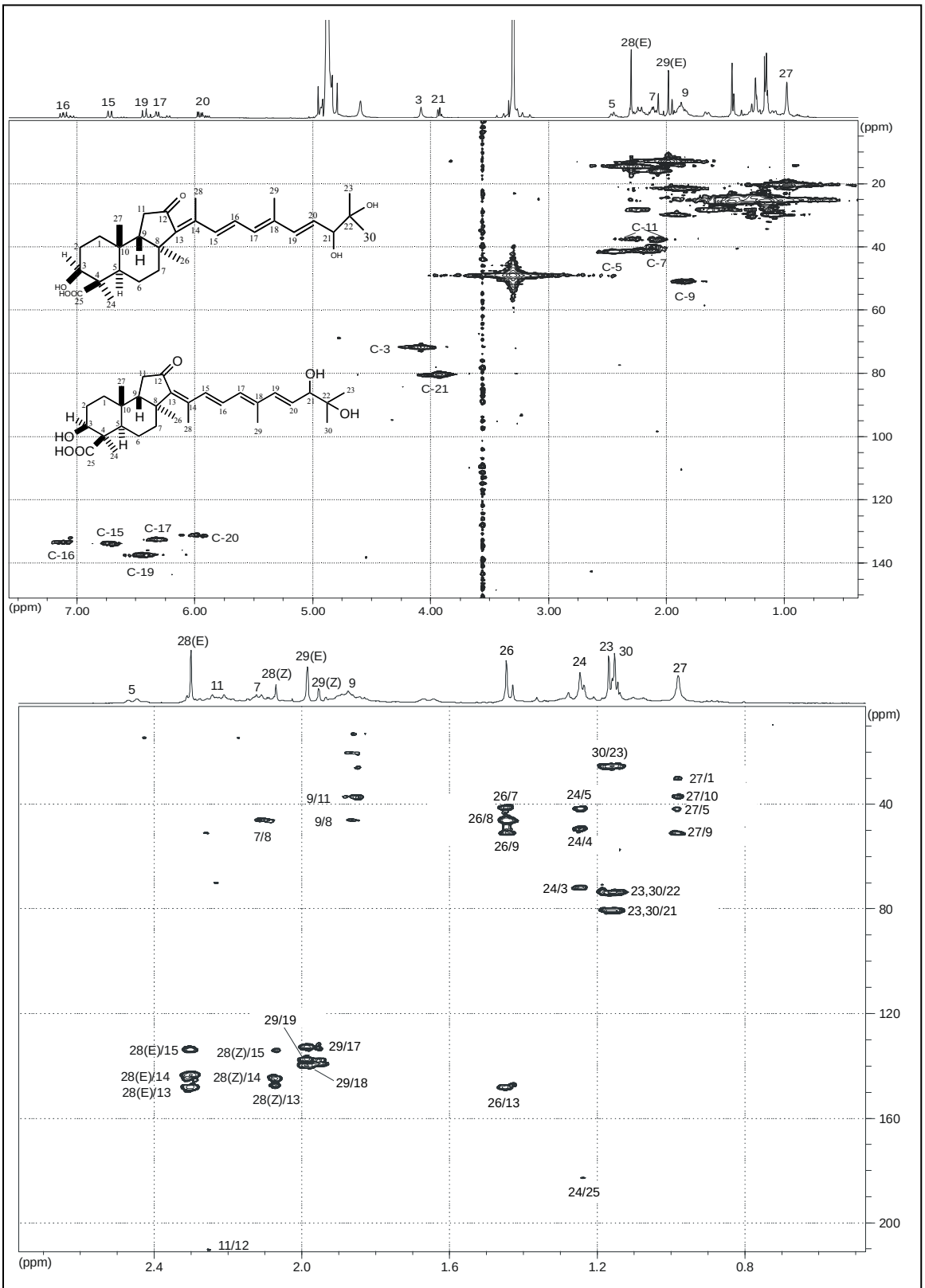

Fig. 3.66: HMQC spectrum of (top) and part of the HMBC spectrum (bottom) of compounds 26 and 27

Table 3.28: NMR data of compounds 26 and 27

Position	^{1}H NMR (ppm), multiplicity (Hz) of 26	^{1}H NMR (ppm), multiplicity (Hz) of 27	^{13}C NMR (ppm) of 26, 27*	HMBC correlations of 26, 27 H ⟶ C
1A	1.91 m	1.91 m	29.9 t	
1B	1.11 m	1.11 m	-	
2A	2.23 m	2.23 m	28.5 t	
2B	1.67 m	1.67 m	-	
3	4.08 br s	4.08 br s	71.7 d	
4	-	-	49.3 s	-
5	2.43 (1H, br d, 12.0 Hz)	2.43 (1H, br d, 12.0 Hz)	41.5 d	
6A,B	1.84 (2H, m)	1.84 (2H, m)	21.5 t	
7A	2.21 m	2.21 m	41.0 t	8
7B	2.14 m	2.14 m	-	
8	-	-	46.1 s	-
9	1.85 m	1.85 m	50.8 d	8, 11
10	-	-	37.0 s	-
11A	2.26 m	2.26 m	37.6 t	
11B	2.13 m	2.13 m	-	
12	-	-	209.9 s	-
13	-	-	148.1 s	-
14	-	-	143.4 s	-
15	6.72 (1H, d, 15.0 Hz)	8.05 (1H, d, 15.0 Hz)	133.7 d	
16	7.11 (1H, dd, 15.0, 11.3 Hz)	7.05 (1H, dd, 15.0, 11.3 Hz)	133.3 d	
17	6.31 (1H, d, 11.3 Hz)	6.22 (1H, d, 11.3 Hz)	132.5 d	
18	-	-	139.8 s	-
19	6.43 (1H, d, 15.8 Hz)	6.39 (1H, d, 15.8 Hz)	137.4 d	
20	5.96 (1H, dd, 15.8, 7.0 Hz)	5.90 (1H, dd, 15.8, 7.0 Hz)	131.1 d	
21	3.92 (1H, t, 7.0)	3.92 (1H,t, 7.0)	80.4 d	
22	-	-	73.5 s	-
23	1.18 (3H, s)	1.16 (3H, s)	25.2 q	21, 22, 30
24	1.25 (3H, s)	1.24 (3H, s)	24.4 q	3, 4, 5, 25
25	-	-	182.7 s	-
26	1.45 (3H, s)	1.43 (3H, s)	25.7 q	7, 8, 9, 13
27	1.01 (3H, s)	1.01 (3H, s)	20.4 q	1, 5, 9, 10
28	2.30 (3H, s)	2.07 (3H, s)	14.7 q	13, 14, 15
29	1.99 (3H, s)	1.95 (3H, s)	12.9 q	17, 18, 19
30	1.16 (3H, s)	1.15 (3H, s)	25.2 q	21, 22, 23

These compounds were measured in CD_3OD at 500 MHz.

* Obtained from the HMQC and HMBC spectra.

3.4.9. Stelliferin riboside (28, known compound)

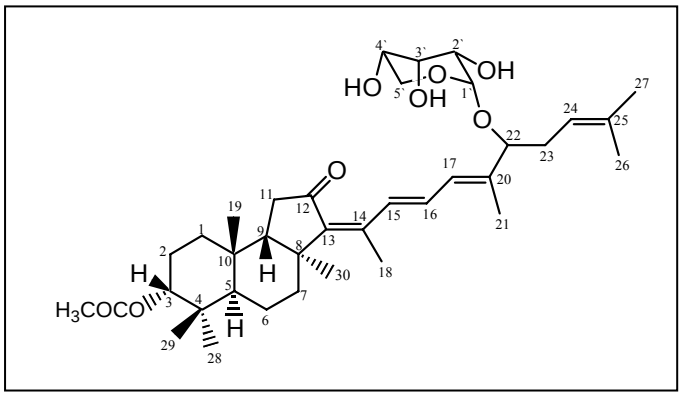

Compound **28** was isolated as a pure light yellowish oil with UV absorbance (MeOH) at λ_{max} 234 and 343 nm, $[\alpha]_D^{20}$ – 100.8 (*c* = 0.2, MeOH). The positive ESIMS of **28** showed a pseudomolecular ion peak at *m/z* 651 $[M+Na]^+$. This molecular weight is compatible with the molecular formula $C_{37}H_{56}O_8$. The ^1H NMR spectrum of compound **28** (see Fig. 3.67 and Table 3.29) revealed the presence of six methyls, two olefinic methyls, one acetoxy function, four olefinic protons, five oxygenated methine protons, and an anomeric proton doublet at 4.40 ppm (1H, d, 4.7 Hz). The five oxygenated methine protons and an anomeric proton suggested the presence of a sugar moiety. The UV spectrum of **28** (λ_{max} 343 nm, MeOH) indicated the presence of a trienone chromophore [Scott, *et al*., 1964]. The side chain substructure of compound **28** was supported by COSY correlations between, H-15 and H-17; H-16 to both H-15 and H-17, the homoallylic coupling H-17 and H-21; H-22 and H-23; H-23 and H-24 and finally, the homoallylic coupling between H-24 and both C*H*$_3$-26 and C*H*$_3$-27. The ^{13}C and DEPT spectra of compound **28** (see Fig 3.68 and Table 3.29) showed the presence of 37 carbons classified to nine methyls, seven methylenes, six oxymethines, six methines, seven quaternary carbons and two carbonyl groups which were comparative to an isomalabaricane triterpenoid aglycone attached to a pentose sugar. The sugar moiety appeared to be α-ribopyranose. The correlation in the COSY spectrum between H-1`and H-2`; H-2`and H-3`; H-3`and H-4`and H-4´and both protons of H-5` proved the sugar to be α-ribopyranose. This is also confirmed by the coupling constant of the anomeric proton (4.7 Hz) [Mohamadi, *et al*., 1990]. The HMBC spectrum of **28** showed connectivity from C*H*$_3$-18 to C-13, C-14 and C-15 indicating that C*H*$_3$-18 was attached at C-14. Similarly, C*H*$_3$-21 showed HMBC correlation to C-22 and C-17 which suggested that C*H*$_3$-21 was attached to C-20. Unfortunately, the attachment of the sugar moiety could not be determined through the

HMBC correlation, but on the other hand, the presence of a cross peak between H-1` and H-22, H-21 in the ROESY experiment confirmed the attachment of the sugar to C-22. Comparison between the NMR data of **28** and those reported for stelliferin riboside confirmed the structure of compound **28** to be identical to the known compound stelliferin riboside [Tabudravu*, et al*., 2001]. The relative sterochemistry of compound **28** was established through the coupling constant values $J_{15,16}$ = 15.5 Hz, $J_{16,17}$ = 11.0 Hz which suggested the 15*E*, 17*E*, geometries characterised for all the isomalabaricane triterpenoids. The sterochemisry of the ring junctions of the tricyclic fragment was determined by the key cross peaks in the ROESY spectrum between H-5 and CH_3-30, CH_3-28; H-3 and CH_3-19,CH_3-29; CH_3-19 and CH_3-29 which also suggested a *trans-syn-trans* sterochemisry characterised for all the isomalabaricane triterpenoids. The downfield shift of H-15 at 8.00 ppm in the ^{1}H NMR of **28** suggested that it was in the deshielding region of the carbonyl group at C-12 which is only possible for a 13*Z*-configuration.

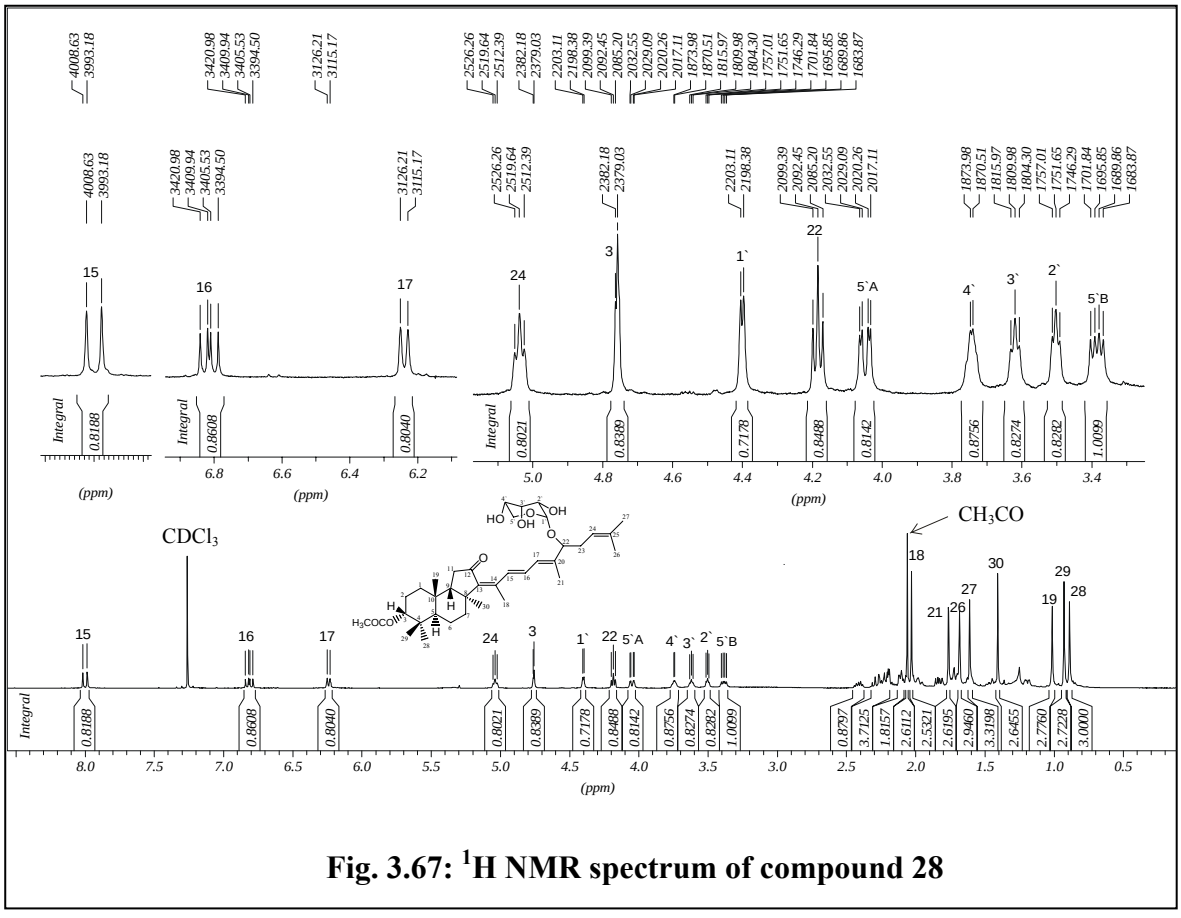

Fig. 3.67: ^{1}H NMR spectrum of compound 28

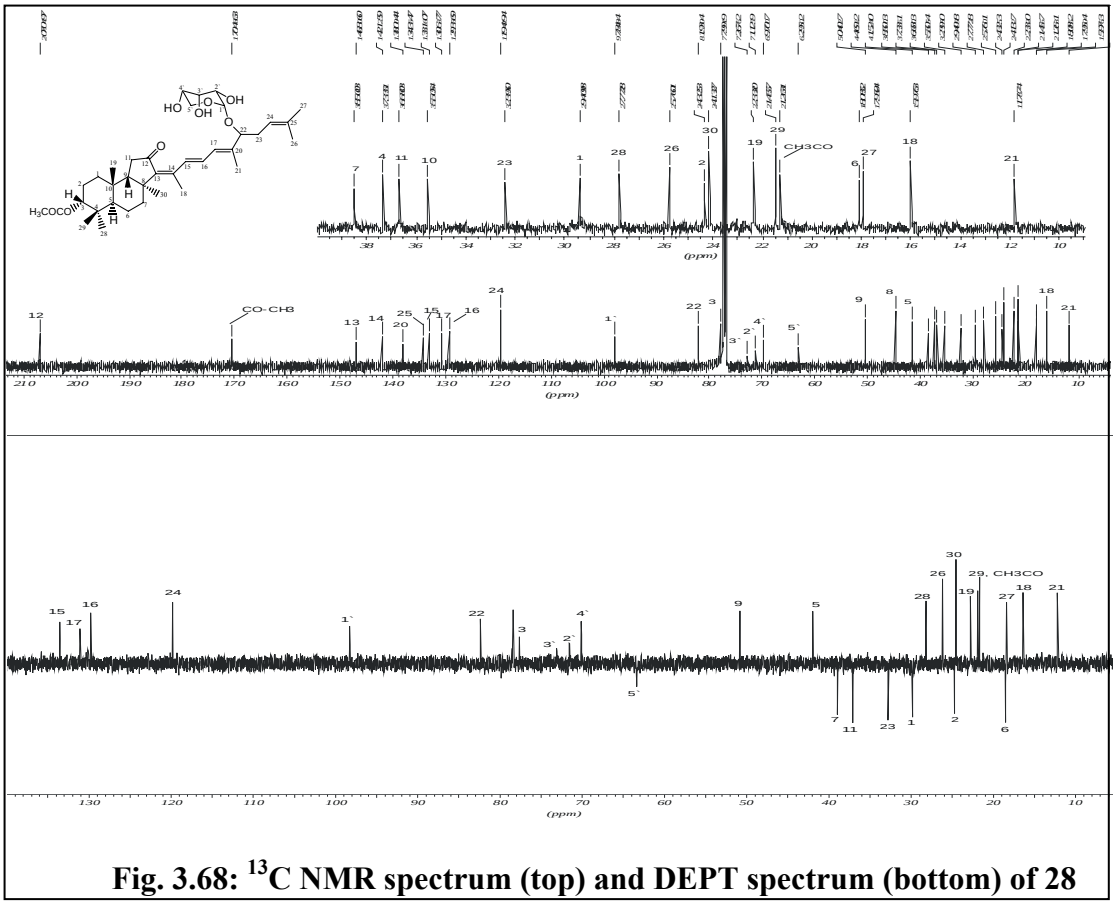

Fig. 3.68: ^{13}C NMR spectrum (top) and DEPT spectrum (bottom) of 28

3.4.10. 13-*E*-Stelliferin riboside (29, new compound)

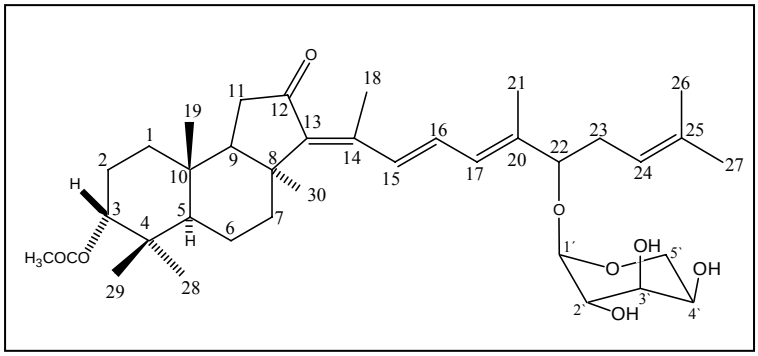

Compound **29** was obtained as yellow oily substance, $[\alpha]_D^{20}$ + 150 (*c* = 0.019, MeOH). It showed a pseudomolecular ion peak in the positive ESIMS at *m/z* 651 $[M+Na]^+$. This molecular weight is compatible with the molecular formula $C_{37}H_{56}O_8$. The ^{1}H NMR of compound **29** (see Fig 3.69 and Table 3.29) indicated the presence of nine methyls, four olefinic protons, seven methylenes and six oxygenated methines. The presence of an anomeric doublet at 4.51 ppm with a coupling constant of 3.9 Hz as exhibited in the ^{1}H NMR spectrum

of compound **29** suggested the presence of α-ribose sugar as present in compound **28**. This is confirmed by the presence of a clearly isolated spin system in the COSY spectrum (see Fig 3.70) typical for a sugar system. Comparison between the molecular weight and ^{1}H NMR spectrum of compound **29** and the known compound stelliferin riboside **28** suggested that compound **29** is a steroisomer of the known compound **28**. The ^{1}H NMR spectrum of **29** was comparable to that of **28,** except for the upfield shift of H-15 (6.63 ppm) which indicated that it is not in the deshielding region of the carbonyl group at C-12. This was also confirmed by the downfield shift of C*H*$_3$-18 (2.33 ppm). This suggested that compound **29** is the 13*E*-isomer of compound **28**. The relative stereochemistry of the tricyclic moiety was determined through ROESY correlation between the pairs H-9/C*H*$_3$-19, as well as H-5/C*H*$_3$-30, which again clearly established a *trans-syn-trans* stereochemistry corresponding to an isomalabaricane skeleton. On the other hand, the attachment of the sugar moiety was confirmed also as mentioned before by the key cross peak between H-1`and both H-22 and H-21 in the ROESY spectrum. This confirmed the attachment of the sugar moiety to C-22 which is compatible with the downfield shift of H-22 at 4.19 ppm.

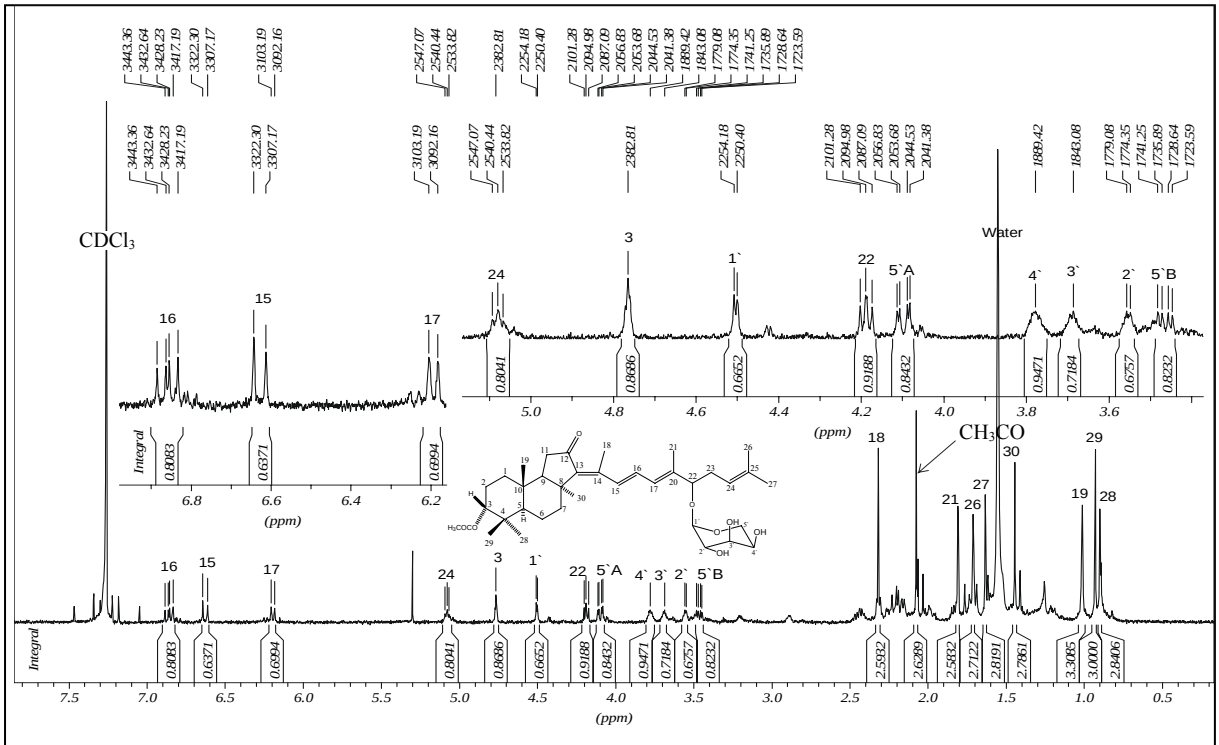

Fig. 3.69: ^{1}H NMR spectrum of compound 29

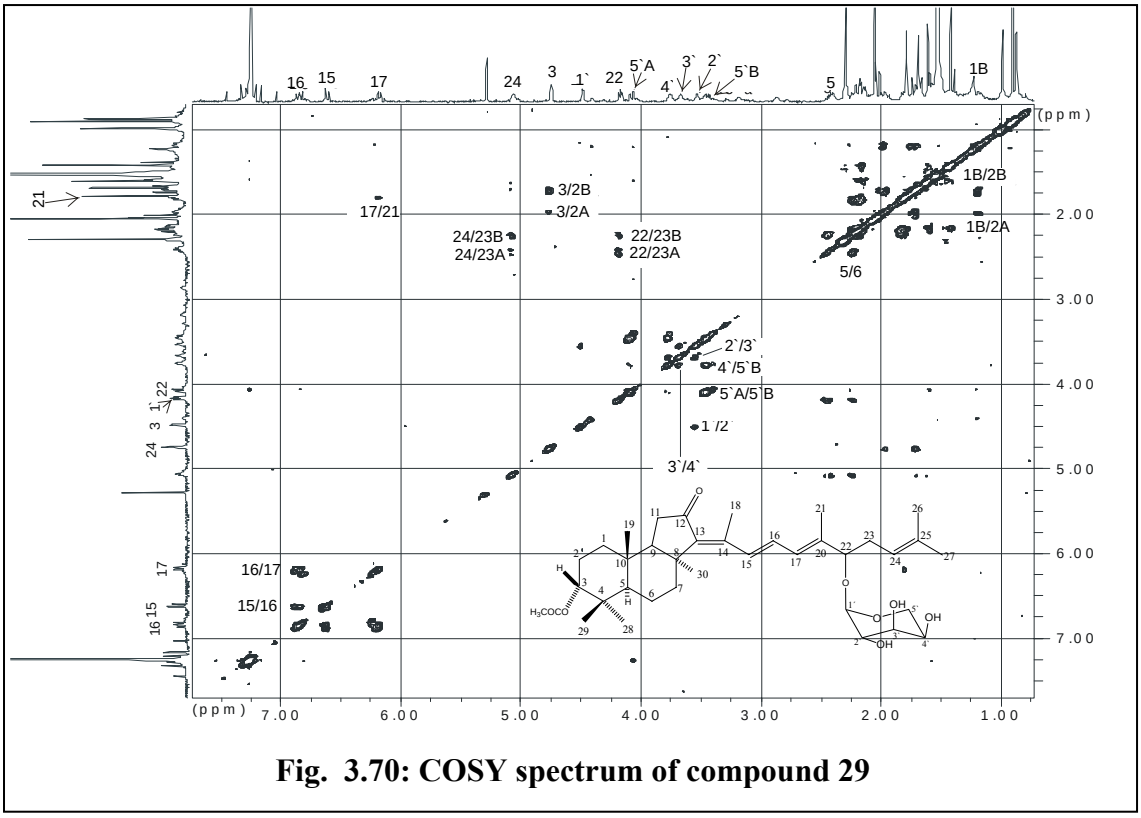

Fig. 3.70: COSY spectrum of compound 29

3.4.11. 3-Hydroxy-stelliferin riboside (30, new compound)

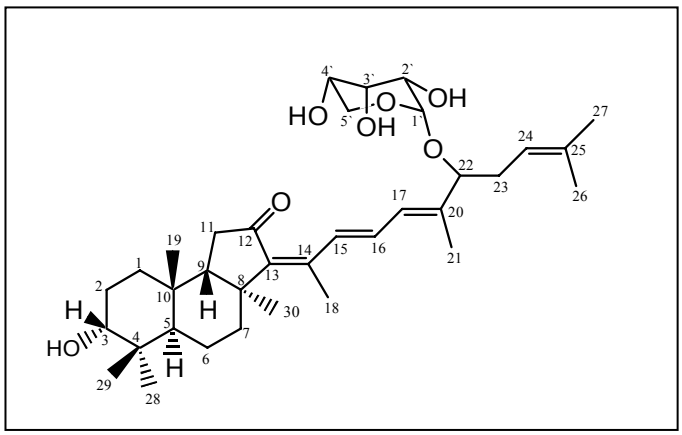

Compound **30** was obtained as a yellow oily substance, $[\alpha]_D^{20}$ – 41.8 (*c* = 0.2, MeOH). It showed a pseudomolecular ion peak in the positive FABMS at *m/z* 609 $[M+Na]^+$. The molecular formula $C_{35}H_{54}O_7Na$ $[M+Na]^+$ was established by HRESIMS ($C_{35}H_{54}O_7Na$, *m/z* 609.3777, calculated 609.3770). The ^1H NMR of compound **30** (see Fig. 3.71 and Table 3.30) showed the presence of eight methyls, seven methylenes, four olefinic protons and six oxygenated methines. Comparison between the ^1H NMR, ^{13}C NMR, HMBC (see Fig. 3.72 and Table 3.30) data of compound **30** and the known compound **28** [Tabudravu, *et al.,* 2001] revealed that compound **30** is closely related to the latter, except for the absence of an acetoxy group at 2.06 ppm which suggested that **30** may be the hydroxyl congener of compound **28**. This was confirmed by the upfield shift of H-3 in **30** at 3.52 ppm in comparison to that of compound **28** at 4.76 ppm. The coupling constant value of the anomeric proton of the ribose sugar (4.7 Hz) confirmed the α-ribopyranose sugar moiety [Tabudravu, *et al*., 2001]. The COSY spectrum of **30** (see Fig. 3.73) established the side chain part and the tricyclic moiety part. The relative stereochemistry of **30** was evaluated through ROESY correlation between the pairs H-9/C*H*$_3$-19, C*H*$_3$-19/C*H*$_3$-29, as well as H-5/C*H*$_3$-30, which clearly established a *trans-syn-trans* stereochemistry corresponding again to an isomalabaricane skeleton. According to the useful model which was described by Tsuda, *et al*. 1991], the presence of ^{13}C chemical shift of 21.8 ppm for the 4β-Me (C-29) is indicative of the presence of a 3α-hydroxyl group while the chemical shift goes generally to the lower field for a 3β-hydroxyl function (17.0 ppm for 4β-Me is generally associated with 3β-hydroxyl group) [Tabudravu, *et al*., 2001]. This was compatible with the presence of a strong ROESY correlation between H-3 and H-9 with C*H*$_3$-19.

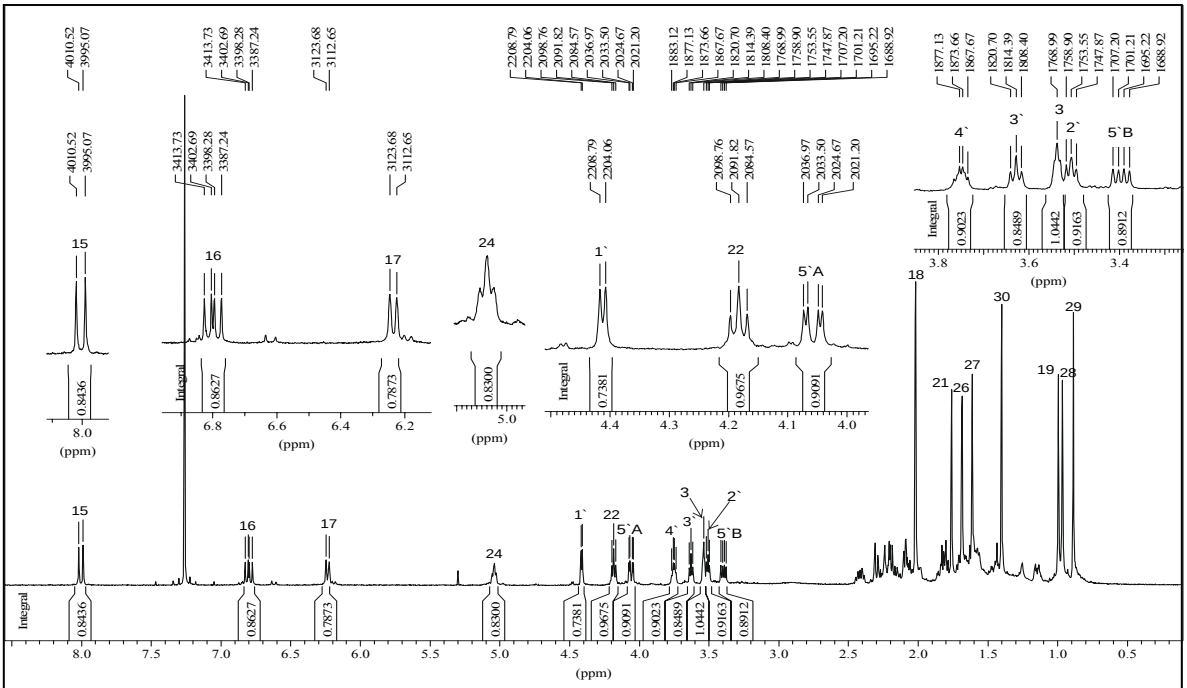

Fig. 3.71: ^{1}H NMR spectrum of compound 30

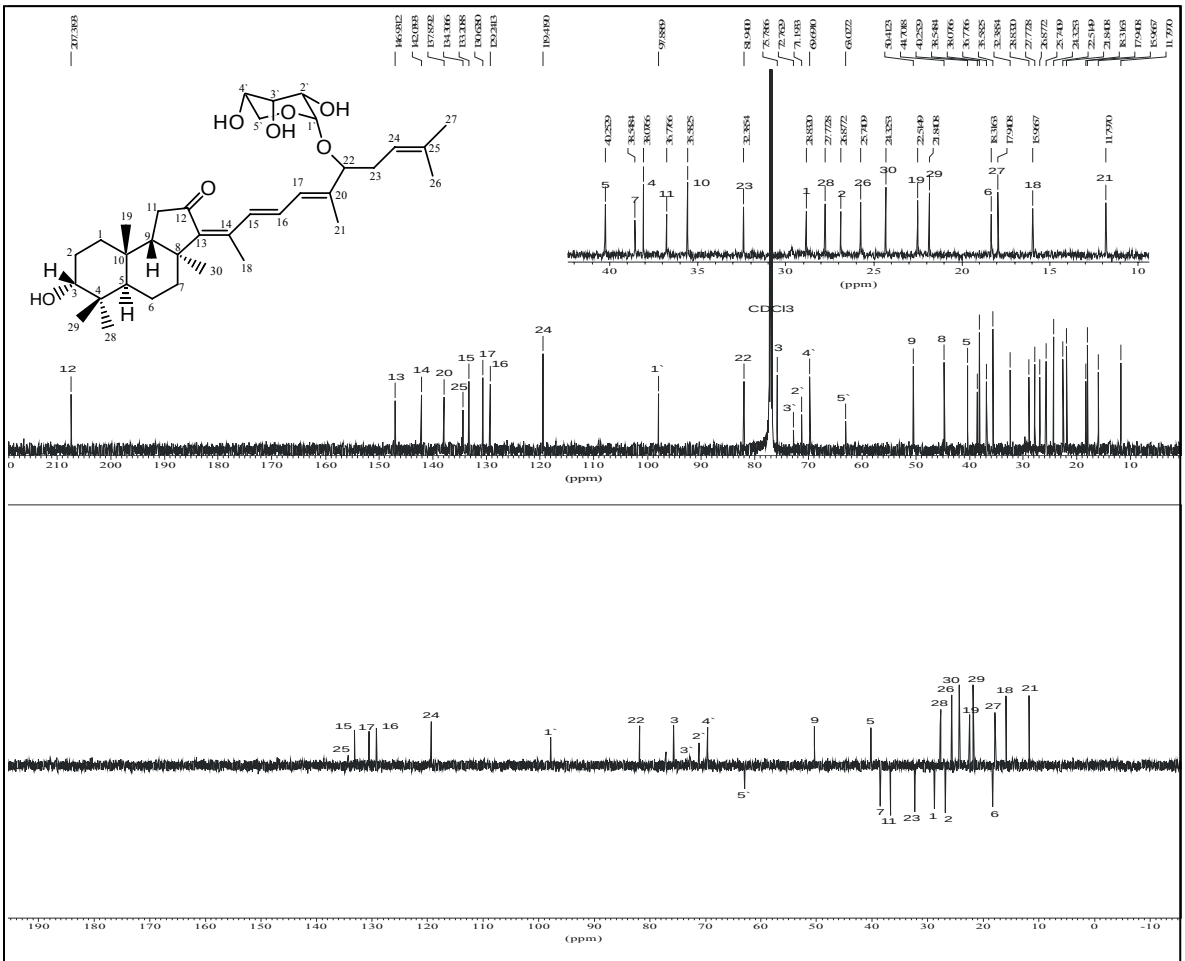

Fig. 3.72: ^{13}C NMR spectrum (top) and DEPT spectrum (bottom) of 30

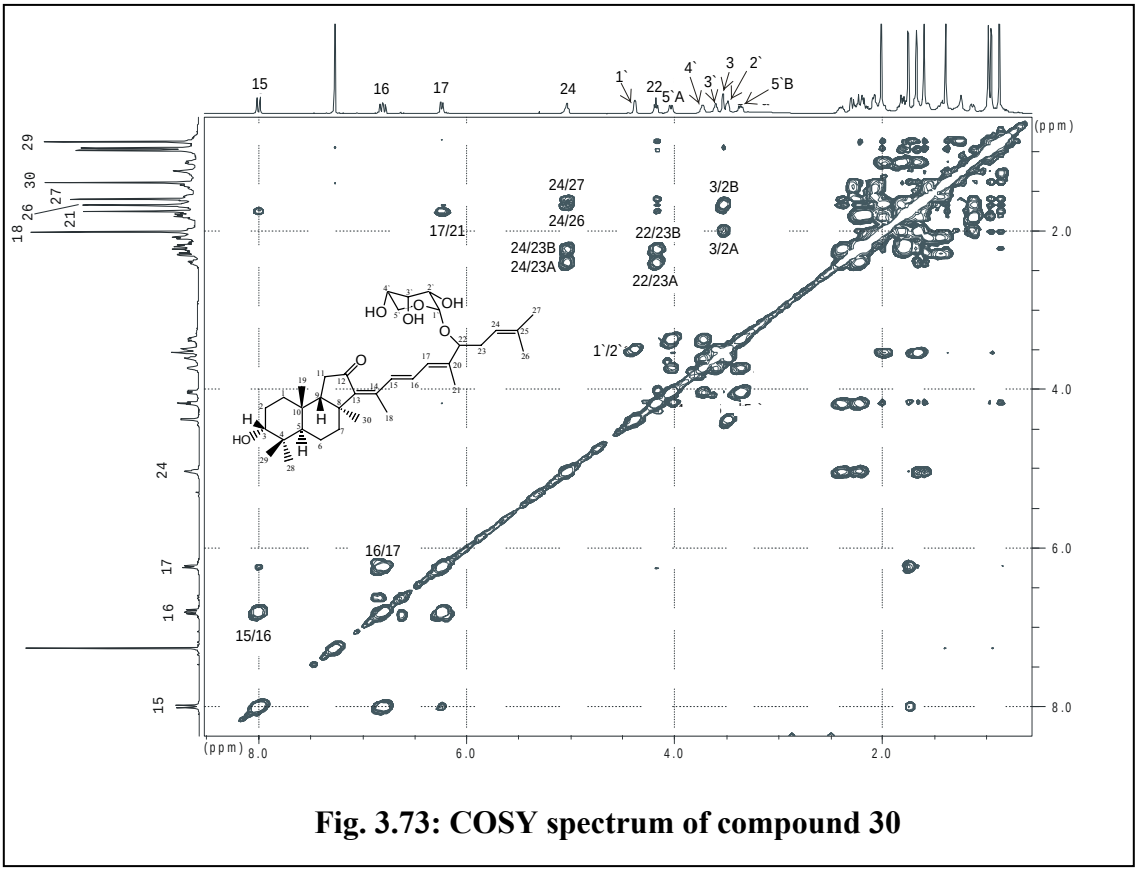

Fig. 3.73: COSY spectrum of compound 30

Table 3.29: NMR data of compounds 28-29

Protons	^{1}H NMR (ppm), multiplicity (Hz) of 28	^{1}H NMR (ppm), multiplicity (Hz) of 29	^{13}C NMR (ppm) of 28
1A,B	1.20 (2H, m)	1.20 (2H, m)	29.4 t
2A	1.95 m	1.99 m	24.3 t
2B	1.72 m	1.72 m	-
3	4.76 (1H, d, 3.2 Hz)	4.77, m	78.0 d
4	-	-	37.3 s
5	2.27 m	2.35 m	41.5 d
6A	1.60 m	1.59 m	18.1 t
6B	1.46 m	1.42 m	-
7A,B	2.08 (2H, m)	2.08 (2H, m)	38.5 t
8	-	-	44.7 s
9	1.79 m	1.83 m	50.4 d
10	-	-	35.5 s
11A,B	2.15 (2H, m)	2.20 (2H, m)	36.7 t
12	-	-	207.1 s
13	-	-	146.8 s
14	-	-	142.1 s
15	8.00 (1H, d, 15.5 Hz)	6.63 (1H, d, 15.4 Hz)	133.2 d
16	6.81(1H, dd, 15.5, 11.0 Hz)	6.86 (1H, dd, 15.4, 11.0 Hz)	129.4 d
17	6.24 (1H, d, 11.0 Hz)	6.19 (1H, d, 11.0 Hz)	130.4 d
18	2.03 (3H, s)	2.33 (3H, s)	16.0 q
19	1.02 (3H, s)	1.02 (3H, s)	22.3 q
20	-	-	138.0 s
21	1.76, s	1.82, s	11.8 q
22	4.18 (1H, t, 7.0 Hz)	4.19 (1H, t, 7.0 Hz)	81.9 d
23	2.17, 2.40, m	2.24, 2.43, m	32.4 t
24	5.04 (1H, t, 7.0 Hz)	5.09 (1H, t, 7.0 Hz)	119.4 d
25	-	-	134.4 s
26	1.69 (3H, s)	1.72 (3H, s)	25.8 q
27	1.61 (3H, s)	1.64 (3H, s)	18.0 q
28	0.89 (3H, s)	0.89 (3H, s)	27.8 q
29	0.93 (3H, s)	0.93 (3H, s)	21.5 q
30	1.41 (3H, s)	1.45 (3H, s)	24.1 q
COC*H*$_3$	2.06 (3H, s)	2.09 (3H, s)	21.3 q
O*C*O	-	-	170.5 s
1`	4.40 (1H, d, 4.7 Hz)	4.51 (1H, d, 3.9 Hz)	97.9 d
2`	3.52 (1H, t, 5.4 Hz)	3.57 (1H, t, 5.4 Hz)	71.1 d
3`	3.62 (1H, t, 6.0 Hz)	3.69 (1H, t, 5.4 Hz)	72.7 d
4`	3.74 (1H, dm, 3.5 Hz)	3.78 m	69.7 d
5`A	4.05 (1H, dd, 11.9, 3.2 Hz)	4.10 (1H, dd, 12.3, 3.2 Hz)	63.0 t
5`B	3.38 (1H, dd, 12.0, 6.0 Hz)	3.46 (1H, dd, 12.3, 6.3 Hz)	-

These compounds were measured in $CDCl_3$ at 500 MHz.

Table 3.30: NMR data of compound 30

Position	^{1}H NMR (ppm), multiplicity (Hz) of 30	^{13}C NMR (ppm) of 30	HMBC correlations of 30 H → C
1A	1.79 m	28.8 t	
1B	1.16 m	-	
2A	1.98 m	26.9 t	
2B	1.69 m	-	
3	3.52 (1H, t, 7.0 Hz)	75.8 d	
4	-	38.1 s	-
5	2.30 m	40.2 d	4, 10, 19
6A	1.59 m	18.3 t	
6B	1.47 m	-	
7A,B	2.10 (2H, m)	38.5 t	
8	-	44.7 s	-
9	1.79 m	50.4 d	8
10	-	35.6 s	-
11A,B	2.20 (2H, m)	36.8 t	8, 12
12	-	207.3 s	-
13	-	146.9 s	-
14	-	142.0 s	-
15	8.01 (1H, d, 15.4 Hz)	133.2 d	
16	6.80 (1H, dd, 15.4, 11.0 Hz)	129.2 d	
17	6.40 (1H, d, 11.0 Hz)	130.6 d	20
18	2.02 (3H, s)	16.0 q	13, 14, 15
19	1.01 (3H, s)	22.5 q	1, 5, 9, 10
20	-	137.9 s	-
21	1.76, s	11.8 q	20, 22
22	4.18 (1H, t, 7.0 Hz)	81.9 d	
23	2.25, 2.40, m	32.4 t	22
24	5.04 (1H, t, 7.0 Hz)	119.4 d	
25	-	134.3 s	-
26	1.69 (3H, s)	25.7 q	24, 25, 27
27	1.61 (3H, s)	17.9 q	24, 25, 26
28	0.97 (3H, s)	27.8 q	3, 4, 5, 29
29	0.89 (3H, s)	21.8 q	3, 4, 5, 28
30	1.40 (3H, s)	24.3 q	7, 8, 9, 13
COC*H*$_3$	-	-	-
O*C*O	-	-	-
1´	4.41 (1H, d, 4,7 Hz)	97.9 d	
2´	3.54 (1H, t, 5.4 Hz)	71.2 d	
3´	3.63 (1H, t, 6.0 Hz)	72.8 d	
4´	3.75(1H, bm, 6.0 Hz)	69.7 d	
5´A	4.06 (1H, dd, 12.3, 3.5, Hz)	63.0 t	
5`B	3.40 (1H, dd, 12.3, 6.3 Hz)	-	

This compound was measured in $CDCl_3$ at 500 MHz.

Bioactivity

Many isomalabaricane triterpenoid compounds isolated from different sponges showed cytotoxicity against different cancer cells like melanoma cells [Meragelman, *et al.*, 2001], epidermoid human carcinoma Kb cells [Bourguet-Kondracki, *et al.*, 2000] or against P-388 murine leukaemia cells [Ryu, *et al.*, 1996]. In our search for new biologically active natural products, all isolated compounds from the sponge *Rhabdastrella globostellata* were tested against different gram positive and gram negative bacteria. Some compounds showed moderate activity against some bacteria while the other were inactive. (see Table 3.31). On the other hand, it was interesting to note that all of the compounds showed a strong or moderate activity against different cancer cells like L5178Y cervix carcinoma cells, Hela mouse lymphoma cells, or PC12 brain tumour cells of rats. The tests were determined using the microculture tetrazolium (MTT) assay, and data were compared to those of untreated controls [Carmichael, *et al.*, 1987]. The results are summarised in (Table 3.32).

Table 3.31: Agar plate diffusion assay of pure compounds isolated from *Rhabdastrella globostellata*.

Compound*	Zone of inhibition (mm)		
	E. coli	***B. subtilis***	***S. cerevisia***
Globostellatic acid A (16)			
(50 µg)	-	-	-
(100 µg)	-	-	-
Globostellatic acid E (17)			
(50 µg)	-	-	-
(100 µg)	-	-	-
Globostellin (19)			
(50 µg)	-	12	n.
(100 µg)	10	13	n.
Globostellatic acid D and M (20 &21)			
(50 µg)	-	-	-
(100 µg)	10	-	-
Globostellatic acid G and H (22&23)			
(50 µg)	-	-	-
(100 µg)	10	-	-
Globostellatic acid I and J (26&27)			
(50 µg)	-	-	-
(100 µg)	-	9	-
Stelliferin riboside (28)			
(50 µg)	-	-	-
(100 µg)	-	-	-
3-Hydroxy-stelliferin riboside (30)			
(50 µg)	-	-	-
(100 µg)	12	-	-

(-): Negative.

* amount tested at µg per disc.

Table 3.32: Cytotoxicity of isolated isomalabarican derivatives against L5178Y, Hela and PC12 cells.

Compounds	L5178Y % of inhibition		Hela % of inhibition		PC12 % of inhibition	
concentration	**10µg/ml**	**3µg/ml**	**10µg/ml**	**3µg/ml**	**10µg/ml**	**3µg/ml**
Globostellatic acid A (16)	100	100	0	0	0	0
Globostellatic acid E (17)	100	42	0	0	0	0
Globostellin (19)	94	66	0	0	0	0
Globostellatic acid D, M (20, 21)	100	100	25	4	42	18
Globostellatic acid D, H (22, 23)	100	100	23	8	41	16
Globostellatic acid I, J (24, 25)	100	24	0	0	0	0
Globostellatic acid K, L (26, 27)	100	100	42	0	30	0
Stelliferin riboside (28)	100	100	56	0	38	0
3-Hydroxy-stelliferin riboside (30)	100	100	100	26	54	33

4. Discussion

4.1. Isolated compounds from sponges collected from the Gulf of Aqaba, Red Sea

The Red Sea has been a focus of attention for many scientists who have been amazed by its clear warm waters and abundance of marine life. The Gulf of Aqaba is one of the two northern V-shaped branches of the Red Sea and is 170 km long, 4-26 km wide and up to 1830 m deep. Many interesting, biologically active compounds have been isolated from the Red Sea, like eryloside A [Carmely, *et al*., 1989], latrunculins A and B [Groweiss, *et al.,* 1983] and sipholenols G, F and H [Kashman, *et al.*, 2001].

4.2. Metabolites isolated from the sponge *Erylus lendenfeldi.*

Steroids or triterpenoid saponins are rarely found in marine sponges, except in the astrophorid sponges [Takada, *et al.,* 2002]. Bioassays revealed that *Erylus lendenfeldi* has a strong deterrent activity against fish. Three steroidal saponins have been isolated from this sponge. The known steroidal saponin eryloside A showed an antifungal activity against *Candida albicans* but was inactive against *S. aureus*.

4.2.1. Steroidal saponins

Saponins are glycosides which even at low concentrations produce a frothing in aqueous solution, because they have surfactant and soap-like properties. The name comes from the Latin sapo, meaning soap. These compounds cause haemolysis, lysis of red blood cells by increasing the permeability of the plasma membrane, and thus they are highly toxic when injected into the blood stream [Dewick, 2002]. Although a large number of new sterol structures have been discovered from marine organisms during the last twenty years, very few secosteroids have been reported. After the discovery in 1972 of the unique 3β, 11-dihydroxy-9,11-secogorgost-5-en-9-one from a gorgonian [Enwall, *et al.*, 1972], two new 9,11-secosterols were isolated from the soft coral *Sinularia sp.* (see Fig. 4.1) [Kazlauskas, *et al.,* 1982] and trihydroxylated 5,6-secosterol known as hipposterol has been isolated from the sponge *Hippospongia communis* (see Fig 4.1) [Madaio, *et al.,* 1988]. The authors have proposed these sterols to originate biogenetically from a 5,6-secosterol through further cleavage of the 9, 10 bond. Recently, the 3β-methoxysteroid, jereisterol A with a rare seco-structure has been isolated from the Pacific sponge *Jereicopsis graphidiophora* [D´Auria, *et al.,* 1991].

4.2.2. Biosynthesis of tetracyclic triterpenes and steroids.

For the biosynthesis of these derivatives the catalysing enzyme folds (3S)-2,3-oxidosqualene in a chair-boat-chair-boat-endo-conformation and the epoxide is opened under catalytic influence by a protonated group on the enzyme. Fourfold cyclization then yields the protosterol carbonium ion I with the side chain at C-17 in the β position. Elimination of H at C-9 forms the double bond C-8-C-9 in lanosterol (see Fig. 4.2, route a) while in the formation of cycloartenol C-9 H is shifted to C-8 with retention of the β-configuration and a new bond is formed between C-19 and C-9 (see route b, Fig. 4.2). Lanosterol and cycloartenol are precursors for steroids which are natural products of great medicinal importance [Samuelsson, 1999].

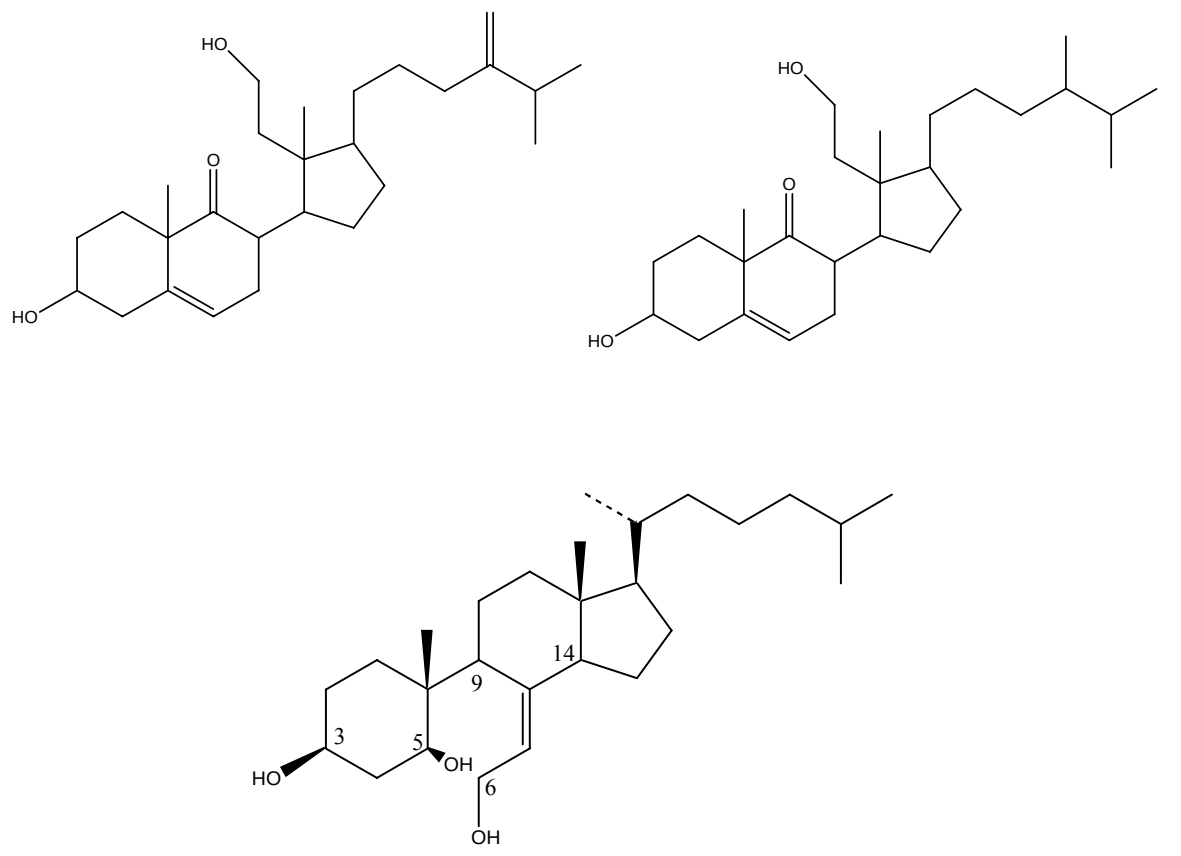

hipposterol

Fig. 4.1: Some new secosteroidal saponins of marine origin

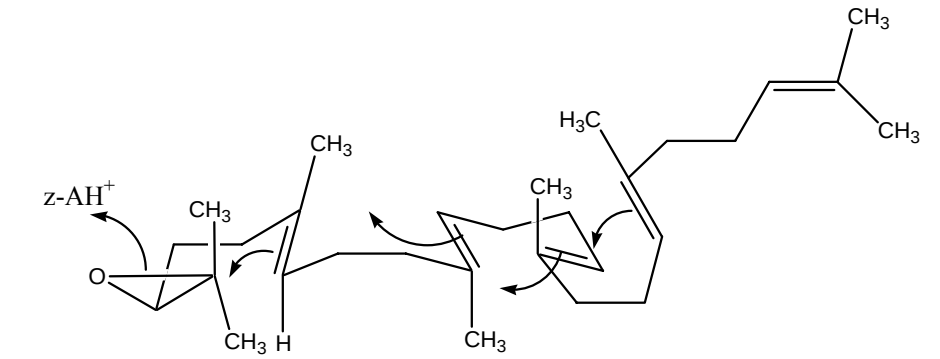

Squalene oxide (chair-boat-chair-boat) endo-conformation

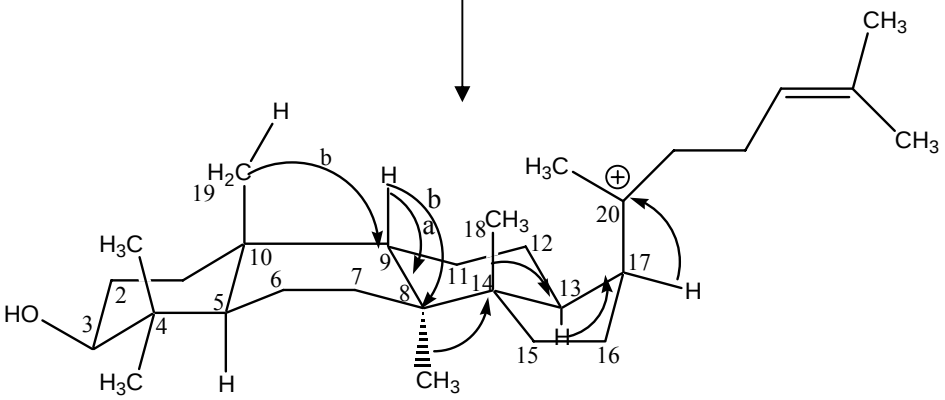

Protosterol carbonium ion I (17-β-side chain)

b

a

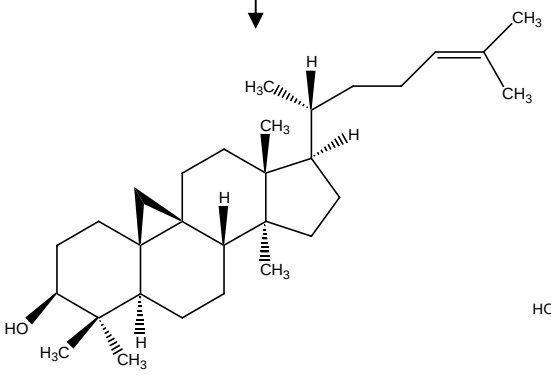

Cycloartenol

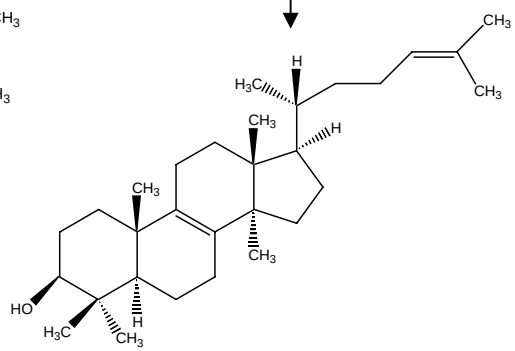

Lanosterol

Fig. 4.2: Biosynthesis of tetracyclic triterpenes and steroids

4.3. Metabolites isolated from the sponge *Negombata corticata*.

In our search to isolate biologically active compounds from marine origin, latrunculin B and M were two known toxic substances isolated from the Red Sea sponge *Negombata corticata*. It was soon realised that all the collections near Sharm-elshikh and in the Gulf of Suez contained the known toxic latrunculin A while those reported from the Gulf of Eilat contained only latrunculin B [Groweiss, *et al.,* 1983]. Trials to isolate latrunculin A or any related compounds from *Negombata corticata* collected from Aqaba have failed and confirm the previous work [Kashman, *et al*., 1980]. Latrunculins have been shown to disrupt micro-filament organisation and exert profound effects on the morphology of non-muscular cells without affecting the organisation of the microtubular system [Kashman, *et al*., 1980; Spector, *et al.*, 1983]. The latrunculins are also potent inhibitors of the microfilament-mediated processes of fertilisation and early development in sea urchin eggs and in mouse oocytes [Schatten, *et al*., 1986].

4.3.1. Structure activity relationship of latrunculins

The interesting action of the latrunculins on the cytoskeletal protein actin [Spector, *et al.*, 1983] raised the question of structure-activity relationships. It was found that blocking the 15-OH group of the ketal (as an OMe ketal) causes a delayed activity of the compound, maybe due to the decomposition of the ketal back into the original lactol [Spector, *et al.*, 1989]. On the other hand, replacing the N*H* proton by alkyls or various benzyls cancels the activity [Blasberger, *et al.,* 1987]. Conversion of the NH to the N-formyl derivative maintained the activity [Kashman, *et al.*, 1989]. Deeper insight into the mode of action of the latrunculins revealed clear differences between latrunculin A and B initiating the preparation of more derivatives of both toxins. Latrunculin B exhibited a strong activity as antimicrobial agent although it has not the double bond flanked by two carbonyl carbons required for the activity of the macrolide [Rodphaya, *et al.*, 1986]. This suggested that this activity may be due to the other functional groups such as the thiazolidinone or the tetrahydropyranyl groups.

4.3.2. Effect of latrunculin B on actin

Latrunculin B is a pharmacological agent that disrupts the actin cytoskeleton in numerous cell types, including budding yeast [Ayscough, *et al.,* 1997]. The origin and structure of latrunculin B are closely related to latrunculin A. This similarity suggests that latrunculin B has a mechanism on actin related to latrunculin A, in which binding of latrunculin A to the monomeric actin (G-actin) prevents its incorporation into microfilaments

[Coue, *et al.,* 1987]. Studies of actin mutants resistant to latrunculin A treatment indicated that latrunculin A specifically binds to a region adjacent to the nucleotide binding cleft [Ayscough, *et al.,* 1997]. Because the structure of latrunculin B is similar to that of latrunculin A, the effects of these latrunculins on yeast actin may be also be analogous. Treatment of yeast cells with latrunculin A causes complete depolymerization of F-actin, leading to a total loss of actin cables and patches [Allen, 2000].

4.3.3. The relationship between the actin cytoskeleton and gene expression

Several studies in mammalian cells identified individual genes induced by disruption of the actin cytoskeleton. Treatment of Hela and WI-38 cells with cytochalasin D (CD), a pharmacologic agent that disrupts F-actin, caused a large increase in the transcription of the proto-oncogene *C-fos* [Zambetti, *et al*., 1991]. In another study, treatment of human epidermoid carcinoma cells with dehydrocytochalasin B, a non-specific agent that disrupts F-actin, activated transcription of ICAM-1 [Norgauer, *et al*., 1995]. Theses studies suggested that disruption of the actin cytoskeleton affects transcript levels of particular genes. However, the fundamental role of the actin cytoskeleton in the regulation of gene expression has not been identified.

4.3.4. Effects of latrunculin B on the actin cytoskeleton in *S. cerevisiae*

After treatment of cells (actin cytoskeleton) with latrunculin B, filamentous (F-actin) was visualized by rhodamine-phalloidin staining followed by fluorescence microscopy. A comparison of the effects of various latrunculin B doses on actin after one h showed that in a sample treated with 10 μM latrunculin B, actin cables were not visible but actin patches remaine somewhat polarized. At 25 μM latrunculin B, actin cables were also not visible and actin patches were found distributed in an analytical pattern throughout the mother and bud cells. These results indicated that latrunculin B disrupted actin cables at the lowest dose treated, while actin patches became progressively more polarized at the dose of latrunculin B was increased, [Allen, 2000].

4.3.5. Latrunculin B treatment causes changes in transcript levels of particular genes.

It is reported that latrunculin B induced disruption of the actin cytoskeleton would affect genes targeted by the *PKCI* MAP kinase pathways. FKSI is targeted by the PKCI pathway and involved in cell responses to stress. It was reported that a minor increase in FKSI levels occured after one h latrunculin B treatment and no change after 2hr treatment. In

contrast, transcript levels of *PPZI*, a gene encoding for a phosphatase whose product plays a role in osmoregulation and the *PKCI* pathway, were clear induced by latrunculin B treatment, particularly after 2hr, [Allen, 2000].

4.3.6. Activation of oocytes by latrunculin A

Actin depolymerization by latrunculin A in mature starfish oocytes induced a massive calcium mobilization that resulted in the discharged of the cortical granules and in the elevation of the fertilization envelope. The calcium liberation started as a circumscribed subplasma membrane hotspot, which is followed by a flash of calcium increase restricted to the cortical layer. The calcium response to spermatozoa (i.e., peripheral hotspot, cortical flash, globalization of the signal) closely mimicked that promoted by latrunculin A. Thus, the initial cortical release of calcium promoted by the sperm may be due to the depolymerization of actin, [Lim, *et al*., 2002].

4.3.7. Biosynthesis of macrolides

As previously mentioned, the latrunculins are the first known 2-thiazolidinone-bearing marine macrolides with 14 or 16 atoms. Furthermore, macrolides are antibiotic compounds produced for example by bacteria of the genus *Streptomyces*, the main structural feature of which is a large lactone ring of acetate origin containing 12, 14, or 16 atoms. Macrolides are biosynthesised by type I polyketide synthases (PKS) i.e. they are organised in a complex of multifunctional proteins [Samuelsson, 1999]. Epothilones are macrolactones produced by the Gram-nagative myxobacterium *Sorangium cellulosum* [Gerth, *et al*., 1996] and has a somewhat related structure to latrunculins which suggests that their biosynthesis involves a type I polyketide synthase (PKS). These enzymes are large multifunctional complexes organized in a modular fashion and catalyze the successive condensation of carboxylic acid residues in a step-wise process. Each protein has one or more modules, each with discrete domains for activities required for the elongation and processing of the polyketide ahin. These must include the β-ketoacyl synthase (KS), acyltransferace (AT) and acyl carrier protein (ACP) domains; β-ketoreductase (KR), dehydratase (DH), enoyl reductase (ER), methyltransferase (MT) or thioestrase (TE) domains may also be present. Sequencing has shown that genes required for the synthesis of each polyketide are clustered on the bacterial chromosome, facilitating their cloning and subsequent characterization. The steps of the biosynthesis of epothilones are represented in Fig 4.3, [Dewick, 2002; Julien, *et al*., 2000].

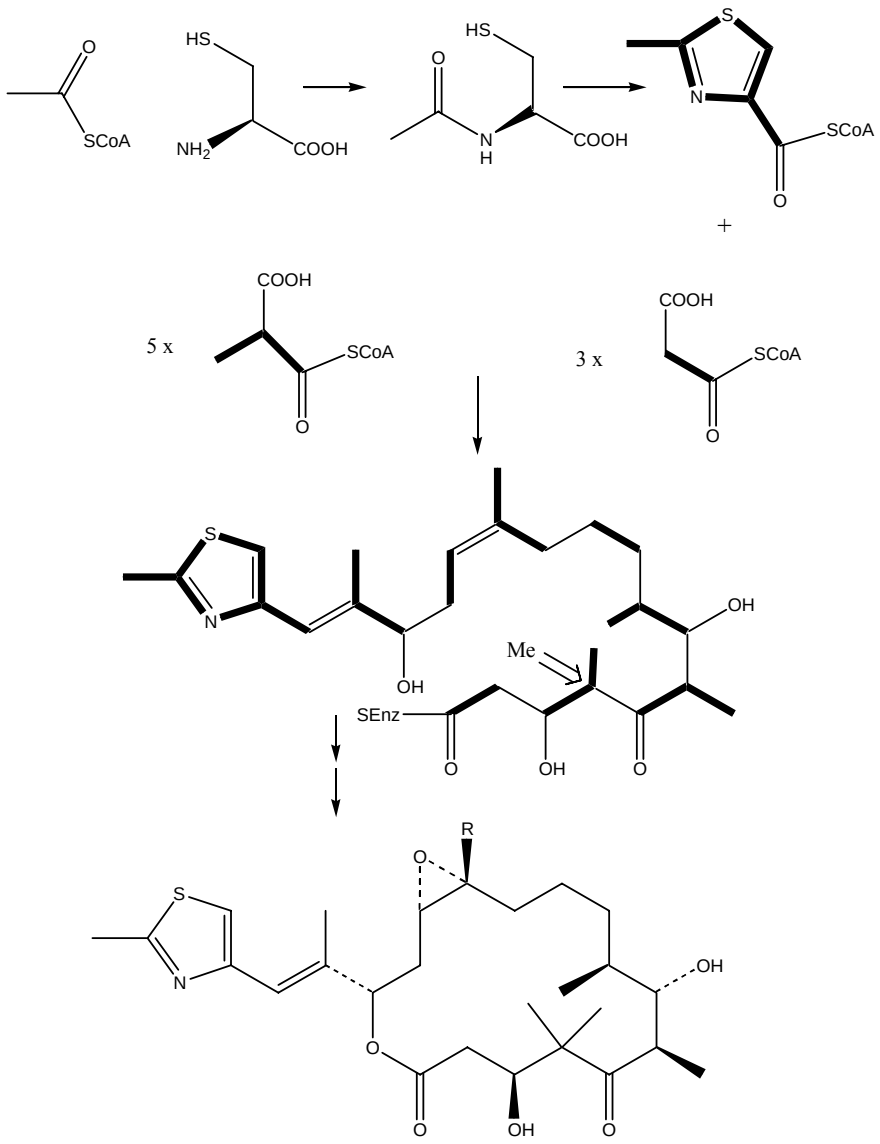

R = Me, epothilone B
R = H, epothilone A

Fig. 4.3: Biosynthesis of epothilones, [Dewick, 2002]

4.4. Metabolites isolated from the sponge *Pseudoceratina purpurea*

Sponges of the order Verongida show a uniform secondary chemistry. Every species examined from this order produces brominated secondary metabolites which are generally assumed to arise biogenetically from 3,5-dibromotyrosine [Cimino, *et al.,* 1983 and 1986; Ireland, *et al.,* 1989]. The sponge *Pseudoceratina purpurea* is a prominent example of this taxonomic group. Typical constituents vary from rather complex to relative simple brominated metabolites. Most of the isolated compounds from this sponge were very simple brominated tyrosine derivative except compound **12** (bisoxazolidinone derivative) and also compound **10** (purealidin R) which are composed of isoxazoline moieties, that are presumably derived from a rearranged tyrosine side chain along with one substituted aromatic ring and form the structural backbone of the other brominated metabolites found in the order Verongida. Since many sponges contain symbiotic micro-organisms in large numbers, there is always the possibility that symbiotic micro-organisms may synthesise the metabolites found in sponges. The presence of brominated metabolites localized within the tissue of the sponge of the order Verongida may be circumstantial evidence that no brominated materials are associated with bacterial cells [Faulkner, 1984].

4.4.1. Biosynthesis of brominated tyrosine derivatives

It is suggested that the small molecular weight constituents of order Verongida such as aeroplysinin-1 and dienone (**8**), are biotransformation products originating from stored precursors of higher molecular weight, such as isofistularin-3 or aerophobin-2 [Teeyapant, 1994]. Teeyapant reported that the proposed enzymatic conversion of isofistularin-3 and aerophobin-2 to aeroplysinin-1 and dienone is of special interest with regard to the biological activities, such as antibiotic, cytotoxic, haemolytic activities of biotransformation products. A possible biogenetic pathway of the active antibiotic compound dienone (**8**) as an example of the simple brominated tyrosine alkaloids, starting from 3,5-dibromotyrosine was proporsed [Cimino, et al., 1983; De Rosa, *et al.,* 1973]. On the other hand, the complete fragmentation of isofistularin-3 in *vitro* enzyme assay [Ebel, 1998] resulted in the formation of bisoxazolidinone derivative (**12**) and dienone (**8**) which suggested that isofistularin-3 was the precursor for our compounds isolated from the sponge *Pseudoceratina purpurea* (see Fig. 4.4).

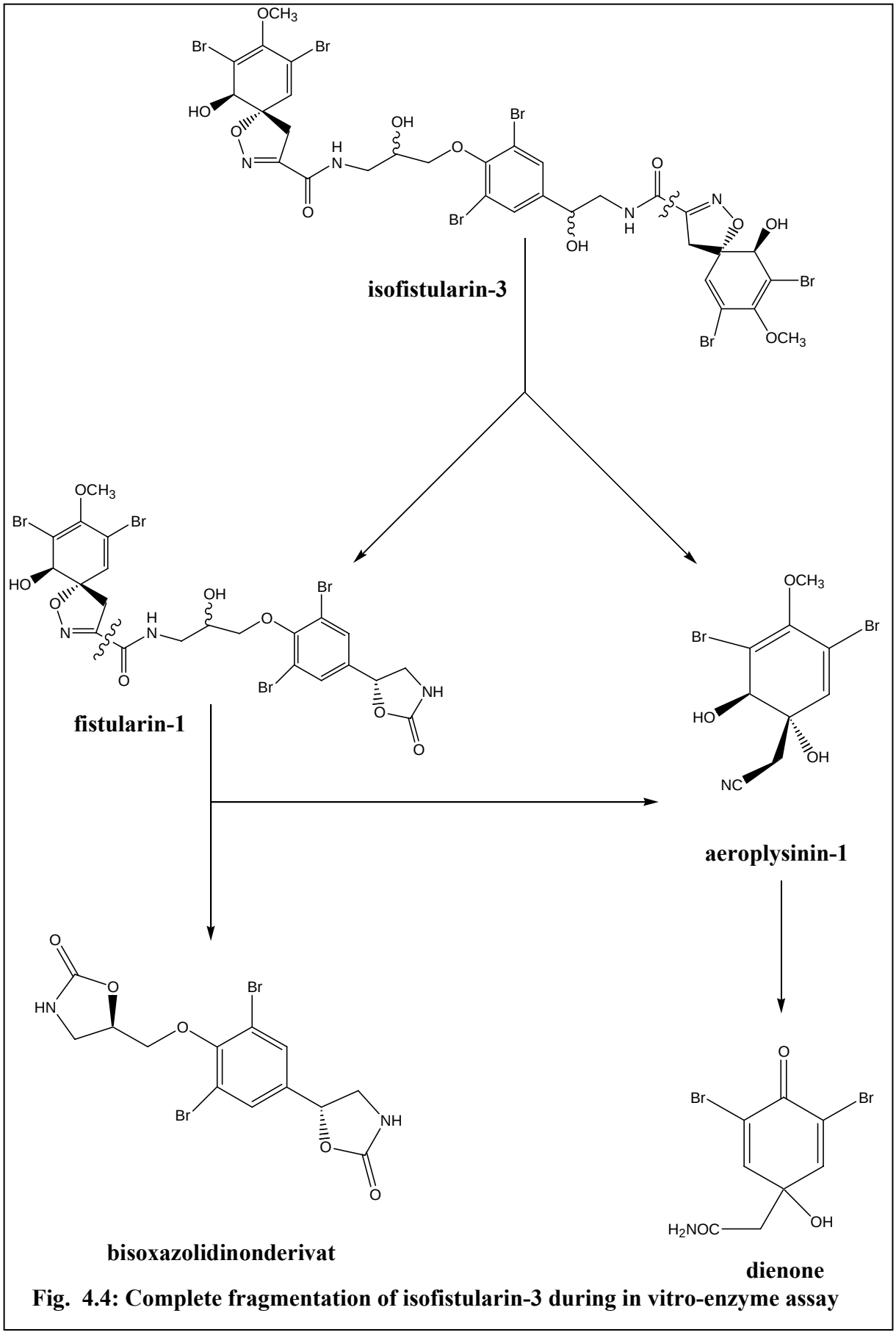

Fig. 4.4: Complete fragmentation of isofistularin-3 during in vitro-enzyme assay

4.4.2. Structure activity relationship of brominated tyrosine alkaloids

According to the results of the antimicrobial test of the isolated compounds from the sponge *Pseudoceratina purpurea* (see Table 3.21) , we can suggest that the presence of an oxo-cyclohexa-2,6-dienyl unit is important for the compounds to have antibacterial effect as shown in dienone (**8**), hydroxydienoic acid (**14**) and hydroxydienoic acid methyl ester (**15**). On the other hand, the hydroxylation or ketal formation of these compounds make them inactive. In the cytotoxicity test (see Table 3.22), dienone (**8**) and hydroxydienoic acid (**14**) were the only active compounds against the three different cancer cells, while compounds (**7**) and dienone diemethoxyketal (**9**) were less active and this activity did not appear in all the three different cancer cells. Thus, the presence of the oxo-cyclohexa-2, 6-dienyl substructure is also very important for cytotoxic activity. Furthermore, we suggest that the presence of the carboxylic acid unit may increase the activity of the compounds against Hela and PC12 cells in comparison to the presence of the acetamide unit.

4.5. Metabolites isolated from the sponge *Rhabdastrella globostellata*

Chemical investigations of sponges in the genus *Stelletta* have resulted in the isolation of steroids, alkaloids and triterpenoids [Su, *et al.,* 1994; Sheikh, *et al.,* 1974]. The triterpenoids belong to the rare isomalabaricane class which has only been reported from *Stelletta* and *Jaspis* species of sponges [Ravi, *et al.,* 1982]. Several isomalabaricanes have been reported to significantly inhibit the growth of L1210 and KB cancer cells. Fourteen **(16-30)** isomalabaricane triterpenoids were isolated from the EtOAc fraction of the Indonesian sponge *Rhabdastrella globostellata.* These compounds showed a strong activity against L5178Y cells. On the other hand, some of them were active against Hela and PC12 cells, while others were inactive (see Table 3.32). Globostellatic acids G-J (**22-25**) have an ethoxy group at position C-21 in the side chain of each compound. It is expected that these compounds may be artefacts. Fortunately, there are two arguments helping to confirm that these compounds are new natural products and not artefacts. The first one was the absence of using ethanol as a solvent at any step during the extraction, fractionation or isolation processes of this sponge. On the other hand, the HPLC chromatogram of the total crude extract of the sponge revealed the presence of two characteristic peaks belong to both of the isomeric mixtures (**22, 23** and **24, 25**).

4.5.1. Isomalabaricane and malabaricane triterpenoid compounds.

Several cytotoxic isomalabaricane triterpenes have been isolated in recent years from sponges of the genera *Stelletta* and *Jaspis* [McCabe, *et al.,* 1982; Kobayashi, *et al.,* 1996]. Embedded in their rather rare isomalabaricane framework is a 4, 4, 8, 10-tetramethylperhydrobenz [e] indene system with *trans-syn-trans* ring junctions which force the central ring into an unfavourable twist-boat conformation. On the other hand, several malabaricane triterpenes were isolated from different plants and also from marine sources, with *trans-anti-trans* ring junctions. The name of malabaricane was coined for the hypothetical hydrocarbon (3S*, 3aR*, 5aS*, 9aS*, 9bS*)-3a,6,6,9a-tetramethyl-3-(1,5,9-trimethyldecyl) perhydrobenz[e]indene [Ravi, *et al*., 1982]. The isolation of malabaricane triterpene is reported from the medicinal plant *Caloncoba echinata* [Ziegler, et al., 2002], while malabaricane triterpene glycosides were isolated from *Adesmia aconcaguensis* [Faini, *et al*., 1995]. The difference in the ^{13}C NMR data of the tricyclic part between isomalabaricane and malabaricane tritepenoids helped to differentiate between the two types. Comparison of ^{13}C NMR data of the previously reported malabaricane triterpene [Ravi, *et al*., 1982] with those of isomalabaricane tritepenoids [Tabudravu, et al., 2001] revealed that the resonance assigned to C-5 of malabaricane tritepenoids showed 6-9 ppm downfield shift in comparison to that in isomalabaricane tritepenoids. Furthermore, resonance assigned to C-9 of malabaricane tritepenoids showed 4-5 ppm upfield shift in comparison to that in isomalabaricane tritepenoids. On the other hand, the chemical shifts for the methyl groups were very similar.

4.5.2. Structure activity relationship of the isomalabaricane triterpenoid compounds.

The cytotoxicity test of the isolated isomalabaricane triterpenes from the sponge *Rhabdastrella globostellata* against different cancer cells showed that all compounds have a strong and specific activity against mouse lymphoma cells. On the other hand, these compounds showed either moderate activity or even no activity against either HELA cervix carcinoma cells or brain tumor PC12 cells. According to these results, it is suggested that the presence of an acetoxy group or hydroxyl group attached to C-3 has no effect on the activity of the compounds against mouse lymphoma cells. Furthermore, for the other types of cancer cells, it is suggested that the presence of an acetoxy group attached to C-3 may decrease the activity of the compounds in comparison to the others with a hydroxyl group attached to C-3.

It is also suggested that, the absence of the carboxylic acid group will decrease the activity of these compounds against the different cancer cells.

5. Summary

Natural products isolated from marine organism such as sponges, fungi and bacteria show a unique structural diversity which may lead to new metabolites which can be used for medicinal purposes. This study involved the isolation, structural elucidation and biological screening of the active constituents of some marine sponges collected from both the Red Sea and Indonesia using different chromatographic techniques and various tools of spectral analysis.

Four sponges have been used in this study and the number of compounds which have been isolated and structurally elucidated are concluded in the next table [Table 5.1).

5.1. The Red Sea sponge *Erylus lendenfeldi*

The sponge *Erylus lendenfeldi* was successively extracted with MeOH and acetone respectively. The combined extracts were concentrated to dryness and partitioned between Petroleum ether, EtOAc, n-BuOH and H_2O, respectively. EtOAc and n-BuOH fractions were pooled since the two fractions were similar to each other. The combined n-BuOH and EtOAc fraction (1.79 g) was subjected to medium pressure column chromatography (MPLC) using normal silica gel as stationary phase and eluted with CH_2Cl_2 / MeOH (70/30). The eluted fractions have been subjected to semi-preparative reversed phase chromatography on RP-18 column, by which three pure compounds have been isolated, the known eryloside A (**1**) and two new compounds, eryloside K (**2**) and eryloside L (**3**). Eryloside A showed moderate activity against *B. subtilis*, *E. coli* and *C. albicans*.

5.2. The Red Sea sponge *Negombata corticata*

The sponge *Negombata corticata* was successively extracted with MeOH and acetone, respectively. The combined extracts were concentrated to dryness and partitioned between petroleum ether, EtOAc, n-BuOH and H_2O respectively. Petroleum ether and EtOAc fractions were combined and subjected to normal phase column chromatography followed by semipreparative HPLC to isolate two pure known and highly active compounds, latrunculin B and M (**4** and **5**). Latrunculin B has a prominent activity as antibiotic and antifungal and as a cytotoxic agent against different leukemia cells.

5.3. The Indonesian sponge *Pseudoceratina purpurea*

The sponge *Pseudoceratina purpurea* was also successively extracted with MeOH and acetone respectively. The combined extracts were concentrated to dryness and partitioned between Petroleum ether, EtOAc, n-BuOH and H_2O, respectively. The EtOAc fraction was subjected to MPLC using different gradient systems followed by normal phase column chromatography and finally semipreparative HPLC to isolate ten known bromotyrosine alkaloids (**6-15**). Some of these compounds showed antibiotic activity while others showed moderate cytotoxic activity.

5.4. The Indonesian sponge *Rhabdastrella globostellata*

The sponge was extracted with MeOH and then with acetone, the solvents were removed under reduced pressure. The crude extract was partitioned between water and EtOAc. The ethyl acetate layer was then subjected to VLC using a gradient system from 100% n-hexane to 100% EtOAc, then 50% MeOH in EtOAc and finally 100% MeOH to have different fractions. Each fraction was purified by normal phase flash chromatography (CH_2Cl_2-MeOH, 95: 5 or 9 :1) followed by semi-preparative reversed phase HPLC using different ratios of MeOH-water to afford twelve new isomalabaricane tritepenoids, in addition to three known isomalabaricane triterpenoids. Some of these compounds showed antibiotic activity. On the other hand, it was interesting that all the isolated compounds showed cytotoxic activity against different cancer cells.

Table 5.1: Summary of the isolated compounds from the different sponges

Compounds	Structure	Name of the sponge	Comment
Eryloside A (**1**)	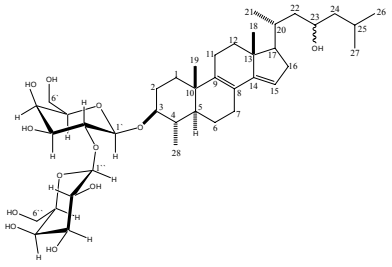	*Erylus lendenfeldi*	known
Eryloside K (**2**)	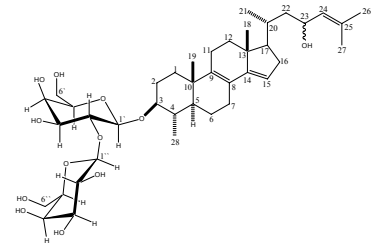	*Erylus lendenfeldi*	new
Eryloside L (**3**)	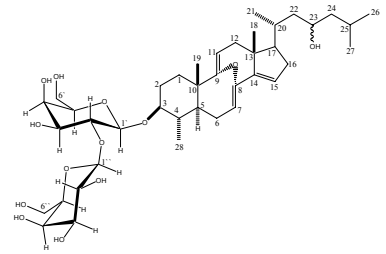	*Erylus lendenfeldi*	new
Latrunculin B (**4**)	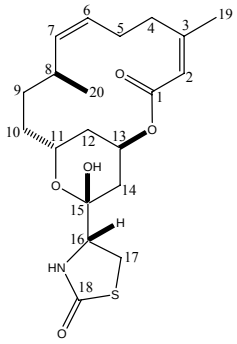	*Negombata corticata*	known
Latrunculin M (**5**)	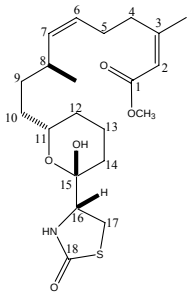	*Negombata corticata*	known

Compounds	**Structure**	**Name of the sponge**	**Comment**
Dienone methoxyethoxyketal (**6**)	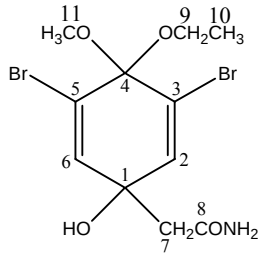	*Pseudoceratina purpurea*	known
3,5- dibromo-4-hydroxy-benzaldehyde (**7**)	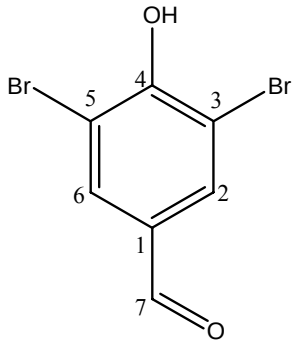	*Pseudoceratina purpurea*	known
Dienone (**8**)	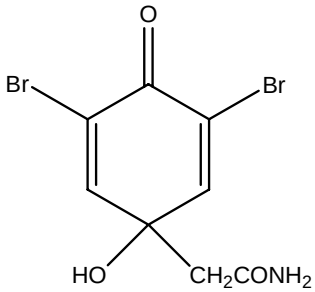	*Pseudoceratina purpurea*	known
Dienone dimethoxyketal (**9**)	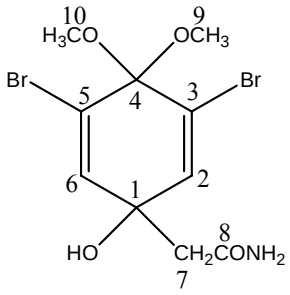	*Pseudoceratina purpurea*	known
Purealidin R (**10**)	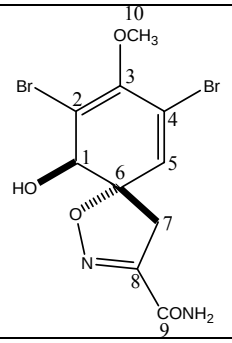	*Pseudoceratina purpurea*	known

Compounds	**Structure**	**Name of the sponge**	**Comment**
2-(3,5-Dibromo-4-hydroxyphenyl)-acetamide (**11**)	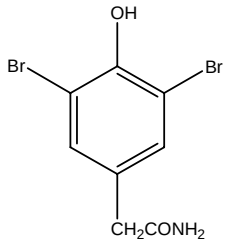	*Pseudoceratina purpurea*	known
Bisoxazolidinone derivative (**12**)	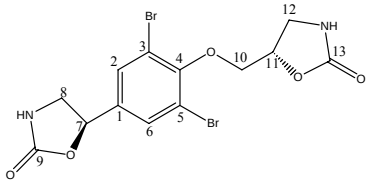	*Pseudoceratina purpurea*	known
3,5-Dibromo-2-hydroxy-4-methoxyphenylacetic acid (**13**)	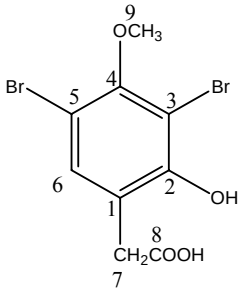	*Pseudoceratina purpurea*	known
Hydroxydienoic acid (**14**)	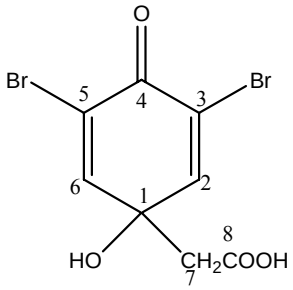	*Pseudoceratina purpurea*	known
Hydroxydienoic acid methyl ester (**15**)	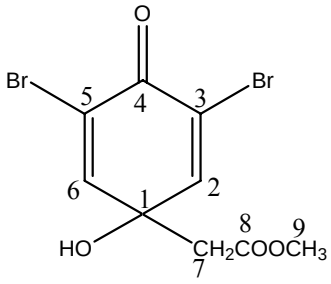	*Pseudoceratina purpurea*	known

Compounds	**Structure**	**Name of the sponge**	**Comment**
Globostellatic acid A (**16**)	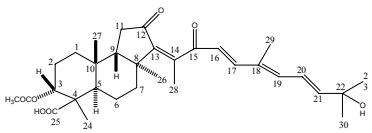	*Rhabdastrella globostellata*	known
Globostellatic acid E (**17**)	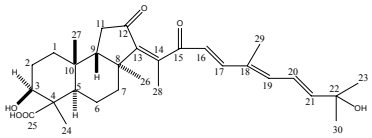	*Rhabdastrella globostellata*	new
Globostellatic acid F (**18**)	Under instructor	*Rhabdastrella globostellata*	new
Globostellin (**19**)	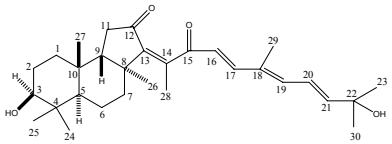	*Rhabdastrella globostellata*	new
Globostellatic acid D (**20**)	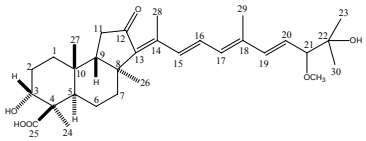	*Rhabdastrella globostellata*	known
Globostellatic acid M (**21**)	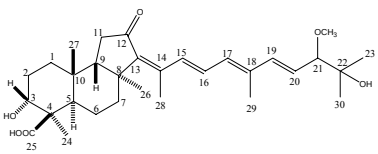	*Rhabdastrella globostellata*	new

Compounds	**Structure**	**Name of the sponge**	**Comment**
Globostellatic acid G (**22**)	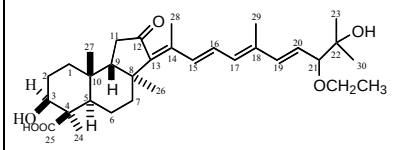	*Rhabdastrella globostellata*	new
Globostellatic acid H (**23**)	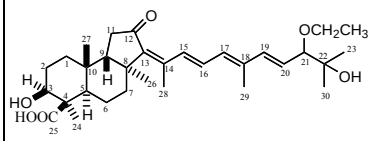	*Rhabdastrella globostellata*	new
Globostellatic acid I (**24**)	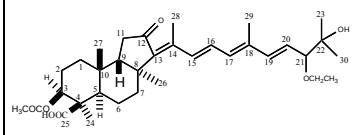	*Rhabdastrella globostellata*	new
Globostellatic acid J (**25**)	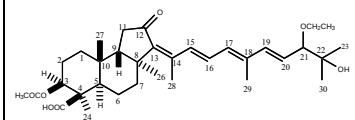	*Rhabdastrella globostellata*	new
Globostellatic acid K (**26**)	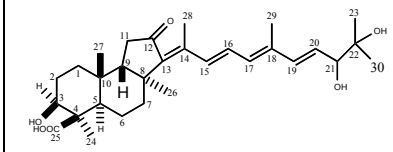	*Rhabdastrella globostellata*	new
Globostellatic acid L (**27**)	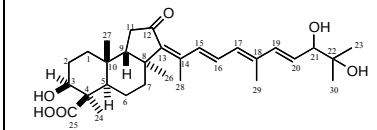	*Rhabdastrella globostellata*	new
Stelliferin riboside (**28**)	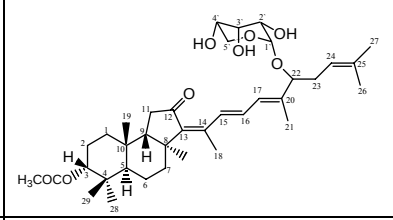	*Rhabdastrella globostellata*	known
13-*E*-Stelliferin riboside (**29**)	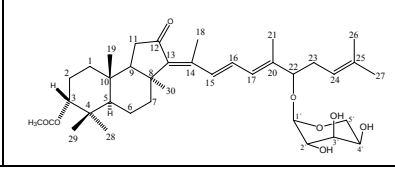	*Rhabdastrella globostellata*	new

Compounds	**Structure**	**Name of the sponge**	**Comment**
3-Hydroxy-stelliferin riboside (**30**)	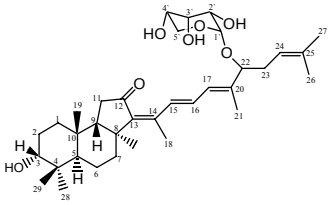	*Rhabdastrella globostellata*	new

6. References

Allen, C. D. C. (2000): *Biology Undergraduate Journal*, , **3**, 141-150.

Ambrosio, M. D.; Guerriero, A. and Pietra, F. (1984): *Helv. Chim. Acta*, **67**, 1484-1492.

Ambrosio, M. D.; Guerriero, A.; Traldiand, P. and Pietra, F. (1982): *Tetrahedron Lett.*, **23**, 4403-4406.

Andersen, R. J. and Faulkner, D. J. (1973): *Tetrahedron Lett.*, **14**, 1175-1178.

Aoki, S.; Higuchi, K.; Ye, Y.; Satari, R. and Kobayashi, M. (2000): *Tetrahedron*, **56**, 1833-1836.

Ayscough, K. R.; Stryker, J.; Pokala, N.; Sanders, M.; Crews, P. and Drubin, D.G. (1997): *J. Cell Biol.,* **137**, 399-416.

Bajaj, A.G. (1979): *Tetrahedron Lett*., 4153-4154.

Bakus, G. J.; Targett, N. M. and Schulte, B. (1986): *J. Chem. Ecol.*, **12**, 951-987.

Blasberger, D.; Carmely, S.; Cojocaru, M.; Spector, I.; Shochet, N. R. and Kashman, Y. (1989): *Liebigs Ann. Chem.*, 1171-1188.

Blasberger, D.; Green, D.; Carmely, S., Spector, I. and Kashman, Y. (1987): *Tetrahedron Lett.,* **28**, 459-462.

Borders, D. B.; Morton, G. O. and Wetzel, E. R. (1974): *Tetrahedron Lett.*, **31**, 2709-2712.

Bourguet-Kondracki, M. L.; Longeon, A.; Debitus, C. and Guyot, M. (2000): *Tetrahedron Lett*., **41**, 3087-3090.

Braekman, J. C. and Daloze, D. (1986): *Pure Appl. Chem*., **58**, 357-364.

Burkholder, P. R. (1973): The ecology of marine antibiotics and coral reefs. In: *Biology and Geology of Coral Reefs* (Jones, O.A. and Endean, R. eds), Academic Press, New York.

Carmely, S.; Roll, M.; Loya, Y. and Kashman, Y. (1989): *J. Nat Prod.*, **52**, 167-170.

Carmichael, J.; DeGraff, W. G.; Gazdar, A. F.; Minna, J. D. and Mitchell, J. B. (1987): *Cancer Res*., **47**, 943-946.

Carmichael, J.; DeGraff, W. G.; Gazdar, A. F.; Minna, J. D. and Mitchell, J. B. (1987): *Cancer Res*., **47**, 943-946.

Chadwick, D. J. and Marsh J. (1990): Bioactive compounds from plants. In: *Ciba Foundation Symposium*, **154**, John Wiley and Sons, Chichester, Sussex, U.K.

Chawla, A. and Dev, S. (1967): *Tetrahedron Lett*., 4837-4843.

Chib, J. S.; Stempien, M. F.; Mierzwa, R. A.; Ruggieri, G. D. and Nigrelli, R. F. (1978): *J. Pharm. Sci.*, **67**, 264-265.

Cimino, G.; De Rosa, S.; De Stefano, S. and Sodano, G. (1986): *Pure Appl. Chem.,* **58**, 375-386.

Cimino, G.; De Rosa, S.; De Stefano, S.; Self, R. and Sodano, G. (1983): *Tetrahedron Lett.,* **24**, 3029-3032.

Coue, M.; Brenner, S. L.; Spector, I. and Korn, E. D. (1987): *FEBS Lett.,* **213**, 316-318.

Cragg, G. M.; Newman, D. J. and Snader, K. M. (1997): *J. Nat. Prod.*, **60**, 52-60.

Cruz, F.; Quijano, L.; Garibay, F. G. and Rios, T. (1990): *J. Nat. Prod.*, **53**, 543-548.

D´Auria, M. V.; Paloma, L. G.; Minale, L. and Riccio, R. (1991): *Tetrahedron Lett.,* **32**, 2149-2152.

De Rosa, M.; Minale, L. and Sodano, G. (1973): *Comp. Biochem. Physiol.,* **45B**, 883-893.

De Silva, E. D. and Scheuer, P. J. (1980): *Tetrahedron Lett.,* **21**, 1611-1614.

Dewick, P. M. (2002): *Medicinal Natural Products*, a biosynthetic approach, ,2nd ed., John Wiley and sons, LTD, England, 104-105.

Ebel, R. (1998): Ph.D. thesis " *Wundinduzierte Biotransformation bromierter Alkaloide in Schwämmen der Gattung Aplysina: Biochemische Charakterisierung und ökologische Bedeutung*".

Enwall, E. L.; Van Der Helm, D.; Nan Hsv, I.; Pattabkiraman, T.; Schmitz, F. J.; Spraggins, R.L. and Weinheimer, A.J. (1972): *J. Chem. Soc. Chem. Commun.*, 251.

Farnsworth, N. R.; Akerele, O.; Bingel, A. S.; Soejarto, D. D. and Guo, Z. (1985): *Bull. WHO*, **63**, 965-981.

Fattorusso, E.; Minale, L. and Sodano, G.(1972): *J. Chem. Soc., Perkin Trans. 1*, 16-18.

Faulkner, D. J. (1984): *Nat. Prod. Rep.,* **1**, 551-598.

Faulkner, D. J. (1988): *Nat. Prod. Rep.*, **5**, 613-663.

Faulkner, D. J. (1990): *Nat. Prod. Rep.*, **7**, 269-307.

Faini, N.; Castillo, M.; Torres, R.; Monache, G.D. and Baitz, E.G. (1995): *Phytochemistry*, **40**, 885-890.

Gao, H.; Kelly, M. and Hamann, M. T. (1999): *Tetrahedron*, **55**, 9717-9726.

Gerrit, J.; Johannis, P. and Johannes, V. (1977): *Carbohydrate Research,* **62**, 349-357.

Gerwick, W. H. and Bernart, M. W. (1992) *Pharmaceutical and bioactive natural products* In: *Marine Biotechnology* **1**. (Attaway, D.H. and Zaborsky, O.R. eds), Plenum Press, New York.

Gerth, K.; Bedorf, N.; Höfle, G.; Irschik; H. and Reichenbach, H. (1996): *J. Antibiot.*, **49**, 560-563.

Glaser, K. B. and Jacobs, R. S. (1986): *Biochem. Pharmacol.,* **35**, 449-450.

Goobes, R.; Rudi, A.; Kashman, Y.; Lian, M. and Loya, Y. (1996): *Tetrahedron*, **52**, 7921-7928.

Gopichand, Y. and Schmitz, F. J. (1979): *Tetrahedron Lett.*, **20**, 3921-3924.

Gribble, G. W. (1992): *J. Nat. Prod.*, **55**, 1353-1395.

Groweiss, A.; Shmueli, U. and Kashman,Y. (1983): *J. Org. Chem.*, **48**, 3512-3516.

Gulavita, N. K.; Wright, A. E.; Kelly-Borges, M. and Longley, R. E. (1994): *Tetrahedron Lett.*, **35**, 4299-4302.

Gullo, V. P. (1994): The discovery of Natural Products with Therapeutic Potential, *Butterworth- Heinemann*, Boston.

Gunawardana, G. P:; Kohmoto, S.; Gunasekera, S. P.; McConnell, O. J. and Koehn, F. E. (1988): *J. Am. Chem. Soc.*, **110**, 4856-4858.

Ireland, C. M.; Molinski, T. F.; Roll, D. M.; Zabriskie, T. M.; McKee, T. C.; Swersey, J. C. and Foster, M. P. (1989), *Natural products peptide in marine organisms*, In: *Bioorganic Marine Chemistry*, **3**, (Scheuer, P.J., ed.) Springer-Verlag, Berlin.

Jacobs, R. S.; Culver, P.; Langdon, R.; O´Brien and White, S. (1985): *Tetrahedron*, **41**, 981-984.

Jaspars, M. (1999): *Chem. Ind.*, 51-55.

Jaspars, M. and Crews, P. (1994): *Tetrahedron Lett.*, **35**, 7501- 7504.

Jongheon, S.; Hyi-Seung, L.; Leeyoung, W.; Jung-Rae, R.; Youngwan, Seo.; Ki, W. C. and Chung, J. S. (2001): *J. Nat. Prod.*, **64**, 767-771.

Julien, B.; Shah, S.; Ziermann, R.; Goldman, R.; Katz, L. and Khosla, C. (2000): *GENE*, **249**, 153-160.

Kashman, Y.; Carmely, S.; Blasberger, D.; Hirsch, S. and Green, D.(1989): *Pure Appl Chem*., **61**, 517-520.

Kashman, Y.; Groweiss, A. and Shmueli, U. (1980): *Tetrahedron Lett.,* **21**, 3629-3632.

Kashman, Y.; Groweiss, A.; Lidor, R.; Blasberger, D. and Carmely, S. (1985): *Tetrahedron*, **41**, 1905-1914.

Kashman, Y.; Yosief, T. and Carmely, S. (2001): *J. Nat. Prod.,* **64**, 175-180.

Kazlauskas, R.; Murphy, P. T.; Ravi, B. N.; Sanders, R. L. and Wells, R. J. (1982): *Aust. J. Chem.* **35**, 69-75.

Kazlauskas, R.; Lidgard, R. O.; Murphy, P. T.; Wells, R. J. and Blunt, J. F. (1981): *Aust. J Chem.,* **34**, 765-786.

Kinghorn, A. D. and Balandrin, M. F. (1993): Human medicinal agents from plants, *ACS*, 205-207.

Kobayashi, J.; Yuasa, K.; Kobayashi, T.; Sasaki, T. and Tsuda, M. (1996): *Tetrahedron*, **52**, 5745-5750.

Kobayashi, J. I.; Honma, K.; Sasaki, T. and Tsuda, M. (1995): *Chem. Pharm. Bull*., **43**, 403-407.

König, G. M. (1992): *Dtsch. Apoth. Ztg.*, **132**, 673-683.

König, G. M. and Wright, A. D. (1996): Planta Med., **62**, 193-211.

Leontein, K.; Lindberg, B. and Lönngren, J. (1977): *Carbohydrate Research.* **62**, 359-362.

Lim, D.; Lange, K. and Santella, L. (2002): *FASEB Journal*, **16**, 1050- 1056.

Lindel, T.; Hoffmann, H.; Hochgürtel, M. and Pawlik, J. R. (2000): *J. Chem. Ecol*., **26**, 1477-1496.

Longely, R. E.; Caddigan, D.; Harmody, D.; Gunasekera, M. and Gunasekera, S. P. (1991): *Transplantation*, **52**, 650-656.

Luesch, H.; Yoshida, W. Y. and Moore, R. E. (2000): *J. Nat. Prod.*, **63**, 611-615.

Madaio, A.; Piccialli, V. and Sica, D. (1988): *Tetrahedron Lett.,* **29**, 5999-6000.

Makarieva, T. N.; Stonik, V. A.; Alcolado, P. and Elyakov, Y. B. (1981): *Comp Biochem Physio B*, **68B**, 481-484.

Marderosian, A.D. (1969): *J. Pharm. Science*, **58**, 1-33.

Mayer, A. M. S.; Glaser, K. B. and Jacobs, R. S. (1988): *J. Pharmcol. Exp. Ther*., **244**, 871-872.

McCabe, T.; Clardy, J.; Minale, L.; Pizza, C.; Zollo, F. and Riccio, R. (1982): *Tetrahedron Lett*., **23**, 3307-3310.

McCaffrey, E. J. and Endean, R. (1985): *Mar. Biol*., **89**, 1-8.

McClintock, J. B. and Baker, B. J. (eds) (2001): *Marine Chemical Ecology*. CRC, Boca Raton, Florida.

McCormick, J. L.; McKee, T. C.; Cardellina II, J. H.; Leid, M. and Boyd, M. R. (1996): *J. Nat. Prod*., **59**, 1047-1050.

McMillan, J. A.; Paul, I. C.; Goo, Y. M. and Rinehart, K. L. (1981): *Tetrahedron Lett.,* **22**, 39- 42.

Meragelman, K.M.; McKee, T. C. and Boyd, M. R. (2001): *J. Nat. Prod*., **64**, 389-392.

Meyer, B. N.; Ferrigni, N. R.; Putnam, J. E.; Jacobsen, L. B.; Nichols, D. E. and McLaughlin, J. L. (1982): *Planta Medica*, **45**, 31-34.

Mohamadi, F.; Richards, N. G. J.; Guida, W. C.; Liskamp, R.; Lipton, M.; Caulfield, C.; Chang, G.; Hendrickson, T. and Still, W. C. (1990): *J. Comput. Chem.*, **11**, 440-467.

Moody, K.; Thomson, R. H.; Fattorusso, E.; Minale, L. and Sodano, G. (1972): *J. Chem. Soc., Perkin Trans. 1*, 18-24.

Neeman, I.; Fishelson, L. and Kashman,Y. (1975): *Mar. Biol.* (Berlin), **30**, 293.

Nishiyama, S. and Yamamura, S. (1985): *Bull. Chem. Soc. Jpn.,* **58**, 3453

Norgauer, J.; Bartels, F.; Gohring, U.; Schopf, E.; Gebicke, H. P.; Kownatzki, E. and Krutmann, J. (1995): *Exp Cell Res*., **219**, 15-20.

Norte, M.; Rodriguez, M. L.; Fernandez, J. J.; Eugern, L. and Estrada, D. M. (1988): *Tetrahedron,* **44**, 4973-4980.

O'Neil, M. J. and Lewis, J. A. (1993) In: *Human Medicinal Agents from Plants* (Kinghorn, A.D. and Balandrin, M.F.,eds) *ACS Symposium Series*, **534**: *American Chemical Society*, Washington DC, 48-55.

Oku, N.; Matsunaga, S.; Wada, S. I.; Watabe, S. and Fusetani, N. (2000): *J. Nat. Prod.*, **63**, 205-209.

Patou, W. F.; Paul, I. C. and Spector, I.; Shochet, N. R.; Blasberger, D. and kashman, Y. (1989): *Cell Motil. Cytoskeleton*, **13**, 127-144.

Pawlik, J. R.; Chanas, B.; Toonen, R. J. and Fenical, W. (1995): *Mar. Ecol. Prog. Ser.*, **127**, 183-194.

Pearse, V.; Pearse, J.; Buchsbaum, M. and Buchsbaum, R.(1987) In: *Living Invertebrates*, Blackwell Scientific Publications, California.

Pechenik, J. A. (2000) In: *Biology of the Invertebrates*, 4th McGraw-Hill companies.

Potts, B. C. M. and Faulkner, D. J. (1992): *J. Nat. Prod.*, **55**, 1701-1717.

Proksch, P. (1991): *BIUZ*, **21**, 26-30.

Proksch, P. (1999): *Chemical defence in marine ecosystems,* In: *Functions of Plant Secondary Metabolites and their Exploitation in Biochemistry* (Wink, M., ed), Academic, Press, Sheffield, 134-154.

Proksch, P. and Ebel, R. (1998): *Ecological significance of alkaloids from marine invertebrates* In: *Alkaloids, Biochemistry, Ecology and Medicinal Applications* (Roberts, M.F. and Wink, M., eds) Plenum, New York, 379-394.

Proksch, P.; Edrada, R. A. and Ebel, R. (2002): *Appl. Microbiol. Biotechnol.*, **59**, 125-134.

Randall, J. E. and Hartman, W. D. (1968): *Mar. Biol.*, **1**, 216-225.

Rao, Z.; Deng, S.; Wu, H. and Jiang, S. (1997): *J. Nat. Prod.*, **60**, 1163-1164.

Ravi, B. N. and Wells, R. J. (1982): *Aust. J. Chem.*, **35**, 39-50.

Ravi, B. N.; Wells, R. J. and Croft, K. D. (1981): *J. Org. Chem.*, **46**, 1998-2001.

Rodphaya, D.; Sekiguchi, J. and Yamada, Y. (1986): *J. Antibiot.*, **39**, 629-635.

Ryu, G.; Matsunaga, S. and Fusetani, N. (1996): *J. Nat. Prod*., **59**, 512-514.

Samuelsson, G.(1999): *Drugs of Natural Origin*, *A Text book of Pharmacognosy*, 4th ed., Kristianstads boktryckeri AB, Kristianstad, Sweden, 305-315.

Sarma, A. S.; Daum, T. and Müller, W. E. G. (1993): *Secondary Metabolites from Marine Sponges*, Ullstein Mosby, Berlin.

Sata, N.; Asai, N.; Matsunaga, S. and Fusetani, N. (1994): *Tetrahedro*n, **50**, 1105-1110.

Scheuer, P. J. (1990): *Science*, **248,** 173-177.

Schneider, U.; Schwenk, H.U. and Bornkamm, G. (1977): *Int. J. Cancer*, **19**, 621-626.

Scott, A. I. (1964): *Interpretation of the Ultraviolet Spectra of Natural products* Pergamon: Oxford

Sharma, G. M. and Burkholder, P. R. (1967a): *J. Antibiot. (Tokyo), Ser. A.,* **20**, 200-203.

Sharma, G. M. and Burkholder, P. R. (1967b): *Tetrahedron Lett.*, **42**, 4147-4150.

Sharma, G. M.; Vig, B. and Burkholder, P. R. (1970): *J. Org. Chem.*, **35**, 2823-2826.

Sheikh, Y. M. and Djerassi, C. (1974): *Tetrahedron*, **30**, 4095-4103.

Sobti, R. R. and Dev, S. (1968): *Tetrahedron Lett*., 2215-2217.

Spector, I.; Shochet, N. R.; Kashman, Y. and Groweiss, A. (1983): *Science*, **214**, 493-495.

Stead, P.; Hiscox, S.; Robinson, P. S.; Pike, N. B.; Sidebottom, P. J.; Roberts, A. D.; Taylor, N. L.; Wright, A. E.; Pomponi, S. A. and Langley, D. (2000): *Bioorg*. *Med*. *Chem*. *lett*., **10**, 661-664.

Su, J. Y.; Meng, Y. H.; Zeng, L. M.; Fu, X. and Schmitz, F. J. (1994): *J. Nat. Prod*., **57**, 1450-1451.

Sundstrom, C. and Nilsson, K. (1976): *Int. J. Cancer*, **17**, 565-577.

Tabudravu, J. N. and Jaspars, M. J. (2001): *J. Nat. Prod*., **64**, 813-815.

Takada, K.; Nakao, Y.; Matsunaga, S.; Van Soest, R.W. M. and Fusetani, N. (2002): *J. Nat. Prod.*, **65**, 411-413.

Tanaka, J. I.; Higa, T.; Bernardinelli, G. and Jefford, C. W. (1996): *Chem. Lett*., 255-256.

Tasdemir, D.; Mangalindan, G. C.; Concepcion, G. P.; Verbitski, S. M.; Rabindran, S.; Miranda, M.; Greenstein, M.; Hooper J. N. A.; Harper, M. K. and Ireland, C. M. (2002): *J. Nat. Prod*., **65**, 210-214.

Teeyapant, R. (1994): Ph.D. thesis "*Brominated Secondary Metabolites of the Marine Sponge Verongia aerophoba and the Sponge Feeding Gastropod Tylodina preversa*: *Identification, Biological Activities and Biotransformation*".

Tsuchiya, S.; Yamaba, M.; Yamaguchi, Y.; Kobayashi, Y.; Konno, T. and Tada, K. (1980): *Int. J. Cancer*, **26**, 171-176.

Tsuda, M.; Ishibashi, M.; Agemi, K.; Sasaki, T. and Kobayashi. J. (1991): *Tetrahedron*, **47**, 2181-2194.

Valeria, D. A. M; Paloma, L. G.; Minale, L. and Riccio, R. (1992): *Tetrahedron*., **48**, 491-498.

Zambetti, G.; Ramsey, E. A.; Bortell, R.; Stein, G. and Stein, J. (1991): *Exp Cell Res*, **192**, 93-101.

Zampella, A.; D´Auria, M. V.; Debitus, C. and Menou, J. L. (2000): *J. Nat. Prod.*, 63, 943-946.

Zhang, W. H. and Che, C. T. (2001): *J. Nat. Prod*., **64**, 1489-1492.

Ziegler, L. H.; Staerk, D.; Christensen, J.; Olsen, C. E.; Sittie, A. and Jaroszewski, J. W. (2002): *J. Nat. Prod*., **65**, 1764-1768.

List of Abbreviations

$[\alpha]_D$	: specific rotation at the sodium D-line
br	: broad signal
CI	: chemical ionization
COSY	: correlation spectroscopy
d	: doublet
dd	: double of doublets
ddd	: double double of doublets
DEPT	: distortionless enhancement by polarization transfer
ED	: effective dose
EI	: electron impact
ESI	: electro spray ionization
eV	: electronvolt
FAB	: fast atom bombardment
HMBC	: heteronuclear multiple bond connectivity
HMQC	: heteronuclear multiple quantum coherence
HPLC	: high performance liquid chromatography
Hz	: herz
LC	: lethal concentration
m	: multiplett
MeOD	: deuterated methanol
MeOH	: methanol
mg	: milligram
mL	: millilitre
MPLC	: medium pressure liquid chromatography
MS	: mass spectroscopy
m/z	: mass per charge
µg	: microgram
µL	: microliter
nm	: nanometer
NMR	: nuclear magnetic resonance
ppm	: part per million
Prep. HPLC	: preparative HPLC

q	: quartet
ROESY	: rotating frame overhauser enhancement spectroscopy
RP-18	: reversed phase C-18
s	: singlett
t	: triplett
TFA	: trifluoroacetic acid
TLC	: thin layer chromatography
UV	: ultra-violet
VLC	: vacuum liquid chromatography

Biographic data

Name:	Mostafa Ahmed Fouad Abdelgawwad
Date of birth:	12. May 1970
Place of birth:	Assiut, Egypt
Nationality:	Egyptian
Civil status:	Married, three children
Address:	Universitätsstrasse 1, 40225 Düsseldorf
Home Address:	El-Minia University, El-Minia, Egypt

Educational Background:

1975 - 1981	Grade school, The University School, Assiut, Egypt.
1981 – 1984	Intermediate School, Assiut Intermediate School, Assiut, Egypt.
1984 – 1987	High School, Naser Higher School, Assiut, Egypt.
1987 – 1992	Bachelor of Science degree in Pharmacy, Assiut University, Assiut, Egypt.
1994 – 1997	Master of Science degree in Pharmacy, Assiut University, Egypt Thesis: Pharmacognostical Studies on *Securigera securidacea*, belonging to family Leguminosae, reputed to have hypoglycemic effect.
June – Sept. 2000	German Language Course, Goethe Institut, Göttingen, Germany.
Oct. 2000 – present	Ph.D. candidate, Institute of Pharmaceutical Biology, HHU, Düsseldorf, Germany.

Employment Record:

1992 – 1994	A Pharmacist in Alcon Pharmaceutical Company, Cairo, Egypt.
1994 – 1997	Demonstrator, Faculty of Pharmacy, Al-Azhar Univeristy, Assiut, Egypt.
1998 – present	Assistant Lecturer, Pharmacognosy Department, Faculty of Pharmacy, El-Minia University, El- Minia, Egypt.